Influence of tumor microenvironment and cancer cells interplay on cutaneous squamous cell carcinoma progression and immunotherapy response

Adrià Archilla Ortega

UNIVERSITAT DE BARCELONA

INFLUENCE OF TUMOR MICROENVIRONMENT AND CANCER CELLS INTERPLAY ON CUTANEOUS SQUAMOUS CELL CARCINOMA PROGRESSION AND IMMUNOTHERAPY RESPONSE

Doctoral thesis memory

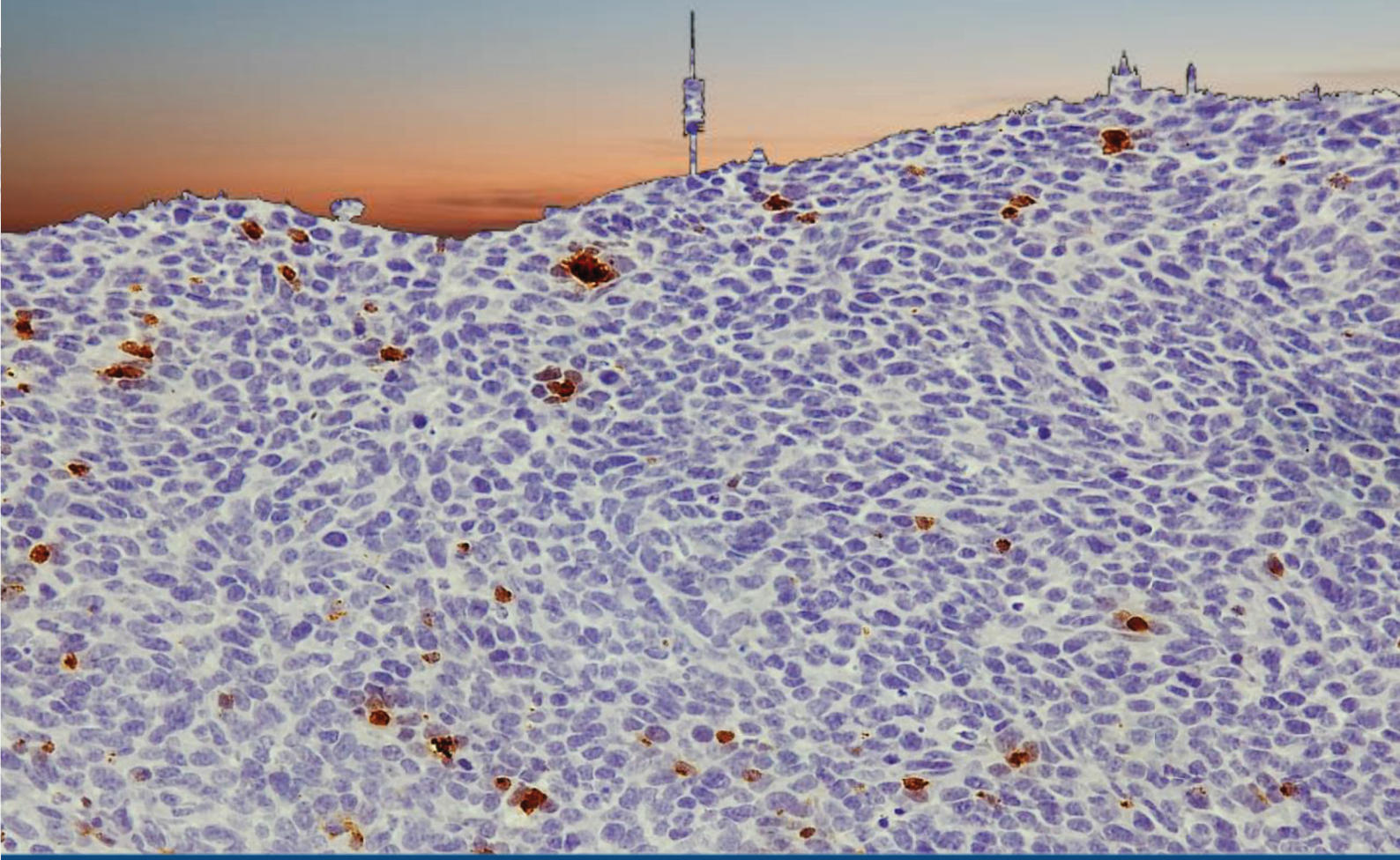

Adrià Archilla Ortega

Barcelona, 2023

IDIBELL

Influence of tumor microenvironment and cancer cells interplay on cutaneous squamous cell carcinoma progression and immunotherapy response

Report presented by Adrià Archilla Ortega to opt for the degree of Doctor from the University of Barcelona

UNIVERSITAT DE BARCELONA - FACULTAT DE MEDICINA

DOCTORAL PROGRAMME IN BIOMEDICINE

This thesis was performed in Cancer and Aging group, integrated in the Oncobell program in the Institut d'Investigació Biomèdica de Bellvitge (IDIBELL)

Dra. Purificación Muñoz Moruno

Director

Dr. Francesc Viñals Canals

Tutor

Adrià Archilla Ortega

Doctoral student

UNIVERSITAT DE BARCELONA

Influence of tumor microenvironment and cancer cells interplay on cutaneous squamous cell carcinoma progression and immunotherapy response

Doctoral thesis memory

Adrià Archilla Ortega

Barcelona, 2023

IDIBELL

Institut d'Investigació Biomèdica de Bellvitge

**“I can accept failure, everyone fails at something.
But I can’t accept not trying.”**

Michael Jordan

ACKNOWLEDGEMENTS

A la meva família, en especial als meus pares per tot el suport que m'han donat. A la meva mare per sempre encoratjar-me a fer tot allò que m'he proposat. Al meu pare per ensenyar-me que les coses ben fetes requereixen temps i no volen preses. A l'Anna per ser una persona tan especial i recolzar-me incondicionalment, gràcies per la paciència. Al Gerard i l'Oriol per haver fet del carrer Manila una segona casa, gràcies per ajudar-me a relativitzar tot el que he viscut.

Al grup PMM, a tots els membres que han passat i he tingut l'oportunitat d'aprendre d'ells. Primerament, a la Puri per donar-me l'oportunitat de fer el doctorat al teu grup i aprendre més del que un pot imaginar, gràcies per obligar-me a treure la millor versió de mi mateix. A la Laura per tota l'expertesa i el coneixement tècnic en la immuno-oncologia. Al Joan pels bons moments i els riures, has estat un gran pilar en el dia a dia. A la Marta i la Carla per haver estat unes bones companyes de treball. Voldria tenir una especial menció per l'Álvaro amb qui vam treballar sis mesos colze a colze i en guardo un dels millors records, gràcies per participar activament en aquest projecte. Finalment, al meu tutor, el Francesc, per haver acceptat aquest rol i sempre donar un cop de mà al nostre grup.

D'aquest viatge em quedo amb les persones amb qui he coincidit i el bon record que m'emporto. A tots els amics del laboratori LRT1. A la meva companya de vida, la Sandra, qui el destí va voler que continuéssim veient-nos diàriament quatre anys més, sense ella no hauria estat el mateix. A la Núria, a qui no tinc paraules per expressar tot el que m'ha ajudat i el suport que ha estat. Les nostres sortides de trail per Collserola van ser sempre reparadores. I a tothom de l'IDIBELL que sempre ha estat disposat a donar un cop de mà en el que fes falta, a la Clara, la Sandra, la Sílvia, la Laura, l'Edgar i un llarg etcètera d'amics.

També voldria agrair a tots els professionals de les plataformes pel seu suport i amabilitat. A la Saioia i el Joan de microscòpia, a la Lola i el Jose d'histologia i a la Rosa de l'estabulari de l'IDIBELL. En especial voldria agrair el suport al Jaume, la Sonia, el Ricard i la Chary de citometria del PCB.

Finalment, voldria agrair al ministeri d'Educació i Ensenyament Superior del Govern d'Andorra pel suport econòmic per a realitzar aquesta tesi doctoral i per haver apostat per la recerca biomèdica.

Malgrat que ha estat un camí difícil sé que en un futur miraré amb nostàlgia aquesta etapa i trobaré a faltar moltes coses. Trobar una cara familiar al passadís, escoltar el matinal de la ràdio a la sala de cultius, la sobretaula de dinar o capturar imatges al microscopi mentre escolto la Sotana o el Búnquer. M'agrada pensar que els bons records d'aquesta etapa perduraran per sobre de les angoixes passades.

INDEX

ABBREVIATIONS

ADCC	Antibody-dependent cell cytotoxicity
AK	Actinic keratosis
APC	Antigen-presenting cell
ARG1	Arginase 1
BafA	Bafilomycin A
BAFF	B Cell-activating factor
BCC	Basal cell carcinoma
BMDM	Bone marrow derived macrophage
BMDM PD	BMDM polarized with conditionate medium from mesenchymal EpCAM-SCC cells
BMDM WD	BMDM polarized with conditionate medium from full epithelial SCC cells
CAFs	Cancer-associated fibroblasts
CEACAM1	Carcinoembryonic antigen-related cell adhesion molecule 1
CIITA	Class II TransActivator
COX-2	Cyclooxygenase-2
CRC	Colorectal carcinoma
CRP	C reactive protein
cSCC	Cutaneous squamous cell carcinoma
CSCs	Cancer stem cells
CSFs	Colony stimulating factors
CTLA-4	Cytotoxic T-lymphocyte-associated molecule 4
CTLs	Cytotoxic T lymphocytes
DAB	3,3'-Diaminobenzidine
DAPI	4'6'-Diamidino-2-Phenylindole
DMBA	Dimethylbenzanthracene
EBV	Epstein-Barr virus
ECM	Extracellular matrix
EGFR	Epidermal growth factor receptor
EMA	European medicines agency
EMT	Epithelial-mesenchymal transition
EndMT	Endothelial-to-mesenchymal transition
ER	Endoplasmic reticulum
ERAD	Endoplasmic reticulum-associated degradation
FACS	Fluorescent activated cell sorter
FDA	Food and drug administration
FGL-1	Fibrinogen-like protein 1
FOXP3	Forkhead box protein P3
GAL-3	Galectin-3
GAL-9	Galectin-9
GAS	Gamma activated sequences
GFP	Green fluorescent protein
GFs	Growth factors
GzmB	Granzyme B
H/E	Hematoxylin and eosin
HCC	Hepatocellular carcinoma
HMGB1	High-mobility group protein 1
HNSCC	Head and neck squamous cell carcinoma
HPV	Human papillomavirus

HS	Horse serum
IC	Immune checkpoint
ICI	Immune checkpoint inhibitor
IF	Immunofluorescence
IFNGR1	Interferon gamma receptor 1
IFNGR2	Interferon gamma receptor 2
IFNs	Interferons
IFN-γ	Interferon-γ
IHC	Immunohistochemistry
IL	Interleukin
iNOS	Induction of nitric oxide synthase
irAEs	Immune-related adverse events
ISG	Interferon-stimulated genes
ISRE	Interferon sensitive response element
JAK1	Janus kinase 1
JAK2	Janus kinase 2
LAG-3	Lymphocyte activation gene-3
LPS	Lipopolysaccharide
mAbs	Monoclonal antibodys
MD/PD-SCCs	Moderate-differentiated/poorly-differentiated squamous cell carcinomas
MDSCs	Myeloid-derived suppressor cells
MET	Mesenchymal-epithelial transition
MHC-I	Major histocompatibility complex class-I
M-MDSCs	Monocytic myeloid-derived suppressor cells
M-MDSCs MD	Splenic M-MDSCs isolated from MD/PD-SCC-bearing mice
M-MDSCs PD	Splenic M-MDSCs isolated from PD-SCC-bearing mice
M-MDSCs WD	Splenic M-MDSCs isolated from WD-SCC-bearing mice
MMPs	Matrix metalloproteinases
MSI	Microsatellite instability
NK	Natural killer
NMSC	Non-melanoma skin cancer
NO	Nitric oxide
NOS2	Nitric oxide synthase 2
NOX-2	NADPH oxidase 2
NS	Not significant
NSCLC	Non-small cell lung cancer
ON	Overnight
ORR	Objective response rate
PARP	Poly (ADP-ribose) polymerase
PBS	Phosphate buffered saline
PD	Progressive disease
PDK	Pyruvate dehydrogenase kinase
PD/S-SCCs	Poorly-differentiated/spindle squamous cell carcinomas
PD-1	Programmed death receptor 1
PDAC	Pancreatic ductal adenocarcinoma
PDGF	Platelet-derived growth factor
PD-L1	Programmed death-ligand 1
PD-SCCs	Poorly-differentiated squamous cell carcinomas

PFA	Paraformaldehyde
PFS	Progression-free survival
PGE2	Prostaglandin E2
PI3K	Phosphoinositide 3-kinase
PMN-MDSCs	Polymorphonuclear myeloid-derived suppressor cells
PMN-MDSCs MD	Splenic PMN-MDSCs isolated from MD/PD-SCC-bearing mice
PMN-MDSCs PD	Splenic PMN-MDSCs isolated from PD-SCC-bearing mice
PMN-MDSCs WD	Splenic PMN-MDSCs isolated from WD-SCC-bearing mice
PMSF	Phenylmethanesulfonylfluoride
PS	Phosphatidylserine
qPCR	Quantitative polymerase chain reaction
RNS	Reactive nitrogen species
ROS	Reactive oxygen species
SCC	Squamous cell carcinoma
SD	Standard deviation
STAT1	Signal transducer and activator of transcription 1
TAMs	Tumor-associated macrophages
TANs	Tumor-associated neutrophils
TAP1	Transporter 1 ATP binding cassette subfamily B member
TAP2	Transporter 2 ATP binding cassette subfamily B member
TBS	Tris-buffered saline
TCR	T-cell receptor
TGFs	Transforming growth factors
TGF-β	Transforming growth factor β
Th-1	T-helper I
Th-17	T-helper 17
Th-2	T-helper II
TIGIT	T cell immunoglobulin and ITIM domain
TIM-3	T-cell immunoglobulin and mucin-domain containing-3
TMB	Tumor mutational burden
TME	Tumor microenvironment
TNFs	Tumor necrosis factors
TNF-α	Tumor necrosis factor α
TPA	12-O-tetradecanoylphorbol-13-acetate
Treg	T regulatory
UVR	Ultraviolet radiation
VEGF	Vascular endothelial growth factor
WD-SCCs	Well-differentiated squamous cell carcinomas

INTRODUCTION

1. CUTANEOUS SQUAMOUS CELL CARCINOMA (cSCC)

1.1 Structure of the skin

The skin is the outermost defense barrier of the body against environmental aggressions and external pathogens. The cellular organization of the skin ensures tissue homeostasis by maintaining a constant number of cells during tissue turnover or after acute injury. This process is accomplished by different populations of stem cells that reside in the skin epidermis, which present an enhanced ability to self-renew and differentiate into distinct cell lineages that will mature into adult tissue (Blanpain & Fuchs, 2009). A highly defined histological organization classifies the human skin into a three-layers tissue. From external to internal layers, the skin is composed of the epidermis, the dermis, and the hypodermis.

The epidermis is a stratified squamous epithelium formed by the interfollicular epidermis and associated structures such as the hair follicle, the sebaceous gland, and the sweat glands. The interfollicular epidermis is composed of several layers of keratinocytes in gradual stages of cell differentiation. In the basal layer, in direct contact with the basal lamina, which separates the epidermis and the dermis, more undifferentiated and proliferative cells are located. The suprabasal layers are the spinous layer, the granular layer, and the stratum corneum (Figure 1). Thus, as the keratinocytes of the basal layer differentiate, they move progressively through the suprabasal layers toward the surface of the epidermis, where they eventually shed (Solanas & Benitah, 2013).

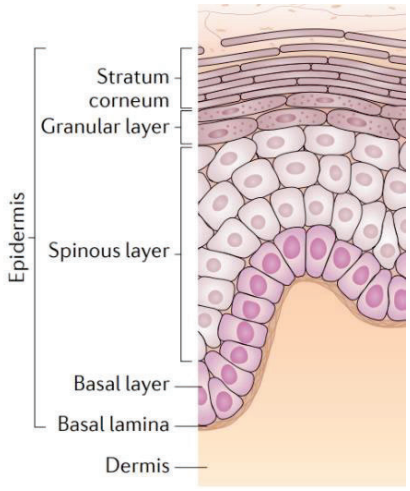

Figure 1. Histological organization of the human interfollicular epidermis. (Adapted from Solanas & Benitah, 2013).

The dermis is a connective tissue composed of collagen, elastin, and reticulin which give characteristic elasticity and flexibility to the skin. The major cellular components in the dermis are fibroblasts but blood vessels, lymphatic vessels, and nerves are also present. Underlying the dermis, the hypodermis layer is found and is characterized by being the thickest layer. Its main cellular components are adipocytes which actively participate in thermoregulation and homeostasis upon inflammatory processes.

Ageing results in structural changes in the skin concomitantly with increased incidence of skin infections and cancer. The epidermis thins, collagen, and elastin are fragmented and there is an altered immune infiltration (Chambers & Vukmanovic-Stejic, 2020). These alterations decrease skin immunity, increasing the susceptibility to experience pathogen infection and to develop cancer.

1.2 Generation of cSCC

Squamous cell carcinoma (SCC) of the skin or cutaneous SCC (cSCC) is the second most common form of non-melanoma skin cancer (NMSC) in humans and accounts for 20% of all NMSCs (Stratigos et al., 2015). The incidence of NMSC has increased in the past decades. Among other factors, this increase is related to poor use of sun protection and increased life expectancy given that NMSC incidence is based on lifetime exposure to risk factors (Lomas et al., 2012). Basal cell carcinoma (BCC), which is the most common form of NMSC, nearly does not cause metastatic lesions (1 case per 14 000 000) and, hence, its associated mortality rate is low. Oppositely, cSCC is characterized by a more aggressive growth and a greater capacity of developing metastases (0.1–9.9%) which cause the lead number of deaths by NMSC (Didona et al., 2018). Given its high prevalence and increased mortality rate in comparison to other NMSCs, cSCC is an increasing problem for health care worldwide.

The main risk factor of cSCC development is cumulative exposition to ultraviolet radiation (UVR), typically sun exposure (de Vries et al., 2012). Hence, elderly becomes a risk factor to present cSCC. In this sense, cSCCs are typically developed in sun exposed anatomic regions and are more frequent in advanced age populations (Fania et al., 2021). Other environmental risk factors consist of X-ray radiation (Karagas et al., 2007) and exposure to chemical agents such as arsenic (Wong et al., 1998). Additionally, risk factors include long inflammatory processes such as those seen in chronic wounds, burns, and ulcers. Immunosuppression, either by therapeutic use for allogenic organ transplantation, therapy of immune-related diseases, or defective skin immunity, is also a risk factor for cSCC appearance (Berg & Otley, 2002). Human papillomavirus (HPV) infection is associated with cSCC development in immunosuppressed patients. Specifically, HPV DNA has been more detected in immunosuppressed cSCC patients compared to immunocompetent cSCC patients indicating that HPV viral infection altogether with poor skin immunity can increase the risk of cSCC appearance (Harwood et al., 2000).

cSCCs are characterized by the uncontrolled proliferation of keratinocytes of the epidermis. The development of cSCC follows a multistage process of malignancy. Initially, the appearance of genetic mutations in keratinocytes due to continuous exposure to cSCC risk factors leads to local damage. Affected skin tissue loses its histological architecture leading to a process of increased keratinization (hyperkeratinization) known as actinic keratosis (AK). AKs are defined as

dysplastic keratinocytic lesions and are considered precancerous. Clinically, AKs can regress, persist as benign AK, or evolve into an invasive cSCC (Criscione et al., 2009). The rate of malignancy of AKs into carcinomas is small but mutations on key genes, as p53 or Ras, lead to expansion of AKs through the epidermis generating *in situ* carcinomas (also known as Bowen's disease) (Marks et al., 1988). Further accumulation of mutations and cellular events promotes the generation of invasive carcinomas characterized by uncontrolled tumor growth (Ratushny et al., 2012). Invasive carcinomas, also referred to as cSCC, can migrate reaching blood and lymphatic vessels, disseminating, and eventually generating metastases in distant organs (Figure 2). Most cSCCs arise from AKs (~97%) despite some *de novo* cSCCs can arise without AK phase. These can be identified by a different histology and are clinically considered more aggressive (Yanofsky et al., 2011). cSCC presents impaired genomic repair that allows rapid acquisition of mutations, as observed with other cancers. In cSCC, UVR-induced inactivation of p53 favoring the genomic instability of keratinocytes.

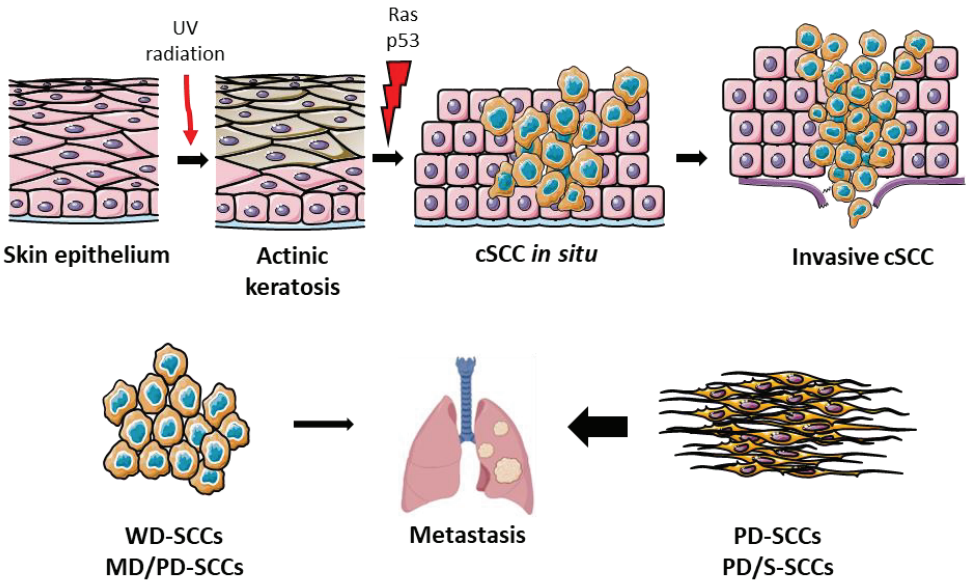

Figure 2. Schematic representation of stages of progression of skin squamous cell carcinomas. The development of SCCs presents a multistage process. After an external stimulus such as ultraviolet radiation (UVR), the skin epithelium can develop actinic keratosis (AK) which can present genetic alterations such as mutations in Ras or p53 causing keratinocytes to start an uncontrolled proliferation giving rise to *in situ* carcinomas. These *in situ* carcinomas can progress towards invasive carcinomas. Most invasive carcinomas conserve epithelial differentiated traits and are classified as well-differentiated (WD-SCCs) or moderate-differentiated/poorly-differentiated SCCs (MD/PD-SCCs). However, some tumors lose epithelial-differentiation features and acquire mesenchymal traits, which are classified as poor-differentiated SCCs (PD-SCCs) or eventually poorly-differentiated/spindle (PD/S-SCCs) and are associated with enhanced recurrence and metastasis.

Invasive cSCC can be graded into four groups depending on their histopathological characteristics. Most of them preserve epithelial differentiation traits and are named well-differentiated SCCs (WD-SCCs). WD-SCC cells exhibit epidermic characteristics with increased keratinization levels and are characterized by presenting big cytoplasmic regions. Secondly, moderate-differentiated/poorly-differentiated SCCs (MD/PD-SCCs) show an increased structural disorder and preserve fewer epithelial characteristics than WD-SCCs. WD-SCCs and MD/PD-SCCs present low frequency of metastasis and good prognosis despite being highly prevalent (Alam & Ratner, 2001). Next, poorly-differentiated SCCs (PD-SCCs) have lost the epithelial differentiation state. These tumors present elongated cells, with pleomorphic nuclei and frequent mitoses. Finally, a rare subtype of cSCCs called poorly-differentiated/spindle SCCs (PD/S-SCCs) are characterized by being completely anaplastic, with a total loss of epithelial differentiation traits that can reach a sarcomatoid spindle cell stage (Evans & Smith, 1980). PD-SCCs and PD/S-SCCs are very relevant in the clinic since they present rapid tumor growth and high frequency of disease recurrence and metastasis that leads to poor patient prognosis (Brantsch et al., 2008) (Brinkman et al., 2015).

1.3 Treatment of cSCC

The prognosis of patients with cSCC is typically good, with a 10-year curation rate of ~89% of patients (Schmults et al., 2013). However, cSCC patients with local recurrences (5-8%) and metastatic disease (3-5%) show a poor prognosis. Recurrent cSCCs present an increased aggressiveness and metastatic capacity (Alam & Ratner, 2001). Around ~87% of metastasis derived from cSCCs are located in lymph nodes, and the remaining metastases are found in distant organs such as the lungs, liver, and brain (Brougham et al., 2012).

The diagnosis of cSCC is based on clinical features including biopsy or excisions and histological confirmation of cutaneous suspicious lesions. The applied treatment to cSCC varies depending on the tumor characteristics such as location, size, and level of invasiveness. The first line of treatment for cSCCs consists of surgical excision with histopathological control of excision margins by post-operative pathologic conventional histology or Mohs micrographic surgery (Stratigos et al. 2015). However, surgery is contra-indicated for patients with tumors located in difficult resection areas, elderly patients, or large tumors. For these patients, radiotherapy and chemotherapy agents (cisplatin, 5-fluorouracil, among others) can be given but have shown poor clinical benefits (Franco et al., 2013). In addition, 5-8% of patients treated with surgery develop recurrences giving rise to locally advanced and metastatic cSCC that are more aggressive than the primary tumor. These recurrent cSCCs can also be treated with radiotherapy and chemotherapy but have also shown low response rates.

Recently, the food and drug administration (FDA) and the European medicines agency (EMA) have approved immunotherapy based on immune checkpoint (IC) inhibitors (ICI) to treat advanced and metastatic cSCCs. Specifically, two monoclonal antibodies (mAbs) against the IC receptor programmed death receptor 1 (PD-1) have proven efficacy to induce a response among patients with advanced cSCC. PD-1 is a receptor present on the surface of T lymphocytes that has a role in downregulating the immune response and preserving self-tolerance. Upon binding to its ligand programmed death-ligand 1 (PD-L1), which is upregulated in multiple tumor types, PD-1 downmodulates T cell cytotoxic activity. PD-1 biological relevance will be further discussed in section 4.1.2. Firstly, the mAb anti-PD-1 cemiplimab showed efficacy in a cSCC metastatic-disease cohort in phase II trials (NCT02383212 and NCT02760498). The objective response rate (ORR), defined as the percentage of patients in a study showing a partial or complete response in a certain time period, of cemiplimab treatment was ~47%. The estimated probability of progression-free survival (PFS) at 12 months, which is the percentage of patients that after the treatment lives with the disease, but it is not worsening, was ~53%. Finally, progressive disease (PD), which measures the percentage of patients presenting cancer that is still growing, spreading, and worsening, affected ~19% of patients (Migden et al., 2018). Similar results were obtained by the treatment of recurrent or metastatic cSCC with the mAb anti-PD-1 named pembrolizumab in the phase II trial (KEYNOTE-629). The ORR of pembrolizumab was ~34%, the PFS estimated probability at 12 months was ~32% and PD affected ~28% of patients (Grob et al., 2020). Despite the initial promising results of ICI, only a subset of patients can benefit from these therapies. Hence, it is necessary to understand the mechanisms that lead advanced and metastatic cSCC to present an incomplete response to ICI to further improve their responsiveness.

1.4 Mouse model of cSCC progression

The study of cSCC biology has been limited by the experimental models used. In order to study the development of cSCC, a chemical carcinogenesis mouse model can be a useful tool. Mice are treated topically with the carcinogenic agent dimethylbenzanthracene (DMBA), which serves as a tumor initiator. Next, tumor promotion is induced by continuous treatment with 12-O-tetradecanoylphorbol-13-acetate (TPA). Mouse cancer models obtained by this approximation are known as two-stage carcinogenesis models. Mouse cSCC models obtained by DMBA/TPA-treated mice have shed light on the process of skin carcinogenesis (P. Y. Huang & Balmain, 2014).

Another possibility to study cSCC biology is the use of genetically modified mice. In this sense, the mouse model K14-HPV16 (keratin 14 – human papillomavirus 16) develops hyperplastic and dysplastic lesions that progress to malignant cSCC (Coussens et al., 1996). HPV infection is involved in the generation and development of SCC malignancies (Lowy et al., 1994). Specifically, HPV16 expresses the E6 and E7 oncoproteins, responsible for inactivating p53 and

the retinoblastoma protein respectively, which are implicated in the control of the cell cycle and cell death. In the case of K14-HPV16 transgenic mice, the oncoproteins E6 and E7 are expressed under the promoter of the keratin 14. Hence, basal keratinocytes of squamous epithelium, which are characterized by expressing keratin 14, also expressed E6 and E7 oncoproteins leading to the appearance of cutaneous dysplastic lesions. After one year, the development of cSCC was observed in 20-30% of K14-HPV16 transgenic mice depending on the mouse genetic background, and generated cSCCs presented distinct grades of differentiation (Coussens et al., 1996).

The described mouse models of cSCC only permit the study of cSCC at a unique progression step while it is known that cSCC presents a multistage development resulting in the formation of invasive tumors (DiGiovanni, 1992). Given this limitation, our group created a mouse model of cSCC progression to study the molecular mechanisms implicated in this malignant process. To this end, K14-HPV16 transgenic mice were treated with carcinogenic agents DMBA and TPA to promote the appearance of cSCCs. Small fragments of spontaneous or chemically induced tumors were implanted subcutaneously in the back of nude mice. When tumors reached a critical size, were removed and a small fragment was serially engrafted in a new immunodeficient mouse during several passages (da Silva-Diz et al., 2016). This process allowed an unlimited growth of cSCC and the generation of different lineages (Figure 3).

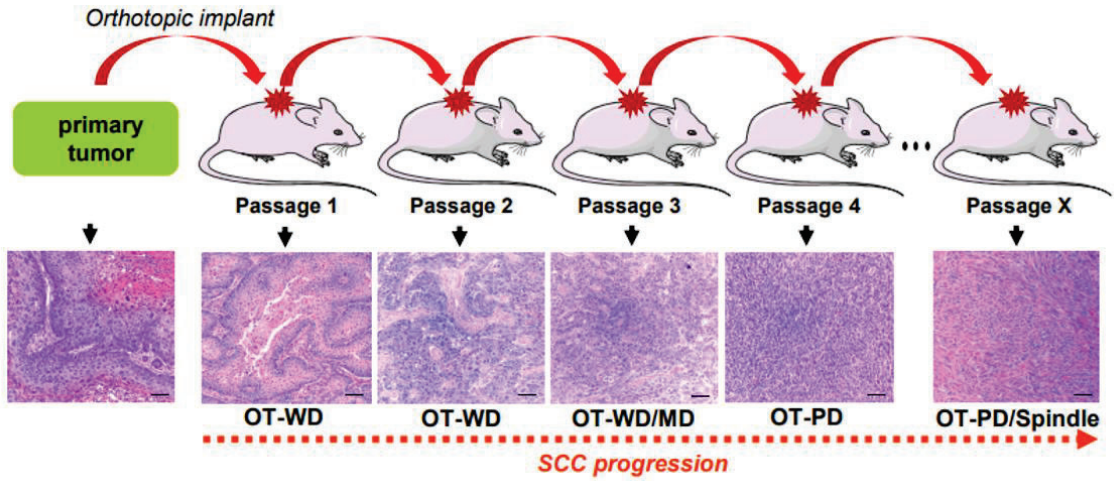

Figure 3. Schematic representation of the process to generate orthotopic cSCC lineages. Spontaneous or chemical-induced (DMBA/TPA treatment) cSCCs generated in K14-HPV16 mice were serially engrafted in immunodeficient mice allowing tumor progression. After several passages, WD-SCCs progressed to PD-SCCs allowing the generation of cSCC lineages and their posterior molecular and cellular study. From da Silva-Diz et al., 2016.

Primary cSCCs obtained after DMBA/TPA treatment in K14-HPV16 mice mostly showed epithelial-like traits while spindle tumors only represented ~5% of the tumors. After the first engraftment, tumors recapitulated the histopathological conditions of the parental tumors. Nevertheless, after serial engraftment over multiple passages, ~62% of WD-SCCs, showing

epithelial traits progressed to MD/PD-SCCs, which evolved to PD-SCCs displaying mesenchymal-like features and finally advanced to PD/S-SCCs, which present spindle-shaped characteristics (da Silva-Diz et al., 2016). Hence, our group concluded that PD-SCCs and PD/S-SCCs are generated through the malignant progression of WD-SCCs. The characterization of these lineages showed that PD/S-SCCs grew faster and had an increased frequency of metastasis in comparison to WD-SCCs. In addition, PD-SCCs compared to WD-SCCs presented an increased presence of tumor-initiating cells or cancer stem cells (CSCs) identified by the co-expression of the molecular markers α6-integrin and CD34, which are markers of hair follicle stem cells (R. J. Morris et al., 2004). Finally, tumor cells from PD/S-SCCs presented downregulated expression of EpCAM and E-cadherin (epithelial-like markers) and upregulated expression of vimentin (mesenchymal-like marker) and epithelial-mesenchymal transition (EMT)-inducing transcript factors (da Silva-Diz et al., 2016). So, enhanced EMT features, and aggressive growth and metastatic capability were characterized in cSCC progression.

Specifically, the EMT is a reversible process that allows an epithelial polarized cell to acquire a mesenchymal phenotype. During EMT activation, epithelial cells lose cell-cell interactions and apical-basal polarity, suffer reorganization of the cytoskeleton, and start expressing extracellular matrix (ECM) degrading enzymes, which facilitates cell migration. In addition, under the EMT program, epithelial cells acquire mesenchymal features such as increased migratory and invasive capacity, and resistance to apoptosis. The induction of the EMT program is observed under physiological conditions during embryogenesis and wound healing. However, the EMT program is also tightly linked to tumor progression and metastasis (Kalluri & Weinberg, 2009). The metastatic potential of tumors has been linked to the loss of epithelial markers, such as E-cadherin, and the acquisition of mesenchymal markers, such as Vimentin, N-cadherin, and Fibronectin (Thiery et al., 2009). The EMT process is mediated by the activation of various transcription factors such as SNAIL, SNAI2, TWIST, ZEB1, and ZEB2 which are referred to as EMT-inducing transcription factors. Initially, the EMT program was considered as the switch between two final states (epithelial *vs.* mesenchymal). However, it was demonstrated that cells oscillate between these two states through hybrid/intermediate states induced by partial activation of the EMT program. In these hybrid/intermediate states tumor cells retain the epithelial phenotype and at the same time express mesenchymal markers (Chaffer et al., 2016) (da Silva-Diz et al., 2018). Importantly, partial EMT and the presence of intermediate states in tumor cells have been linked to poor patient prognosis and decreased survival in HNSCCs (Pal et al., 2021), in SCCs including cSCC, HNSCC, esophageal SCC, and cervical SCC (Liao et al., 2021), and breast cancer (Yamashita et al., 2018). Some studies indicate that after dissemination, tumor cells must reverse their mesenchymal state to endow colonization and growth of metastatic lesions in distant organs. This process is known as mesenchymal-epithelial transition (MET) and typically involves the

repression of EMT-transcription factors. These findings have also been observed for cSCC metastasis, where it was shown that the transcription factor Twist1 promotes EMT but once disseminated tumor cells had arrived at distant organs the inactivation of Twist1 and EMT was essential to proliferate and metastasize (Tsai et al., 2012).

More recently, our group demonstrated that during cSCC progression, SCC cancer cells can acquire a strong plasticity defined as the ability to progress from an epithelial to a mesenchymal-like state undergoing a progressive EMT. Specifically, epithelial cancer cells from MD/PD-SCCs show a plastic phenotype primed to switch to mesenchymal-like cancer cells, which later progress to a full mesenchymal state. In this sense, epithelial plastic $EpCAM^{+}$ SCC cells isolated from MD/PD-SCCs can be classified into $EpCAM^{high}$ SCC cells or plastic $EpCAM^{low}$ SCC cells depending on their EpCAM expression. $EpCAM^{high}$ SCC cells can lose epithelial differentiation traits becoming $EpCAM^{low}$ SCC cells, which can finally progress to $EpCAM^{-}$ mesenchymal-like SCC cells. Both plastic $EpCAM^{high}$ and plastic $EpCAM^{low}$ SCC cells show strong plasticity, can lose epithelial traits, and induce the expression of mesenchymal markers such as vimentin and EMT-inducing transcription factors, finally resulting in the progression to mesenchymal-like SCC cells. These events are induced during *in vivo* cSCC growth, indicating that TME-derived signals regulate the acquisition of mesenchymal-like features (López-Cerda et al, unpublished results).

2. HEAD AND NECK SQUAMOUS CELL CARCINOMA (HNSCC)

2.1 Generation of HNSCC

Head and neck SCC (HNSCCs) are a group of heterogeneous tumors originating in the mucosal epithelium of the oral cavity, pharynx, larynx, and sinonasal tract. HNSCC stands for ~90% of head and neck cancers and is the sixth most common cancer with an increasing incidence worldwide (Ferlay et al., 2019). The 5-year survival expectancy of HNSCC patients is approximately ~66% (Pulte & Brenner, 2010). HNSCCs are mainly caused by tobacco and alcohol consumption or infection with HPV16. Consequently, HNSCCs can be ranked into HPV-negative and HPV-positive HNSCCs, having this last subgroup a better prognosis. While HPV-negative HNSCCs are mainly associated with oral cavity and larynx cancers, HPV-positive HNSCCs are typically pharynx cancers (Johnson et al., 2020). Given its high prevalence, the management of HNSCCs represents a global healthcare challenge.

Development of HNSCC has been tightly linked to the exposition of individuals to various risk factors including tobacco consumption, continuous alcohol intake, exposure to environmental pollutants, or viral infection with HPV or Epstein-Barr virus (EBV). Some of these risk factors present different prevalence depending on the gender or cultural habits such as smoking or high alcohol intake. HPV infection that causes HNSCC is typically transmitted by oral sex in the not vaccinated population and is more common in men (Gillison et al., 2008).

Transformed mucosal epithelial cells from the oral cavity, pharynx, and larynx originate HNSCCs. The heterogeneous nature of HNSCCs is explained by the specific anatomical location of the cell of origin. The histological progression to invasive HNSCCs follows a multistage process similar to cSCC. This process begins with epithelial cell hyperplasia (enlargement of tissue by cell proliferation), continued by dysplasia (abnormal growth or development of cells) that can advance towards a carcinoma *in situ* that ultimately results in the appearance of invasive carcinoma (Figure 4). Specific genetic alterations occur in each stage. These genetic modifications typically cause the inactivation of suppressor genes *CDKN2A* and *TP53* in the early stages of HNSCC progression and *phosphatase and tensin homolog* (*PTEN*) at later stages (Johnson et al., 2020). The initiating and early events of HPV-negative HNSCC are caused by the carcinogenic agents present in tobacco smoke including nitrosamines, benzopyrene, and polycyclic aromatic hydrocarbons. These carcinogens, and their derived metabolites, can form DNA adducts leading to genetic mutations. Alcohol consumption synergizes with tobacco to promote carcinogenesis by solving carcinogens (Pai & Westra, 2009). For HPV-positive HNSCCs, the initiating event is infection with HPV, mainly HPV16. In HNSCC cells, the HPV genome is usually integrated at a single genomic site. The genome of HPV consists of seven early genes (E1-E7) and two late genes (L1 and L2). E1-E5 genes encode proteins for viral replication and transcription while L1 and L2 genes encode the viral capsid proteins. E6 and E7 proteins are responsible for promoting the oncogenic transformation as described in section 1.4.

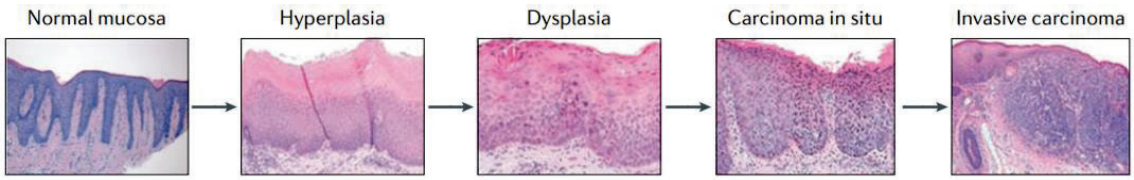

Figure 4. Stages of progression of HNSCC. The mucosal epithelium from the oral cavity, pharynx, and larynx is the location of origin of HNSCC. HNSCC progression follows a histological order that begins with mucosal hyperplasia, followed by dysplasia, the appearance of carcinomas *in situ* that finally transforms into invasive carcinomas. From Johnson et al., 2020.

2.2 Treatment of HNSCC

The diagnosis of HNSCC is done by histopathological analysis of the primary tumor. The histopathological range of HNSCC is characterized by cellular origin and squamous differentiation. Well-differentiated HNSCCs resemble stratified epithelium with cells organized in layers and irregular levels of keratinization are found. Poorly differentiated HNSCCs are characterized by loss of organized stratification and keratinization. Most HPV-negative HNSCCs are well-differentiated while HPV-positive HNSCCs are commonly poorly differentiated. HPV infection is analyzed in all oropharyngeal tumors. Next, HNSCCs are staged to determine the

anatomical origin. The median age of diagnosis for HPV-negative HNSCCs is ~66 years while for HPV-positive HNSCCs is ~53 years (Windon et al., 2018).

Given the high heterogeneity of HNSCCs, the treatment of every patient is determined by the anatomical site, stage, and tumor characteristics. The first line of treatment includes resection, radiation, and systemic therapy in the highest curative combination. Small primary HNSCCs are treated by resection or radiation. For oral cavity tumors, surgery is recommended while pharyngeal and laryngeal tumors are commonly treated with radiation. These therapies can be combined with the use of chemotherapy like cisplatin or targeted therapies such as epidermal growth factor receptor (EGFR) inhibitors (Johnson et al., 2020). In 2016, for the treatment of recurrent and metastatic HNSCC, the FDA and the EMA approved the use of the ICI pembrolizumab and nivolumab, which block PD-1 function. These therapies are given to patients presenting PD-L1^{+} expressing tumors. Since 2019, immunotherapy based on ICI is also the first line of treatment for unresectable or metastatic HNSCCs. A phase 3 study (KEYNOTE-048) of pembrolizumab efficacy to treat recurrent or metastatic HNSCC showed an ORR of ~23%, median overall survival of ~15 months, and did not improve PFS (Burtness et al., 2019). Another phase 3 clinical trial (NCT02105636) analyzed the efficacy of nivolumab treatment in recurrent and metastatic HNSCC. This study concluded that nivolumab treated patients presented an ORR of ~13%, median overall survival of ~8 months, and also did not improve PFS (Ferris et al., 2016). These results pinpoint that uniquely a subset of patients suffering recurrent and metastatic HNSCCs benefit from immunotherapy. It is necessary to understand why some recurrent and metastatic HNSCCs do not respond to ICI to further enhance the response and duration of these therapies.

3. TUMOR MICROENVIRONTMENT (TME)

3.1 Definition of the tumor microenvironment (TME)

The tumor microenvironment (TME) is composed by the ensemble of host cells, molecular components, and blood vessels forming the tumor that are not strictly cancer cells. A reciprocal interplay between tumor cells, and the TME exists. Tumor cells can modulate the microenvironment and the TME directly affects tumor growth, aggressiveness, and metastatic capabilities. Intercellular communication between the TME and tumor cells is a complex framework that includes growth factors, cytokines, chemokines, exosomes, and cell-free DNA, among other mechanisms that are recently emerging (Baghban et al., 2020). Exploiting the mechanisms that regulate the interplay between the TME and tumor cells can be useful as a novel strategy to develop and increase the efficacy of therapeutic interventions against cancer. Initially, it was thought that exclusively targeting the TME might represent an approach for any cancer. However, the complexity of the TME function has hindered this approach (Xiao & Yu, 2021).

Depending on the tumor type, stage of progression, cellular, and molecular characteristics the TME can present tumor-suppressive activities or a tumor-supporting role (Quail & Joyce, 2013) (Salmon et al., 2019). Multiple strategies targeting the TME have been developed with different degrees of efficacy including depletion of tumor-supporting infiltrating cells or transformation towards an anti-tumor suppressive profile (Bejarano et al., 2021). Finally, the TME composition has been linked to acquired resistance to standard-of-care anticancer treatments such as chemotherapy and radiotherapy or TME-targeting therapies (Khalaf et al., 2021) (Klemm & Joyce, 2015).

3.1.1 Cellular components of the TME

The cellular content of the TME differs between tumor types (S. Cheng et al., 2021) (H. Luo et al., 2022) (Zheng et al., 2021). Nonetheless, common cellular components that can be found in the TME include stromal fibroblasts, immune cells, endothelial cells, and pericytes.

Activated stromal fibroblasts located in the TME are known as cancer-associated fibroblasts (CAFs) and can support tumor growth through several processes. CAFs are a heterogenous population that results from the expansion of local resident fibroblasts and/or the interconversion of endothelial cells, pericytes, and adipocytes (Ping et al., 2021) (Xing et al., 2010). Consequently, CAFs do not express a common surface marker. Diverse mechanisms promote CAFs activation such as transforming growth factor β (TGF-β) signaling, inflammatory signals, physiological stress, DNA damage, and Notch signaling. Once fibroblasts are activated in the tumor context, become more proliferative and can facilitate tumor growth and invasiveness. CAFs secrete soluble factors including the vascular endothelial growth factor (VEGF) which promotes angiogenesis (B. Huang et al., 2019). Most ECM proteins and components are secreted by CAFs, which orchestrate tumor architecture. Hence, CAFs are directly related to tumor aggressiveness and metastasis through remodeling ECM. In addition, the structure of ECM also influences drug delivery and therapy response. CAFs directly interplay with other cell types infiltrating the TME including immune cells by secreting cytokines and chemokines like interleukin (IL)-6, CXCL12, and CCL2 (Xiang et al., 2022). Furthermore, metabolic effects derived from CAFs have been observed in the TME. CAFs promote amino acid depletion which interferes with adaptive immunity against tumor cells and the appearance of lactate inducing a more acidic TME which has been linked to tumor growth (Sahai et al., 2020).

Immune cells from the innate and adaptive immune systems are also recruited in the TME. The innate immunity function is the first defense against pathogens and is composed of multiple immune cell types including macrophages, neutrophils, natural killer cells, and dendritic cells. This last immune population works as the link between the innate and adaptive immune systems. Adaptive or acquired immunity learns and remembers specific antigens from pathogens providing

long-term defense. This immunity includes the immune populations of dendritic cells, $CD4^+$ T helper lymphocytes, $CD8^+$ T cytotoxic lymphocytes, and B lymphocytes. Tumor-infiltrating immune cells play a key role in tumor progression and therapy response and will be discussed in detail in section 3.2.

Endothelial cells are responsible for regulating and forming blood vessels in the tumor ensuring O_2 and nutrients supply in a process named angiogenesis. Specifically, endothelial cells form a single cell layer around blood vessels controlling the flow of fluid into a tissue. CD34 is selectively expressed in vascular endothelial cells and serves as a molecular marker to identify this cell population. At the initial stages, tumor development relies on passive diffusion for nutrients and O_2 transport. Once tumors reach a critical size tumor metabolism causes a hypoxic and acidic TME (Boedtkjer & Pedersen, 2020). At this point, hypoxia-induced factors promote vessel development by endothelial cells. In this process, endothelial cells secrete platelet-derived growth factor (PDGF) and VEGF that stimulates the formation of new blood vessels. Blood vessels generated in the TME are immature and lack strong cell-to-cell attachments enabling cancer cells to transverse and disseminate (Sobierajska et al., 2020). Endothelial cells also affect immune cell infiltration and stromal fibroblast rearrangement. In addition, endothelial cells can undergo a transition known as endothelial-to-mesenchymal transition (EndMT) where endothelial cells are able to convert to fibroblasts in response to external stimuli such as TGF-β (van Meeteren & ten Dijke, 2012) (Wermuth et al., 2017). Hence, it has been reported that endothelial cells are a source of CAFs (Zeisberg et al., 2007) (Potenta et al., 2008). Pericytes are mural cells that situate around endothelial cells in the capillaries. Pericytes concomitantly with endothelial cells regulate the formation of blood vessels and vascular permeability and are also found within the TME (R. Sun et al., 2021). Pericytes are involved in tumor angiogenesis and regulate immune cells recruitment to the TME by secreting cytokines and chemokines. It has been reported that pericytes secrete IL-33 (Y. Yang et al., 2016), CXCL12 (Asada et al., 2017), and CECR1 (C. Zhu et al., 2017) resulting in the recruitment of immunosuppressive cells.

3.1.2 Non-cellular components of the TME

Non-cellular components of the TME include the ECM, exosomes, circulating free DNA, and apoptotic bodies (Baghban et al., 2020). Additionally, soluble molecules such as cytokines, chemokines, growth factors, and metabolites are present in the TME establishing a complex signaling network (Labani-Motlagh et al., 2020). Recent evidence points out that soluble molecules can promote tumor progression and modulate response to therapy. Hence, in certain tumors, soluble molecules present in the TME might actively support cancer development (W. Huang et al., 2018).

The ECM provides the physical structure of tumor cells and cellular components of the TME. It is composed of fibrous proteins (collagen and elastin), glycoproteins (fibronectin and laminin), proteoglycans (heparan sulfate), and glycosaminoglycans (hyaluronic acid). CAFs are the major supplier of components of the ECM but other cells participate in building and modeling the ECM. Matrix metalloproteinases (MMPs) are enzymes responsible for degrading the ECM proteins which allow the remodeling of ECM, promoting tumor growth and metastasis (Kessenbrock et al., 2010). Dynamic crosstalk mediated by cytokines, growth factors, and soluble molecules occurs in the ECM. In addition, drug delivery is affected by the composition of the ECM. Of high relevance is the role of collagen within the TME since it is the most abundant component and contributes to cancer fibrosis. Collagen synthesis can be regulated by tumor cells and can affect tumor cell behavior by altering integrins and tyrosine kinases signaling (S. Xu et al., 2019).

3.2 Tumor-infiltrating immune cells

The tumor immune microenvironment is composed of the immune cells that are recruited within the tumor and its periphery. Depending on the presence and the location of specific immune cell populations, tumors can be classified into immune-desert, immune-excluded, and immune-inflamed phenotypes (Figure 5), some of them associated with poor therapy response (Binnewies et al., 2018). Immune-inflamed tumors are referred to as “hot tumors” while immune-desert tumors and immune-excluded are considered to be “cold tumors” (Y.-T. Liu & Sun, 2021).

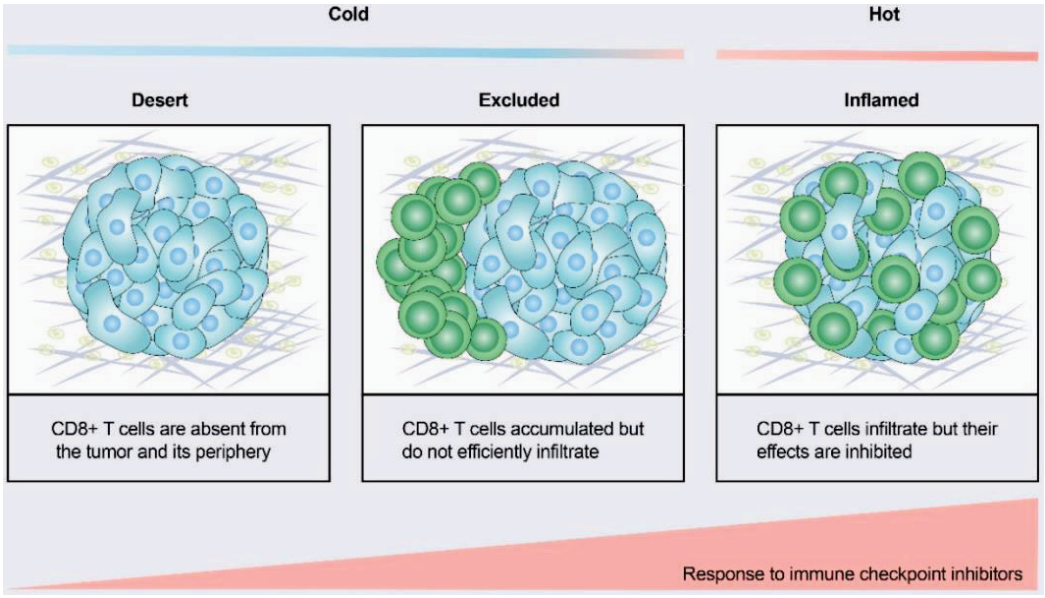

Figure 5. Tumor immune microenvironment classification. According to $CD8^+$ T cell infiltration, tumors can be classified as immune-desert, immune-excluded, and immune-infiltrated/inflamed. In immune-desert tumors, $CD8^+$ T cells cannot be found either in the tumor core or the periphery. In immune-excluded tumors, $CD8^+$ T cells accumulate in the periphery but cannot enter the tumor core. In immune-inflamed tumors, $CD8^+$ T cells can infiltrate inside the tumor core. From Liu & Sun, 2021.

In immune-desert tumors, $CD8^+$ T cells are not recruited into the tumor core, the periphery of the tumor, or the stroma while in immune-excluded tumors, $CD8^+$ T cells are restricted along the border of the tumor mass or in the stroma but cannot enter inside the tumor core. This is relevant since activated $CD8^+$ T cells can identify and eliminate tumor cells by establishing proximal contact. Specifically, T-cell receptors (TCRs) of $CD8^+$ T cells need to recognize peptides presented by the major histocompatibility complex class-I (MHC-I) of tumor cells. Hence, in immune-excluded tumors, despite $CD8^+$ T cells presenting a close location to the tumor, they are not able to identify tumor cells. These cold tumors are characterized by low MHC-I expression, low mutational load making the tumor cells less immunogenic, and low PD-L1 expression which is a protein involved in the inhibition of $CD8^+$ T cell function (see details in section 4.1.2). The presence of immunosuppressive cells, including myeloid-derived suppressor cells (MDSCs), M2-like macrophages, and T regulatory (Treg) cells, also inhibit $CD8^+$ T cell function and are thought to be responsible to prevent $CD8^+$ T cell intratumor infiltration (Beatty et al., 2015). Immune-excluded phenotypes have been observed in various epithelial-derived cancers such as melanoma (Herbst et al., 2014), colorectal carcinoma (CRC) (Mlecnik et al., 2016), and pancreatic ductal adenocarcinoma (PDAC) (Ademmer et al., 1998) and have been linked to lack or poor response to IC blockade immunotherapies.

Immune-inflamed tumors are characterized by a high infiltration of $CD8^+$ T cells into the tumor allowing proximal contact with tumor cells. These tumors are characterized by increased PD-L1 expression, high tumor mutational burden (TMB) making tumor cells more immunogenic, and enhanced interferon-γ (IFN-γ) signaling which is a marker of cytotoxic activity by $CD8^+$ T cells. Tumors that presented an immune-inflamed profile are more responsive to immunotherapy based on ICI (Galon & Bruni, 2019). Of note, the immune microenvironment of a tumor can be heterogenous containing sites with different phenotypes that may evolve with disease progression and in response to therapeutic interventions (Bindea et al., 2013). Given its predominant role in therapy response, modulating the immune cell infiltration to “fire up” the TME has been tested to improve the response of immunotherapies based on ICI (Duan et al., 2020) (Roma-Rodrigues et al., 2019). However, limited benefits have been observed in particular tumor conditions which are probably explained by the complex microenvironment context and the high heterogeneity within the TME.

3.2.1 Effector immune cells

Activated $CD8^+$ T cells, also known as cytotoxic T lymphocytes (CTLs), and natural killer (NK) cells are effector immune cells characterized by the ability to identify and eliminate tumor cells. $CD8^+$ T cells participate in adaptive immunity while NK cells form part of innate immunity. Cytotoxicity arises by Perforin and Granzyme B (GzmB) lysis, and despite $CD8^+$ T cells and NK

cells act mechanistically in a similar way, these cell populations identify target cells by different processes. Importantly, the activity of CTLs and NK cells is tightly controlled by the balance of positive and negative signals upon detecting a target cell in order to ensure self-tolerance and homeostasis. An unprecise controlled activity of effector immune cells has been related to severe autoimmune events (Walter & Santamaria, 2005) (Zitti & Bryceson, 2018).

Activated $CD8^+$ T cells are lymphocytes of the acquired immune system that can recognize and target viral infected and malignant tumor host cells. CTLs express TCRs that interact with peptides presented through the MHC-I complex by nucleated cells. Through the interaction between TCR and MHC-I, CTLs can identify and eliminate malignant host cells that express viral or oncogenic antigens. Each immature $CD8^+$ T cell in a naïve state expresses a different TCR and only become activated when interacting with dendritic cells, which are professional antigen-presenting cells (APCs). DCs carry viral or oncogenic antigen that matches the TCR of the immature $CD8^+$ T cell. To become completely functional, the costimulatory receptor CD28 expressed by $CD8^+$ T cells must interact with their ligands CD80 and CD86 expressed by APCs. Once an activated $CD8^+$ T cell detects an antigen through the TCR, the $CD8^+$ T cell is expanded and eliminates the antigen-expressing host cell secreting perforin and GzmB (Raskov et al., 2021). Phenotypically, mouse CTLs can be detected by the co-expression of the marker CD3 and CD8.

NK cells are cytotoxic lymphocytes of the innate immune system with the ability to recognize and eliminate stressed host cells in the absence of antigen presentation by MHC-I. NK cells express multiple activator and inhibitory receptors that allow them to identify cell surface markers of stress. In addition, the lack of expression of MHC-I promotes the cytotoxic activity of NK cells. The final balance between positive and negative signals activating NK cells that can sense through multiple receptors allows them to eliminate host cells that present cellular stress, or malignancy such as tumor cells (Myers & Miller, 2021) (Shimasaki et al., 2020). In the tumor context, NK cells present a complementary role to $CD8^+$ CTLs since NK cells are in charge of eliminating tumor cells lacking MHC-I expression. Mechanistically, once NK cells have been activated, they release perforin and GzmB to eliminate the target cell. Phenotypically, mouse NK cells can be detected by the expression of NK marker NK1.1 together with the lack of expression of CD3.

To ensure self-tolerance and homeostasis, CTLs and NK cells peripheral activity is closely controlled. In physiological conditions, the release of immunosuppressive molecules by Treg cells, M2-like macrophages, and MDSCs dampens CTLs and NK cells cytotoxic activity in inflammation and infection situations (Gabrilovich & Nagaraj, 2009) (R. Kim et al., 2006). Furthermore, activated CTLs and NK cells express IC receptors, which are mostly inhibitory receptors that dampen the cytotoxic activity of effector immune cells upon binding to their IC ligands and will be discussed in detail in section 4.1.

3.2.2 Tumor-associated macrophages (TAMs)

Macrophages are differentiated myeloid cells originating from monocytic precursors that eliminate infectious agents by phagocytosis, regulate adaptive immunity by antigen presentation, and participate in tissue repair. According to their polarization state and functional role, macrophages can be classified into classically activated or M1 macrophages, and alternatively activated or M2 macrophages. M1 macrophages are activated by T-helper I (Th-1) cells derived cytokines and/or pathogen components such as lipopolysaccharide (LPS). M1-like macrophages secrete pro-inflammatory cytokines including tumor necrosis factor α (TNF-α), IL-1β, and IL-6 among others. On the other side, M2 macrophages are activated by T-helper II (Th-2) derived cytokines and present an immunosuppressive profile. M2-like macrophages secrete immunosuppressive cytokines such as IL-4, IL-10, and IL-13, express the enzyme Arginase 1 (ARG1), and produce VEGF and MMPs facilitating tumor malignancy (Yunna et al., 2020). Specifically, macrophages recruited to the tumor site are known as tumor-associated macrophages (TAMs) and can present pro-tumorogenic or anti-tumorogenic functions. While M1-like TAMs mainly present a tumoricidal function, M2-like TAMs promote tumor progression (B.-Z. Qian & Pollard, 2010) (J. Liu et al., 2021). Despite both M1 and M2 macrophages can be found infiltrating a tumor, the TME can promote the polarization towards an M2-like profile through hypoxia and cytokines such as IL-4. In addition, the M1/M2 nomenclature has been proven to be simplistic and it is currently known that macrophages can change their polarity in response to external stimuli presenting intermediate phenotypes (S. K. Biswas & Mantovani, 2010) (Martinez & Gordon, 2014). Phenotypically, murine macrophages can be identified by the expression of CD11b and F4/80 markers. M2-like macrophages also express CD206 and CD163 while M1-like macrophages do not express these markers.

Immunosuppressive M2-like TAMs alter anti-tumor immunity by impairing $CD8^+$ and NK cells cytotoxic activity by several mechanisms. Firstly, M2 macrophages secrete immunosuppressive cytokines such as IL-10, TGF-β, and prostaglandins. In addition, M2 macrophages express high levels of ARG1 that depletes the amino acid L-arginine from the microenvironment preventing $CD8^+$ T cell function (Chanmee et al., 2014). Finally, M2-like macrophages express the IC ligands PD-L1/-L2 and CD80/86 which bind respectively to PD-1 and cytotoxic T-lymphocyte-associated molecule 4 (CTLA-4) IC receptors, resulting in effector cells inhibition (Lim et al., 2002) (Y. Liu et al., 2020).

3.2.3 Myeloid-derived suppressor cells (MDSCs)

MDSCs are a heterogeneous group of immune cells that arise from an aberrant expansion of immature cells from the myeloid lineage. MDSCs are characterized by presenting a potent immunosuppressive activity and are expanded under pathological conditions such as chronic

infection or cancer (Gabrilovich & Nagaraj, 2009). Similarly to differentiated myeloid cells, MDSCs interact with other immune cells from the adaptive and acquired immune system. Tumors presenting high levels of MDSCs infiltration are associated with poor clinical outcomes and therapy resistance (Gabrilovich et al., 2012). MDSCs can be classified into two main subpopulations: granulocytic or polymorphonuclear MDSCs (PMN-MDSCs), and monocytic MDSCs (M-MDSCs). PMN-MDSCs resemble neutrophils with less phagocytic capability while M-MDSCs present similarities to immunosuppressive M2-like macrophages. Phenotypically, murine PMN-MDSCs can be identified by the expression of the markers $CD11b^{+}$ $Ly6G^{+}$ $Ly6C^{low}$ and murine M-MDSCs by $CD11b^{+}$ $Ly6G^{-}$ $Ly6C^{high}$ (Veglia et al., 2021). PMN- and M-MDSCs can be recruited into the tumor by tumor-cell derived cytokines and chemokines described in section 5.1.

MDSCs cells exert a strong immunosuppressor activity inhibiting NK and T cells cytotoxicity and impairing macrophages M1-like polarization by several mechanisms: i) induction of immunosuppressive Treg cells and M2-like TAMs through the secretion of IL-10 and IFN-γ; ii) expression of ARG1 enzyme; iii) production of free radical molecules including reactive oxygen species (ROS) and nitrogen species (RNS) through NADPH oxidase 2 (NOX-2) and nitric oxide synthase 2 (NOS2) respectively; iv) induction of nitric oxide synthase (iNOS), which produces nitric oxide (NO) limiting lymphocytes homing into tumors; v) expression of IL-10, TGF-β, cyclooxygenase-2 (COX-2), and prostaglandin E2 (PGE2) which directly inhibits effector immune cells function; vi) upregulation the expression of IC ligands such as PD-L1, inhibiting CTLs activity through IC receptors interaction (Groth et al., 2019).

3.2.4 T Regulatory (Treg) cells

Treg cells are a subset of $CD4^{+}$ $CD25^{+}$ lymphocytes responsible for limiting the cytotoxic functions of T and NK cells in peripheral tissues maintaining self-tolerance in physiological conditions. Treg cells express the transcription factor forkhead box protein P3 (FOXP3) which serves as an exclusive lineage-specifying into Treg cells (Rudensky, 2011). Physiologically, Treg cells are recruited into inflammatory sites where they limit the immune response. In the tumor context, Treg cells promote tumor growth and development by limiting anti-tumor immune response and their recruitment have been mainly linked to poor clinical outcome in cancer patients (Togashi et al., 2019).

Immunosuppressive activity of Treg cells interferes with T cell function and suppresses tumor-antigen presentation. Treg cells indirectly enhance tumor growth by inhibiting APCs function which results in impaired antitumor immunity (Nishikawa & Koyama, 2021). Additionally, Treg cells secrete soluble factors such as IL-10, IL35, and TGF-β that modulate innate immune cell populations (von Boehmer & Daniel, 2013). Specifically, Treg cells recruit immunosuppressive

M2-like macrophages and MDSCs to the tumor site. Treg cells also upregulate the expression of IC ligands directly inhibiting $CD8^+$ T cell function.

3.2.5 Other tumor-infiltrating immune cells

T helper cells are $CD4^+$ T lymphocytes that recognize peptides presented by MHC class II molecules and regulate effective immune responses. Depending on the phenotypic characteristics and the specific cytokine production, $CD4^+$ T cells can be divided into different subsets which mainly include Th-1 and Th-2, among others (Luckheeram et al., 2012). Cytokines released by $CD4^+$ T helper cells, regulate the survival, proliferation, and programming of memory CTLs which reside in peripheral tissues after an infection is cleared, providing a potent early response after later exposition to the same antigen (Pennock et al., 2013). In the tumor context, $CD4^+$ T helper cells regulate an extensive range of immune responses depending on the microenvironment stimuli. Th-1 cells present a proinflammatory profile and enhance $CD8^+$ T cell activity and M1-like macrophage polarization by secreting IL-2 and IFN-γ. Indeed, the recruitment of Th-1 cells within the tumor has been associated with positive clinical outcomes. On the other side, Th-2 cells promote the humoral immune response by secreting IL-4 and stimulating eosinophils, basophils, and B cells (Basu et al., 2021). Importantly, the increase of Th-2/Th-1 ratio has been associated with poor prognosis in patients suffering from breast cancer (Hong et al., 2013) and uterine cervical cancer (W. Lin et al., 2020).

Neutrophils are granulocytic myeloid cells and the most abundant circulating leukocytes in the blood. Neutrophils can phagocyte pathogens and serve as the first line of defense against pathogenic infections (Nauseef & Borregaard, 2014). In the context of cancer, neutrophils can present pro-tumor and anti-tumor activities by secreting different cytokines depending on the tumor type and development stage. Indeed, neutrophils have been shown to present different phenotypes depending on the TME signals (Que et al., 2022). Similarly to macrophages, neutrophils located in the tumor have been named tumor-associated neutrophils (TANs) and have been functionally classified as N1-like if they present anti-tumor activities or N2-like if they present pro-tumor activities. Specifically, it was observed that TGF-β signaling polarized neutrophils towards an N2 pro-tumor profile (Fridlender et al., 2009). However, N1-like and N2-like neutrophil cell populations are defined by their functional phenotype since no differentiating cell surface markers have yet been described (Giese et al., 2019).

Dendritic cells are professional APCs responsible for promoting immunity or tolerance by processing and displaying antigens to T cells. Despite dendritic cells are low frequently located within the TME, they exert a central role in regulating the adaptive immune response against tumor cells by capturing and presenting tumor antigens to $CD8^+$ T cells (Y. S. Lee & Radford, 2019). Dendritic cells within the TME are initially programmed to present anti-tumor functions.

However, TME pressure can induce dendritic cells towards a more tolerogenic state which ends up supporting tumor progression (Gardner & Ruffell, 2016). In addition, dendritic cells also secrete immunomodulatory signals through cell-to-cell contact and cytokines that orchestrate the adaptive and innate immune response (Wculek et al., 2020).

B cells are lymphocytes responsible for secreting antibodies and cytokines in the humoral response. Typically, B cells can be found in the margins of the tumors or infiltrating lymph nodes close to the tumor. Like most immune cells, B cells can display pro-tumorigenic and anti-tumorigenic activities (Engelhard et al., 2021). The anti-tumorigenic activities of B cells include the secretion of cytokines that stimulate effector immune cells such as IFN-γ and IL-12, and the production of antibodies against tumor antigens that mediate antibody-dependent cell cytotoxicity (ADCC). However, B cells can present pro-tumor activities under certain TME stimuli. Then, B cells secrete immunosuppressive cytokines such as IL-10 and TGF-β promoting the recruitment of Treg cells and MDSCs to the tumor site (Sharonov et al., 2020).

4. IMMUNE CHECKPOINT (IC) BLOCKADE IMMUNOTHERAPY

4.1 Immunotherapy based on immune checkpoint (IC) blockade

Last decades immunotherapy has emerged as a clinical option to treat cancer patients. Unlike conventional therapies such as chemotherapy, radiotherapy, or targeted therapy, immunotherapy is based on stimulating the host immune system to identify and target cancer cells. Antibody-based immunotherapies allow the modulation of the immune response against tumors. Specifically, the use of IC blockade antibodies against CTLA-4, PD-1, and PD-L1 have been approved in clinics to treat several tumor types (Archilla-Ortega et al., 2022).

ICs are signaling pathways that regulate the immune system response. In physiological states, ICs pathways are crucial regulators of the immune response maintaining self-tolerance and preventing autoimmunity. Specifically, IC receptors are mainly inhibitory receptors expressed by activated $CD8^+$ T cells and NK cells which dampen cytotoxicity upon binding to their specific IC ligands (E. S. Kim et al., 2016). Immunosuppressive cells including M2-like macrophages, Treg cells, and MDSCs express IC ligands controlling the peripheral immune response ensuring a proportional response by effector immune cells. However, the uninterrupted interaction between IC receptors, expressed by $CD8^+$ T cells and NK cells, and their respective ligands, leads to a dysfunctional state in cytotoxic cells known as exhaustion. These mechanisms can be exploited by cancer cells in tumor immune evasion, which consist of the strategies of tumor cells to evade the host's immune response. Specifically, tumor cells upregulate the expression of IC ligands and recruit immunosuppressive cells preventing anti-tumor immunity. By this, tumor cells establish what is known as an immunosuppressive TME, which is associated with impaired anti-tumor

immunity, increased tumor aggressiveness, and poor clinical outcome (M. Wang et al., 2017) (Moon et al., 2021).

Inhibition of IC signaling by disrupting the interaction between IC receptors and IC ligands is a promising strategy to therapeutically activate anti-tumor immunity (Figure 6). The IC receptors CTLA-4 and PD-1 were the first IC pathways to be blocked in preclinical models and are the most studied ones (Pardoll, 2012) (Pandey et al., 2022). However, a plethora of different IC receptors have been described in $CD8^+$ T cells and NK cells and its blockade is currently being addressed as a possible anticancer treatment in clinical trials (Marin-Acevedo et al., 2021) (Archilla-Ortega et al., 2022). As mentioned before, antibodies against CTLA-4, PD-1, and PD-L1 were approved by the FDA and the EMA to treat different tumor types. However, we are far from completely exploiting the potential of ICI therapies. Despite the blockade of IC pathways has shown clinical benefits in some patients, a considerable percentage of patients present short-duration response or no response (Aslan et al., 2020). The existence of these innate and acquired resistances to IC blockade points out the need to improve efficacy by administrating the correct treatment, or combination of treatments, to the correct tumor type in the stage of progression appropriated.

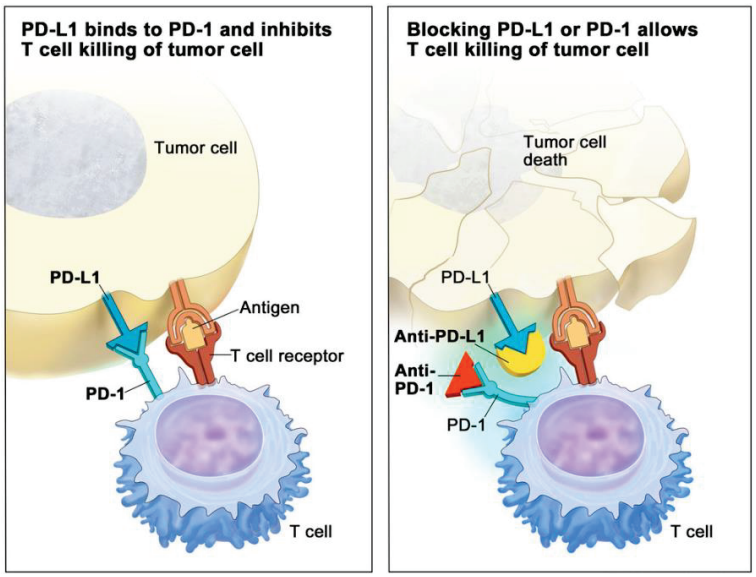

Figure 6. Immune checkpoint blockade strategy. IC ligands such as PD-L1 can be expressed by tumor cells preventing T cell cytotoxic activity against tumor cells. When disrupting the interaction of the receptor PD-1 with its ligands PD-L1 by using blockade antibodies T cells can reactivate and eliminate tumor cells. From National Cancer Institute, U.S. Govt. (n.d.) *Immune checkpoint inhibitors.* National Cancer Institute. https://www.cancer.gov/about-cancer/treatment/types/immunotherapy/checkpoint-inhibitors

To achieve an effective response to ICI therapy, clonal proliferation and activation of antigen-experienced T cells in the TME are required. This process has been named cancer-immunity cycle (Figure 7). Briefly, tumor antigens are captured and processed by dendritic cells, which present processed antigens to T cells through MHC-I molecules. T cells that can bind and recognize tumor antigens are primed and activated. Activated T cells traffic and infiltrate into the tumor core. T

cells recognize tumor cells by the interaction of the TCR with the specific tumor antigen displayed by the MHC-I. Once T cells have recognized a target cell, T cells secrete perforin and GzmB to kill tumor cells (D. S. Chen & Mellman, 2013) (Pio et al., 2019). As previously described, NK cells can eliminate tumor cells independently from cytotoxic T cells. NK cells target cells presenting oncogenic and stress surface markers or lack of MHC-I expression. Furthermore, activated NK cells also exert an immunomodulatory effect impacting and enhancing all the steps of the cancer-immunity cycle (Huntington et al., 2020) (M. Wang et al., 2022).

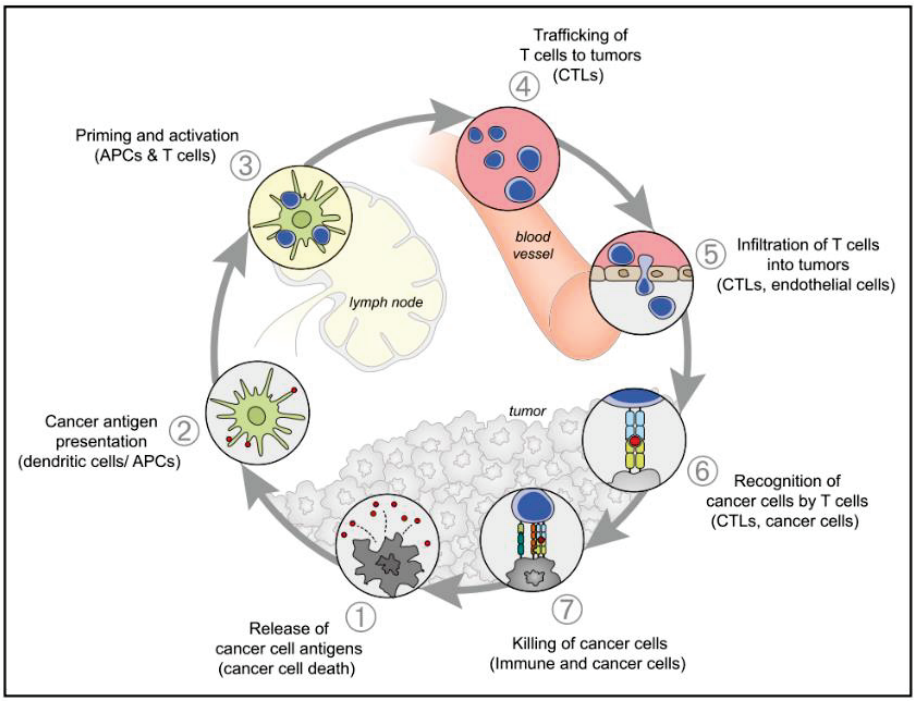

Figure 7. The cancer-immunity cycle. The generation of anti-tumor immunity can be described as a cyclic process where T cells that recognize tumor antigens are activated, and they mobilize to the tumor core to eliminate cancer cells. From Chen & Mellman, 2013.

4.1.1 CTLA-4 axe

CTLA-4 was the first IC receptor described**.** CTLA-4 binds to its IC ligands CD80 and CD86 and exerts negative signals in T cells inhibiting T-cell proliferation and function. The ligands CD80 and CD86 also bind to the T-cell activator receptor CD28, but with lower affinity than to CTLA-4. Hence CTLA-4 and CD28 compete for the binding of CD80 and CD86 (Rowshanravan et al., 2018). CTLA-4 regulates the initial stages of $CD8^+$ T cell activation, ensuring tolerance to self-antigens in, what is known as, central tolerance. This process occurs in the lymph nodes where APCs activate $CD8^+$ T cells. Blockade of CTLA-4 showed increased T cell proliferation and cytotoxicity. In addition, Treg cells also express CTLA-4 and its signaling stimulates immunosuppressive functions (Wing et al., 2008). Anti-CTLA-4 administration in preclinical tumor models caused the rejection of tumors that were pre-established by stimulating $CD8^+$ CTLs response against tumor cells. Given these strong results, CTLA-4 was the first IC that moved to

the clinic. The mAb against CTLA-4 named ipilimumab was the first IC blockade antibody approved for treating patients with advanced melanoma. However, given the central role of CTLA-4 regulating the initial stages of T-cell proliferation and function, anti-CTLA-4 therapies produce secondary autoimmune events, also known as immune-related adverse events (irAEs) which can cause the stop of the treatment administration to patients (Dougan et al., 2021). Ipilimumab is often combined with anti-PD-1 antibodies like nivolumab and it has been observed they present a synergic effect.

The exclusive use of anti-CTLA-4 antibodies in patients suffering from cSCC is limited to a few case reports (Alberti & Bossi, 2021). Patients with metastatic melanoma altogether with advanced or metastatic cSCC were administrated with ipilimumab and presented a durable remission of both pathologies (Day et al., 2017). Another case report described a complete response of a patient with metastatic cSCC to the combination of ipilimumab and nivolumab (Miller et al., 2017). The administration of ipilimumab (anti-CTLA-4) to treat cSCC patients is currently being tested in one clinical trial combined with nivolumab (anti-PD-1), to date, no results have yet been reported (NCT04620200).

The single administration of the anti-CTLA-4 antibody ipilimumab is also being tested to treat HNSCC patients in clinical phase trials (Ferris et al., 2022). Despite that, other clinical trials have demonstrated that the administration of anti-CTLA-4 antibodies combined with anti-PD-1 antibodies did not improve the antitumor response in comparison to anti-PD-1 single blockade in locally advanced and recurrent HNSCC (Siu et al., 2019) (Ferris et al., 2020) (Ferris et al., 2021).

4.1.2 PD-1/PD-L1 axe

The IC receptor PD-1 delivers inhibitory signals to $CD8^+$ T cells upon binding to its ligands PD-L1 and PD-L2. PD-1 signaling decreases T cell proliferation and cytotoxic activities (Y. Han et al., 2020). In contrast to CTLA-4, PD-1 regulates the activity of T cells in peripheral tissues upon inflammatory processes to prevent autoimmunity. Activated T cells induce the expression of PD-1. Tumor-infiltrating lymphocytes express high levels of PD-1 along other IC receptors, which have been associated with an exhausted phenotype (Ahmadzadeh et al., 2009). When activated by its ligands, PD-1 inhibits TCR downstream signaling by recruiting the phosphatase SHP2 (Freeman et al., 2000). Treg cells also express PD-1, and PD-1 signaling promotes their immunosuppressive activities. In addition, PD-1 expression can also be detected in NK cells under pathological situations inhibiting NK cell function. The blockade of the PD-1 axis with either anti-PD-1 or anti-PD-L1 mAbs has been shown to promote anti-tumor immunity and decrease tumor growth in mouse tumor models. Specifically, inhibition of the PD-1 signaling promotes $CD8^+$ T cells and NK cells anti-tumor activities (Pesce et al., 2017). The blockade of PD-1 axis is the most applied ICI in the clinics. The combinatory blockade of PD-1/PD-L1 and CTLA-4 is

also being administrated in clinics. In addition, PD-1/PD-L1 blockade therapies present fewer secondary events than anti-CTLA-4 making them a good option to combine with other treatments (Dougan et al., 2021).

The blockade of PD-1 signaling by administrating anti-PD-1 antibodies has shown positive clinical responses in patients suffering from advanced and metastatic cSCC (Aboul-Fettouh et al., 2021). Treatment of advanced and metastatic cSCC with cemiplimab (anti-PD-1) presented ORRs of ~47% (Migden et al., 2018), ~44% (Migden et al., 2020), and ~45% (Rischin et al., 2020). Former studies tested other anti-PD-1 antibodies such as cemiplimab and pembrolizumab to treat advanced and metastatic cSCC with ORRs of ~42% (In et al., 2021), ~41% (Maubec et al., 2020), and ~59% (Salzmann et al., 2020). In addition, the administration of anti-PD-L1 antibodies such as avelumab is being tested in clinical trials to treat advanced and metastatic cSCC without published results yet (NCT03944941). Anti-PD-1 therapies have been approved to be administered in the clinics to treat patients suffering from advanced and metastatic cSCC as commented in detail in section 1.3. Still, a significant percentage of patients diagnosed with advanced or metastatic cSCC do not benefit from anti-PD-1 interventions.

Blockade of PD-1 signaling with nivolumab and pembrolizumab has proven therapeutic benefits in recurrent HNSCCs (Shibata et al., 2021). Treatment of recurrent and metastatic HNSCCs with nivolumab presented ORRs of ~13% (Ferris et al., 2016) and 12% (Ferris et al., 2021). While the treatment of these advanced HNSCCs with pembrolizumab presented an ORR of ~23% (Burtness et al., 2019) and ~15% (Cohen et al., 2019). Additionally, the anti-PD-L1 antibody durvalumab is currently being tested alone or in combination with the anti-CTLA-4 antibody tremelimumab to treat oropharyngeal squamous cell carcinoma, a subtype of HNSCC (Ferrarotto et al., 2020). As described in section 2.2, anti-PD-1 therapies have been approved to treat patients suffering from recurrent and metastatic HNSCC. Nonetheless, a large percentage of HNSCC patients still do not benefit from anti-PD-1 intervention.

4.1.3 Other ICs axis

Besides CTLA-4 and PD-1, a plethora of different IC receptors are expressed by $CD8^+$ T cells and NK cells inhibiting their function. From these multiple ICs, LAG-3, TIM-3, and TIGIT stand out and are currently being targeted in clinical trials. These receptors, despite presenting a similar function to CTLA-4 and PD-1, present singular and unique characteristics and signaling pathways. Importantly, exhausted $CD8^+$ T cells and NK cells co-express various IC receptors and the simultaneous blockade of some of them may present benefits in comparison to single-blockade strategies (Archilla-Ortega et al., 2022). However, up to date, few clinical trials have analyzed the clinical relevance of blocking LAG-3, TIM-3, and TIGIT in advanced cSCC and HNSCC.

Lymphocyte activation gene-3 (LAG-3) is an IC receptor expressed by $CD8^+$ T cells and NK cells. LAG-3 regulates peripheral tolerance by binding to its ligands Galectin-3 (GAL-3), HLA class II, fibrinogen-like protein 1 (FGL-1), and LSECTin (Anderson et al., 2016). Cancer cells upregulate the expression of LAG-3 IC ligands preventing anti-tumor immunity by effector immune cells. In addition, LAG-3 is also expressed by Treg cells promoting suppressor functions. Mechanistically, LAG-3 downstream signals remain largely unknown but end up interfering with T-cell activation. Blockade of LAG-3 increases $CD8^+$ T cells function and delays tumor growth. Simultaneous blockade of LAG-3 and PD-1 synergized to delay tumor growth (Burova et al., 2019). Anti-LAG-3 mAbs are being studied in clinical trials either as a single agent or combined with other anti-IC antibodies.

No studies targeting LAG-3 have been done in cSCC however, the expression of LAG-3 was detected in tumor-infiltrating lymphocytes of cSCC patients indicating a high potentiality to target LAG-3 signaling with anti-LAG-3 therapies and enhance antitumor immunity (S. Wu et al., 2020). A mouse model of HNSCC was used to test the blockade of LAG-3 and it was shown that anti-LAG-3 antibodies reduced tumor growth and increased $CD8^+$ T cell cytotoxicity (Deng et al., 2016). Various ongoing phase II clinical trials are testing the anti-LAG-3 antibody relatlimab in HNSCC patients. Specifically, relatlimab is being studied in combination with nivolumab in patients with recurrent and metastatic HNSCC (NCT04080804, NCT04326257). These clinical studies are still recruiting patients and the results are expected to be posted in 2026.

T-cell immunoglobulin and mucin-domain containing-3 (TIM-3) is another IC receptor expressed by T cells and NK cells that tightly modulate effector immune response. TIM-3 ligands are Galectin-9 (GAL-9), carcinoembryonic antigen-related cell adhesion molecule 1 (CEACAM1), phosphatidylserine (PS), and high-mobility group protein 1 (HMGB1). Ligands activating TIM-3 are upregulated by certain tumor types inhibiting T cell and NK cell function. Blocking TIM-3 signaling could reverse the exhausted phenotype of $CD8^+$ T cells that were infiltrating tumors. TIM-3 activation leads to inhibition of the kinase LCK, which is downstream of the TCR activation signaling in T cells (Davidson et al., 2007). Blockade of TIM-3 signaling activates $CD8^+$ T cells against tumor cells. Additionally, the co-blockade of TIM-3 and PD-1 increases the regression of murine glioma in comparison to single-blockade agents (J. E. Kim et al., 2017). TIM-3 blockade antibodies are also being tested in clinical trials as monotherapy or in combination with other IC blockade antibodies.

Anti-TIM-3 therapies have not been tested in cSCC to date. In a phase I study the anti-TIM-3 agent sabatolimab alone and combined with an anti-PD-1 mAb safety and tolerability were validated in multiple solid tumors including HNSCC patients (Curigliano et al., 2021). In addition, another phase I clinical trial is evaluating a bispecific antibody anti-PD-1/TIM-3 in

patients suffering from metastatic HNSCC among other advanced and metastatic solid tumors (NCT03708328).

T cell immunoglobulin and ITIM domain (TIGIT) is an IC receptor also expressed by activated T cells and NK cells that impairs its function upon binding to its ligands. TIGIT ligands are PVR, nectin-2, and nectin-3 which are expressed by APCs and tumor cells. Specifically, TIGIT interacts with PVR with the highest affinity. In addition. DNAM-1 is a co-stimulatory receptor expressed by T cells and NK cells that competes with TIGIT for the binding of PVR and nectin-2 (Sanchez-Correa et al., 2019). Upon binding its ligands, TIGIT recruits SHP-1 phosphatase that interferes with activation signals in T and NK cells (Joller et al., 2011). Anti-TIGIT treatment promotes tumor regression by enhancing $CD8^+$ T cell response. Dual blockade of TIGIT with PD-1 or TIM-3 presented anti-tumor synergistic effects. As LAG-3 and TIM-3, TIGIT blockade is being analyzed in clinical trials as a single or combinatory agent against different tumor types.

The blockade of the IC TIGIT has not been addressed yet to treat cSCC. In HNSCC, the anti-TIGIT antibody tiragolumab is being tested alone or combined with anti-PD-L1 antibodies in two phase II clinical trials (NCT03708224, NCT04665843) without posted results yet.

4.2 Resistance to IC blockade therapies

Despite IC blockade therapies have improved clinical outcomes in various cancer types, only a minority of patients present a durable response (Fares et al., 2019). Three groups of patients treated with ICI can be identified: a) those that present a long-term response (responders), b) those that never respond to therapy (innate/primary resistance), and c) those who initially responded but eventually present disease progression (acquired/secondary resistance) (Sharma et al., 2017). In addition, defining patients as responders and non-responders is challenging given the heterogeneity of responses to ICI observed. The response to the blockade of IC pathways varies depending on the tumor type and stage of progression. Mechanisms of innate and acquired resistance are not fully elucidated in part to the incomplete understanding of molecular processes leading to a beneficial IC blockade strategy. Moreover, multiple factors can impact anti-tumor immunity and consequently immunotherapy response. These have been classified as host-intrinsic factors such as the TME and the immune system, host genomics and epigenomics, host systemic factors, and the composition of the circulating microbiota. Host-extrinsic factors such as exposure to environmental hazards, lifestyle and psychosocial factors, and microbial infections can also impact on anti-tumor immunity (Morad et al., 2021). Hence, the understanding of ICI resistance mechanisms is gaining more levels of complexity since many factors can impact anti-tumor immunity and consequently lead to the failure of ICI.

Several resistance mechanisms to ICI prevent an optimal function of the cancer immunity cycle (D. Liu et al., 2019) (Schoenfeld & Hellmann, 2020). These resistance mechanisms can be

grouped into tumor-cell intrinsic features and tumor-infiltrating immune and stromal cell features (Figure 8). It is necessary to keep in consideration that these mechanisms do not happen individually in the tumor context, and their combination will conditionate the outcome of the therapeutic intervention.

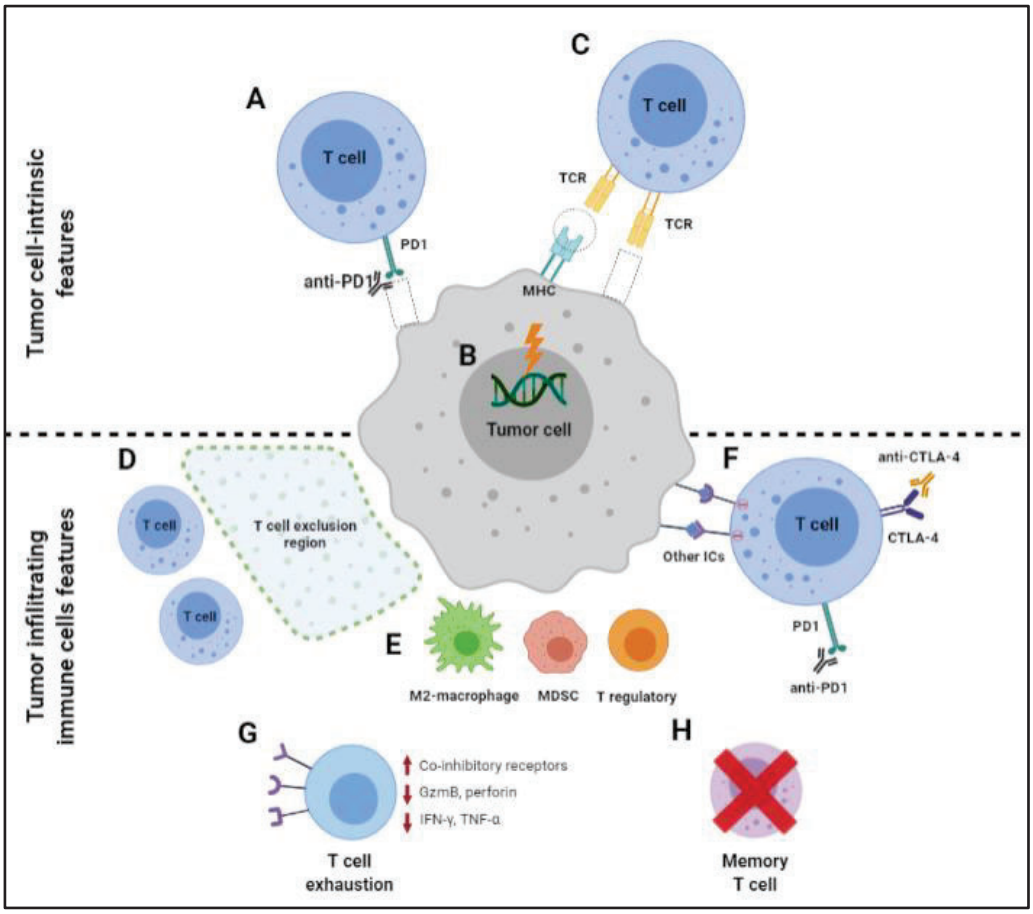

Figure 8. Resistance mechanisms to IC inhibition therapies. A, Alterations in PD-L1 expression. **B**, Oncogenic mutations. **C**, Deficiencies in antigen presentation due to low TMB or downregulation of MHC-I expression. **D**, T cell exclusion. **E,** Recruitment of immunosuppressive immune cells. **F,** Co-expression of other immune checkpoint receptors. **G,** T cell dysfunction and exhaustion. **H**, Impaired formation of memory T cells.

The tumor-cell intrinsic features refer to the set of changes that intrinsically a tumor cell experiences and are linked to resistance to ICI therapies (Kalbasi & Ribas, 2020). Alterations in PD-L1 expression levels in cancer cells have been linked to ICI outcomes with controversial results. The presence of PD-L1^{+} tumor cells has been associated with successful PD-1/PD-L1-based therapies, whereas negative PD-L1 tumors are expected to exhibit primary resistance (C. Sun et al., 2018) (Figure 8A). Nevertheless, PD-L1 expression is highly variable between tumors which can be due to intratumor heterogeneity and lack of standardized PD-L1 quantification methods between clinical studies (F. Yang et al., 2021). In this sense, the use of PD-L1 expression as a predictive biomarker of response to anti-PD-1/PD-L1 therapy is not good since some patients

with PD-L1 negative tumors respond to PD-1 signaling blockade (L. Horn et al., 2017) (Zheng, 2017). One proposed explanation for this observation is that infiltrating myeloid immune cells can also express PD-L1, which would lead to the activation of PD-1 signaling in effector immune cells and inhibit their cytotoxicity (Bocanegra et al., 2019). More recently new studies pointed out that PD-L1 expression in circulating tumor cells has shown the potential to be used as predictive biomarkers to PD-1 signaling inhibitors in hepatocellular carcinoma (HCC) and would be a more reliable biomarker (Su et al., 2022).

Mutations affecting oncogenes have also been linked to IC blockade resistance. Genetic mutations that have been linked to resistance to anti-PD-1/PD-L1 include EGFR activating mutations, MYC overexpression, poly (ADP-ribose) polymerase (PARP) inhibition, alterations in INF-γ signaling pathway such as loss-of-function mutations in β2-microglobulin, pyruvate dehydrogenase kinase (PDK) amplifications, PTEN loss, inactivating mutations in JAK1 and JAK2, and phosphoinositide 3-kinase (PI3K)/Akt activating mutations (Cretella et al., 2019) (Schoenfeld & Hellmann, 2020) (Figure 8B).

Tumor cells are recognized by CTLs through the expression of neoantigens derived from genetic/epigenetic alterations as mutations or the overexpression of oncogenes. Tumor cells presenting a high number of genetic alterations are likely to be more immunogenic and present a higher TMB score. Generally, tumors with high TMB, such as melanoma, cSCC, non-small cell lung cancer (NSCLC), HNSCC, or microsatellite instability (MSI) colorectal cancer are expected to be sensitive tumors to ICI-based therapy, although a large percentage of these tumors showed a poor response to this therapy (Yarchoan et al., 2017) (Chan et al., 2019). In this regard, a higher TMB has been reported in responder patients compared to non-responders with the same tumor condition including NSCLC (Rizvi et al., 2015), melanoma (Van Allen et al., 2015), and urothelial carcinoma (Rosenberg et al., 2016). Indeed, the TMB is not always a reliable predictor of response since other tumor features can also contribute to the final response to ICI-based therapy (Chan et al., 2019). In addition, for proper cytotoxic T-cell recognition, tumor cells need to express tumor antigens through MHC-I molecules. Genetic alterations that disrupt the machinery of MHC-I antigen presentation have been described in different tumor cells (Figure 8C). These include the downregulation of MHC-I expression and loss of heterozygosity of β2-microglobulin among others and will be discussed in detail in section 4.2.1.

The tumor-infiltrating immune and stromal cell features refer to the set of cellular events happening in the TME that causes resistance to ICI therapies. The spatial location of effector cells is important for the accomplishment of anti-tumor response since a proximal contact between activated T cells and tumor cells is needed for correct anti-tumor immunity. When activated CTLs cannot enter inside the tumor cores, a process that is known as T-cell exclusion and is influenced

by the composition of tumor-infiltrating immune and stromal cells (Y. Zhang et al., 2020). The presence of immunosuppressive cells such as MDSCs and M2-like macrophages, and specific subgroups of CAFs and their derived cytokines regulate the spatial distribution of CTLs and promote T-cell exclusion (Feig et al., 2013) (Figure 8D). For example, secreted IL-10 by M2-like macrophages prevent the tumor recruitment of T cells trapping them in the stroma in mammary cancer (Ruffell et al., 2014). RNS derived from MDSCs metabolism alter chemokine signaling within the tumoral context preventing the contact of T cells with tumor cells (Molon et al., 2011). CAFs can restrict the infiltration of T cells into the tumor core by modulating the composition of the ECM or by secreting the cytokine CXCL12 (Joyce & Fearon, 2015).

The composition of the TME impacts ICI therapy outcome. TMEs enriched in neutrophils, M1-like TAMs, CTLs, and DCs are typically associated with good prognostics and efficacy of ICI therapies (Raftopoulou et al., 2022) (Russo & Nastasi, 2022). On the other side, the presence of immunosuppressive cells, such as MDSCs, Treg, and M2-like TAMs are linked to a poor response to IC blockade (Galon & Bruni, 2019). This is mainly due to immunosuppressive cells secrete local immunosuppressive factors and express IC ligands that dampen CTLs function and prevent proper antigen processing function within the TME (Saleh & Elkord, 2019) (Nakamura & Smyth, 2020) (Figure 8E).

Beyond CTLA-4 and PD-1, CTLs can express other IC receptors that upon binding to their respective ligands, impair T cell effector function. Cancer cells express their respective ligands to evade the attack of cytotoxic immune cells. The activation of alternative IC receptors rather than the ones being targeted by the anti-IC treatment causes IC blockade therapy resistance (E. S. Kim et al., 2016) (Figure 8F). Hence, simultaneous blockade of different immune checkpoints is a good strategy to recover the functionality of T cells and has proven increased antitumor responses in comparison to single blockade strategies (Zhouhong et al., 2021) (Archilla-Ortega et al., 2022).

The sustained exposure of CTLs to antigens leads to a dysfunctional state known as exhaustion in which T cells lose their proliferation and effector functions. This effect is observed in chronic viral infections and cancer and prevents the obtention of durable responses of IC blockade treatment. Exhausted T cells are characterized by the co-expression of various IC receptors, do not exhibit cytotoxic activity, present reduced mRNA levels of perforin and granzyme B, and do not secrete effector cytokines such as IFN-γ and TNF-α (Wherry & Kurachi, 2015) (W. Jiang et al., 2020) (Figure 8G). After persisting antigenic stimulation, CTLs undergo epigenetic changes that lead to the exhausted phenotype. Within the first stages of exhaustion, T cells can restore functionality after PD-1 blockade (A. C. Huang et al., 2017) (Tough et al., 2020). However, if these reinvigorated CTLs cannot eliminate tumor cells and antigenic stimulation persists, T cells acquire fixed epigenetic modifications and become re-exhausted T cells (Philip et al., 2017). This

re-exhausted state makes T cells unresponsive to anti-PD-1 therapy (Pauken et al., 2016). In addition, one of the biggest drawbacks of ICI therapies is the lack of long-term durable responses. For that, effector T cells must differentiate into effector memory cells (Qingjun et al., 2020). However, epigenetic changes that occur during T-cell exhaustion impair the formation of T-memory cells (Y. Jiang et al., 2015) (Pauken et al., 2016) (Figure 8H). Specifically, chromatin remodeling that suffer T cells in an exhausted state prevents the differentiation of effector T cells into T-memory cells (Tough et al., 2020).

4.2.1 Defective MHC-I antigen processing and presentation

The antigen presentation is a key process to ensure anti-tumor immunity. Cancer cells must present intracellular neoantigens through MHC-I to be recognized by CTLs. Hence, tumor cells can bypass immune surveillance and become invisible to CTLs by losing the expression of MHC-I (Dhatchinamoorthy et al., 2021). If activated $CD8^+$ cells cannot identify tumor cells, IC blockade stimulation of $CD8^+$ T cells will hardly present benefits. Understanding class I antigen processing downregulation is crucial to elucidate the mechanisms of cancer progression and resistance to ICI therapies. By contrast, MHC-II participates in antigen processing and the presentation of extracellular peptides. Consequently, despite MHC-II is also crucial in developing immune responses, its implication in tumor surveillance is not as relevant as MHC-I. Whereas class I MHC is expressed in all nucleated cells, class II MHC is restricted to APCs including dendritic cells, macrophages, and monocytes. In addition, non-professional APCs can express MHC-II in pathologic situations such as autoimmune processes (Lipski et al., 2017).

Structurally, MHC-I is a non-covalently linked heterodimer consisting of an α polymorphic polypeptide chain (heavy chain) where presented peptides bind, and a non-polymorphic β2-microglobulin chain. Presented peptides are generated from degraded intracellular proteins through the proteasome. Cytosolic proteins, after being ubiquitinated, are driven towards the proteasome to be cleaved into peptides ranging from 16 to 20 amino-acid length (Tanaka, 2009). These peptides are translocated into the endoplasmic reticulum (ER) thanks to ER transporter TAP proteins which are a heterodimer formed of transporter 1 ATP binding cassette subfamily B member (TAP1), and transporter 2 ATP binding cassette subfamily B member (TAP2). In the luminal side of ER, the MHC-I α-chain and β2-microglobulin chain are synthetized and assembled thanks to the chaperone calreticulin. In addition, the glycoprotein Tapasin and the oxidoreductase ERp57 mediate the interaction between newly assembled MHC-I molecules and TAP transports allowing optimal loading of the presented peptide. Besides having the right length, not all peptides present affinity to bind to the MHC-I and only high-affinity peptides will be assembled to empty MHC class I molecules. In fact, IFN-γ induces the formation of immunoproteasomes, a type of proteasome that produces peptides with high affinity to class I MHC chains. The loading peptide

needs to be cut between 8-to-9 amino-acid length by ERAP to fit in the groove of the empty MHC-I molecule (F. Zhou, 2009). After loading of MHC class I with a high-affinity peptide, the interaction between Tapasin, TAP transporters, calreticulin, ERp57, and MHC-I disappears and the complex peptide/MHC-I is able to mature through the Golgi apparatus. Finally, MHC-I with the high-affinity peptide arrives at the cell membrane through exocytic vesicles. Once, the MHC-I complex is located on the cell surface displays intracellular antigens to activated $CD8^+$ T cells (Figure 9).

Defects in any step of the antigen processing pathway will prevent the correct loading of the high-affinity peptide to the MHC-I and its maturation towards de Golgi apparatus until the cell membrane. Moreover, alterations in antigen presentation pathway components such as losing the expression of immunoproteasomes, TAP1, TAP2, ERAP, and Tapasin as well as mutations in β2-microglobulin have been detected in different cancers and work as immune evasion mechanisms by downregulating the cell surface expression of MHC-I (Reeves & James, 2017). Unmature and unstable MHC-I molecules are retained inside the ER preventing its maturation towards the cell membrane. Ultimately, these MHC-I can be degraded in the lysosome (Dhatchinamoorthy et al., 2021). Lack of MHC-I cell surface expression due to defects in antigen processing pathway makes cancer cells invisible for $CD8^+$ CTLs and can contribute to resistance to immunotherapies based on ICI.

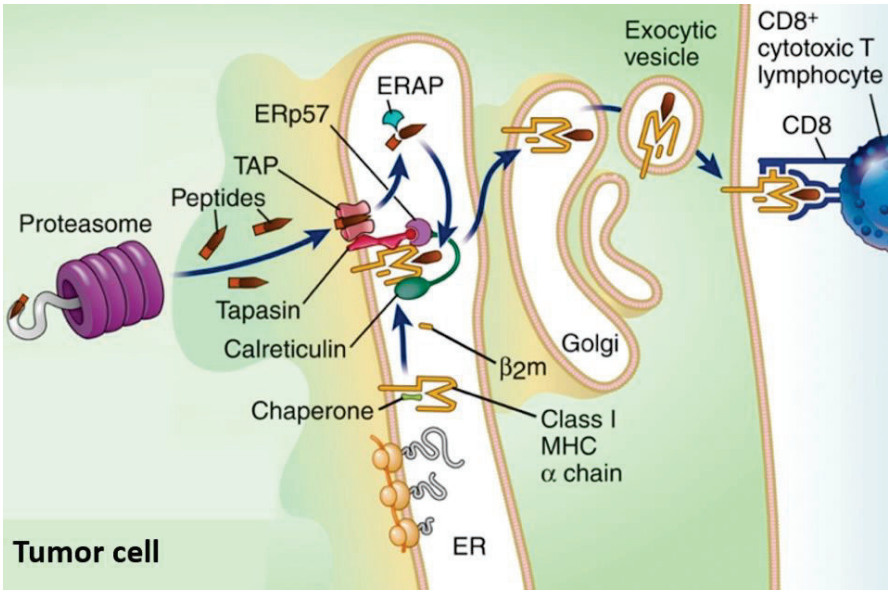

Figure 9. MHC-I antigen processing pathway. Intracellular proteins after being degraded by the proteasome, are translocated to the ER through the TAP heterodimer (TAP1 and TAP2). Then peptides with the correct length and high affinity to MHC-I molecules are loaded with the help of Tapasin, calreticulin, and ERp57. After that, the peptide/MHC-I complex goes through Golgi to complete its maturation until the cell membrane where is recognized by $CD8^+$ CTLs. Modified from Abul K, Abbas. et al. Cellular and molecular immunology, Elsevier, 2021.

4.2.2 Impaired IFN-γ signaling

Given the crucial role of MHC-I in $CD8^+$ T cells dependent anti-tumor immunity its regulation has consequences for tumor immune evasion. The expression of MHC-I α heavy chain and β2-microglobulin as well as MHC-I antigen processing machinery including TAP1, TAP2, Tapasin, and ERAP is coordinated by similar gene control elements that bind to their promoter and enhancer regions. These include various transcription factors such as NLRC5, IRF1/IRF2, and NF-κB (Jongsma et al., 2019). Importantly, NLRC5, IRF1, and IRF2 transcription factors are not essential for cell viability, hence their expression can be lost in tumor cells (Matsuyama et al., 1993) (A. Biswas et al., 2012). The stimulation with interferons, especially with IFN-γ, increases the expression of MHC-I and antigen processing components. Specifically, IFN-γ upregulates the expression of IRF-1 and NLRC5 (Der et al., 1998). Upon an infection, T cells induce the expression of interferons enhancing the detection of infected cells. In the cancer context, mice presenting defects in interferon pathways presented increased cancer incidence (Kaplan et al., 1998).

IFN-γ is a cytokine mainly expressed by $CD8^+$ CTLs, NK cells, and Th-1 cells. Upon binding to its receptor, a heterodimer formed by interferon gamma receptor 1 (IFNGR1) and interferon gamma receptor 2 (IFNGR2), IFN-γ initiates a tyrosine kinase cascade. Intracellular Janus kinase 1 (JAK1) binds to the cytosolic tail of IFNGR1 and Janus kinase 2 (JAK2) binds to the cytosolic tail of IFNGR2. JAK1 and JAK2 trans-phosphorylates in tyrosine residues creating a binding pattern to recruit the signal transducer and activator of transcription 1 (STAT1). When bound to JAK1 and JAK2, JAKs phosphorylate tyrosine residues of STAT1 promoting its dimerization and translocation to the nucleus. Homodimers of phospho-STAT1 bind to the elements of gamma activated sequences (GAS) in the promotor region of interferon-stimulated genes (ISG). This promotes the expression of IRF1 and NLRC5. As a result, IRF1 and NLRC5 drive MHC-I expression by binding to IFN sensitive response element (ISRE) and W/S, X1, X2, and Y1 boxes, respectively, both located in the promotor region of MHC class I (Jongsma et al., 2019) (Dhatchinamoorthy et al., 2021) (Figure 10). This promotes the expression of MHC-I and antigen-processing proteins such as TAP1, TAP2, Tapasin, and ERAP. In addition, IRF1 also promotes the expression of MHC-II and PD-L1. MHC-II expression is controlled by the transcriptional regulator Class II TransActivator (CIITA) which is induced by IRF1 (Muhlethaler-Mottet et al., 1998). By contrast, IRF1 directly induces PD-L1 expression by binding to its promoter (Garcia-Diaz et al., 2017) (Shi, 2018).

The IFN-γ signaling signature refers to a set of genes that are induced by IFN-γ signaling in a cell and are involved in a range of biological processes, including immune response, inflammation, cell growth, and apoptosis. The IFN-γ signaling signature can serve as a biomarker of IFN-γ

activity and can be used to study the role of IFN-γ in physiological and pathological conditions (Benci et al., 2016). Importantly, IFN-γ signaling signature correlates with immunotherapy response in cancer patients (Grasso et al., 2020). In addition, the ratio between the IFN-γ signaling signature to the immunosuppression signature positively correlates with response to anti-PD-1 treatment in melanoma patients (Cui et al., 2021).

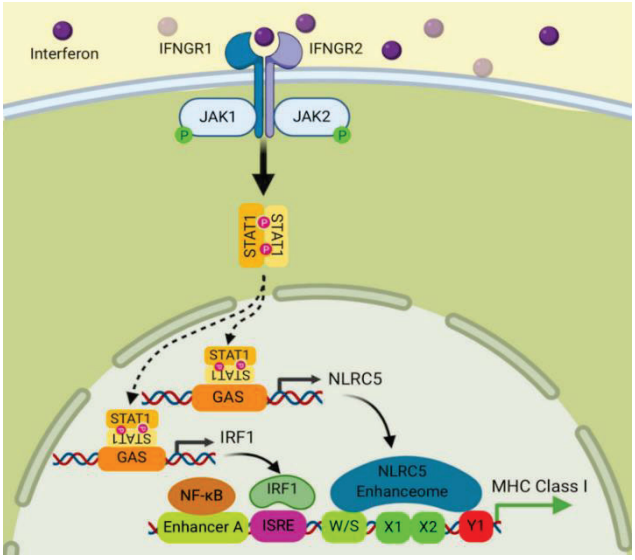

Figure 10. IFN-γ signaling stimulates MHC-I expression. The binding of IFN-γ to its receptors promotes the phosphorylation of STAT1, which translocate to the nucleus and promotes the expression of IRF1 and NLRC5. IRF1 and NLRC5 are responsible for driving the gene expression of MHC class I and antigen processing proteins. From Dhatchinamoorthy et al., 2021.

5. CYTOKINE INTERPLAY WITHIN TME

Cytokines are soluble proteins with low molecular weight involved in cell signaling. Cytokines are produced by multiple cell types and are involved in autocrine, paracrine, and endocrine cell communication. Cytokines are molecules with pleiotropic effects since the same cytokine can act on more than one cell type producing multiple biological actions (Saxton et al., 2023). Given that cytokines cannot cross the lipid barrier, they exert their effects by signaling through cell surface receptors. Cytokines participate in immunity modulating the maturation and responsiveness of immune cells. Specifically, cytokines control the immune response to inflammation, infection, trauma, and cancer (Foster, 2001). In addition, cytokines exhibit redundancy, which means that multiple cytokines exert similar actions producing a shared biological action (C. Liu et al., 2021). Hence, cytokines establish a complex network of cellular communication.

Cytokines constitute a heterogeneous set of factors, which includes several families such as interleukins (ILs), tumor necrosis factors (TNFs), interferons (IFNs), transforming growth factors (TGFs), colony-stimulating factors (CSFs), growth factors (GFs), and chemokines (Khan, 2019). However, due to cytokines present redundancy and pleiotropism, this classification has changed over time and may be slightly different depending on the consulted bibliography. Initially, ILs were referred to cytokines produced by immune cells. However, later it was demonstrated that these factors were also secreted by other cell types and participate in distinct physiological

processes (Briukhovetska et al., 2021). TNFs are mediators of inflammatory reactions and play an important role in chronic inflammatory diseases (Chu, 2013) while IFNs present a key role in regulating innate and adaptive immunity (Pestka et al., 2004). CSFs regulate the proliferation and differentiation of monocytic and granulocytic hematopoietic cells (Hamilton, 2008). GFs are involved in the regulation of cell proliferation and differentiation, as well as in hematopoiesis, angiogenesis, migration, and apoptosis (Barrientos et al., 2008). Finally, chemokines are considered chemotactic cytokines given their capacity to induce chemotaxis and recruit specific immune cells located nearby. Cytokines can also be classified as pro-inflammatory or anti-inflammatory depending on their role. Pro-inflammatory cytokines include TNF-α, IL-1β, IL-6, IL-8, IL-12, and IFNs among others. By contrast, anti-inflammatory cytokines include TGF-β, IL-4, IL-6, IL-10, and IL-1RA among others (Wojdasiewicz et al., 2014) (Singh et al., 2022).

Cytokines are active transducers of cell communication within the TME. While some cytokines participate in host anti-tumor response, others support tumor progression (S. Lee & Margolin, 2011) (R. M. Morris et al., 2022). Dysregulated cytokine secretion by tumor cells, stromal cells, and immune cells is observed in all stages of cancer progression (Propper & Balkwill, 2022). Specifically, some cytokines have been extensively linked with pro-tumor effects. TGF-β has a direct effect on tumor cells either by promoting cell survival, proliferation, and EMT or by acting as tumor suppressor inhibiting tumor cells proliferation depending on the tumor pathological characteristics (Baba et al., 2022). IL-1β promotes tumor cell proliferation, dysregulated cytokine response, and abnormal ECM production (Rébé & Ghiringhelli, 2020). IL-4 and IL-10 also participate in promoting an immunosuppressive TME by recruiting immunosuppressive cells such as Treg cells, MDSCs and M2-like TAMs (Mirlekar, 2022) (Y. Li et al., 2023). Furthermore, IL-6 and VEGF promote angiogenesis (Y.-H. Huang et al., 2016). By contrast, other cytokines promote anti-tumor effects: IL-2 enhances NK and T cell response, Th-1 proliferation, and antibody production by B cells (Bachmann & Oxenius, 2007, p. 2). IFN-γ signaling directly enhances the cytotoxic activity of lymphocytes (Pestka et al., 2004). IL-12 stimulates NK and T cell proliferation and cytotoxicity (Oka et al., 2020) while IL-15 promotes the persistent activity of $CD8^+$ CTLs and NK cells (Briukhovetska et al., 2021). In addition, the cytokine signaling network within the TME may vary depending on the stage of progression and individual tumor features (Hinshaw & Shevde, 2019) (Q. Wang et al., 2023). Given the role of cytokines modulating the immune response, their pharmacological target with single-agent cytokine-based therapies has been assayed for cancer treatment. However, clinical trials presented limited therapeutic benefits (Propper & Balkwill, 2022). Last decade, the explosion of immunotherapy has increased the interest in a better understanding of the modulation of the TME by cytokines as possible combinatory targets to boost immune response and ameliorate irAEs.

5.1 Role of chemokines recruiting immunosuppressive cells

Chemokines are a family of cytokines that were initially characterized for their chemoattractant function for different leukocyte populations (Griffith et al., 2014). Chemokines can attract specific immune cell populations and can modulate the TME profile. In addition, chemokines act on non-immune cells, and regulate numerous processes, such as angiogenesis, tumor growth, and metastasis development (Vandercappellen et al., 2008). Chemokines are the largest subfamily of cytokines being formed by approximately 50 ligands. Chemokines are characterized by the presence of 2 cysteine (C) residues in the N-terminal which are essential for their three-dimensional structure. Hence, chemokines are subdivided into four subgroups depending on the exact location of the first 2 C residues: C-chemokines, CC-chemokines, CXC-chemokines, and CX_3C-chemokines (X represents any amino acid) ("Chemokine," 2009). Importantly, chemokines present a high redundancy with many ligands binding different receptors and receptors binding multiple ligands (Nagarsheth et al., 2017). In the tumoral context, chemokines can be secreted by immune cells, stromal cells, and tumor cells. Given that chemokines regulate the location and function of immune cells they can present pro-tumor and anti-tumor immunity (Ozga et al., 2021). The final effect of chemokines depends on the stage of tumor progression, the activation state of the immune response, and the balance between effector and regulatory target cells (Ozga et al., 2021).

Unraveling the chemoattract signals that cause the establishment of an immunosuppressive TME by attracting immunosuppressive cells is of high interest. Immunosuppressive cells are recruited into tumors in response to chemokines, but also other cytokines such as TGFs, GFs, ILs, and CSFs (Lorenzo-Sanz & Muñoz, 2019). Macrophages are recruited to tumor sites in response to CCL2, CCL3, CCL4, CCL7, CCL8, CSF1, CSF2, macrophage-stimulating protein (MSP), PDGF, VEGF, and TGF-β (Joyce & Pollard, 2009) (B.-Z. Qian et al., 2011). Then, macrophages may differentiate into an M2-like profile in response to IL-4, IL-10, and IL-3 (N. Wang et al., 2014). M-MDSCs are recruited into tumor mainly by CCL2 and CCL5 while PMN-MDSCs are recruited in response to CXCL1, CXCL2, CXCL5, CXCL6, CXCL8, CXCL12, CCL2, CCL3, and CCL15 (Kumar et al., 2016). Finally, it has been described that Treg cells are recruited to the tumor by CCL17, CCL22, CCL28, and CXCL12 (Mizukami et al., 2008). Importantly, the expression levels of cytokine receptors in immune cells can change in response to external stimuli (O'Shea et al., 2019) (Propper & Balkwill, 2022). In addition, as mentioned before, there is an overlap and redundancy in cytokine signaling reflecting the complexity of the recruitment of immune cells to the TME.

OBJECTIVES

The studies carried out by our laboratory have shown that the presence of mesenchymal-like SCC cancer cells and the establishment of an immunosuppressive TME has been associated with resistance to ICI immunotherapy in advanced mouse cSCC. In addition, previous studies indicate that immunosuppressive cells can enhance tumor progression by promoting EMT on cancer cells of different tumor types. However, it remains unknown if these immunosuppressive cells promote cSCC progression toward a mesenchymal-like state. We hypothesize that cytokines produced by specific populations of tumor-infiltrating immune cells could be inducing the switch of cancer cells to the mesenchymal state, promoting cSCC progression. In turn, mesenchymal cancer cell-derived factors may drive the conversion of tumor immune-microenvironment toward an immunosuppressive state, which is characterized by the recruitment of immunosuppressive cells that block antitumor response. This scenario may be responsible for resistance to ICI therapies in cSCCs.

The main aim of this project is to characterize the crosstalk between tumor-infiltrating immune cells and cancer cells that is responsible for promoting the mesenchymal-like state of SCC cells, and the recruitment of immunosuppressive cells in advanced cSCCs.

The specific objectives of the present thesis are:

1. Identify tumor-infiltrating immune cells-derived cytokines responsible for promoting the mesenchymal-like state of cancer cells during mouse cSCC progression.

2. Determine cancer cell-derived cytokines and mechanisms involved in the recruitment of immunosuppressive cells, which contribute to the exhaustion of cytotoxic T cells in advanced mouse cSCCs.

3. Study alternative strategies to promote the anti-tumor response of ICI therapies in advanced cSCCs.

4. Study of patient cSCC and HNSCC cell characteristics associated with resistance to ICI therapy.

MATERIALS AND METHODS

1. *In vitro* cell culture of primary SCC cells and treatments

Primary SCC mouse cells previously obtained in the laboratory were used. Specifically, cancer cells from WD-SCCs (full epithelial cancer cells), MD/PD-SCCs (Plastic EpCAM$^+$ cancer cells), PD-SCCs (mesenchymal-like EpCAM$^-$ cancer cells) and PD/S-SCCs (full mesenchymal cancer cells) were plated and cultured in DMEM-F12 GlutaMAX medium (Life Technologies, 31331093) with 1X B27 (Life Technologies, 17504044) and 1% penicillin/streptomycin (Biowest, L0022-100) (Table 1). Cells were grown in a 60 mm treated cell culture dish (Corning, 353002) in a humidified incubator at 37ºC and 5% CO_2. Primary SCC cells were previously transduced with the plasmid MSCV-IRES-GFP and can be identified by enhanced Green fluorescent protein (GFP) expression.

Primary SCC cells	Origin	Differentiation degree
2C3	WD-SCCs	Full epithelial SCC cells
3A		
Plastic S2T2 EpCAM$^+$	MD/PD-SCCs	Plastic EpCAM$^+$ SCC cells
Plastic S5T2 EpCAM$^+$		
S3T1 EpCAM$^-$	PD-SCCs	Mesenchymal EpCAM$^-$ SCC cells
6G2 EpCAM$^-$		
468-8A	PD/S-SCCs	Full mesenchymal SCC cells

Table 1: Primary SCC cells and its degree of differentiation.

Primary SCC cells were subcultured when reached ~80% confluence. Cell passaging was performed by carefully washing the plates with phosphate buffered saline (PBS) 1X (Life Technologies, 11593377) and adding 2X trypsin-EDTA 0.5% (Life Technologies, 10779413). Once cells were detached, DMEM high glucose GlutaMAX medium (Life Technologies, 31966047) supplemented with 10% FBS (Life Technologies, 10270106) and 1% antibiotic-antimycotic (Biowest, L0010-100) was added and centrifuged at 1.200 rpm for 4 minutes. The supernatant was removed, and cells were resuspended at desired dilution in the culturing medium.

Full epithelial cancer cells (2C3 and 3A) and mesenchymal-like EpCAM$^-$ cancer cells (S3T1 EpCAM$^-$ and 6G2 EpCAM$^-$) were used to perform *in vitro* assays. For IFN-γ treatment, 350 000 full epithelial cancer cells or 400 000 mesenchymal-like EpCAM$^-$ cancer cells were seeded in 6-well plates (Corning, 353046) with 10 ng/mL of IFN-γ (R&D systems, 485-MI) or PBS in culture medium (DMEM-F12 GlutaMAX with 1X B27 medium and 1% P/S) for 48 hours. Then, treated cells were analyzed by fluorescent activated cell sorter (FACS) analysis or cell pellets were collected for RNA and western blot analysis.

The selective inhibitor of the methyltransferase EZH2, GSK126 (Selleckchem, S7061), was used to treat full epithelial cancer cells or mesenchymal-like EpCAM$^-$ cells. Specifically, 200 000 2C3

SCC cells or 300 000 S3T1 EpCAM$^-$ SCC cells were seeded in 6-well plates with 5 µM of GSK126 or dimethyl sulfoxide (Sigma, D4540) in culture medium for 72 hours. Treated cells were then analyzed by FACS analysis or cell pellets were collected for RNA and western blot assays.

To inhibit the autophagic flux, Bafilomycin A (BafA, Sigma, B1793) was used to treat mesenchymal-like EpCAM$^-$ cells. Specifically, 400 000 S3T1 EpCAM$^-$ SCC cells were seeded in 6-well plates with 200 nM of BafA or DMSO in the culture medium for 24 hours. Treated cells were then analyzed by FACS analysis or cell pellets were collected for western blot analysis.

2. Tumor-cell grafting and *in vivo* treatments

Isolated GFP$^+$ full epithelial SCC cells from WD-SCCs, GFP$^+$ epithelial EpCAM$^+$ SCC cells from MD/PD-SCCs and GFP$^+$ mesenchymal-like EpCAM$^-$ SCC cells from PD-SCCs (#10 000 cells) were mixed 1:1 with matrigel basement membrane matrix (Corning, 356234), and subcutaneously engrafted in the back skin of 6–8-week syngeneic males (C57Bl6/FVB F1 background). Tumor growth volume was monitored every 2-3 days by applying $V = \pi/6 \times L \times W^2$. Tumors were resected when reached a critical size for processing by flow cytometry and immunohistology assays. Animal housing, handling and all procedures involving mice were approved by the Institutional Animal Care and Use Committee IDIBELL (Barcelona, Spain), in accordance with the Spanish national guidelines and regulations. Mice were housed at 2-5 animals per cage with a 12-hour light/dark cycle at a constant temperature of 23ºC with food and water *ad libitum*.

To study the role of CXCL1 and CXCL2 signaling on tumor growth and tumor immune landscape, PD-SCCs were generated in immunocompetent syngeneic mice by engrafting S3T1 EpCAM$^-$ cells as described above. Once tumors were palpable (approximate volume of 14 mm^3) mice were randomly assigned to a group and treated intraperitoneally with the selective small-molecule antagonist of CXCR2 (CXCL1 and CXCL2 receptor) SB225002 6 days per week at a dose of 2 mg/kg or with solvent solution (Table 2). SB225002 powder was solubilized according to the manufacturer's instructions by adding sequentially 10% DMSO >> 40% PEG300 >> 5% Tween-80 >> 45% saline. Once tumors achieved a critical size (approximately after 30 days of treatment) were excised and processed.

To assess the function of CSF3 signaling on tumor growth and tumor immune landscape, PD-SCCs were generated in immunocompetent syngeneic mice by engrafting S3T1 EpCAM$^-$ cells as described above. Once tumors were palpable (approximate volume of 14 mm^3) mice were randomly assigned to a group and treated with anti-CSF3 or anti-IgG$_1$ 2 days per week at a dose of 10 µg (Table 2). Anti-CSF3 or anti-IgG$_1$ drugs were reconstituted at 0.5 mg/mL in sterile PBS according to the manufacturer's instructions. Once tumors achieved a critical size (approximately after 30 days of treatment) were excised and processed.

To determine the role of CCL2 signaling on tumor growth and tumor immune landscape, PD-SCCs were generated in immunocompetent syngeneic mice by engrafting S3T1 EpCAM$^-$ cells as described above. Once tumors were palpable (approximate volume of 14 mm^3) mice were randomly assigned to a group and treated with anti-CCL2 or anti-IgG 2 days per week at a dose of 200 µg (Table 2). Once tumors achieved a critical size (approximately after 30 days of treatment) were excised and processed.

***In vivo* treatment**	**Clone**	**Source**
Anti-mouse G-CSF Antibody	67604	R&D systems (MAB414)
Rat IgG_1 Isotype control	43414	R&D systems (MAB005)
*InVivo*Mab anti-mouse/human/rat CCL2	2H5	BioXCell (BE0185)
*InVivo*Mab polyclonal Armenian hamster IgG	/	BioXCell (BE0091)
SB225002	/	MedChemExpress (HY-16711)

Table 2: Drugs used in *in vivo* treatments.

3. Fluorescent activated cell sorter (FACS) analysis and isolation of SCC cells

To analyze mouse tumors fresh samples were mechanically minced and enzymatically digested ON at 37ºC in soft mix with RPMI 1640 GlutaMAX medium (Life Technologies, 61870044) supplemented with 10% FBS (Life Technologies, 10270106), 20 mM HEPES (Sigma, H3537), 1% antibiotic-antimycotic (Biowest, L0010-100), 28.8 U/ml collagenase type I (Sigma, C0130) and 0.42 U/ml dispase (Life Technologies, 17105041). Obtained cell suspensions were filtered with a 70 µm cell strainer (Corning, 087712) and depleted of erythrocytes by incubating with ACK lysis buffer (Lonza, BP1-548E) for 10 min at RT. Endothelial cells were depleted by incubating in a rotary mixer with a purified rat anti-mouse CD31 antibody (1/100, BD Bioscience, 550274) for 30 min at 4ºC, and then with Dynabeads anti-rat IgG (3/100, Life Technologies, 11035) for 30 min at 4ºC. For cell surface staining, ~100.000 isolated cells were incubated with flow cytometry antibodies (Table 3) in blocking buffer (5% FBS in PBS) with 0.01 µg/µL IgG (Sigma, I5381) for 30 min at 4ºC. Next, cells were washed with wash buffer (0.5% BSA, 2 mM EDTA in PBS) and resuspended in analysis buffer (2% FBS, 2 mM EDTA in PBS). Viability was determined by DAPI (Thermo Scientific, 62248) staining exclusion. FACS analysis and sorting were performed in BD Bioscience Fusion II equipment. Obtained data were analyzed using FlowJo 10.6 Software.

Antibody	**Clone**	**Dilution**	**Source**
CD11b APC	M1/70	1/250	BioLegend (101212)
CD11b PE	M1/70	1/200	BD Bioscience (557397)
CD11b PE/Cyanine7	M1/70	1/250	BioLegend (101215)
CTLA-4 PE/Cyanine7	UC10-4B9	1/250	BioLegend (106313)

LAG-3 PE/Cyanine7	C9B7W	1/250	BioLegend (125225)
PD-L1 PE/Cyanine7	10F.9G2	1/200	BioLegend (124313)
PD-1 APC/Cyanine7	29F.1A12	1/350	BioLegend (135223)
CD3ε APC	145-2C11	1/300	BioLegend (100311)
EpCAM APC-eF780	G8.8	1/400	eBioscience (47-5791-82)
TIM-3 PE/Cyanine7	B8.2C12	1/250	BioLegend (134009)
CD4 PE/Cyanine7	RM4-5	1/300	BioLegend (100527)
CD45 PE	30-F11	1/350	TONBO (50-0451-U100)
CD8a PE	53-6.7	1/400	BioLegend (100707)
F4/80 PE	BM8	1/200	BioLegend (123110)
Ly-6C PE/Cyanine7	HK1.4	1/150	BioLegend (128017)
Ly-6G APC	1A8	1/150	BioLegend (127613)
MHC-I (H-2K^b) PE/Cyanine7	AF6-88.5	1/200	BioLegend (116519)
MHC-II (I-A/I-E) PE/Cyanine7	M5/114.15.2	1/400	BioLegend (107629)
NK-1.1 PE	PK136	1/400	BioLegend (108707)
TIGIT PE/Cyanine7	1G9	1/250	BioLegend (142107)

Table 3: Cell surface mouse conjugated antibodies used in flow cytometry assays.

4. Patient cSCC and HNSCC samples

Samples of cSCC and HNSCC patients treated with ICI therapy were supplied by the Plastic Surgery and Pathology Units of the Hospital Universitari de Bellvitge (Barcelona, Spain). Sample collection protocol was supervised and approved by the Research Ethics Committee of the Hospital Universitario de Bellvitge (Barcelona, Spain). All patients were fully informed about the study before giving their signed consent to be included in it.

5. Bone marrow derived macrophages (BMDM) culture

To obtain primary cultures of BMDM fresh femur and tibiae from euthanized mice were processed. Muscle tissue was removed from bones and the end of bones was cut off using disposable scalpers. Femur and tibia were put inside a 200 µL Eppendorf with a hole in the bottom (opened with a needle). This 200 µL Eppendorf was centrifuged at the highest speed for 15 seconds inside a 1.5 mL Eppendorf. A red pellet on the bottom of the 1.5 mL Eppendorf is formed which includes the bone marrow. Pellets were resuspended with macrophage induction medium (DMEM high glucose GlutaMAX, 10% FBS, 1% A/A, 25 mM HEPES (Sigma, H0887) and 10 ng/mL CSF1 (Peprotech, 315-02)) and cells were seeded in 100 mm cell culture dish untreated at a ratio of 5 dishes per leg for 5-7 days in a humidified incubator at 37ºC and 5% CO_2. Then, monocytes were induced into macrophages. Macrophage polarization was achieved by culturing induced macrophages with the macrophage induction medium supplemented with soluble molecules 10 ng/mL LPS (Sigma, L2630) or 10 ng/mL IL-4 (Sigma, I1020) for 24 hours or by

culturing induced macrophages with 72-hour conditioned medium from primary SCC cells with 10 ng/mL CSF1 for 24 hours. Polarized macrophages were collected to be analyzed by RT-qPCR or cultured for 48 hours in DMEM-F12 GlutaMAX medium with 1X B27 and 1% P/S to obtain BMDM conditioned medium for further experiments.

6. Splenic MDSCs analysis and sorting

For splenic MDSCs obtention, mice were euthanized, and the spleen was collected into RPMI 1640 GlutaMAX medium with 10% FBS, 20 mM HEPES and 1% A/A. Using a plunger end of a 1 mL syringe the spleens were gently mashed through a 70 μm cell strainer. Obtained single cell suspensions were depleted of erythrocytes by incubating with ACK lysis buffer for 3 min at 4ºC. Isolated splenocytes were incubated with conjugated antibodies (Table 3) in blocking buffer (5% FBS in PBS) with 0.01 μg/μL IgG for 30 min at 4ºC, then washed with 0.5% BSA, 2 mM EDTA in PBS, and finally resuspended in analysis buffer (2% FBS, 2 mM EDTA in PBS). FACS-sorting was performed in BD Bioscience Fusion II equipment. PMN-MDSCs ($CD11b^+$ $Ly6C^+$ $Ly6G^+$) and M-MDSCs ($CD11b^+$ $Ly6C^+$ $Ly6G^-$) were sorted into RPMI 1640 GlutaMAX medium with 10% FBS, 20 mM HEPES, and 1% A/A and cultured in DMEM-F12 GlutaMAX medium with 1X B27 and 1% P/S for 48 hours in a humidified incubator at 37ºC and 5% CO_2. Next, splenic MDSCs conditioned medium and cell pellets were collected for further analysis.

7. RNA extraction, reverse transcription and quantitative real-time PCR analysis

RNA was extracted from isolated cells by using TRIzol Reagent (Invitrogen, 15596026) and chloroform and precipitated by isopropanol and ethanol. Isolated RNA was quantified in Nanodrop 2000. Reverse transcription was performed using the kit High-Capacity cDNA Reverse Transcription kit (Applied Biosystems, 4374966). 2 ug of RNA were retrotranscribed into cDNA following the indicated conditions: 10 min at 25ºC, 2 hours at 37°C and 10 min at 85°C. Quantitative real-time PCR reactions were carried out in triplicate by mixing 20 ng of cDNA with 1X PowerUp SYBR Green Master Mix (Applied biosystems, A25742) and 500 nM of specific forward and reverse primers targeting each gene of interest (Table 4). *Gapdh* and *Ppia* were used to normalize the gene expression values for all mouse samples. Quantitative Polymerase Chain Reaction (qPCR) was performed using the QuantStudio 7 Pro machine (Applied biosystems) following the indicated conditions: 2 min at 50ºC, 10 min at 95 ºC and 40 cycles of 15 sec 95ºC + 1 min 65ºC followed by standard melting curve dissociation. Relative gene expression was calculated using the $2^{-\Delta\Delta Ct}$ analysis method with *Gapdh* and *Ppia* as housekeeping genes.

Gene	Forward (5' - 3')	Reverse (5' - 3')
Arg1	TTTTAGGGTTACGGCCGGTG	CCTCGAGGCTGTCCTTTTGA
β2-microglobulin	TCACACTGAATTCACCCCCA	TCACATGTCTCGATCCCAGT
Cd163	GTGCTGGATCTCCTGGTTGT	CGTTAGTGACAGCAGAGGCA

Csf1	AGTGGAAGTGGAGGAGCCAT	TGGTGAGGGGTCATAGAATCC
Cxcl10	ATGACGGGCCAGTGAGAATG	TCGTGGCAATGATCTCAACAC
Cxcl2	CCAAAAGATACTGAACAAAGGCA	CGAGGCACATCAGGTACGA
Cxcl9	GCCATGAAGTCCGCTGTTCT	TAGGGTTCCTCGAACTCCACA
Gapdh	AGGTCGGTGTGAACGGATTTG	TGTAGACCATGTAGTTGAGGTCA
Gas6	GGAGGCCTGCCAGAAGTATC	TGCTTGTACGAGGCCGTATC
Hnrnpr	CCAGCTCTGCCCTGCATAAT	GGCCTGCCTCTATCAGTGTC
Il-1b	TGCCACCTTTTGACAGTGATG	TGATGTGCTGCTGCGAGATT
Il-6	ACCAGAGGAAATTTTCAATAGGC	TGATGCACTTGCAGAAAACA
Infgr1	GGTGCCTGTACCGACGAATG	AGTCCAGGAACCCGAATACAC
Infgr2	CGAAACAACAGCAAATGCCTC	CAATGCGAAGATGCCCAACG
Inos	TCCTGGACATTACGACCCCT	CTCTGAGGGCTGACACAAGG
Irf-1	ATTGACAGCCCTCGAGGAAAC	TTCGTGATCGACGCATGTCA
Mex-3c	GTCGGACGCCAGGGTTGTAA	ATGGGTTCTTCACCACGAACA
Mhc-I (H-2d)	ACCCAGGACATGGAGCTTGT	GCTCCAAGGACACCCAGAAC
Mhc-II	AAGCTTTGACCCCCAAGGTG	GGAGCCTCATTGGTAGCTGG
Pd-l1	CGCCTGCAGATAGTTCCCAA	AGCCGTGATAGTAAACGCCC
Pd-l2	TGCTGGGTGCTGATATTGACA	GGGGCTGTCACGGTGAATAA
Ppia	GTTCATGCCTTCTTTCACCTTCCC	CAAATGCTGGACCAAACACAAACG
Tap1	AAGTCTGGACCACGAGTGTCT	TGACAGCCCCTCTGATCACC
Tap2	GCAGACGACTTCATAGGGGAAAT	TCTCCAGTTCTGTAGGGCCTG
Tapasin	ATACTTCAAGGTGGATGACCCG	GACTTCTAGCCCACTTCGCC
Tnf-α	GCCTCTTCTCATTCCTGCTTG	CTGATGAGAGGGAGGCCATT

Table 4: Primers for mouse mRNA quantification in qRT-PCR assays.

8. Histology, immunohistochemistry and immunofluorescence assays

Mouse and patient tumor samples were fixed in 4% formaldehyde (PanReac, 252931) overnight (ON) at 4ºC. Next, samples were paraffin-embedded and sectioned at 4 µm using a microtome (Leica). To quantify necrotic areas, tumor sections were stained with hematoxylin and eosin (H/E) and mounted with DPX mounting medium (Sigma, 06522). Tumor sections were captured using bright-field microscopy (Nikon Eclipse 80i). Tumor micrographs were overlapped to obtain whole digital sections of tumors. Next, viability was analyzed with the Weka Training Segmentation Plugin available in the Fiji Image J software, which combines machine learning algorithms with selected image features to produce pixel-based segmentations. The selection of viable and necrotic regions (identified by nuclear fragmentation) provides a labeled result for the whole tumor section, from which the percentages of viable and necrotic areas were calculated.

Mouse and patient tumor paraffin-embedded sections were deparaffinized and antigen retrieval was performed using 10 mM sodium citrate (pH 6.0) or 10 mM TRIS / 1 mM EDTA (pH 9.0), depending on the primary antibody. Endogenous peroxidase activity was blocked with 3% hydrogen peroxide (Millipore, 107210) for 10 min at RT. Next, samples were blocked with 5% horse serum (HS, Life Technologies, 16050122) in Tris-buffered saline (TBS) buffer 1X (TBS; 10 mM Tris-HCl pH 8, 150 mM NaCl) with 0,1% Tween-20 (Merck, 9005-64-5) for 1h at RT, and incubated with primary antibodies (Table 5) ON in 3% HS in TBS 1X with 0,1% Tween-20 at 4ºC in a humidified chamber. For immunohistochemistry (IHC) detection, sections were incubated with a secondary antibody (Table 6) in 3% HS in TBS 1X with 0,1% Tween-20 for 1h at RT, followed by 3,3'-Diaminobenzidine (DAB) developing system (Dako, K3468). Tumor sections were then counterstained with hematoxylin, mounted with permanent DPX mounting medium and captured using bright-field microscopy (Nikon Eclipse 80i). For immunofluorescence (IF) detection, samples were incubated with secondary antibodies (Table 6) in 3% HS in TBS 1X with 0,1% Tween-20 for 1h at room temperature. Nuclei were stained with 4'6'-Diamidino-2-Phenylindole (DAPI, Life Technologies, D3571) 1/5000 for 10 min at RT. Samples were mounted with Vectashield mounting medium (Palex, 416397), and micrographs were captured with a Leica TCS SP5 confocal microscope. All images were analyzed with Fiji Image J software.

Reactivity	Antibody	Host	Source	Retrieval	Use
Mouse	CD163	Rb	Abcam (ab182422)	10 mM sodium citrate (pH 6.0)	IHC: 1/100
	CD8α (D4W2Z)	Rb	Cell Signaling (98941)	10 mM sodium citrate (pH 6.0)	IHC: 1/50
	FoxP3 (D608R)	Rb	Cell Signaling (12653)	10 mM sodium citrate (pH 6.0)	IHC: 1/100
	GzmB	Gt	R&D systems (AF1865)	10 mM sodium citrate (pH 6.0)	IHC: 1/50
	Ly6-G/Ly6C (Gr-1)	Rt	R&D systems (MAB1037)	10 mM sodium citrate (pH 6.0)	IF: 1/200
Human	CD8α (144B)	Ms	Abcam (ab17147)	10 mM TRIS / 1 mM EDTA (pH 9.0)	IF: 1/50
	PD-1 (EPR4877 2)	Rb	Abcam (ab137132)	10 mM TRIS / 1 mM EDTA (pH 9.0)	IF: 1/100

Table 5: Primary antibodies used in immunohistochemistry and immunofluorescence mouse and human assays. Gt, Goat; Ms, Mouse; Rb, Rabbit; Rt, Rat. IF, immunofluorescence; IHC, immunohistochemistry.

Antibody	Host	Source	Use
Anti-Mouse Alexa Fluor 647	Gt	Invitrogen (A21235)	IF: 1/200
Anti-Rabbit Alexa Fluor 568	Dy	Invitrogen (A10042)	IF: 1/200
Anti-Rat Alexa Fluor 546	Gt	Invitrogen (A11081)	IF: 1/400
Anti-Rabbit EnVision+System-HRP	-	Dako (K4003)	IHC: -
Anti-Goat Immunoglobulins/HRP	Rb	Dako (P044901-2)	IHC: 1/100

Table 6: Secondary antibodies used in immunohistochemistry and immunofluorescence assays. Dy, Donkey; Gt, Goat; Rb, Rabbit. IF, immunofluorescence; IHC, immunohistochemistry.

9. Obtention of total protein lysates and western blotting (WB)

To extract proteins, obtained cell pellets were resuspended in 80 µL of lysis buffer: 350 mM NaCl, 50 mM Tris pH 8, 5 mM EDTA, 0.5% NP_4O, 10% glycerol, cOmplete protease inhibitor cocktail 1X (Roche, 11697498001), PhosSTOP 1X (Roche, 4906845001), 2 mM NaF, 0.1 mM Na_3VO_4, 1 mM DTT, 1 mM phenylmethanesulfonylfluoride (PMSF) and 0.1% SDS. Cell pellets were then maintained for 20 minutes at 4ºC in lysis buffer, sonicated at 30kHz 1 Cycle 100% amplitude for 10 seconds twice (UP50H, Biotech) and centrifugated at 12.000 rpm for 10 min at 4ºC. Obtained supernatants were transferred into new Eppendorf and total protein concentration was measured using Bradford's protein assay (Bio-rad, 5000006). The absorbance lectures were quantified at λ=595 nm using the BioTek PowerWave XS microplate reader.

Protein extracts were mixed with 1X SDS-Page sample loading buffer (4X: 50 mM Tris-HCl pH 6.8, 2% SDS, 10% glycerol, 12.5 mM EDTA, 0.02 bromophenol blue, 12% 2-mercaptoethanol). Samples were heated for 5 min at 95ºC to denature proteins. Electrophoresis was performed after loading 40 µg of protein from each condition in 10% polyacrylamide gel and ran under 100V for 2h in electrophoresis buffer (25 mM Tris-HCl, 192 mM Glycine, 1% SDS). Then, proteins were transferred via wet blotting system to 0,2 µm Amersham Protran Western blotting nitrocellulose membranes (Sigma, GE10600001) for 2h at 200 mA in transfer buffer (25 mM Tris-HCl pH 8.3, 192 mM Glycine, 20% methanol). Next, membranes were stained with Ponceau S solution (Sigma, P7170). Membranes were washed with 1X TBS 0,1% Tween 20 and blocked a least for 1 hour with 5% BSA in TBS-Tw at RT in agitation. Membranes were incubated O/N at 4ºC in agitation with primary antibody solution (Table 7). The next day, membranes were rinsed with TBS-Tw 3 times for 10 min and incubated with secondary antibody (Table 7) diluted in 5% milk TBS-Tw for 1 hour at RT with agitation. Membranes were then washed with TBS-Tw 3 times and incubated with the ECL western blotting detection reagents (Sigma, GERPN2209) to detect specific protein bands. Detection of the labeling was achieved by chemiluminescence analysis at chemidoc (Amersham Imager 600). The intensity of the bands was quantified using the Fiji Image J software.

Antibody	Host	Source	Use	Secondary antibody
Anti-β-actin-HRP	Ms	Sigma (A3854)	1/500 000 in 5% milk TBS-Tw	N/A
Anti-Histone H3 (D1H2)	Rb	Cell signaling (4499)	1/50 000 in 5% milk TBS-Tw	1/2000 Goat Anti-Rabbit Immunoglobulins/HRP (Dako, P0448)
Anti-Tri-Methyl-Histone H3 (Lys27) (C36B11)	Rb	Cell signaling (9733)	1/1000 in 5% milk TBS-Tw	1/2000 Goat Anti-Rabbit Immunoglobulins/HRP (Dako, P0448)
Anti-LC3	Rb	MBL (PD014)	1/1000 in 5% milk TBS-Tw	1/2000 Rabbit Anti-Rat Immunoglobulins/HRP (Dako, P0450)
Anti-MHC-I	Rt	Biorad (MCA2398)	1/500 in 5% milk TBS-Tw	1/2000 Rabbit Anti-Rat Immunoglobulins/HRP (Dako, P0450)
Anti-p-STAT1 (Tyr701) (58D6)	Rb	Cell signaling (9167)	1/1000 in 1% milk TBS-Tw	1/2000 Goat Anti-Rabbit Immunoglobulins/HRP (Dako, P0448)

Table 7: Primary and secondary antibodies used in western blot assays. Rb, Rabbit; Rt, Rat; Ms, Mouse.

For Histones detection a different procedure was performed to ensure the separation of proteins from DNA. Cell pellets were resuspended in Laemmli buffer 1X (0.0625 M Tris-HCl pH 6.8, 2% SDS. 15% glycerol and 0.01% bromophenol blue), sonicated 10 seconds three times and quantified by measuring the absorbance at λ=260 nm in the Nanodrop 2000. 20 µg of samples were loaded with Laemli buffer supplemented with 1.25% 2-mercaptoethanol in 15% polyacrylamide gel and ran under 100V for 2h in electrophoresis buffer. Then, proteins were transferred via wet blotting system to 0,2 µm Amersham Protran Western blotting nitrocellulose membranes at 10 V in transfer buffer O/N at 4ºC. The next day, membranes were washed three times with TBS-Tw and incubated with primary antibodies (Table 7) for 2 hours at RT in agitation. After the primary antibody incubation, the procedure was followed as described above.

10. Immunocytochemistry

To analyze antigen expression and location in *in vitro* cells immunocytochemistry assays were performed. Round cover glasses (Harvard Apparatus, BS4 64-0702) were introduced into a 24-well plate (Corning, 353047) and treated with poly-L-lysine (Sigma, P4832) to ensure cell attach. Full epithelial cancer cells (2C3) and mesenchymal-like EpCAM$^-$ cancer cells (S3T1 EpCAM$^-$) were seed (#40 000 cells) and cultured for 48 hours in a humidified incubator at 37ºC and 5% CO_2. Next, cells were washed with PBS, fixed with 4% paraformaldehyde (PFA) for 15 min at

RT and washed again. Cells were then permeabilized by adding 0.1% Triton PBS 10 min a RT and washed with PBS. Next, cells were blocked with 5% BSA PBS 0,1% Tw (PBS-Tw) for 2 hours at RT and incubated with primary antibody rabbit anti-MHC class I (Abcam, ab281901) in 3% BSA PBS-Tw O/N at 4ºC. The next day, cells were washed with PBS-Tw and incubated with secondary antibody Anti-Rabbit Alexa Fluor 568 in 3% BSA PBS-Tw for 1 hour at RT. Cells were then washed with PBS and nuclei were stained with DAPI 1/5000 for 10 min at RT. Finally, cells were mounted with Vectashield mounting medium, and micrographs were captured with a Leica TCS SP5 confocal microscope. All images were analyzed with Fiji Image J software.

11. Mouse cytokine proteome profiler

Cytokines secreted by full epithelial cancer cells and mesenchymal-like EpCAM$^-$ cancer cells were detected using the mouse cytokine array proteome profiler array (R&D systems, ARY006), which are membranes spotted with a duplicate of antibodies against 40 different mouse cytokines. The array was proceeded as indicated by the manufacturer and 600 µL of the conditioned medium was loaded into each membrane. Cytokines secreted by splenic MDSCs were detected using the mouse XL cytokine array proteome profiler array (R&D systems, ARY028), which are membranes spotted with a duplicate of antibodies against 111 different mouse cytokines (Table 8). The array was proceeded as indicated by the manufacturer and 400 µL of the conditioned medium was loaded into each membrane.

Detection of the labeling was achieved by chemiluminescence analysis at chemidoc (Amersham Imager 600). The intensity of the dots was quantified using the Fiji Image J software.

Coordinate 1	Coordinate 2	Analyte / Control	Entrez Gene ID
A1	A2	Reference Spot	N/A
A3	A4	Adiponectin/Acrp30	11450
A5	A6	Amphiregulin	11839
A7	A8	Angiopoietin-1	11600
A9	A10	Angiopoietin-2	11601
A11	A12	Angiopoietin-like 3	30924
A13	A14	BAFF/BLyS/TNFSF13B	24099
A15	A16	C1q R1/CD93	17064
A17	A18	CCL2/JE/MCP-1	20296
A19	A20	CCL3/CCL4/MIP-1α/β	20302/20303
A21	A22	CCL5/RANTES	20304
A23	A24	Reference Spot	N/A
B3	B4	CCL6/C10	20305
B5	B6	CCL11/Eotaxin	20292
B7	B8	CCL12/MCP-5	20293
B9	B10	CCL17/TARC	20295
B11	B12	CCL19/MIP-3β	24047
B13	B14	CCL20/MIP-3α	20297
B15	B16	CCL21/6Ckine	18829
B17	B18	CCL22/MDC	20299
B19	B20	CD14	12475
B21	B22	CD40/TNFRSF5	21939
C3	C4	CD160	54215
C5	C6	Chemerin	71660

C7	C8	Chitinase 3-like 1	12654
C9	C10	Coagulation Factor III	14066
C11	C12	Complement Component C5/C5a	15139
C13	C14	Complement Factor D	11537
C15	C16	C-Reactive Protein / CRP	12944
C17	C18	CX3CL1/Fractalkine	20312
C19	C20	CXCL1/KC	14825
C21	C22	CXCL2/MIP-2	20310
D1	D2	CXCL9/MIG	17329
D3	D4	CXCL10/IP-10	15945
D5	D6	CXCL11/I-TAC	56066
D7	D8	CXCL13/BLC/BCA-1	55985
D9	D10	CXCL16	66102
D11	D12	Cystatin C	13010
D13	D14	DKK-1	13380
D15	D16	DPPIV/CD26	13482
D17	D18	EGF	13645
D19	D20	Endoglin/CD105	13805
D21	D22	Endostatin	12822
D23	D24	Fetuin A/AHSG	11625
E1	E2	FGF acidic	14164
E3	E4	FGF-21	56636
E5	E6	Flt-3 Ligand	14256
E7	E8	Gas 6	14456
E9	E10	G-CSF	12985
E11	E12	GDF-15	23886
E13	E14	GM-CSF	12981
E15	E16	HGF	15234
E17	E18	ICAM-1/CD54	15894
E19	E20	IFN-γ	15978
E21	E22	IGFBP-1	16006
E23	E24	IGFBP-2	16008
F1	F2	IGFBP-3	16009
F3	F4	IGFBP-5	16011
F5	F6	IGFBP-6	16012
F7	F8	IL-1α/IL-1F1	16175
F9	F10	IL-1β/IL-1F2	16176
F11	F12	IL-1ra/IL-1F3	16181
F13	F14	IL-2	16183
F15	F16	IL-3	16187
F17	F18	IL-4	16189
F19	F20	IL-5	16191
F21	F22	IL-6	16193
F23	F24	IL-7	16196
G1	G2	IL-10	16153
G3	G4	IL-11	16156
G5	G6	IL-12 p40	16160
G7	G8	IL-13	16163
G9	G10	IL-15	16168
G11	G12	IL-17A	16171
G13	G14	IL-22	50929
G15	G16	IL-23	83430
G17	G18	IL-27 p28	246779
G19	G20	IL-28A/B	330496/338374
G21	G22	IL-33	77125
G23	G24	LDL R	16835
H1	H2	Leptin	16846
H3	H4	LIF	16878
H5	H6	Lipocalin-2/NGAL	16819
H7	H8	LIX	20311
H9	H10	M-CSF	12977
H11	H12	MMP-2	17390
H13	H14	MMP-3	17392
H15	H16	MMP-9	17395

H17	H18	Myeloperoxidase	17523
H19	H20	Osteopontin	20750
H21	H22	Osteoprotegerin/TNFRSF11B	18383
H23	H24	PD-ECGF/Thymidine phosphorylase	72962
I1	I2	PDGF-BB	18591
I3	I4	Pentraxin 2/SAP	20219
I5	I6	Pentraxin 3/TSG-14	19288
I7	I8	Periostin/OSF-2	50706
I9	I10	Pref-1/DLK-1/FA1	13386
I11	I12	Proliferin	18811
I13	I14	Proprotein Convertase 9/PCSK9	100102
I15	I16	RAGE	11596
I17	I18	RBP4	19662
I19	I20	Reg3G	19695
I21	I22	Resistin	57264
J1	J2	Reference Spots	N/A
J3	J4	E-Selectin/CD62E	20339
J5	J6	P-Selectin/CD62P	20344
J7	J8	Serpin E1/PAI-1	18787
J9	J10	Serpin F1/PEDF	20317
J11	J12	Thrombopoietin	21832
J13	J14	TIM-1/KIM-1/HAVCR	171283
J15	J16	TNF-α	21926
J17	J18	VCAM-1/CD106	22329
J19	J20	VEGF	22339
J21	J22	WISP-1/CCN4	22402
J23	J24	Negative Control	N/A

Table 8. Antibodies for cytokine detection and their location within the membrane.

12. ELISA

To analyze the *in vitro* secretion of CXCL1 and CXCL2 $7 \cdot 10^5$ full epithelial SCC cells and $8 \cdot 10^5$ mesenchymal EpCAM$^-$ SCC cells were seeded in 6-well plates and cultured for 48 hours in a humidified incubator at 37ºC and 5% CO_2 in DMEM-F12 GlutaMAX medium with 1X B27 and 1% penicillin/streptomycin. After this, the medium was collected and centrifuged at 12.000 rpm for 10 minutes at 4ºC. Next, the supernatant was collected for the ELISA analysis. The PeproTech ELISA kit (Mini ABTS ELISA Development kit) to detect CXCL1 (900-M127) and CXCL2 (900-M152) was used together with the ABTS ELISA Buffer Kit (900-K00) following the manufacturer's recommendations. Subsequently, the substrate solution (TMB Liquid Substrate) was added and incubated for 20 minutes at room temperature for color development. The absorbance was measured at 450 nm in a VICTOR X Multilabel Plate reader (PerkinElmenr, Inc).

13. Statistical analysis

Statistical tests and graphs were generated using GraphPad Prism 6 (GraphPad Software Inc.). Data is presented as mean ± standard deviation (SD). Statistical analysis was performed applying unpaired two-tailed Student's *t*-test to determine the significance of group differences in each experiment. Significant differences between tumor growth were analyzed by repeated measures ANOVA test. Statistically significant differences between compared groups are represented as: not significant (ns) $p>0.05$; * $p\leq0.05$; ** $p\leq0.01$; *** $p\leq0.001$.

RESULTS

CHAPTER 1: IDENTIFICATION OF TUMOR-INFILTRATING IMMUNE CELLS-DERIVED CYTOKINES RESPONSIBLE FOR PROMOTING THE MESENCHYMAL-LIKE STATE OF CANCER CELLS DURING MOUSE cSCC PROGRESSION

Previous results of the group demonstrated that the infiltrate of immune cells with immunosuppressive features was increased in PD-SCCs as compared to WD-SCCs. Specifically, Treg cells, M-MDSCs, M2-like macrophages, and exhausted $CD8^+$ T cells populations are more strongly recruited into PD-SCCs. In addition, the blockade of PMN-MDSCs recruitment after anti-GR1 treatment in MD/PD-SCCs (containing epithelial plastic cancer cells) decreases the acquisition of mesenchymal traits in cancer cells. Hence, these results suggest that MDSCs-derived signals could be responsible for promoting the acquisition of mesenchymal-like traits by cancer cells during cSCC progression, as described in other tumor types such as breast cancer (Ouzounova et al., 2017) (H. Zhu et al., 2017) and nasopharyngeal carcinoma (Z.-L. Li et al., 2015). In addition, macrophages recruitment and polarization changed concomitantly with cSCC progression suggesting that derived cytokines from macrophages could also play an active role in cSCC progression and acquisition of mesenchymal characteristics. Macrophages derived factors and cytokines have also been described to enhance the acquisition of mesenchymal traits and promote EMT in different tumor conditions such as gastric cancer (W. Li et al., 2019) and lung cancer (Techasen et al., 2012). In addition, previous studies from our group also showed that cSCC progression succeed in athymic nude mice, which are deficient in Treg cells, indicating that Treg cells were not necessary to acquire mesenchymal-like traits in our cSCC model. However, it has not been tackled which specific cytokines secreted by MDSCs or macrophages could be promoting the advance toward a mesenchymal phenotype in cSCCs.

Initially, tumor-infiltrating macrophages and MDSCs from WD-SCCs and PD-SCCs were isolated in order to study if their derived secreted factors and cytokines were promoting the acquisition of mesenchymal features of cSCC tumor cells. To this end, WD-SCCs and PD-SCCs were grown in immunocompetent syngeneic mice by engrafting full epithelial SCC cells or mesenchymal $EpCAM^-$ SCC cells, respectively. Once tumors achieved critical size were excised and enzymatically digested with collagenase and dispase. Two enzymatic digestion protocols were tested: 3 hours *vs.* O/N digestion. Next, $CD11b^+$ $Ly6C^+$ $Ly6G^+$ cells (PMN-MDSCs), $CD11b^+$ $Ly6C^+$ $Ly6G^-$ (M-MDSCs), $CD11b^+$ $F4\text{-}80^+$ $CD206^-$ cells (M1-like macrophages) and $CD11b^+$ $F4\text{-}80^+$ $CD206^+$ (M2-like macrophages) infiltrating in WD-SCCs and PD-SCCs were sorted by flow cytometry to establish primary cultures for 48 hours (Figure 11). However, we obtained low cell sorting recovery rates and sorted immune cells were not viable for a short *in vitro* culture. This could be because enzymatic digestion might be producing cellular damage or immune cells could be highly sensitive to cellular stress during the process of cell sorting.

Alternative methods to obtain macrophages and MDSCs with a similar polarization to that *in vivo* described when infiltrating cSCCs at different stages of progression were explored.

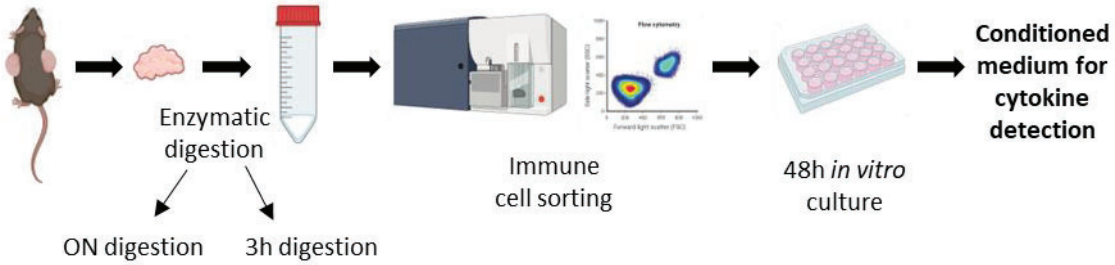

Figure 11. Strategy to isolate tumor-infiltrating immune cells from WD-SCC and PD-SCC tumors. WD-SCCs and PD-SCCs were excised and enzymatically digested 3 hours or O/N with collagenase and dispase to obtain a single-cell suspension. Next, immune cells were sorted by FACS and *in vitro* cultured for 48 hours.

1.1 Generation of bone marrow-derived macrophages (BMDM) and splenic MDSCs *in vitro* cultures with similar characteristics to the respective immune cell populations when infiltrating cSCCs

To study macrophages, BMDMs from tumor-bearing mice were isolated and differentiated to a macrophage phenotype by the treatment with CSF1 for 5 to 7 days (Warren & Vogel, 1985). BMDM can be polarized to M1 or M2-like macrophages by the treatment with soluble factors (Figure 12A). BMDM were differentiated with recombinant LPS or murine IL-4 as a positive control of M1-like and M2-like profiles, respectively (Ying et al., 2013). Hematopoietic cells were differentiated into macrophages by the addition of the cytokine CSF1, which promotes hematopoietic stem cells differentiation into macrophages. Hematopoietic cells that were not stimulated with CSF1 did not proliferate and survive, while induced macrophages by CSF1 presented a characteristic attachment to the cell plate (Figure 12B). BMDM isolated from WD-SCC- or PD-SCC-bearing mice polarized with LPS induced the expression of *Il-1β*, *Tnf-α*, *Il-6*, *Cxcl9*, and *Cxcl10*, which are M1-like markers (Jayasingam et al., 2019) (Figure 13A). Oppositely, the polarization of BMDM isolated from WD-SCC- and PD-SCC-bearing mice with IL-4 induced the expression of *Cd163*, *Arg1*, *Pd-l2*, and *Gas6*, which are M2-like markers (Jayasingam et al., 2019) (Figure 13B). Hence, independently if BMDM were isolated from WD-SCC or PD-SCC-bearing mice LPS polarization induced the expression of M1-like markers while IL-4 polarization induced the expression of M2-like markers.

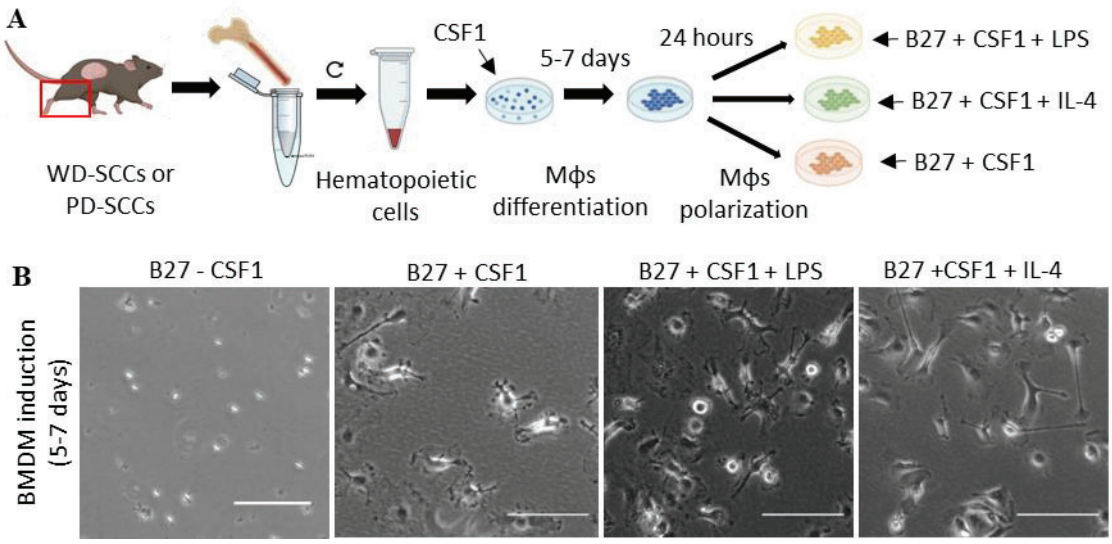

Figure 12. Procedure to isolate and polarize BMDM with soluble molecules. (**A**) Strategy to obtain BMDM cultures. Femur and tibiae were put inside a 200 µL Eppendorf with a hole in the bottom. After centrifugation, a red pellet is formed containing the bone marrow. Cells were seeded with CSF1 for 5-7 days and then obtained BMDM polarized with CSF1 and soluble molecules for 24 hours. (**B**) Representative images of obtained BMDM without CSF1 or with CSF1 and polarized 24 hours with CSF1 alone or combined with LPS or IL-4. Scale bar: 100 µm.

BMDM can polarize towards a similar profile as tumor-infiltrating macrophages (tumor-associated macrophages) if they are incubated with the conditioned medium from cancer cells (Al-Rayahi et al., 2017). BMDMs from WD-SCC-bearing mice were treated with conditioned medium from *in vitro* culture of full epithelial SCC cells and BMDMs from PD-SCC-bearing mice with conditioned medium from *in vitro* culture of EpCAM$^-$ cells from mesenchymal SCCs (Figure 14A). BMDM polarized with conditioned medium from full epithelial SCC cells slightly induced the expression of the M1-like markers *Cxcl10*, *Il-1β*, and *Il-6* in comparison to non-polarized BMDM (F12 B27 group) (Figure 14B). However, the expression levels of the M1 markers *Tnf-α* and *Cxcl9* were not increased in BMDM polarized with conditioned medium from full epithelial SCC cells. By contrast, BMDM with conditioned medium from mesenchymal EpCAM$^-$ SCC cells slightly induced the expression of the M2-markers *Arg1*, *Cd163*, and *Gas6* in comparison to non-polarized BMDM (Figure 14C). The expression of the M2-marker *Pd-l2* was not increased in BMDM polarized with conditioned medium from mesenchymal EpCAM$^-$ SCC cells. Secreted factors from full epithelial SCC cells promote the expression of certain M1-markers while secreted factors from mesenchymal EpCAM$^-$ SCC cells promote the expression of specific M2-markers (Figure 14D). Hence, our results indicate that tumor cells polarize BMDM towards M1-like or M2-like profiles with particularities. This matches the current knowledge of macrophage polarization where it has been shown that the M1/M2 macrophage categorization is an oversimplistic approach and there is a continuum of multiple intermediate phenotypes between

M1-like and M2-like states (Nahrendorf & Swirski, 2016). These data go in accordance with previous characterization of WD-SCCs and PD-SCCs immune landscape (Lorenzo-Sanz et al., under-review manuscript) where it was shown that they were mainly infiltrated by M1-like macrophages or M2-like macrophages, respectively. Once BMDM were polarized to a similar profile to the one observed in the TME, they were rinsed to ensure the removal of secreted factors from SCC tumor cells, and fresh medium was added for 48 hours. These conditioned mediums during 48 hours of *in vitro* culture of polarized BMDM were collected to study the capability of secreted factors to induce the acquisition of mesenchymal features of plastic EpCAM^{+} SCC cells.

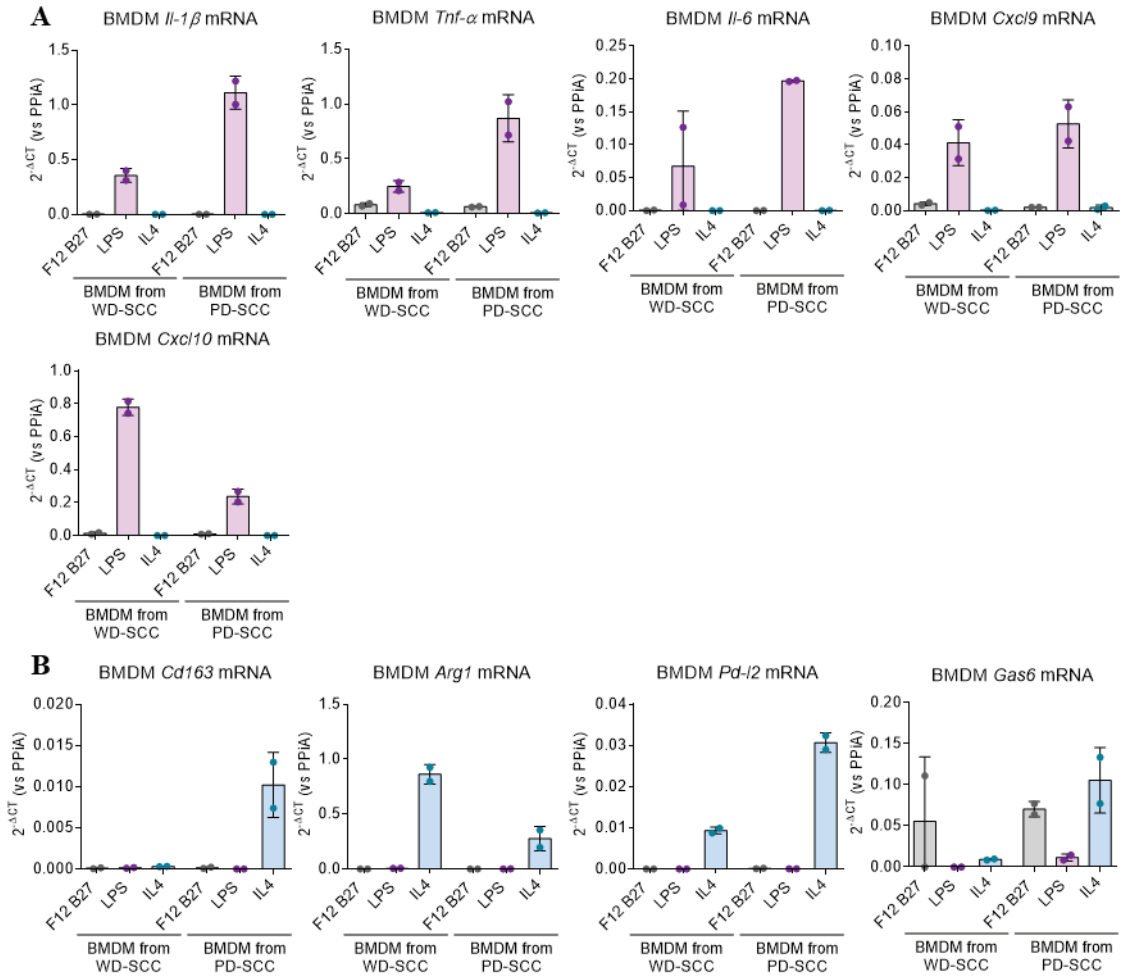

Figure 13. BMDM from WD-SCC or PD-SCC-bearing mice polarized with LPS express M1-like markers while those polarized with IL-4 express M2-like markers. Results shown (mean ± SD) the mRNA levels normalized to *Ppia* of (**A**) M1-like marker genes and (**B**) M2-like marker genes on the indicated BMDM cell cultures polarized with CSF1 + F12 B27 alone (control) or CSF1 + F12 B27 combined with LPS or IL-4. BMDM from WD-SCCs and PD-SCC-bearing mice were polarized with LPS and IL-4. Dots represent independent experiments (*n=2*).

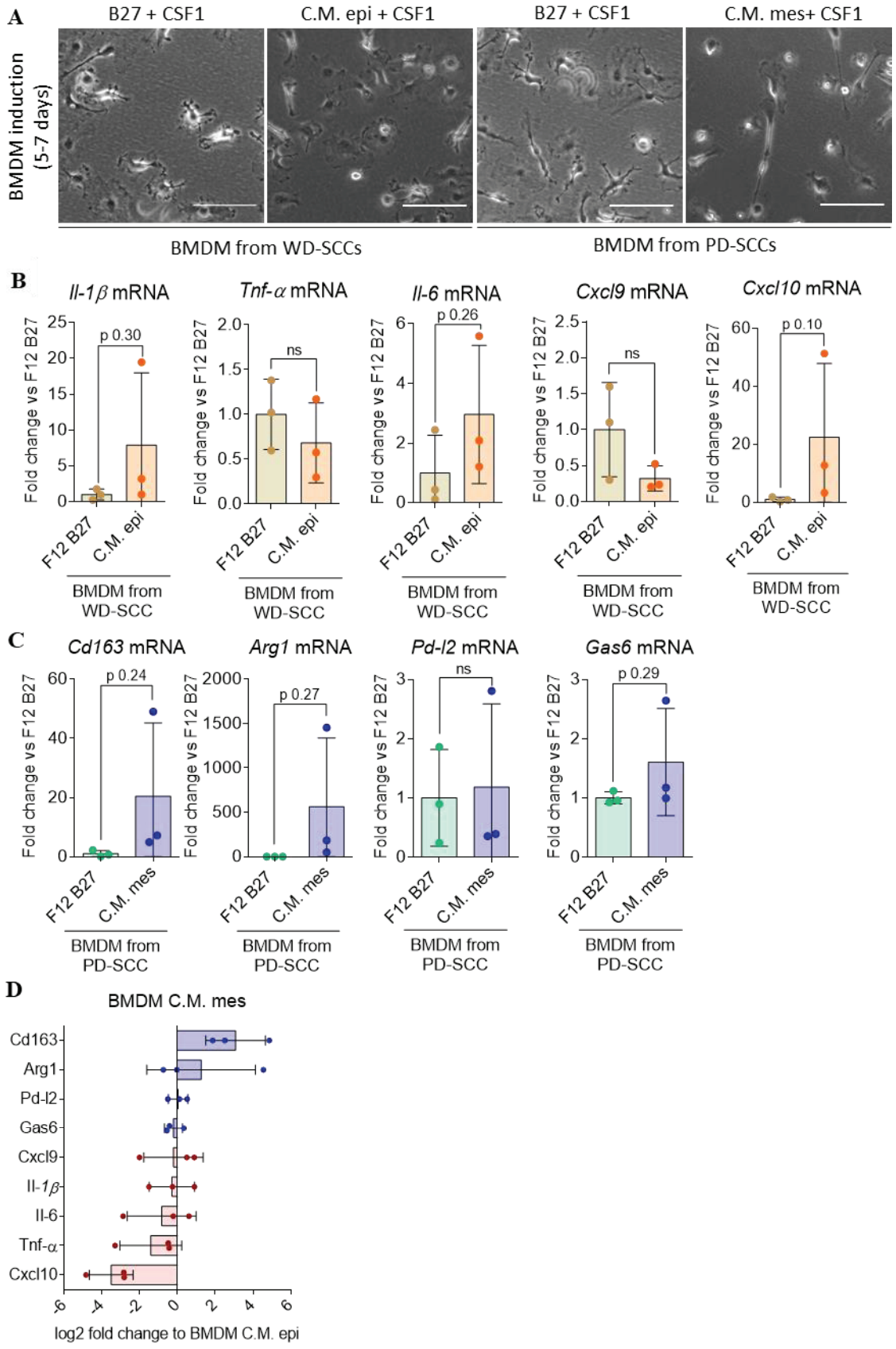

Figure 14. Figure legend on next page.

Figure 14. Characterization of mouse BMDM polarized with conditioned medium from full epithelial SCC cells or with conditioned medium from mesenchymal EpCAM$^-$ SCC cells. (**A**) Representative images of BMDM polarized with CSF1 alone (F12 B27) or combined with conditioned medium from full epithelial SCC cells or from mesenchymal EpCAM$^-$ SCC cells. Scale bar: 100 µm. (**B**) Results show (mean ± SD) the mRNA level fold change to control F12 B27 normalized to *Gapdh* and *Ppia* of M1-like marker genes in BMDM polarized with conditioned medium from full epithelial SCC cells. (**C**) Results show (mean ± SD) the mRNA level fold change to control F12 B27 normalized to *Gapdh* and *Ppia* of M2-like marker genes in BMDM polarized with conditioned medium from mesenchymal EpCAM$^-$ SCC cells. (**F**) Results show (mean ± SD) the $\log_2$ of mRNA fold change of M1- and M2-like markers expression in BMDM polarized with conditioned medium from mesenchymal EpCAM$^-$ SCC cells *vs* BMDM polarized with conditioned medium from epithelial SCC cells. Only BMDM from WD-SCC-bearing mice were polarized with conditioned medium from full epithelial SCC cells while only BMDM from PD-SCC-bearing mice were polarized with conditioned medium from mesenchymal EpCAM$^-$ cells. Dots represent independent experiments (*n=3*). Statistical significance of the differences observed between compared groups was analyzed using unpaired two-tailed Student's T-test. ns: p>0.05. C.M. epi: conditioned medium from full epithelial SCC cells; C.M. mes: conditioned medium from mesenchymal EpCAM$^-$ SCC cells.

MDSCs are expanded in the spleen of tumor-bearing mice and show immunosuppressive capabilities (C. Liu et al., 2007). To study MDSCs, spleens from mice carrying WD-SCCs (composed of full epithelial SCC cells), MD/PD-SCCs mixed tumors (composed of plastic EpCAM$^+$ and plastic EpCAM$^-$ SCC cells), and PD-SCCs (composed of mesenchymal EpCAM$^-$ SCC cells) were collected. Splenocytes were obtained by a gentile mechanical disruption of spleens. Next, splenic MDSCs were sorted by flow cytometry and *in vitro* cultured for 48 hours (Figure 15A). Specifically, CD11b$^+$ Ly6C$^+$ Ly6G$^+$ cells (PMN-MDSCs) and CD11b$^+$ Ly6C$^+$ Ly6G$^-$ cells (M-MDSCs) were sorted. According to the literature, the spleens of tumor-bearing mice were bigger than the ones from tumor-free mice. As cSCC advanced the spleens were increasingly larger (Figure 15B). In addition, the presence of immune myeloid cells within the spleen, identified by the surface expression of CD11b$^+$, also increased as cSCC advanced and spleens were larger (Figure 15C). The proportion of PMN-MDSCs and M-MDSCs within CD11b$^+$ cells was similar in spleens from tumor-free mice and WD-SCC, MD/PD-SCC, and PD-SCC-bearing mice. Given that the presence of CD11b$^+$ cell population was increased in spleens from tumor-bearing mice and the proportion of PMN-MDSCs and M-MDSCs within CD11b$^+$ cells was maintained, the global presence of MDSCs in spleens from tumor-bearing mice was higher. Both PMN-MDSC and M-MDSC populations were more abundant in the spleens as cSCC progressed and spleens were aberrantly bigger (Figure 15D).

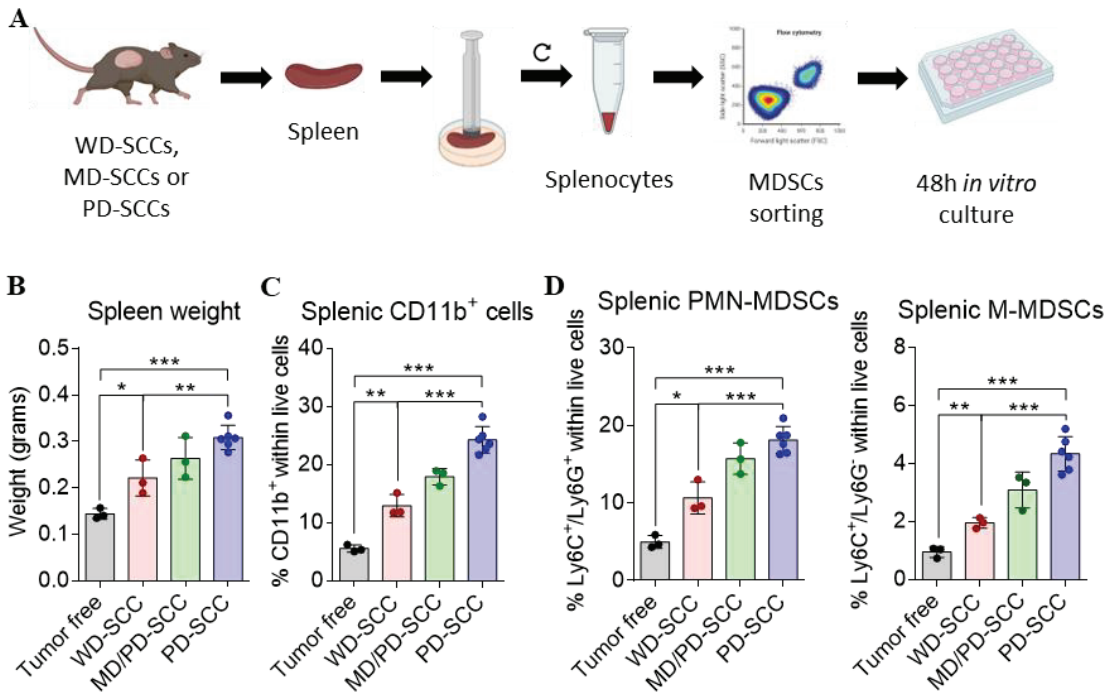

Figure 15. Isolation strategy of splenic MDSCs from WD-SCC-, MD/PD-SCC-, and PD-SCC-bearing mice. (**A**) Strategy to obtain splenic MDSCs cultures. Spleens were gently mashed through a cell strainer using a plunger end of a syringe obtaining single-cell suspensions. MDSCs were sorted by FACS and *in vitro* cultured for 48 hours. (**B**) Results show (mean ± SD) the fresh weight of excised spleens. Results show (mean ± SD) the percentage of (**C**) splenic CD11b$^+$ within live cells, (**D**) splenic PMN-MDSCs (Ly6C$^+$ Ly6G$^+$), and M-MDSCs (Ly6C$^+$ Ly6G$^-$) within live cells, as analyzed by flow cytometry. Dots represent independent experiments (*n=3-6*). Statistical significance of the differences observed between compared groups was analyzed using unpaired two-tailed Student's T-test. * p≤0.05; ** p≤0.01; *** p≤0.001.

After 48 hours of *in vitro* culture MDSCs expression markers were characterized. A little amount of RNA was obtained from splenic MDSCs and a pool of splenic MDSCs cultures was performed to analyze the expression of several MDSCs markers. Splenic MDSCs expressed *Arg1*, *Inos*, and *Mhc-II*, which are markers of MDSCs populations (Figure 16). *Arg1* expression in splenic MDSCs (both PMN-MDSCs and M-MDSCs) showed a slightly upregulation concomitantly with cSCC progression. Similar behavior was observed in the expression of *Inos* in splenic M-MDSCs while in splenic PMN-MDSCs *Inos* expression was the highest in PMN-MDSCs from MD/PD-SCCs spleens. Finally, *Mhc-II* expression in splenic PMN-MDSCs and M-MDSCs did not show a clear trend during cSCC progression. The characterization of splenic MDSCs showed that PMN-MDSCs and M-MDSCs slightly expressed more immunosuppressive markers *Arg1* and *Inos* when isolated from spleens of PD-SCC-bearing mice than from spleens of WD-SCC-bearing mice, while *Mhc-II* expression remained unaltered (Figure 16). This suggests that MDSCs in the spleen of PD-SCC-bearing mice exhibited more immunosuppressive features than those from

WD-SCC-bearing mice, accordingly to our previous data which showed that M-MDSCs were more frequently infiltrating PD-SCCs than WD-SCCs and presented higher immunosuppressive capabilities (Lorenzo-Sanz et al., under-review manuscript). Conditioned mediums from splenic MDSCs were recovered after 48 hours to analyze the capability of secreted factors to induce the switch to mesenchymal-like states of plastic EpCAM^{+} SCC cells from MD/PD-SCCs, which are epithelial SCC cells with the ability to lose epithelial-differentiation traits and acquire mesenchymal features under specific stimuli (Lopez-Cerda et al., submitted manuscript).

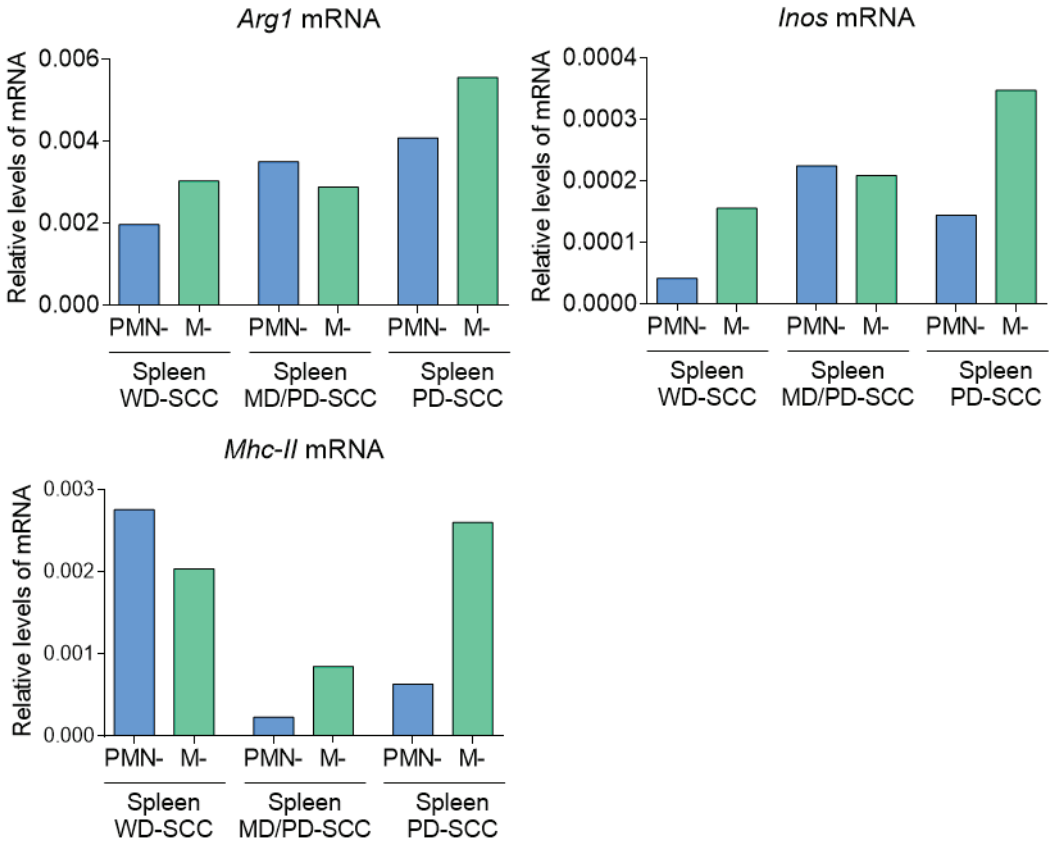

Figure 16. Characterization of the pool of PMN-MDSCs and M-MDSCs cell cultures from spleens from WD-SCC-, MD/PD-SCC-, or PD-SCC-bearing mice. Results show the mRNA levels normalized to *Ppia* of the indicated genes. Data was obtained from the pool of various (3-5) splenic PMN-MDSCs and M-MDSCs *in vitro* cultures for 48 hours. PMN-: PMN-MDSCs; M-: M-MDSCs.

1.2 Study of the capacity of polarized BMDM and splenic MDSC secreted factors to induce the acquisition of mesenchymal-like features in plastic SCC cells

MD/PD-SCCs were generated by injecting plastic EpCAM^{+} SCC cells into immunocompetent syngeneic mice. Once tumors reached a critical size were excised and enzymatically digested to obtain a single-cell suspension. Plastic EpCAM^{high} and plastic EpCAM^{low} SCC cells with the ability to lose epithelial differentiation traits and gain mesenchymal features (Lopez-Cerda et al., submitted manuscript) were sorted by FACS. Specifically, plastic SCC cells can progress from

EpCAM^{high} to EpCAM^{low} and from EpCAM^{low} to EpCAM^{-} when cultured *in vitro* and during *in vivo* tumor growth. To study if secreted factors by polarized BMDM or splenic MDSCs further promoted the acquisition of mesenchymal characteristics, EpCAM^{high} and EpCAM^{low} plastic SCC cells were sorted and *in vitro* cultured with the conditioned medium from the studied immune populations for 4 days. Then, the resulting percentage of EpCAM^{high}, EpCAM^{low}, and EpCAM^{-} tumor cells was evaluated by flow cytometry (Figure 17). Two distinct plastic SCC cells were used to obtain derived plastic SCC cells: plastic S5T2 EpCAM^{+} SCC cells and plastic S2T2 EpCAM^{+} SCC cells (Table 9).

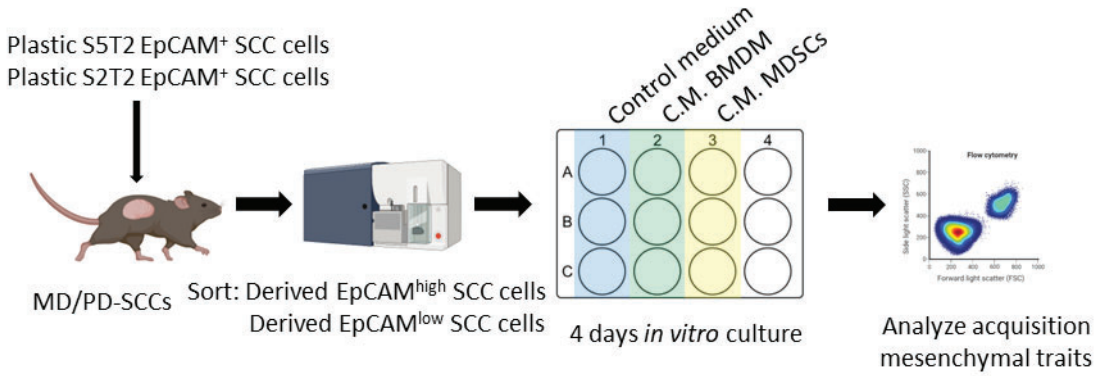

Figure 17. Design of mesenchymal traits acquisition experiment. Strategy to obtain plastic EpCAM^{+} SCC cells and test the acquisition of mesenchymal features. MD/PD-SCCs were excised and enzymatically digested O/N with collagenase and dispase to obtain a single-cell suspension. Next, EpCAM^{high} and EpCAM^{low} SCC cells were sorted by FACS and *in vitro* cultured for 4 days with conditioned medium from polarized BMDM or splenic MDSCs. C.M.: conditioned medium.

Plastic SCC cells	Derived plastic SCC cells
Plastic S5T2 EpCAM^{+}	PL-5 EpCAM^{high} / PL-5 EpCAM^{low}
Plastic S2T2 EpCAM^{+}	PL-2 EpCAM^{high} / PL-2 EpCAM^{low}

Table 9. Derived plastic SCC cells isolated by cell sorting. Plastic S5T2 EpCAM^{+} and plastic S2T2 EpCAM^{+} cells were injected in immunocompetent syngeneic mice to generate MD/PD-SCCs. PL-5 EpCAM^{high} and PL-5 EpCAM^{low} cells were sorted from MD/PD-SCCs generated from plastic S5T2 EpCAM^{+} cells. PL-2 EpCAM^{high} and PL-2 EpCAM^{low} cells were sorted from MD/PD-SCCs generated from plastic S2T2 EpCAM^{+} cells.

The characterization of PL-5 EpCAM^{high} and PL-2 EpCAM^{high} cells by flow cytometry showed that after a period of *in vitro* culture, a percentage of EpCAM^{high} cells progressed to EpCAM^{low} in both cell types. However, neither PL-5 EpCAM^{high} nor PL-2 EpCAM^{high} cells completely lose epithelial marker EpCAM after 7 or 14 days of *in vitro* culture (Figure 18A). When PL-5 EpCAM^{low} and PL-2 EpCAM^{low} cells were established and characterized by flow cytometry it was observed that most of EpCAM^{low} cells reversed to EpCAM^{high} after 4 days of *in vitro* culture.

Longer culture time allowed a percentage of EpCAM^{high} cells to progress back to EpCAM^{low} cells in both cell types, although without losing the expression of EpCAM (Figure 18B). Hence, PL-5 EpCAM^{low} and PL-2 EpCAM^{low} cells presented a certain degree of switch from a more epithelial state (EpCAM^{high}) to a less epithelial and more mesenchymal state (EpCAM^{low}) but did not completely lose the expression of EpCAM. Previously our group characterized EpCAM^{low} SCC cells and observed that these cells partially lose epithelial characteristics and concomitantly gain mesenchymal features, presenting a strong plasticity (Lopez-Cerda et al., submitted manuscript).

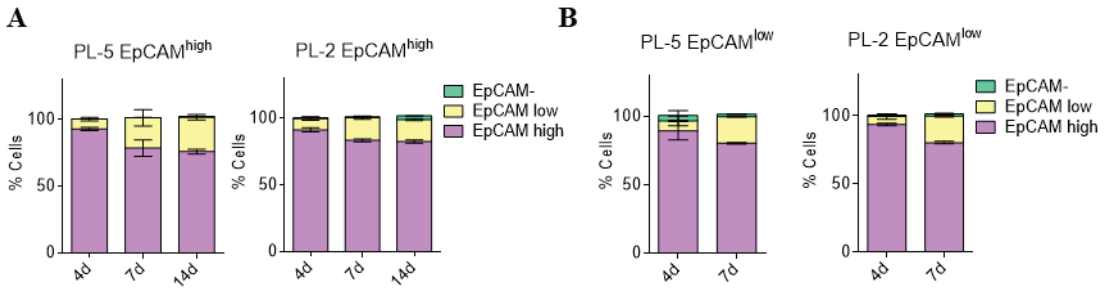

Figure 18. Characterization of obtained plastic EpCAM^{+} SCC cells. Results shown the percentage of EpCAM^{high}, EpCAM^{low}, and EpCAM^{-} SCC cells (mean ± SD) after *in vitro* culture of sorted (**A**) PL-5 EpCAM^{high} and PL-2 EpCAM^{high} SCC cells for 4 days, 7 days, or 14 days without a conditioned medium (F12 B27 alone) and (**B**) PL-5 EpCAM^{low} and PL-2 EpCAM^{low} SCC cells for 4 days or 7 days without a conditioned medium (F12 B27 alone), as analyzed by flow cytometry. Data obtained from 3 independent experiments (*n=3*).

Next, PL-5 EpCAM^{high} and PL-2 EpCAM^{high} SCC cells were cultured for 4 days with a control medium (F12 B27) or with conditioned medium of polarized BMDM or splenic MDSCs cell cultures. As a control, PL-5 EpCAM^{high} and PL-2 EpCAM^{high} cells were treated with the conditioned medium from SCC tumor cells used to polarize BMDM. The conditioned mediums containing secreted factors from the full epithelial SCC cells or mesenchymal EpCAM^{-} SCC cells did not induce the acquisition of mesenchymal traits of PL-5 EpCAM^{high} and PL-2 EpCAM^{high} cells (Figure 19). Hence, possible remaining secreted factors from full epithelial SCC cells or mesenchymal EpCAM^{-} SCC cells when polarizing BMDM will not affect the acquisition of mesenchymal features by plastic SCC cells.

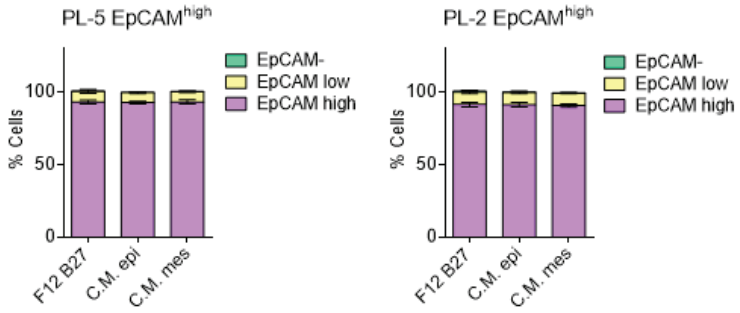

Figure 19. Secreted factors from full epithelial SCC cells or mesenchymal EpCAM$^-$ SCC cells do not promote the acquisition of mesenchymal-like features in plastic EpCAM^{high} SCC cells. Results shown (mean ± SD) the percentage of EpCAM^{high}, EpCAM^{low}, and EpCAM$^-$ SCC cells after *in vitro* culturing PL-5 EpCAM^{high} and PL-2 EpCAM^{high} SCC cells for 4 days without (F12 B27) or with the indicated conditioned medium, as analyzed by flow cytometry. Data obtained from 2-4 independent experiments (*n=2-4*). C.M. epi: conditioned medium from full epithelial SCC cells; C.M. mes: conditioned medium from mesenchymal EpCAM$^-$ SCC cells.

Secreted factors from BMDM polarized with conditioned medium from full epithelial SCC cells (BMDM WD) did not enhance the switch from EpCAM^{high} to EpCAM^{low} or EpCAM$^-$ cells. By contrast, secreted factors from BMDM polarized with conditioned medium from mesenchymal EpCAM$^-$ cells (BMDM PD) significantly increased the appearance of EpCAM^{low} SCC cells in comparison to F12 B27 but did not induce a complete loss of the EpCAM marker in both PL-5 EpCAM^{high} and PL-2 EpCAM^{high} cells (Figures 20A, 20C). Secreted factors from splenic PMN-MDSCs and M-MDSCs from WD-SCC-bearing mice (MDSCs WD) and MD/PD-SCC-bearing mice (MDSCs MD/PD) did not promote the appearance of EpCAM^{low} nor EpCAM$^-$ SCC cells. Nonetheless, secreted factors by splenic PMN-MDSCs isolated from PD-SCC-bearing mice (PMN-MDSCs PD) slightly increased the appearance of EpCAM^{low} and EpCAM$^-$ cells in PL-5 EpCAM^{high} and PL-2 EpCAM^{high} cells (Figures 20A, 20C). Conditioned medium by splenic M-MDSCs isolated from PD-SCC-bearing mice (M-MDSCs PD) promoted the acquisition of mesenchymal traits by significantly increasing the percentage of EpCAM^{low} and EpCAM$^-$ cells in comparison to F12 B27 in PL-5 EpCAM^{high} and PL-2 EpCAM^{high} SCC cells (Figures 20A-20D). Therefore, secreted factors by splenic M-MDSCs from PD-SCC-bearing mice exhibited the highest ability to induce the acquisition of mesenchymal-like features in plastic SCC cells.

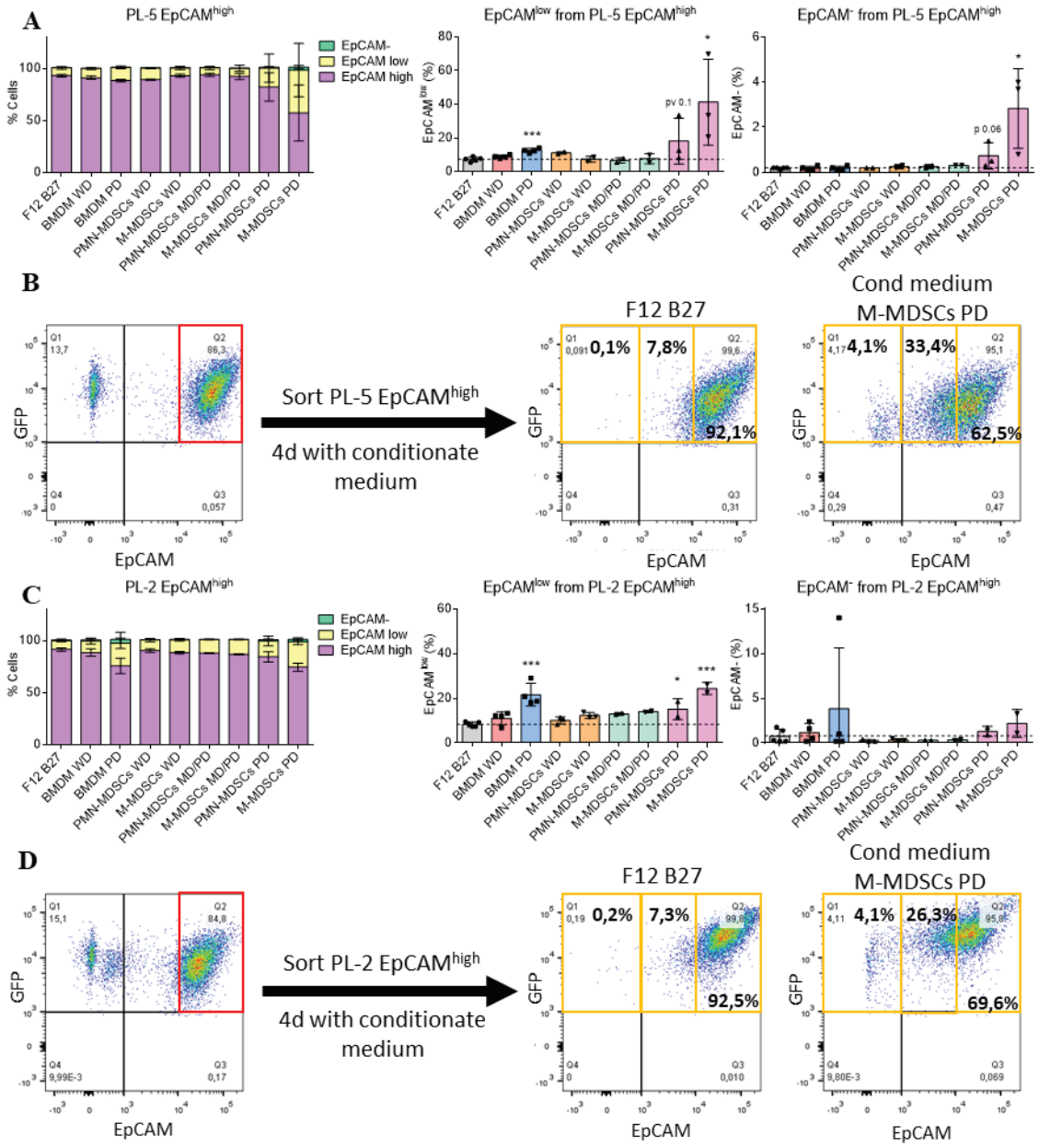

Figure 20. Secreted factors by splenic M-MDSCs from PD-SCC-bearing mice promote the advance of plastic SCC EpCAM^{high} cells to EpCAM^{low} cells. Results shown (mean ± SD) the percentage of EpCAM^{high}, EpCAM^{low}, and EpCAM^{-} SCC cells after *in vitro* culturing sorted (**A**) PL-5 EpCAM^{high} SCC cells and (**C**) PL-2 EpCAM^{high} SCC cells for 4 days without (F12 B27) or with the indicated conditioned medium, as analyzed by flow cytometry. Representative flow cytometry dot plots of sorted (**B**) PL-5 EpCAM^{high} SCC cells and (**D**) PL-2 EpCAM^{high} SCC cells after 4 days growing without (F12 B27) or with the indicated conditioned medium. (**A** and **C**) Dots represent independent experiments (*n=2-4*). Significant differences between analyzed group vs control F12 B27 were evaluated via unpaired two-tailed Student's T-test. * p≤0.05; ** p≤0.01; *** p≤0.001. BMDM WD / PD: BMDM *in vitro* polarized with conditioned medium from full epithelial SCC cells / mesenchymal EpCAM^{-} SCC cells; MDSCs WD / MD/PD / PD: splenic MDSCs from WD-SCCs / MD/PD-SCCs / PD-SCC-bearing mice.

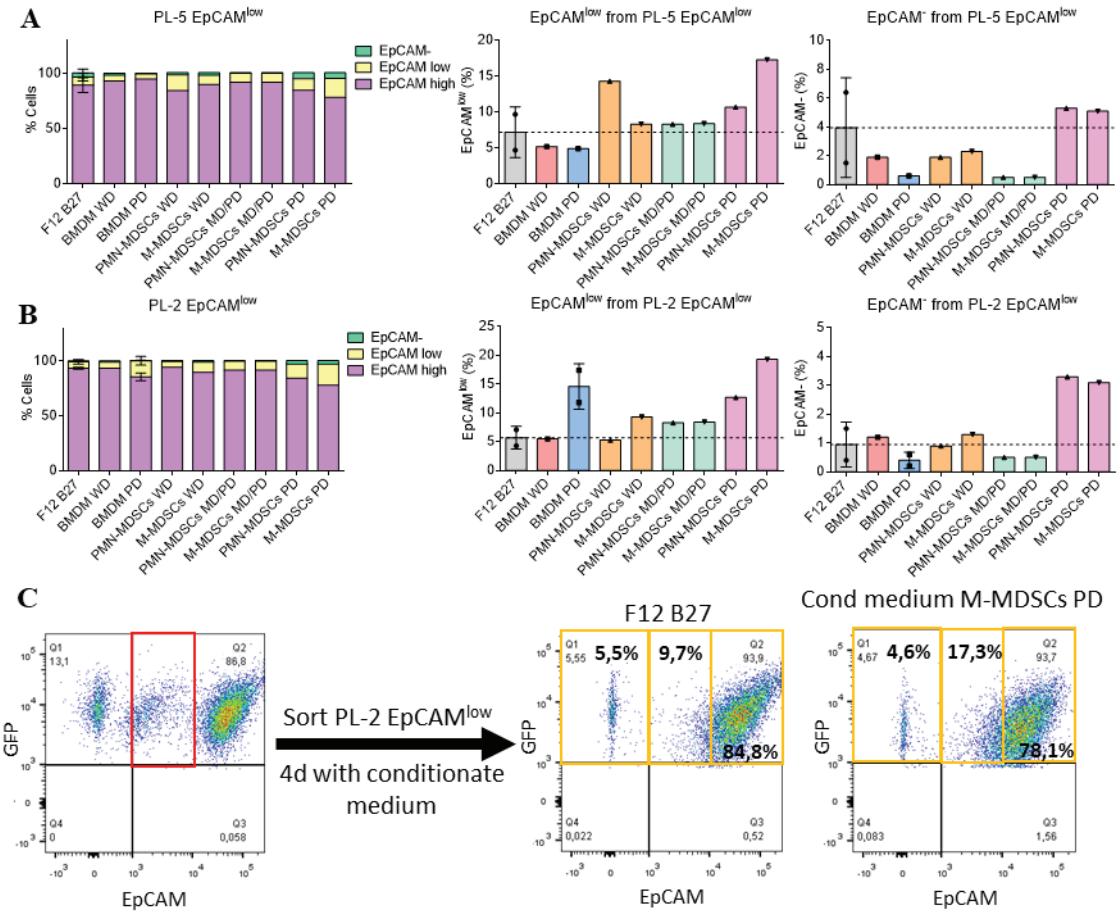

Figure 21. Secreted factors from splenic MDSCs from PD-SCC-bearing mice do not promote the advance of tumor EpCAM^{low} cells to EpCAM^{-} cells. Results shown (mean ± SD) the percentage of EpCAM^{high}, EpCAM^{low}, and EpCAM^{-} SCC cells after *in vitro* culturing sorted (**A**) PL-5 EpCAM^{low} SCC cells and (**B**) PL-2 EpCAM^{low} SCC cells for 4 days without (F12 B27) or with the indicated conditioned medium, as analyzed by flow cytometry. Representative flow cytometry dot plots of sorted (**C**) PL-5 EpCAM^{low} SCC cells after 4 days growing without (F12 B27) or with the indicated conditioned medium. (**A** and **B**) Dots represent independent experiments (*n=1-2*). BMDM WD / PD: BMDM *in vitro* polarized with conditioned medium from full epithelial SCC cells / mesenchymal EpCAM^{-} SCC cells; MDSCs WD / MD/PD / PD: splenic MDSCs from WD-SCCs / MD/PD-SCCs / PD-SCC-bearing mice.

Similarly, it was analyzed whether secreted factors by polarized BMDM or splenic MDSCs could induce the acquisition of mesenchymal-like traits in PL-5 EpCAM^{low} and PL-2 EpCAM^{low} SCC cells. These cell types were cultured for 4 days with a control medium (F12 B27) or with conditioned medium from the immune cell populations studied. Secreted factors by PMN-MDSCs and M-MDSCs from PD-SCC-bearing mice induced the emergence of EpCAM^{low} and EpCAM^{-} in both PL-5 EpCAM^{low} and PL-2 EpCAM^{low} cells (Figures 21A-21C). The other conditioned mediums from polarized BMDM and splenic MDSCs did not show a clear trend to increase the percentage of EpCAM^{low} or EpCAM^{-} SCC cells (Figures 21A-21B). Hence, secreted factors from

polarized BMDM or splenic MDSCs may promote the loss of epithelial traits of plastic EpCAM^{low} SCC cells. More experiments should be addressed in the future to confirm these results.

1.3 Identification of cytokines secreted by splenic M-MDSCs responsible for promoting the mesenchymal-like state of cancer cells during mouse cSCC progression

The conditioned medium from splenic M-MDSCs isolated from PD-SCC-bearing mice showed the strongest effect promoting the acquisition of mesenchymal-like features. Specifically, secreted factors from M-MDSCs presented the highest capability of inducing the switch of plastic EpCAM^{high} SCC cells to EpCAM^{low} SCC cells. To identify the secreted cytokines that may be involved in this process, it was used a mouse XL cytokine array proteome profiler array (R&D systems) which is a membrane-based sandwich immunoassay. Capture antibodies are spotted in duplicate on nitrocellulose membranes bind to 111 different cytokines. Captured cytokines are detected with biotinylated antibodies and visualized using chemiluminescent reagents. The obtained signal is proportional to the amount of cytokine bound. The cytokines secreted by splenic M-MDSCs from WD-SCC-bearing mice, which did not induce the acquisition of mesenchymal features in plastic cancer cells, were compared to cytokines secreted by splenic M-MDSCs from PD-SCC-bearing mice, which promoted the switch from plastic EpCAM^{high} SCC cells to EpCAM^{low} SCC cells (Figure 22A). As could be expected, a different pattern of secreted cytokines was detected between the conditioned medium of splenic M-MDSCs from WD-SCCs and splenic M-MDSCs from PD-SCC-bearing mice (Figure 22B). The quantification of upregulated and downregulated secreted cytokines in splenic M-MDSCs from PD-SCC-bearing mice identified BAFF, CRP, IL-2, IL-28A/B, CCL20, C1qR1, CCL21, Angiopoietin-like 3, Complement factor D, and IL-7 as the 10 most upregulated secreted cytokines, while CXCL2, IL-6, Lipocalin-2, CXCL1, Chitinase 3-like 1, MMP-9, G-CSF, Myeloperoxidase, IL-12p40, and CCL22 as the 10 most downregulated secreted cytokines (Figure 22C).

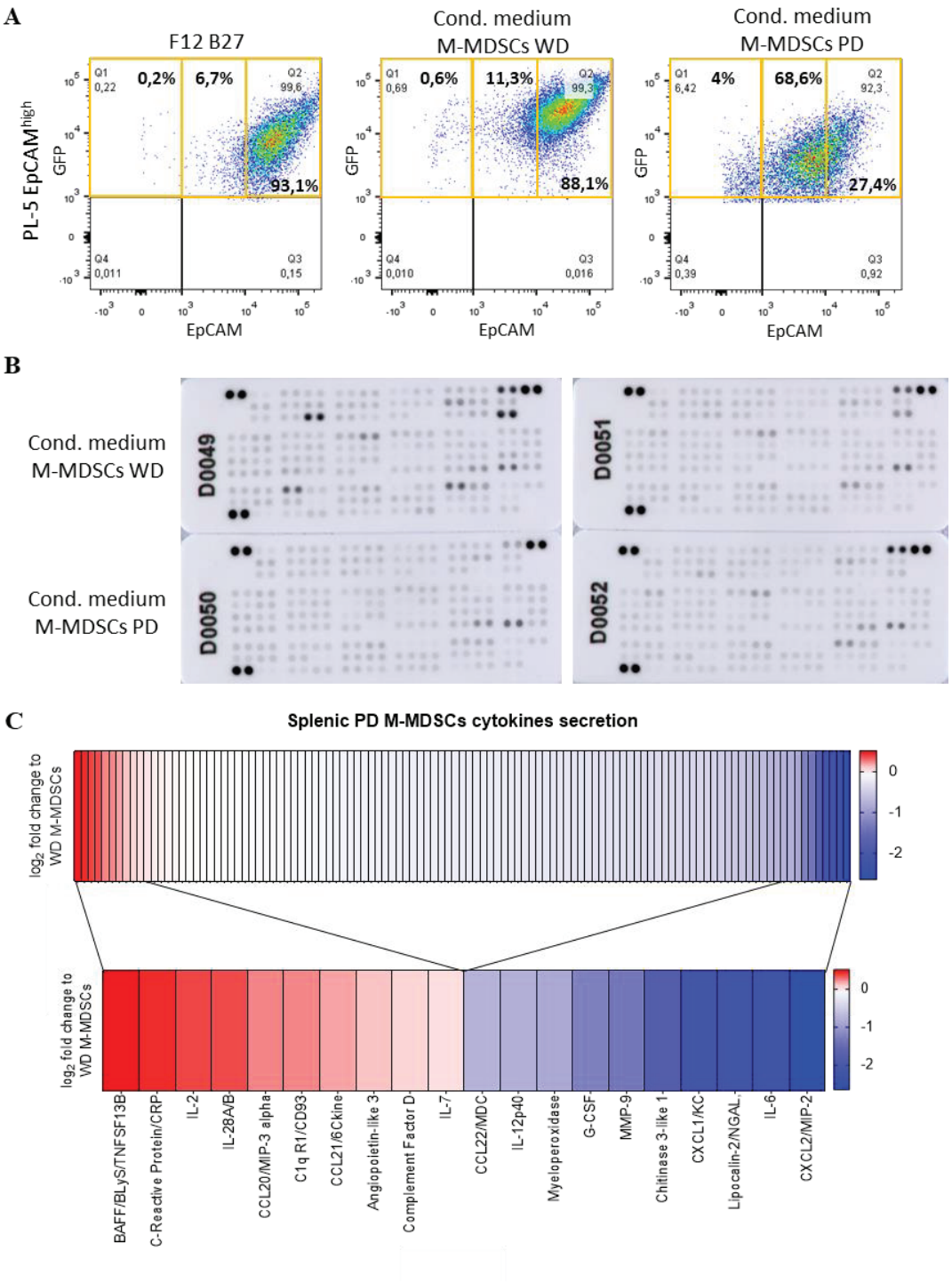

Figure 22. Splenic M-MDSCs from WD-SCC- and PD-SCC-bearing mice present a different cytokine secretion profile. (**A**) Representative flow cytometry dot plots of PL-5 EpCAM^{high} SCC cells after 4 days without (F12 B27) or with the indicated conditioned medium used in the cytokine array. (**B**) Representative image of cytokine detection using the mouse XL cytokine array proteome profiler array. (**C**) Results show (mean) the $\log_2$ of the fold change of secreted cytokines by M-MDSCs from the spleen of PD-SCC-bearing mice normalized to cytokines secreted by M-MDSCs from the spleen of WD-SCC-bearing mice. Top 10 upregulated and downregulated cytokines secreted by M-MDSCs from the spleen of PD-SCC-bearing mice in comparison to M-MDSCs from the spleen of WD-SCC-bearing mice are presented. Data obtained from 2 independent experiments (*n=2*).

CHAPTER 2: DETERMINE CANCER CELL-DERIVED CYTOKINES AND MECHANISMS INVOLVED IN THE RECRUITMENT OF IMMUNOSUPPRESSIVE CELLS, WHICH CONTRIBUTE TO THE EXHAUSTION OF CYTOTOXIC T CELLS IN ADVANCED MOUSE cSCCS

A previous RNA microarray study of our group identified gene expression alterations associated with cSCC progression by comparing the whole gene expression profile of 3 different populations of full epithelial SCC cells isolated from WD-SCCs, 3 different populations of plastic EpCAM$^+$ and plastic EpCAM$^-$ SCC cells isolated from MD/PD-SCCs and 3 different populations of mesenchymal EpCAM$^-$ SCC cells isolated from PD-SCCs (Lopez-Cerda et al., submitted manuscript) (Figure 23). The previous analysis of this RNA microarray revealed differences in the gene expression between the different SCC cell populations and defined the gene signature of SCC cells in each step of cSCC progression (Figure 24). This allowed our group to study which genes were differently expressed in full epithelial SCC cells, plastic EpCAM$^+$ SCC cells, plastic EpCAM$^-$ SCC cells, and mesenchymal EpCAM$^-$ SCC cells. It was observed that there is an important change in the transcriptomic profile when plastic EpCAM$^+$ SCC cells switched to plastic EpCAM$^-$ SCC cells (Lopez-Cerda et al., submitted manuscript). However, it has not been studied specifically which cytokines are upregulated in cancer cells during the acquisition of the mesenchymal state, which could be actively recruiting immunosuppressive cells and establishing the characteristic immunosuppressive TME of PD-SCCs (Lorenzo-Sanz et al., under-review manuscript).

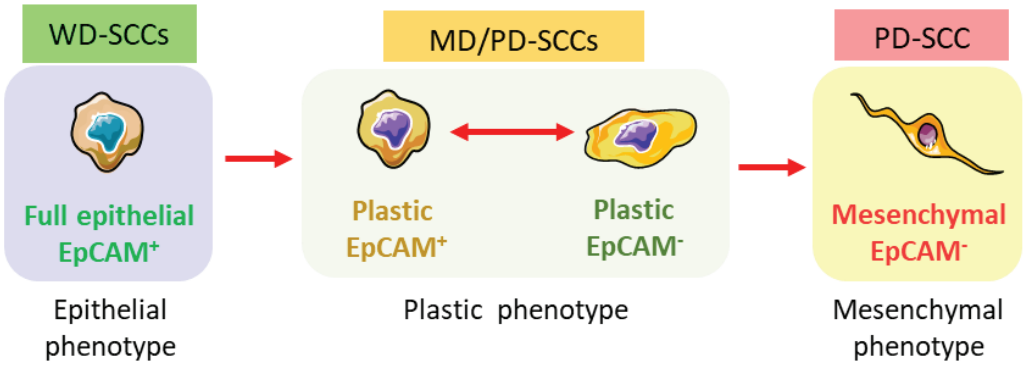

Figure 23. Schema of cSCC progression model from WD-SCCs to MD/PD-SCCs, and PD-SCCs. WD-SCCs are composed of full epithelial SCC cells, MD/PD-SCCs are composed of plastic EpCAM$^+$ and plastic EpCAM$^-$ cells, and PD-SCCs are composed of mesenchymal EpCAM$^-$ SCC cells.

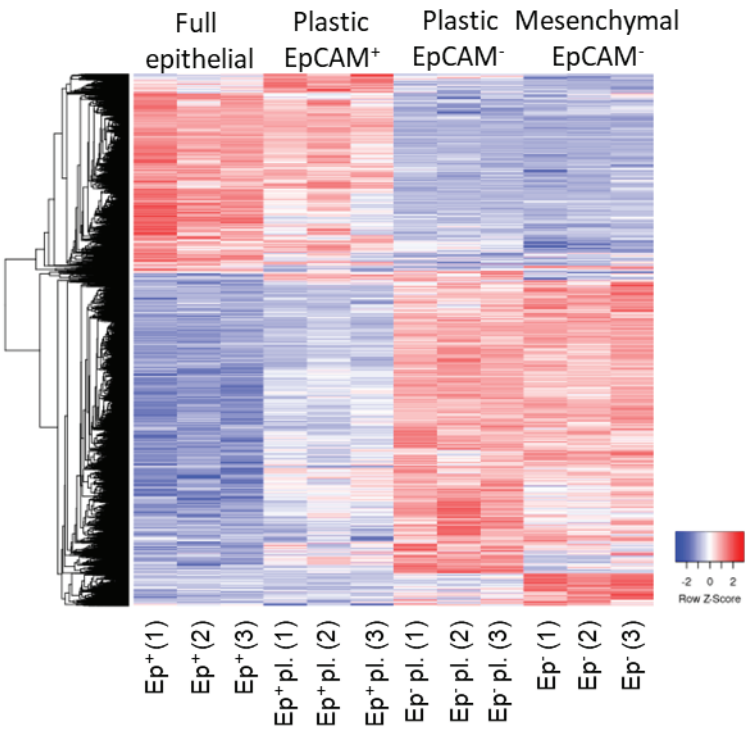

Figure 24. Full epithelial, plastic EpCAM$^+$, plastic EpCAM$^-$, and mesenchymal EpCAM$^-$ SCC cells present different gene expression signature. Heat map of differentially expressed genes between full epithelial EpCAM$^+$, plastic EpCAM$^+$, plastic EpCAM$^-$, and mesenchymal EpCAM$^-$ SCC cells sorted from WD-SCCs, MD/PD-SCCs, and PD-SCCs, respectively obtained from an RNA microarray analysis and calculated as Z score of gene expression.

2.1 Identification and validation of secreted cytokines by mesenchymal EpCAM$^-$ SCC tumor cells that promote the recruitment of immunosuppressive cells in advanced SCCs

A deeper analysis of the RNA microarray permitted the identification of upregulated and downregulated biological processes in SCC cell populations. When comparing the gene signatures of full epithelial SCC cells and mesenchymal EpCAM$^-$ SCC cells (the two extreme populations) the gene ontology bioinformatic analysis showed that cell migration, cell adhesion, wound healing, collagen fibril organization, and cell chemotaxis processes were upregulated in mesenchymal EpCAM$^-$ SCC cells. Additionally, keratinocyte differentiation, keratinization, peptide cross-linking, the establishment of the skin barrier, and epidermis development processes were downregulated in mesenchymal EpCAM$^-$ SCC cells (Figure 25A). The results of this analysis support our previous findings of cSCC progression model where WD-SCCs containing full epithelial SCC cells present an epithelial-like phenotype characterized by a clear histological organization of the epidermis with keratinized layers. By contrast, PD-SCCs containing mesenchymal EpCAM$^-$ SCC cells lose the epithelial histological organization and cellular migration is enhanced. Mesenchymal EpCAM$^-$ SCC cells upregulate the expression of secreted factors, glycoproteins, disulfide bond proteins, and extracellular matrix proteins (Figure 25B). Next, the 10 most upregulated cytokines RNA expression in mesenchymal EpCAM$^-$ SCC cells in comparison to full epithelial SCC cells were identified: *Cxcl2*, *Csf1*, *Grem1*, *Lif1*, *Cxcl10*, *Cxcl14*, *Csf2*, *Cx3cl1*, *Spp1*, and *Bmp2* (Figure 25C). Specifically, CXCL2, CSF1, and CSF2 were selected as cytokines candidates to recruit immunosuppressive cells in advanced SCCs since according to the bibliography they actively participate in establishing an immunosuppressive TME in other

tumor conditions. Each of these cytokines presents a particular gene expression across cSCC progression which ends in an increased expression in mesenchymal EpCAM- SCC cells (Figure 25D).

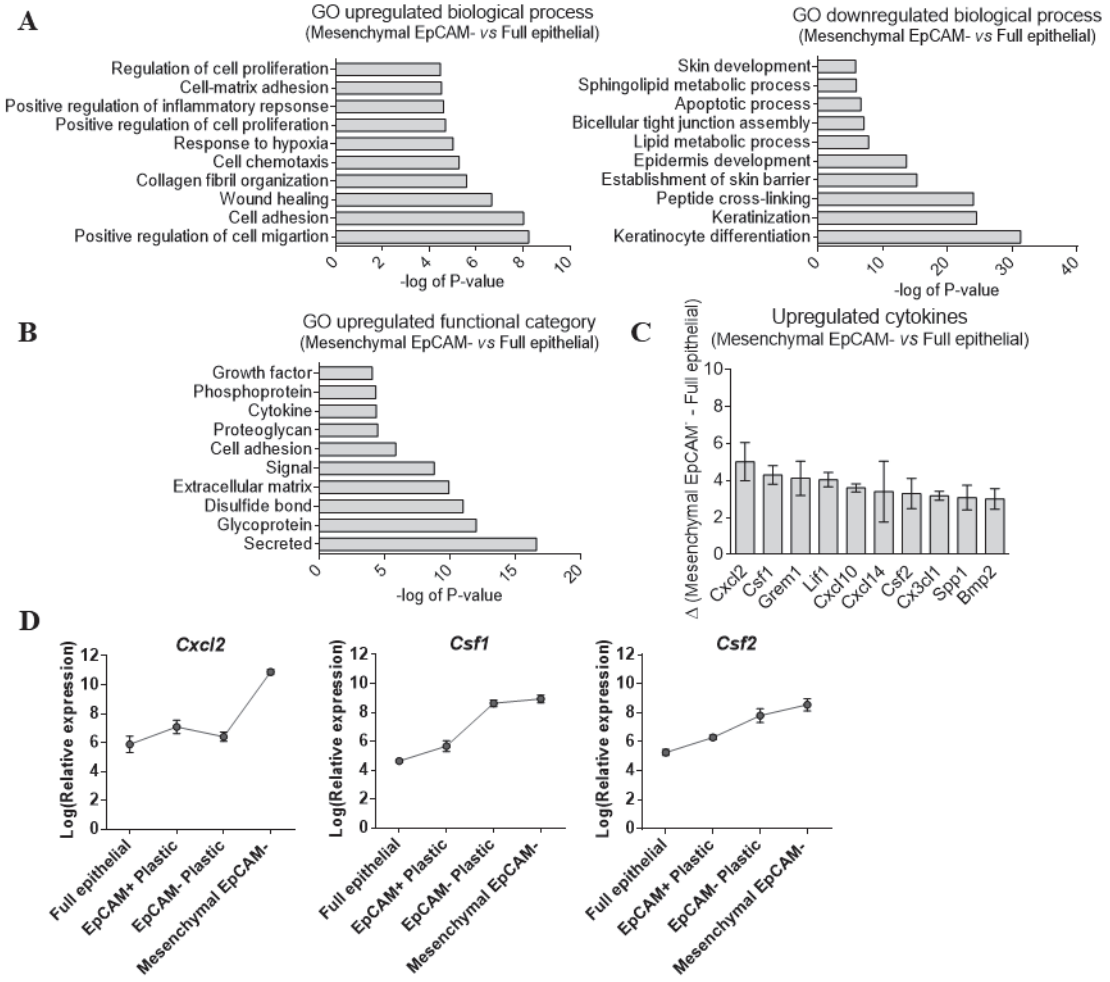

Figure 25. RNA microarray gene ontology analysis identifies upregulated expression of cytokines in mesenchymal EpCAM- SCC cells. (**A**) Results show the -log of the P-value of the gene ontology enrichment analysis performed using DAVID bioinformatics resources on upregulated and downregulated groups of genes (full epithelial SCC cells - mesenchymal EpCAM- SCC cells) classified based on gene fold changes above 2. (**B**) Results show the -log of the P-value of the functional category enrichment analysis performed using DAVID bioinformatics resources on the upregulated genes groups (full epithelial SCC cells -mesenchymal EpCAM- SCC cells) classified based on gene fold changes above 2. (**C**) Results show (mean ± SD) the relative expression of the top 10 upregulated cytokines comparing full epithelial SCC cells to mesenchymal EpCAM- SCC cells. (**D**) Results show (mean ± SD) the relative expression of candidate cytokines profile expression across the different cSCC cancer cell states. Data obtained from 3 biological replicates (*n=3*).

Next, the expression of the candidate cytokines to establish an immunosuppressive TME was analyzed in *in vitro* growing full epithelial and mesenchymal EpCAM- SCC cells by RT-qPCR to validate the RNA microarray obtained data. *Cxcl2* expression levels in full epithelial and

mesenchymal EpCAM$^-$ SCC cells remained unchanged in contrast to the data obtained in the RNA microarray (Figure 26A). The expression of *Csf1* was significantly increased in mesenchymal EpCAM$^-$ SCC cells in comparison to full epithelial SCC cells and *Csf2* expression was slightly higher in mesenchymal EpCAM$^-$ SCC cells (Figure 26A). In addition, we analyzed the expression of CXCL1 since this cytokine signals through the same receptor as CXCL2 (CXCR2) and have also been described to recruit immunosuppressive cells. *Cxcl1* expression was significantly increased in mesenchymal EpCAM$^-$ SCC cells in comparison to full epithelial SCC cells which was not observed in the RNA microarray (Figure 26A). Next, the secretion of CXCL1 and CXCL2 was analyzed by ELISA. *In vitro* growing full epithelial and mesenchymal EpCAM$^-$ SCC cells secreted similar amounts of CXCL1 and CXCL2 (Figure 26B). Hence, some divergences were observed between the RNA data obtained from the microarray analysis of SCC cells grown *in vivo* and the RT-qPCR and the protein quantification by ELISA in full epithelial SCC cells and mesenchymal EpCAM$^-$ SCC cells grown *in vitro*.

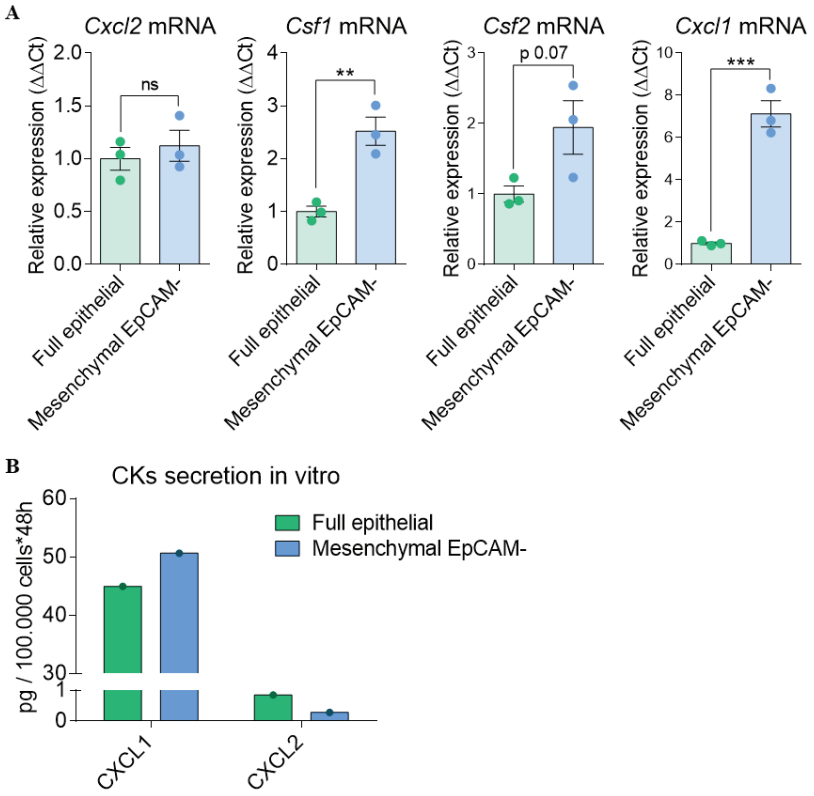

Figure 26. Full epithelial and mesenchymal EpCAM$^-$ SCC cells present a unique cytokine expression and secretion profile. (**A**) Results show (mean ± SD) the mRNA fold change of the indicated genes in mesenchymal EpCAM$^-$ SCC cells as compared to full epithelial SCC cells. RNA expression was normalized to *Gapdh* and *Ppia*. (**B**) Results show the amount of CXCL1 and CXCL2 secreted in the culture medium of the indicated cells, as determined by ELISA assays. Dots represent independent experiments (*n=1-3*). Significant differences between full epithelial and mesenchymal EpCAM$^-$ groups were evaluated by unpaired two-tailed Student's T-test. ns: p>0.05; ** p≤0.01; *** p≤0.001.

To further characterize the secretion of cytokines by cancer cells at different stages of cSCC progression, WD-SCCs and PD-SCCs were grown by engrafting full epithelial and mesenchymal EpCAM$^-$ SCC cells respectively in immunocompetent syngeneic mice. Primary cell cultures of full epithelial SCC cells from WD-SCCs and mesenchymal EpCAM$^-$ SCC cells from PD-SCCs were freshly obtained to ensure that cancer cells resemble the most *in vivo* cancer cells. Conditioned mediums with secreted factors from tumor cells were collected after 48 hours of *in vitro* culture (Figure 27). Secreted cytokines were identified using a mouse cytokine proteome profiler (R&D systems). These membranes detect 40 different cytokines and work with the same principle as the membranes described in section 1.3. Full epithelial SCC cells and mesenchymal EpCAM$^-$ SCC cells presented a different cytokine secretion profile. While full epithelial SCC cells secreted IL-1ra, mesenchymal EpCAM$^-$ SCC cells secreted CXCL1, CCL2, TIMP1, CSF3, and to a lesser extent CXCL2, CSF1, and CXCL10 (Figures 28A-28B). Given that CXCL1, CCL2, and CSF3 are highly secreted by mesenchymal EpCAM$^-$ cells and their signaling promoted the recruitment of immunosuppressive cells in other tumor models, their signaling were blocked in PD-SCCs to analyze their role in recruiting immunosuppressive cells in advanced SCCs.

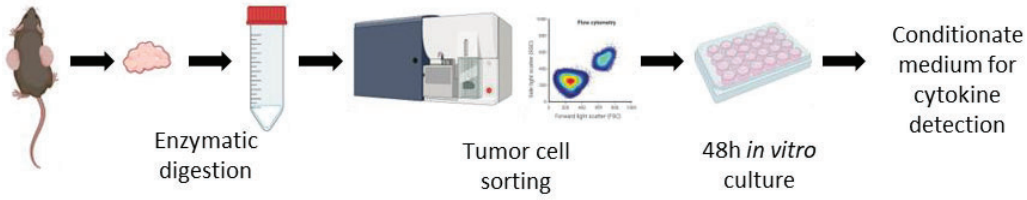

Figure 27. Experimental schema for obtaining conditioned medium from full epithelial SCC cells from WD-SCCs and mesenchymal EpCAM$^-$ SCC cells from PD-SCCs. WD-SCCs and PD-SCCs were excised and enzymatically digested O/N with collagenase and dispase to obtain a single-cell suspension. Next, full epithelial SCC cells and mesenchymal EpCAM$^-$ SCC cells were sorted by FACS and *in vitro* cultured for 48 hours.

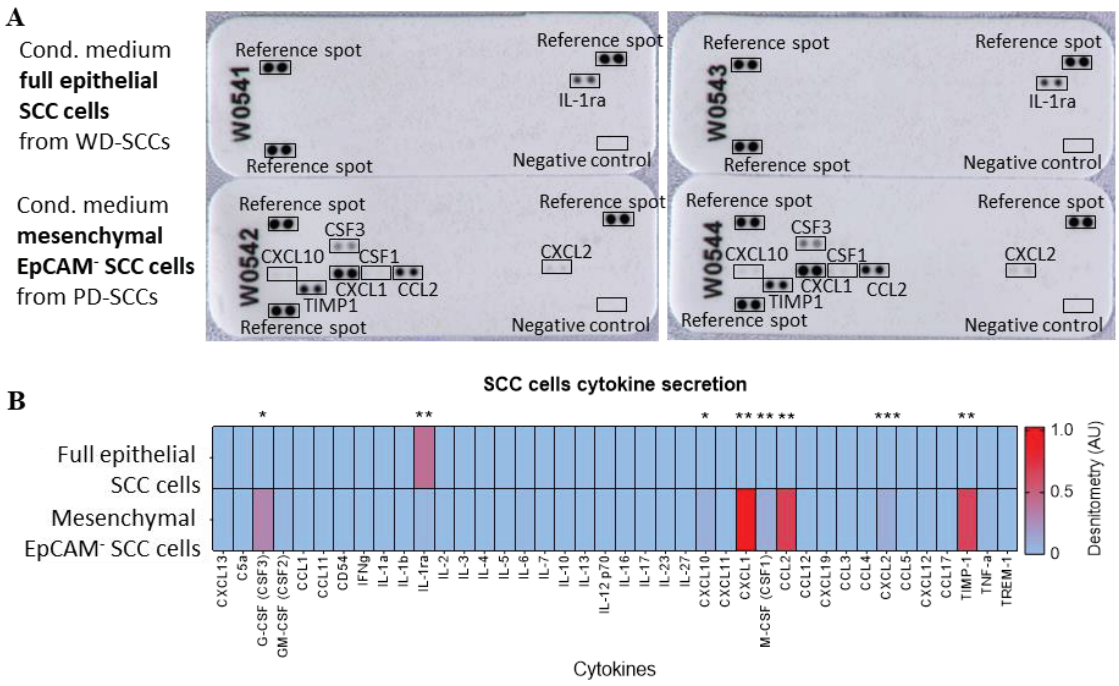

Figure 28. Full epithelial SCC cells from WD-SCCs and mesenchymal EpCAM- SCC cells from PD-SCCs present a different cytokine secretome. (**A**) Representative image of cytokine detection using the mouse cytokine proteome profiler array. (**B**) Results (mean) presented as a heat map of the densitometry analysis of the indicated cytokines. Data obtained from 2 independent experiments (*n=2*). Significant differences between full epithelial and mesenchymal EpCAM- groups were evaluated by unpaired two-tailed Student's T-test. * p≤0.05; ** p≤0.01; *** p≤0.001.

2.2 Study the relevance of CXCL1, CSF3 and CCL2 stablishing an immunosuppressive TME in PD-SCCs

To block CXCL1 signaling, mesenchymal EpCAM- SCC cells were engrafted in immunocompetent syngeneic mice and once PD-SCCs were palpable, mice were treated 6-day a week with the CXCR2 (CXCL1 and CXCL2 receptor) antagonist SB225002 or control solution (vehicle). Blockade of CXCR2 signaling did not delay PD-SCCs growth and did not reduce cellular viability nor the percentage of tumor cells (GFP^+ $CD45^-$ cells), immune cells ($CD45^+$ cells), or stromal cells (GFP^- $CD45^-$ cells) in PD-SCCs, as analyzed by flow cytometry (Figures 29A-29C). PD-SCCs remained mainly composed of EpCAM- SCC cells and the presence of tumor $EpCAM^+$ cells were not increased by SB225002 treatment (Figure 29D). Blockade of CXCR2 function with SB225002 did not modify the recruitment of myeloid-lineage immune cells ($CD11b^+$ cells) and macrophages into PD-SCCs (Figure 30A). According to the bibliography, CXCR2 signaling promotes the recruitment of neutrophils, PMN-MDSCs (Katoh et al., 2013), and Treg cells (Lv et al., 2014a) to the TME in different tumor conditions. However, SB225002 treatment did not alter PMN-MDSCs neither M-MDSCs recruitment in PD-SCCs (Figure 30B).

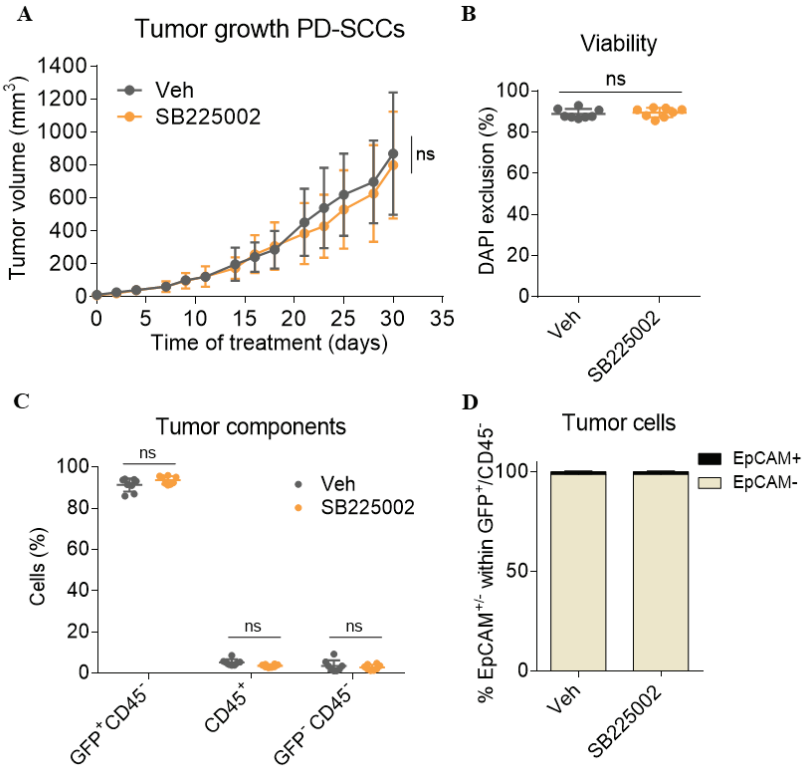

Figure 29. SB225002 treatment does not affect PD-SCCs growth. (**A**) Results show the tumor volume in mm^3 (mean ± SD) indicating the growth kinetics of Vehicle and SB225002 treated tumors. Results show (mean ± SD) (**B**) the percentage of DAPI exclusion cell population, defining tumor viability; (**C**) the percentage of tumor cells ($GFP^+/CD45^-$ cell population), leukocytes ($CD45^+$ cell population), and fibroblasts ($GFP^-/CD45^-$ cell population); and (**D**) the percentage of $EpCAM^-$ and $EpCAM^+$ tumor cells ($EpCAM^{+/-}$ within $GFP^+/CD45^-$ cell population) in PD-SCCs as determined by flow cytometry. Each dot represents a single tumor (*n=8*). Statistical significance of the differences observed between Vehicle and SB225002 treated tumors were analyzed by unpaired two-tailed Student's T-test. ns: p>0.05.

PD-SCCs treated with SB225002 presented increased tumor recruitment of $CD8^+$ T cells and slightly increased presence of T helper cells, while NK cell recruitment remained unchanged (Figure 31). SB225002 treatment did not increase the percentage of necrotic regions in PD-SCCs (Figure 32A). However, effector immune cell cytotoxicity, as tested by the expression of GzmB ($GzmB^+$ cells), was increased, while Treg cells ($FoxP3^+$ cells) recruitment was reduced under SB225002 treatment (Figures 32B-32C). Hence, blockade of CXCL1/CXCL2 derived signaling with SB225002 reduced the immunosuppressive environment of PD-SCCs and increased the presence of active cytotoxic effector cells. However, these effects were not sufficient to alter PD-SCC growth or viability.

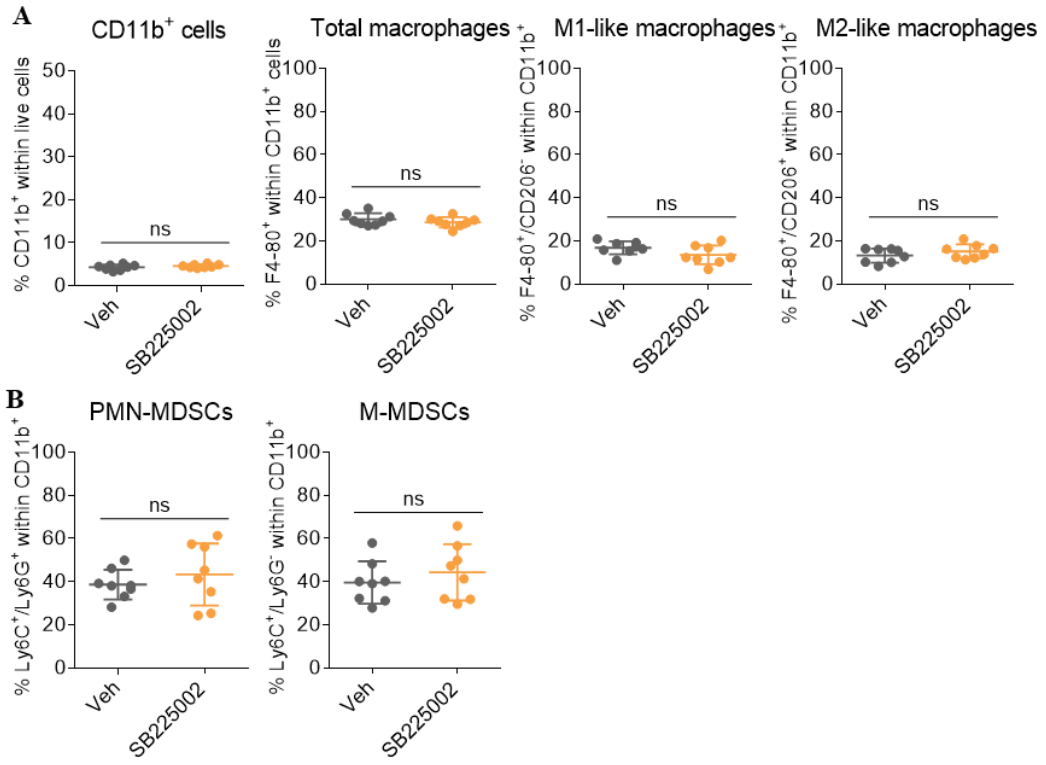

Figure 30. Myeloid cells recruitment into PD-SCCs is not affected by SB225002 treatment. Quantification of the percentage (mean ± SD) of recruited (**A**) myeloid cells ($CD11b^+$ within live cells), total macrophages ($F4\text{-}80^+$ within $CD11b^+$ cell population), M1-like macrophages ($F4\text{-}80^+/CD206^-$ within $CD11b^+$ cell population), and M2-like macrophages ($F4\text{-}80^+/CD206^+$ within $CD11b^+$ cell population); and (**B**) PMN-MDSCs ($Ly6C^+/Ly6G^+$ within $CD11b^+$ cell population) and M-MDSCs ($Ly6C^+/Ly6G^-$ within $CD11b^+$ cell population) into PD-SCCs, as analyzed by flow cytometry. Each dot represents a single tumor (*n=8*). Statistical significance of the differences observed between Vehicle and SB225002 treated tumors were analyzed by unpaired two-tailed Student's T-test. ns: $p>0.05$.

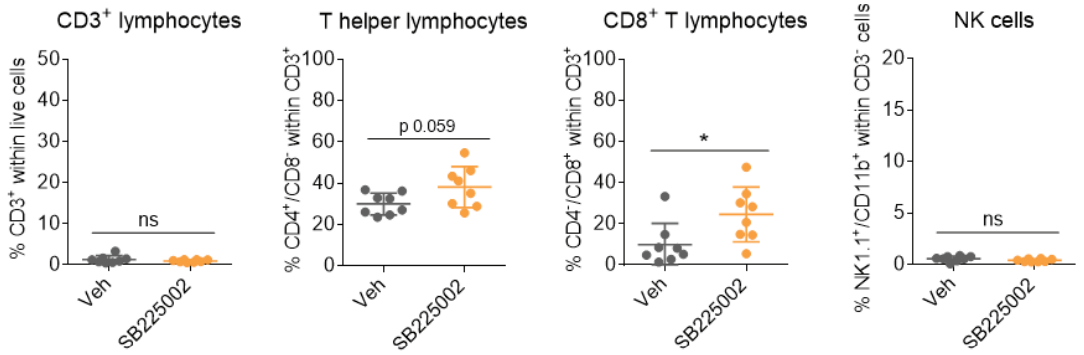

Figure 31. PD-SCCs treated with SB225002 present increased infiltration of $CD8^+$ T cells. Quantification of the percentage (mean ± SD) of recruited T lymphocytes ($CD3^+$ cell population within live cells), T helper lymphocytes ($CD4^+/CD8^-$ within $CD3^+$ cell population), $CD8^+$ T lymphocytes ($CD4^-/CD8^+$ within $CD3^+$ cell population), and NK cells ($NK1.1^+/CD11b^+$ within $CD3^-$ cell population) into PD-SCCs, as analyzed by flow cytometry. Each dot represents a single tumor (*n=8*). Statistical significance of the differences observed between Vehicle and SB225002 treated tumors were analyzed by unpaired two-tailed Student's T-test. ns: $p>0.05$; * $p\leq0.05$.

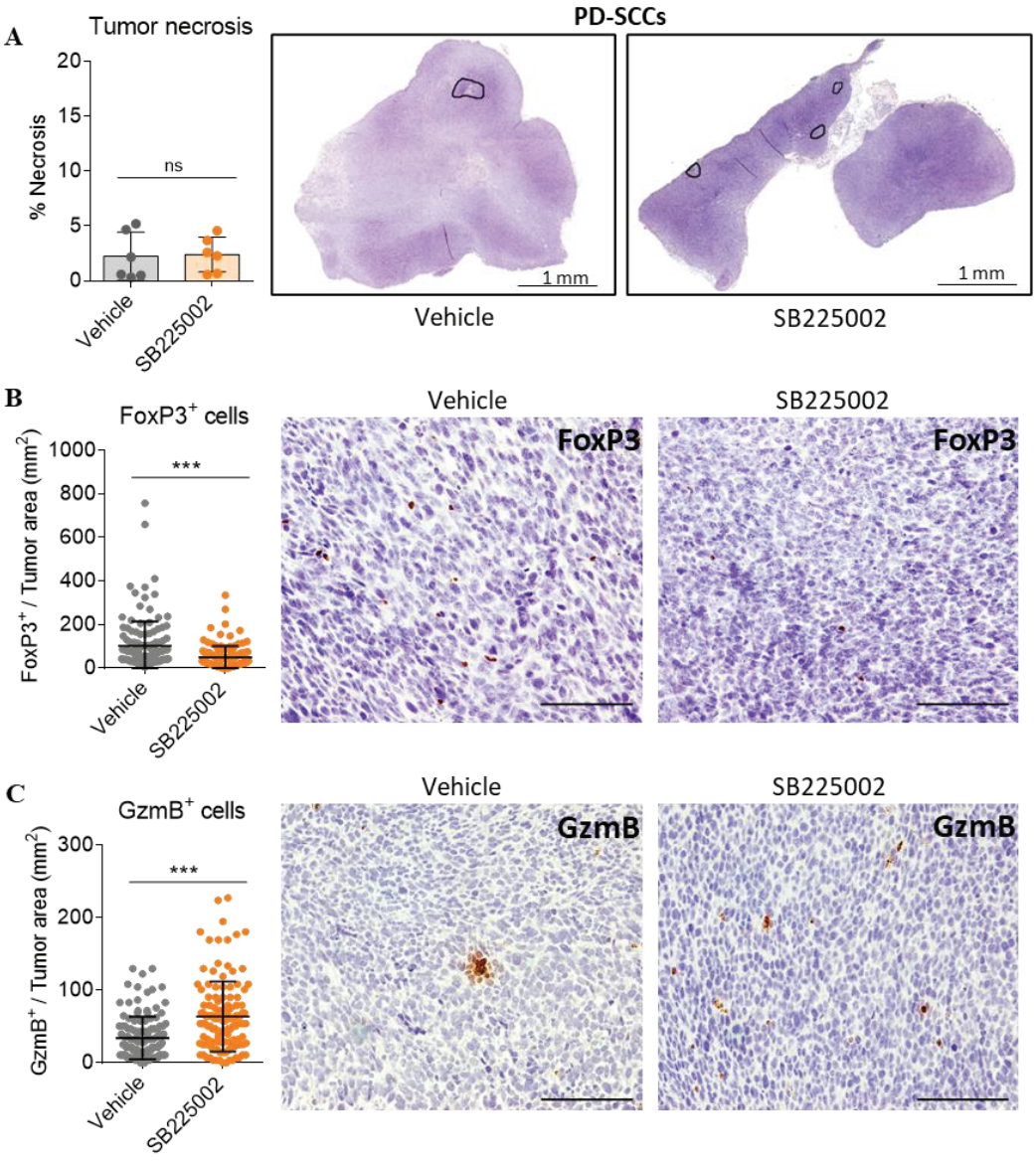

Figure 32. PD-SCCs treated with SB225002 recruit less immunosuppressive Treg cells and more cytotoxic GzmB$^+$ cells. (**A**) Quantification of the percentage (mean ± SD) of tumor necrotic area and representative H/E section of PD-SCCs treated with Vehicle or SB225002, where necrotic areas are marked with black lines. Scale bar: 1 mm. Each dot represents a single tumor (*n=6*). Frequency (mean ± SD) of (**B**) FoxP3$^+$ (Treg) cells and (**C**) cytotoxic (GzmB$^+$) cells per tumor area and representative immunohistochemistry images of Vehicle and SB225002 treated tumors. Scale bar: 100 µm. Data obtained from 6 independent samples per group (*n=6*) and quantified from 20 images per sample. Statistical significance of the differences observed between Vehicle and SB225002 treated tumors were analyzed by unpaired two-tailed Student's T test. ns: $p>0.05$; *** $p\leq0.001$.

Blockade of CSF3 signaling in PD-SCCs was achieved using an anti-CSF3 antibody. Mesenchymal EpCAM$^-$ SCC cells were engrafted in immunocompetent syngeneic mice and once PD-SCCs were palpable, mice were treated 2 days a week with anti-CSF3. Inhibition of CSF3 derived signaling did not significantly alter PD-SCCs growth kinetics (Figure 33A). The cellular viability and the percentage of tumor cells (GFP$^+$ CD45$^-$ cells), immune cells (CD45$^+$ cells), or stromal cells (GFP$^-$ CD45$^-$ cells) remained unchanged in PD-SCCs after anti-CSF3 treatment (Figures 33B-33C). PD-SCCs were mainly composed of EpCAM$^-$ tumor cells and the presence of tumor EpCAM$^+$ cells were not increased with anti-CSF3 treatment (Figure 33D). Blockade of CSF3 function did not modify the recruitment of myeloid-lineage immune cells (CD11b$^+$ cells) neither macrophages into PD-SCCs (Figure 34A). It has been described that CSF3 recruits neutrophils and PMN-MDSCs to the TME in different tumor conditions (J. Li et al., 2018). Accordingly, anti-CSF3 administration decreased PMN-MDSCs recruitment into PD-SCCs (Figure 34B). However, the recruitment of M-MDSCs into PD-SCCs was slightly increased with anti-CSF3 intervention (Figure 34B).

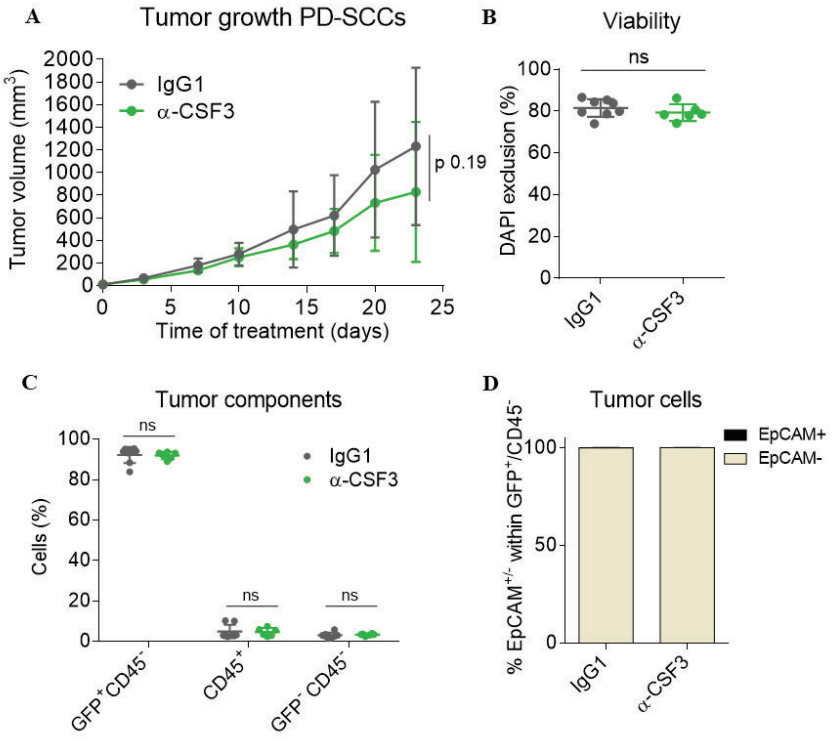

Figure 33. Anti-CSF3 treatment does not affect PD-SCCs growth. (**A**) Results show the tumor volume in mm^3 (mean ± SD) indicating the growth kinetics of IgG1 and anti-CSF3 treated tumors. Results show (mean ± SD) (**B**) the percentage of DAPI exclusion cell population, defining tumor viability; (**C**) the percentage of tumor cells (GFP$^+$/CD45$^-$ cell population), leukocytes (CD45$^+$ cell population), and fibroblasts (GFP$^-$/CD45$^-$ cell population); and (**D**) the percentage of EpCAM$^+$ and EpCAM$^-$ tumor cells (EpCAM$^{+/-}$ within GFP$^+$/CD45$^-$ cell population) in PD-SCCs as determined by flow cytometry. Each dot represents a single tumor (*n=6-8*). Statistical significance of the differences observed between IgG1 and anti-CSF3 treated tumors were analyzed by unpaired two-tailed Student's T-test. ns: p>0.05.

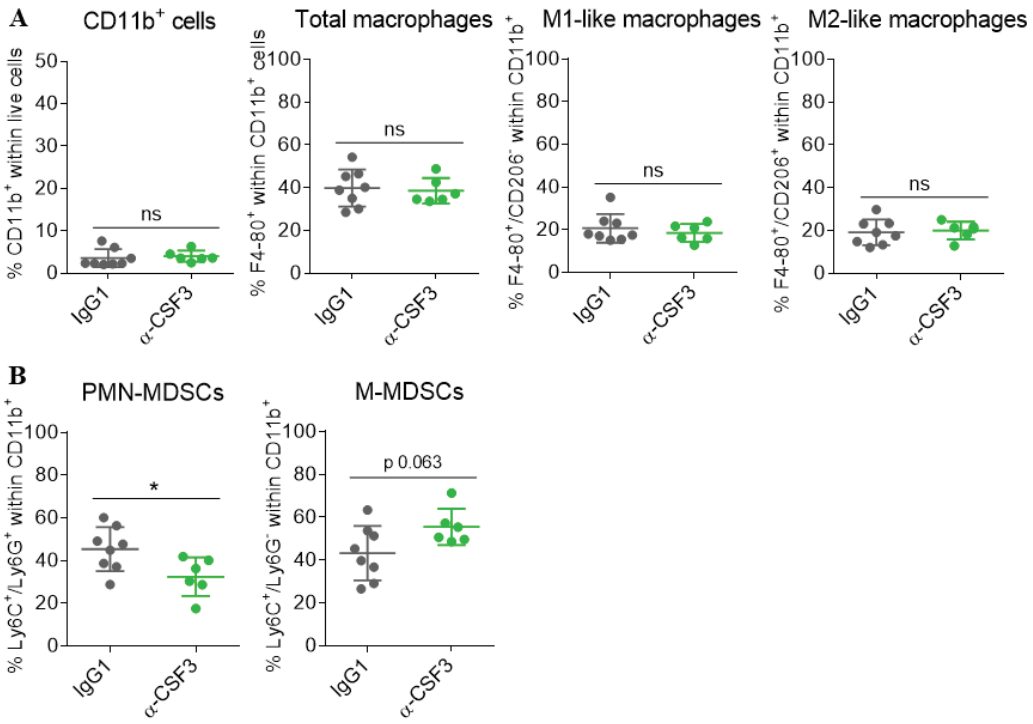

Figure 34. Anti-CSF3 treatment reduces the recruitment of PMN-MDSCs into PD-SCCs. Quantification of the percentage (mean ± SD) of recruited (**A**) myeloid cells ($CD11b^+$ within live cells), total macrophages ($F4\text{-}80^+$ within $CD11b^+$ cell population), M1-like macrophages ($F4\text{-}80^+/CD206^-$ within $CD11b^+$ cell population), and M2-like macrophages ($F4\text{-}80^+/CD206^+$ within $CD11b^+$ cell population); and (**B**) PMN-MDSCs ($Ly6C^+/Ly6G^+$ within $CD11b^+$ cell population) and M-MDSCs ($Ly6C^+/Ly6G^-$ within $CD11b^+$ cell population) into PD-SCCs as analyzed by flow cytometry. Each dot represents a single tumor (*n=6-8*). Statistical significance of the differences observed between IgG1 and anti-CSF3 treated tumors were analyzed by unpaired two-tailed Student's T-test. ns: $p>0.05$; * $p\leq0.05$.

PD-SCCs treated with anti-CSF3 did not present increased recruitment of T helper cells, $CD8^+$ T cells, nor NK cells (Figure 35). Blockade of CSF3 did not alter the percentage of necrotic regions in PD-SCCs nor the recruitment of Treg cells ($FoxP3^+$ cells) (Figures 36A-36B). Despite the total number of $CD8^+$ cells and Treg cells were not altered, anti-CSF3 caused an increased presence of $GzmB^+$ cells (Figure 36C). So, anti-CSF3 treatment ultimately enhanced cytotoxic activity by effector immune cells.

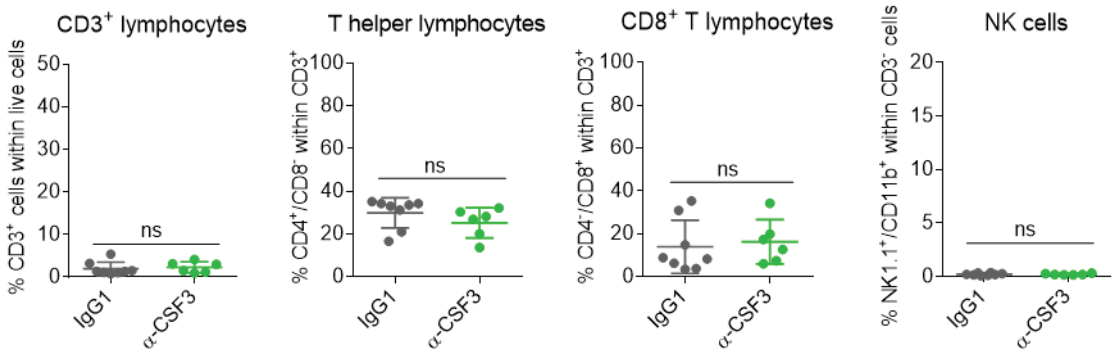

Figure 35. Anti-CSF3 treatment did not alter the recruitment of lymphoid cells into PD-SCCs. Quantification of the percentage (mean ± SD) of recruited T lymphocytes ($CD3^+$ cell population within live cells), T helper lymphocytes ($CD4^+/CD8^-$ within $CD3^+$ cell population), $CD8^+$ T lymphocytes ($CD4^-/CD8^+$ within $CD3^+$ cell population), and NK cells ($NK1.1^+/CD11b^+$ within $CD3^-$ cell population) into PD-SCCs, as analyzed by flow cytometry. Each dot represents a single tumor (*n=6-8*). Statistical significance of the differences observed between IgG1 and anti-CSF3 treated tumors were analyzed by unpaired two-tailed Student's T-test. ns: $p>0.05$.

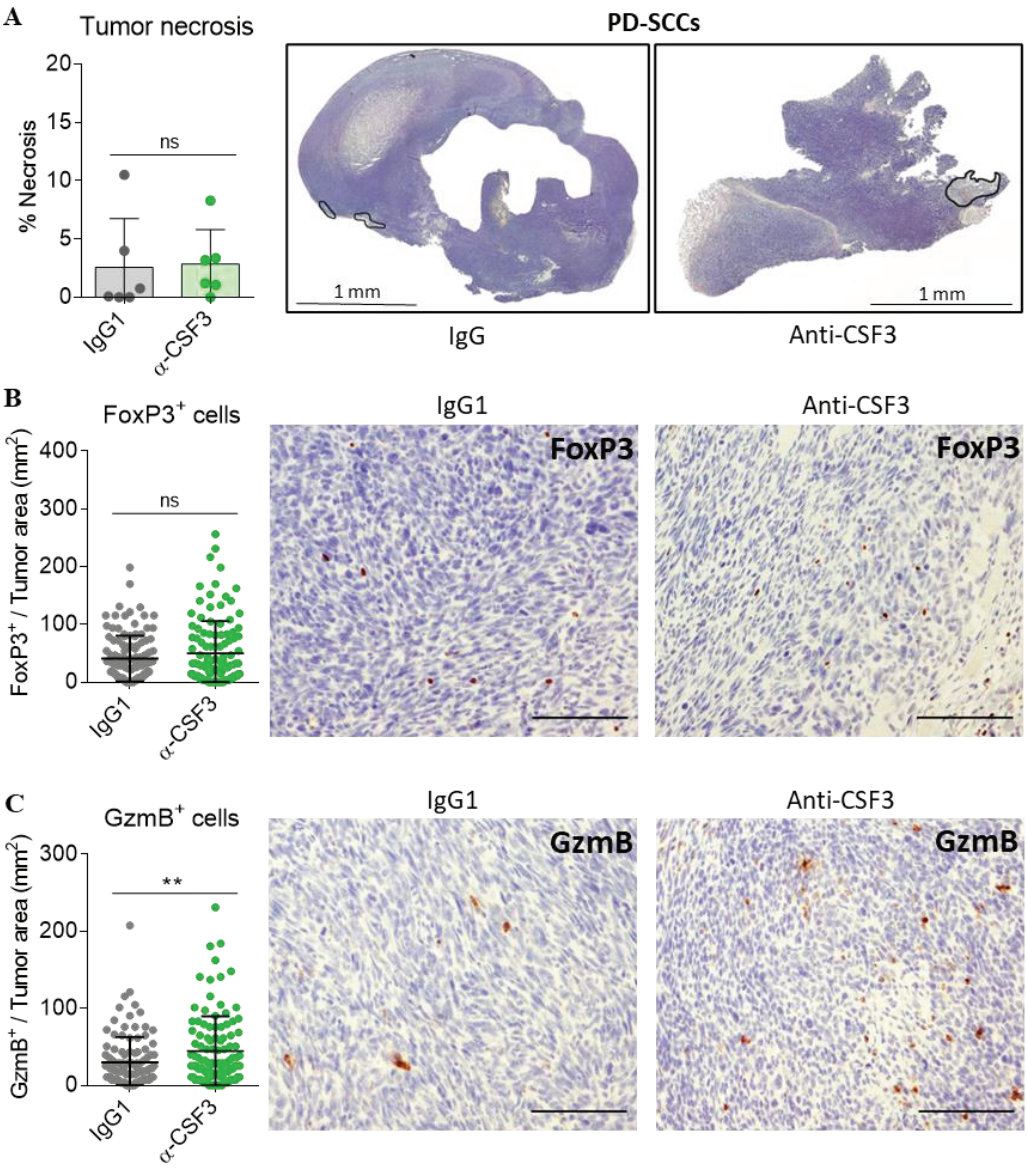

Figure 36. Anti-CSF3 treatment enhances the recruitment of cytotoxic GzmB$^+$ cells into PD-SCCs. (**A**) Quantification of the percentage (mean ± SD) of tumor necrotic area and representative H/E section of PD-SCCs treated with IgG1 or anti-CSF3, where necrotic areas are marked with black lines. Scale bar: 1 mm. Each dot represents a single tumor and the mean ± SD for each group is shown (*n=6*). Frequency (mean ± SD) of (**B**) FoxP3$^+$ (Treg) cells and (**C**) cytotoxic (GzmB$^+$) cells per tumor area and representative immunohistochemistry images of IgG1 and anti-CSF3 treated tumors. Scale bar: 100 µm. Data obtained from 6 independent samples per group (*n=6*) and quantified from 20 images per sample. Statistical significance of the differences observed between IgG1 and anti-CSF3 treated tumors were analyzed by unpaired two-tailed Student's T test. ns: $p>0.05$; ** $p\leq0.01$.

To block CCL2 signaling, mesenchymal EpCAM$^-$ SCC cells were engrafted in immunocompetent syngeneic mice and once PD-SCCs were palpable, mice were treated 2 days a week with anti-CCL2. Blockade of CCL2 signaling did not affect PD-SCCs growth (Figure 37A). In addition, tumor viability and the percentage of tumor cells (GFP$^+$ CD45$^-$ cells), immune cells (CD45$^+$ cells), or stromal cells (GFP$^-$ CD45$^-$ cells) were not modified by the anti-CCL2 intervention (Figures 37B-37C). CCL2 recruits macrophages (H. Yang et al., 2020) and Treg cells (Mondini et al., 2019) to the TME of different tumor types. In this sense, the blockade of CCL2 signaling decreased infiltration of total macrophages and specifically of M1-like macrophages into PD-SCCs. Furthermore, the blockade of CCL2 signaling slightly decreased tumor recruitment of M2-like macrophages without achieving statistical significance (Figure 38A). By contrast, the recruitment of MDSCs cell populations remained unchanged with anti-CCL2 treatment in PD-SCCs (Figure 38B).

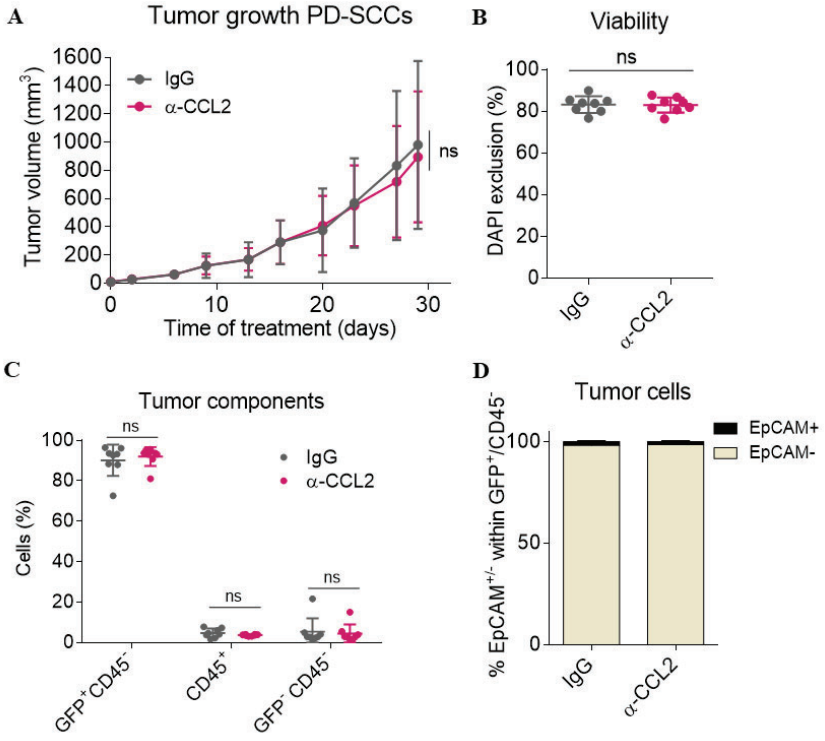

Figure 37. Anti-CCL2 treatment does not affect PD-SCCs growth. (**A**) Results show the tumor volume in mm^3 (mean ± SD) indicating the growth kinetics of IgG and anti-CCL2 treated tumors. Results show (mean ± SD) (**B**) the percentage of DAPI exclusion cell population, defining tumor viability; (**C**) the percentage of tumor cells (GFP$^+$/CD45$^-$ cell population), leukocytes (CD45$^+$ cell population), and fibroblasts (GFP$^-$/CD45$^-$ cell population); and (**D**) the percentage of EpCAM$^+$ and EpCAM$^-$ tumor cells (EpCAM$^{+/-}$ within GFP$^+$/CD45$^-$ cell population) in PD-SCCs as determined by flow cytometry. Each dot represents a single tumor (n=8). Statistical significance of the differences observed between IgG and anti-CCL2 treated tumors were analyzed by unpaired two-tailed Student's T-test. ns: p>0.05.

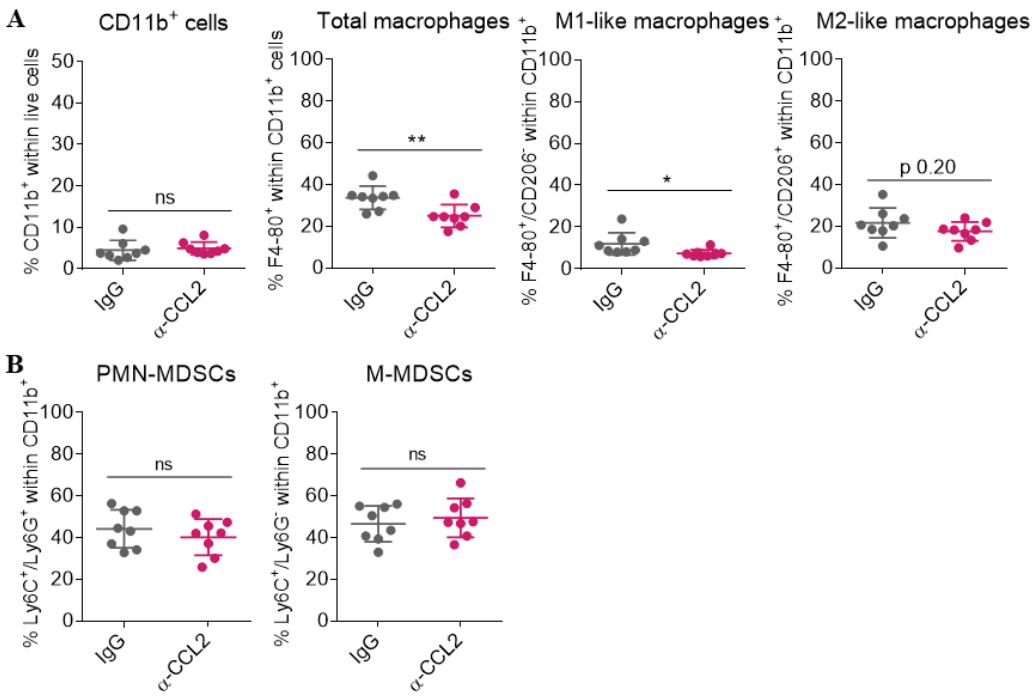

Figure 38. Anti-CCL2 treatment reduces the recruitment of macrophages into PD-SCCs. Quantification of the percentage (mean ± SD) of recruited (**A**) myeloid cells ($CD11b^+$ within live cells), total macrophages ($F4\text{-}80^+$ within $CD11b^+$ cell population), M1-like macrophages ($F4\text{-}80^+/CD206^-$ within $CD11b^+$ cell population), and M2-like macrophages ($F4\text{-}80^+/CD206^+$ within $CD11b^+$ cell population); and (**B**) PMN-MDSCs ($Ly6C^+/Ly6G^+$ within $CD11b^+$ cell population) and M-MDSCs ($Ly6C^+/Ly6G^-$ within $CD11b^+$ cell population) into PD-SCCs, as analyzed by flow cytometry. Each dot represents a single tumor (*n=8*). Statistical significance of the differences observed between IgG and anti-CCL2 treated tumors were analyzed by unpaired two-tailed Student's T-test. ns: $p>0.05$; * $p\leq0.05$; ** $p\leq0.01$.

Blockade of CCL2 signaling did not increase the recruitment of T helper cells, $CD8^+$ T cells, or NK cells into PD-SCCs (Figure 39). Anti-CCL2 treatment slightly increased the presence of tumor necrotic areas in PD-SCCs despite not achieving statistical significance (Figure 40A). In addition, a reduced presence of immunosuppressive Treg cells ($FoxP3^+$ cells) and increased recruitment of active effector cells ($GzmB^+$ cells) was observed in PD-SCCs treated with anti-CCL2 (Figures 40B-40C). These results indicate that anti-CCL2 decreases the immunosuppressive TME of PD-SCCs. Modifying and reducing the recruitment of immunosuppressive cells by inhibiting CXCL1/CXCL2, CSF3, and CCL2 signaling in PD-SCCs ultimately results in increased activity of cytotoxic cells, although it is not enough to alter tumor growth kinetics or tumor cell viability.

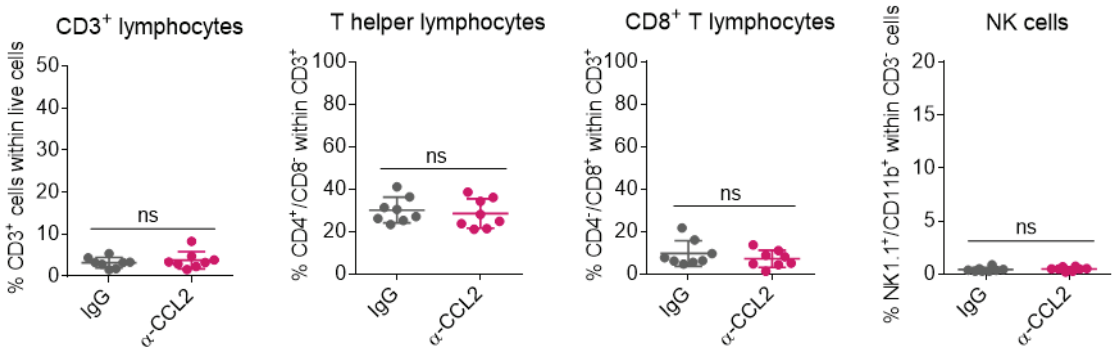

Figure 39. T cells and NK cells infiltrating PD-SCCs are not altered in response to anti-CCL2 treatment. Quantification of the percentage (mean ± SD) of recruited T lymphocytes ($CD3^+$ cell population within live cells), T helper lymphocytes ($CD4^+/CD8^-$ within $CD3^+$ cell population), $CD8^+$ T lymphocytes ($CD4^-/CD8^+$ within $CD3^+$ cell population), and NK cells ($NK1.1^+/CD11b^+$ within $CD3^-$ cell population) into PD-SCCs, as analyzed by flow cytometry. Each dot represents a single tumor (*n=8*). Statistical significance of the differences observed between IgG and anti-CCL2 treated tumors were analyzed by unpaired two-tailed Student's T-test. ns: p>0.05.

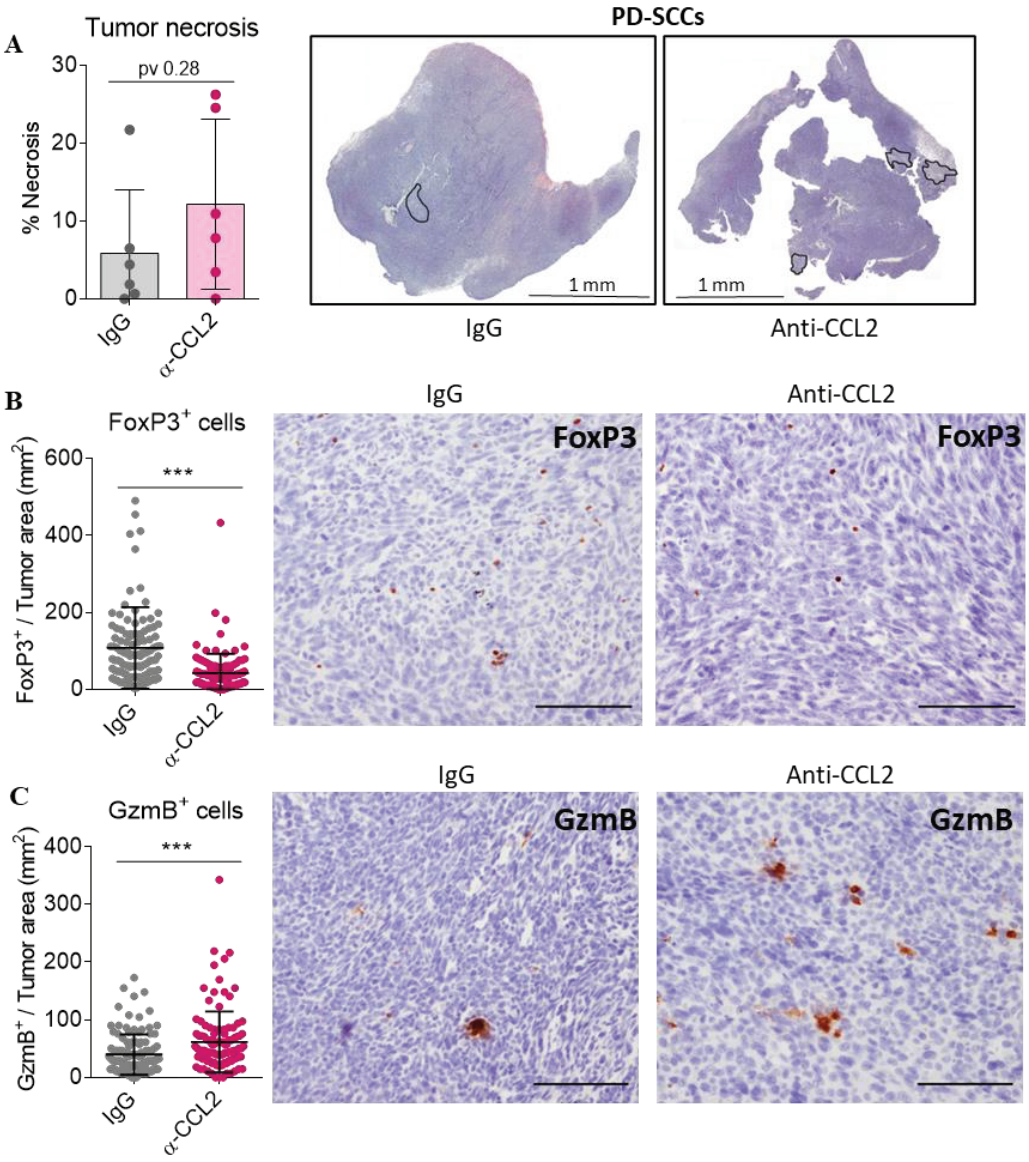

Figure 40. Anti-CCL2 treatment reduces the recruitment of immunosuppressive Treg cells and increases the infiltration of cytotoxic GzmB$^+$ cells in PD-SCCs. (**A**) Quantification of the percentage (mean ± SD) of tumor necrotic area and representative H/E section of PD-SCCs treated with IgG or anti-CCL2, where necrotic areas are marked with black lines. Scale bar: 1 mm. Each dot represents a single tumor and the mean ± SD for each group is shown (*n=6*). Frequency (mean ± SD) of (**B**) FoxP3$^+$ (Treg) cells and (**C**) cytotoxic (GzmB$^+$) cells per tumor area and representative immunohistochemistry images of IgG and anti-CCL2 treated tumors. Scale bar: 100 μm. Data obtained from 6 independent samples per group (*n=6*), quantified from 20 images per sample, and represented as mean ± SD. Statistical significance of the differences observed between IgG1 and anti-CCL2 treated tumors were analyzed by unpaired two-tailed Student's T test. ns: $p>0.05$; ** $p\leq0.01$.

2.3 Analysis of the role of CXCL12 promoting an immunosuppressive TME in PD/S-SCCs

A recent study revealed that the dual blockade of CXCL12/CXCR4 and PD-L1/PD-1 pathways prevented the establishment of an immunosuppressive TME in an ovarian cancer mode (Zeng et al., 2019). Simultaneous blockade of CXCL12/CXCR4 signaling by the antagonist of CXCR4 AMD3100 and PD-L1/PD-1 signaling by anti-PD-1 antibody reduced ovarian cancer growth and prolonged survival of tumor-bearing mice. Specifically, mice treated with AMD3100 + anti-PD-1 presented increased effector T-cell infiltration and function, decreased intratumor Treg cells presence and increased conversion of Treg cells into T helper cells, decreased recruitment of MDSCs, and increased M2-to-M1 macrophage polarization in the tumor (Zeng et al., 2019). These effects of remodeling the TME and establishing a less immunosuppressive profile were observed in single treatments and synergized when combined AMD3100 with anti-PD-1.

We took advantage of a previous study done in our group where it was demonstrated that CXCL12 (also known as SDF-1) autocrine signaling promoted metastasis in advanced skin carcinoma (Bernat-Peguera et al., 2019). Specifically, full mesenchymal SCC cells were engrafted in immunocompetent syngeneic mice and once PD/S-SCCs were palpable, mice were treated daily with AMD3100 or a control solution (Figure 41A). Our previous studies showed that AMD3100 treatment did not delay PD/S-SCCs tumor growth but reduced lung metastasis lesions in immunocompetent syngeneic mice (Figures 41B-41C). The characterization of *Cxcl12* expression determined that full mesenchymal SCC cells from PD/S-SCCs expressed *Cxcl12* while full epithelial SCC cells from WD-SCCs scarcely expressed this cytokine (Figure 41D). This was further corroborated by CXCL12 secretion analysis by ELISA where it was shown that full mesenchymal SCC cells from PD/S-SCCs were secreting more CXCL12 to the medium (Figure 41E). In addition, our group observed that fibroblasts from both WD-SCCs and PD/S-SCCs were expressing *Cxcl12* (Figure 41F). This was further corroborated by the fact that SDF-1 could be detected in stromal regions of WD-SCCs while in PD/S-SCCs SDF-1 was detected homogeneously in the tumor cells regions (Figure 41G) (Bernat-Peguera et al., 2019). We further validated the *Cxcl12* expression in the different cancer cell populations identified during cSCC progression, and we observed that *Cxcl12* was expressed by full mesenchymal SCC cells from PD/S-SCCs while full epithelial SCC cells from WD-SCCs and mesenchymal EpCAM^{-} SCC cells from PD-SCCs were expressing low levels of *Cxcl12* (Figure 42A). Total tumor lysates expressed more *Cxcl12* than their specific tumor cells suggesting that *Cxcl12* could be expressed by the stromal components. However, the expression levels of *Cxcl12* by total tumors were significantly lower in comparison to full mesenchymal SCC cells (Figures 42A-42B). Given the low expression of *Cxcl12* in WD-SCCs and PD-SCCs, we focused our efforts on determining how the lack of CXCL12 signaling could impact the TME of PD/S-SCCs. We hypothesized that blockade of

CXCL12 signaling in PD/S-SCCs by AMD3100 treatment could reduce the immunosuppressive TME as observed in mouse ovarian cancer. To test this hypothesis, we analyzed the samples from (Bernat-Peguera et al., 2019) in order to characterize the recruitment of immune cells.

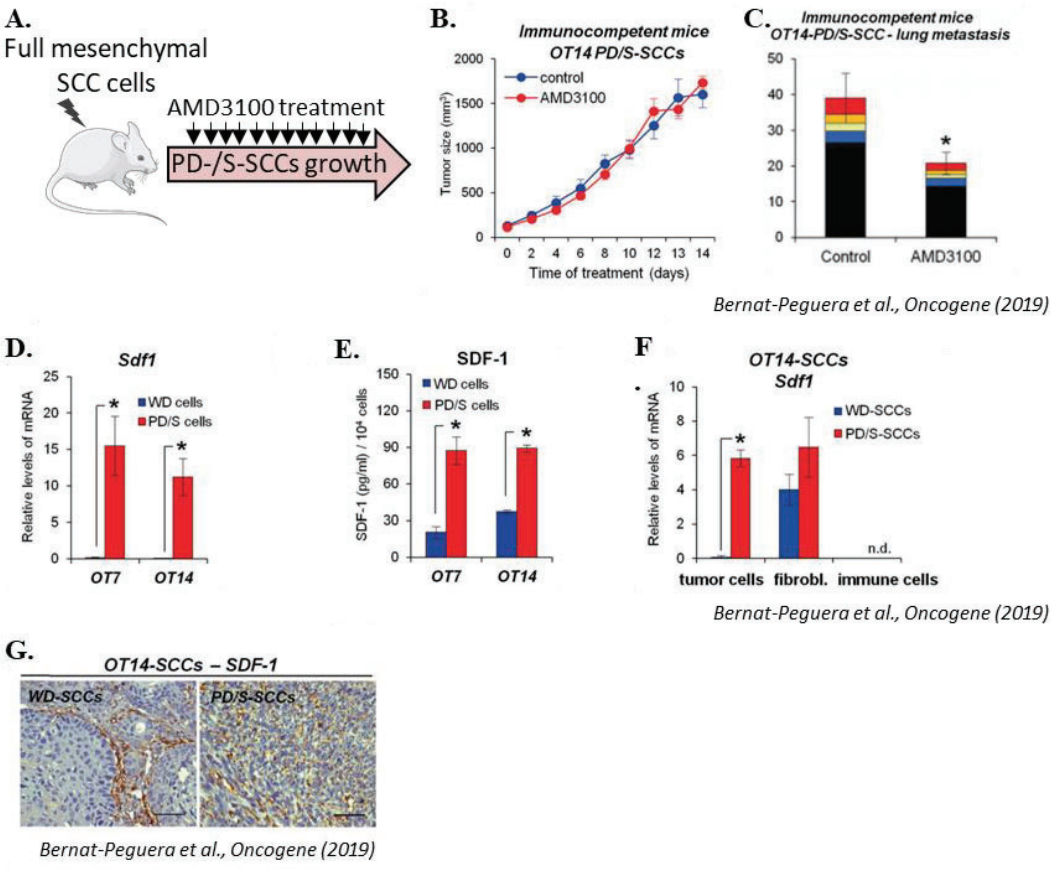

Figure 41. Full mesenchymal SCC cells from PD/S-SCCs express Sdf1 (CXCL12) and AMD3100 treatment decreases PD/S-SCCs derived metastasis. (**A**) Experimental scheme for the treatment of PD/S-SCCs with Vehicle or AMD3100. Full mesenchymal SCC cells were subcutaneously engrafted in immuncompetent syngeneic mice and once PD/S-SCCs were palpable mice were intraperitoneally treated with AMD3100 (15 mg/kg; diluted in sterile serum), or serum *(n=7)*. (**B**) Growth kinetics (means ± SE of tumor size, mm^3) of control and AMD3100 treated PD/S-SCCs (seven tumors per group) growing in immunocompetent mice. (**C**) Mean of metastatic foci (± SE) per lung section (categorized by size, mm^2) in mice with PD/S-SCC and the indicated treatments (six mice per group). (**D**) Mean (± SE) of *Sdf1* mRNA levels relative to *Gapdh*, as quantified by qRT-PCR in *in vitro* growing tumor cells isolated from WD-SCC (WD cells) and PD/S-SCCs (PD/S cells) of the indicated tumor lineages (two different primary cell cultures per tumor type and lineage). (**E**) SDF-1 concentration in the culture medium of the indicated cells (two primary culture cells per group and lineage), as quantified by ELISA assays. (**F**) Mean (± SE) levels of *Sdf1* mRNA relative to *Gapdh*, as quantified by qRT-PCR in tumor cells ($\alpha6\text{-integrin}^+/CD45^-/CD31^-$ cells), immune cells ($\alpha6\text{-integrin}^-/EpCAM^-/CD45^+/CD31^-$ cells), and fibroblasts ($\alpha6\text{-integrin}^-/EpCAM^-/CD45^-/CD31^-$ cells), isolated from OT14 WD-SCCs and PD/S-SCCs (two different samples per group) by FACS-sorter. (**G**) Representative images of the SDF-1 immunodetection in paraffin sections of WD-SCCs and PD/S-SCCs of OT14 lineage. Scale bar: 100 µm. *, significant differences between the compared groups (t-test; $p \leq 0.05$). Adapted from Bernat-Peguera et al., Oncogene (2019).

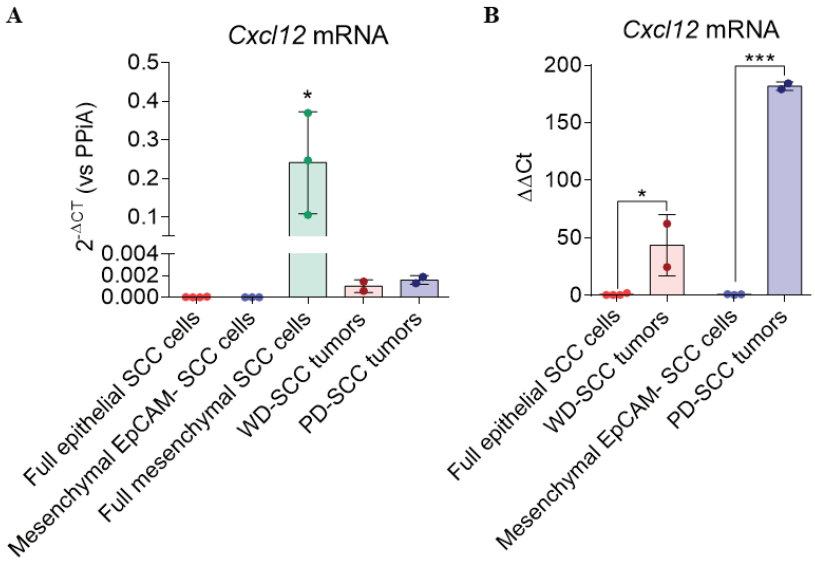

Figure 42. Full epithelial and mesenchymal EpCAM$^-$ SCC cells do not express *Cxcl12*. (**A**) Results show (mean ± SD) the *Cxcl12* mRNA levels normalized to *Ppia* expression in the indicated tumor cells or tumor lysates. Data obtained from 2-4 independent experiments (*n=2-4*). Statistical significance of the differences observed between groups was analyzed using one-way ANOVA followed by Tuckey's multiple comparison test. * p≤0.05. (**B**) Results show (mean ± SD) the *Cxcl12* mRNA level fold change of WD-SCCs and PD-SCCs tumors to its tumor cells normalized to *Gapdh* and *Ppia* expression. Data obtained from 2-4 independent experiments (*n=2-4*). Statistical significance of the differences observed between compared groups was analyzed by unpaired two-tailed Student's T-test. * p≤0.05; ** p≤0.01.

AMD3100 treatment decreased the recruitment of CD8$^+$ T cells and Treg cells (FoxP3$^+$ cells) into PD/S-SCCs (Figures 43A-43B). Despite the reduced presence of CD8$^+$ cells, the ratio of CD8$^+$ and Treg cells was increased upon AMD3100 treatment, suggesting that these fewer CD8$^+$ cells might be more active thanks to an even greater reduction in Treg cells infiltration (Figure 43D). In this sense, activated effector cells expressing GzmB (GzmB$^+$ cells) were more present in PD/S-SCCs upon AMD3100 treatment (Figure 43C). The presence of macrophages with an M2 profile (CD163$^+$ cells) was also decreased in PD/S-SCCs treated with AMD3100 (Figure 44A). In contrast, infiltration of GR1$^+$ cells, which includes both polymorphonuclear and monocytic MDSC subtypes, remained unchanged in PD/S-SCCs with AMD3100 treatment (Figure 44B). However, the blockade of CXCL12 signaling did not increase the necrotic areas on PD/S-SCCs (Figure 45). Therefore, blocking CXCL12 signaling decreases the presence of immunosuppressive cells in PD/S-SCCs. Despite reducing the immunosuppression, the single blockade of CXCL12 was not sufficient to decrease PD/S-SCCs tumor growth or increase tumor necrosis.

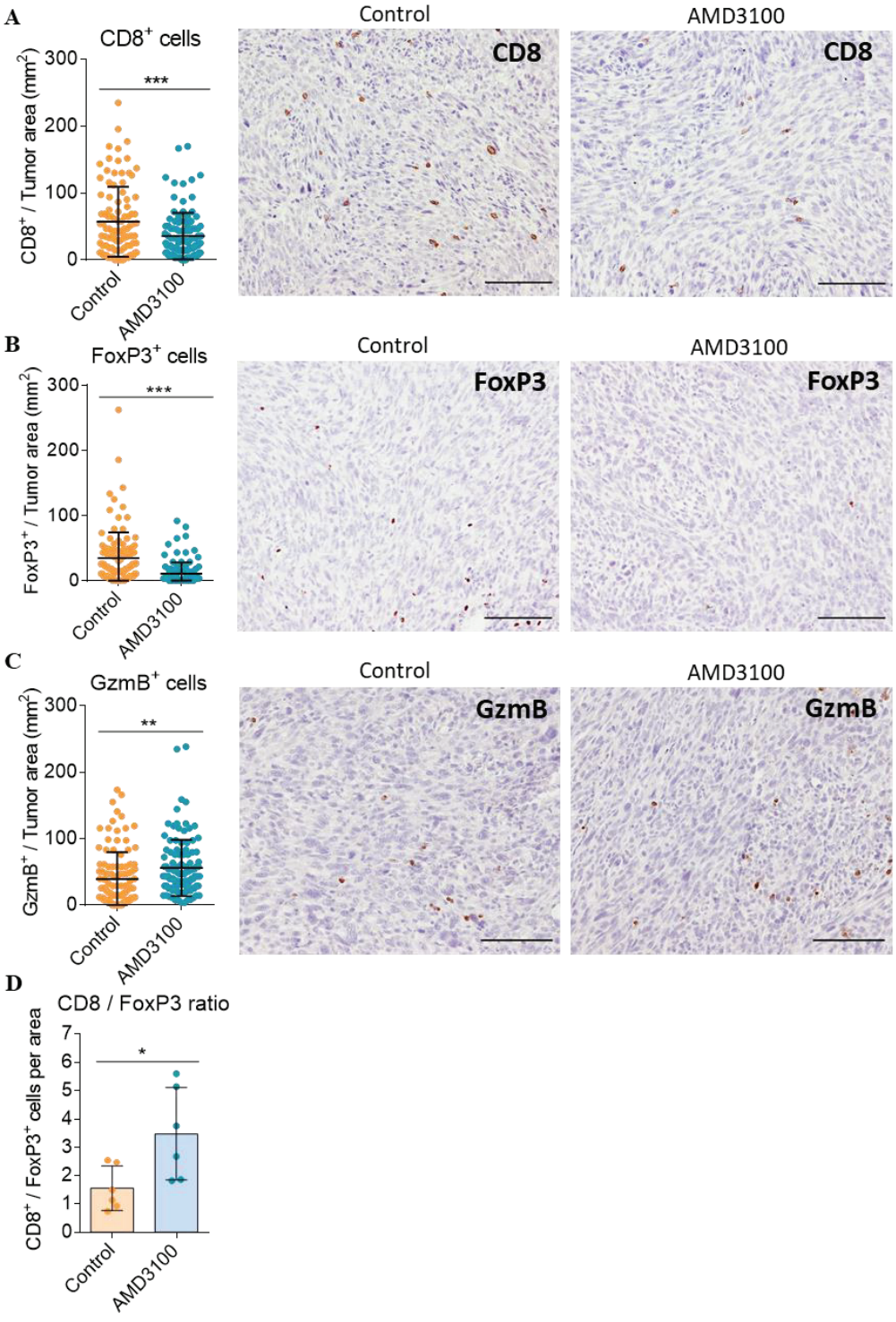

Figure 43. AMD3100 promoted a less immunosuppressive TME in PD/S-SCCs by increasing the CD8 *vs.* FoxP3 ratio and the recruitment of cytotoxic GzmB$^+$ cells. Frequency (mean ± SD) of (**A**) CD8$^+$ cells, (**B**) FoxP3$^+$ (Treg) cells and (**C**) cytotoxic (GzmB$^+$) cells per tumor area and representative immunohistochemistry images of control and AMD3100 treated tumors. Scale bar: 100 µm. (**D**) Quantification (mean ± SD) of CD8 *vs.* FoxP3 cells ratio per tumor area. Data obtained from 6 independent samples per group (*n=6*) and quantified from 20 images per sample**.** Statistical significance of the differences observed between control and AMD3100 treated tumors were analyzed by unpaired two-tailed Student's T test. * p≤0.05; ** p≤0.01; *** p≤0.001.

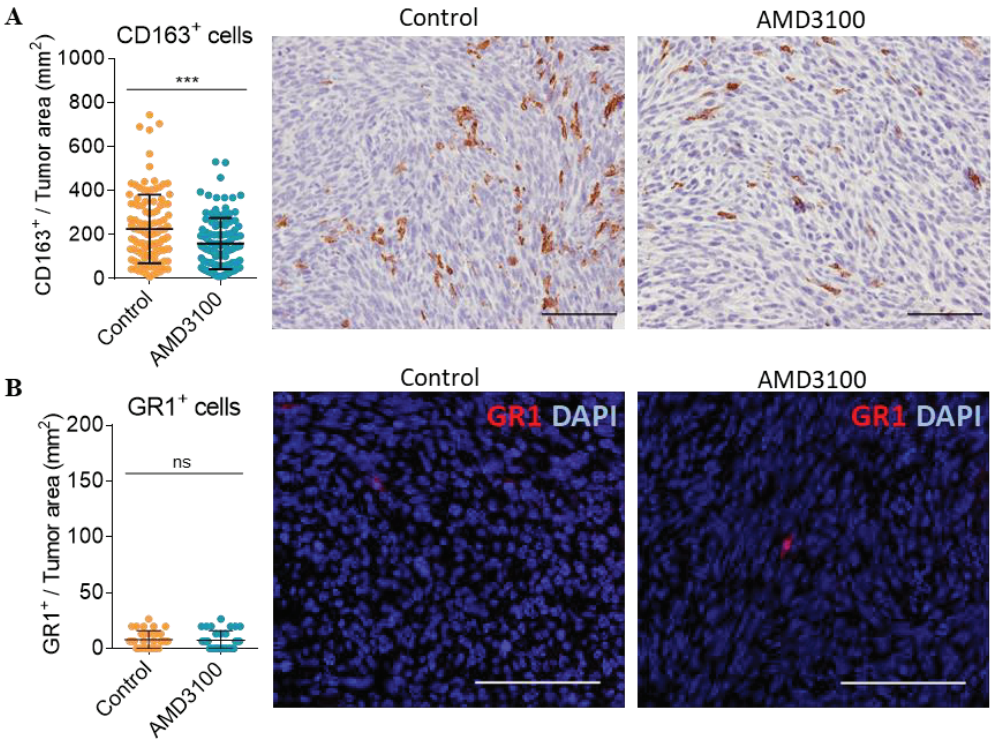

Figure 44. AMD3100 treatment reduces the infiltration of M2-like macrophages in PD/S-SCCs. (**A**) Frequency (mean ± SD) of $CD163^+$ cells (M2-like macrophages) per tumor area and representative immunohistochemistry images of control and AMD3100 treated tumors. Scale bar: 100 µm. Data obtained from 6 independent samples per group (*n=6*) and quantified from 20 images per sample. (**B**) Frequency (mean ± SD) of $GR1^+$ cells per tumor area and representative immunofluorescence images of GR1 (red) in control and AMD3100 treated tumors. Cell nuclei were stained with DAPI (blue). Scale bar: 100 µm. Data obtained from 3 independent samples per group (*n=3*) and quantified from 10 images per sample. Statistical significance of the differences observed between control and AMD3100 treated tumors were analyzed by unpaired two-tailed Student's T test. ns: $p>0.05$; *** $p\leq0.001$.

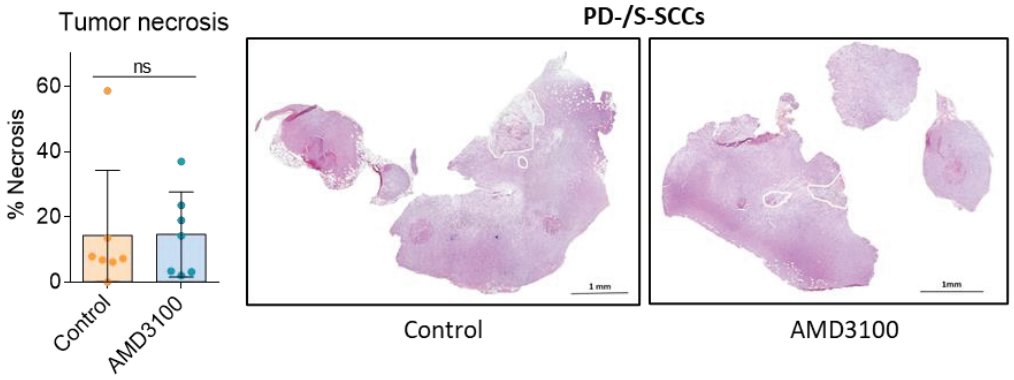

Figure 45. AMD3100 treatment does not increase necrosis of PD/S-SCCs tumors. Quantification of the percentage (mean ± SD) of tumor necrotic area and representative H/E section of PD/S-SCCs treated with control solution or AMD3100, where necrotic areas are marked with white lines. Scale bar: 1 mm. Each dot represents a single tumor (*n=7*). Statistical significance of the differences observed between control and AMD3100 treated tumors were analyzed by unpaired two-tailed Student's T test. ns: p>0.05.

CHAPTER 3: STUDY ALTERNATIVE STRATEGIES TO PROMOTE ANTI-TUMOR RESPONSE OF ICI THERAPIES IN ADVANCED cSCCS

The expression of MHC-I by cancer cells is fundamental for CD8+ T cells to identify and eliminate malignant cells. In addition, PD-L1 expression has been proposed as a predictive marker of anti-PD-1/PD-L1 response in patients (C. Sun et al., 2018). Previous results from our laboratory indicated that epithelial cancer cells from WD-SCCs expressed cell surface MHC-I and PD-L1 while mesenchymal cells from PD-SCCs cells did not express cell surface MHC-I neither PD-L1. We aimed to validate these observations in primary SCC cell cultures and study the possible mechanisms leading to the lack of cell surface expression of MHC-I and PD-L1 in advanced SCC tumor cells.

3.1 Characterize the transcriptional status of MHC-I and antigen processing genes in cSCC cells

To study the mechanisms that prevent MHC-I and PD-L1 cell surface expression, two full epithelial primary SCC cell cultures (2C3 and 3A cells) and two mesenchymal EpCAM$^-$ SCC cell cultures (S3T1$^-$ and 6G2$^-$ cells) were used. The expression of *Mhc-I*, *Mhc-II*, *Pd-l1*, and MHC-I antigen processing genes such as *Tap1*, *Tap2*, *Tapasin*, and *β2-microglobulin* was analyzed by RT-qPCR in basal conditions. Mesenchymal EpCAM$^-$ SCC cells showed a downregulated expression of *Mhc-I*, *Mhc-II*, and *Pd-l1* mRNA as compared to full epithelial SCC cells (Figures 46A-46C). Furthermore, the expression of *Tap1* was reduced in mesenchymal EpCAM$^-$ SCC cells, while the expression of *Tap2*, *Tapasin*, and *β2-microglobulin* did not vary between full epithelial and mesenchymal EpCAM$^-$ SCC cells (Figure 47). Hence, these results demonstrate that

transcriptional downregulation of *Mhc-I*, *Mhc-II*, *Pd-l1*, and *Tap1* genes is induced in mesenchymal EpCAM- SCC cells.

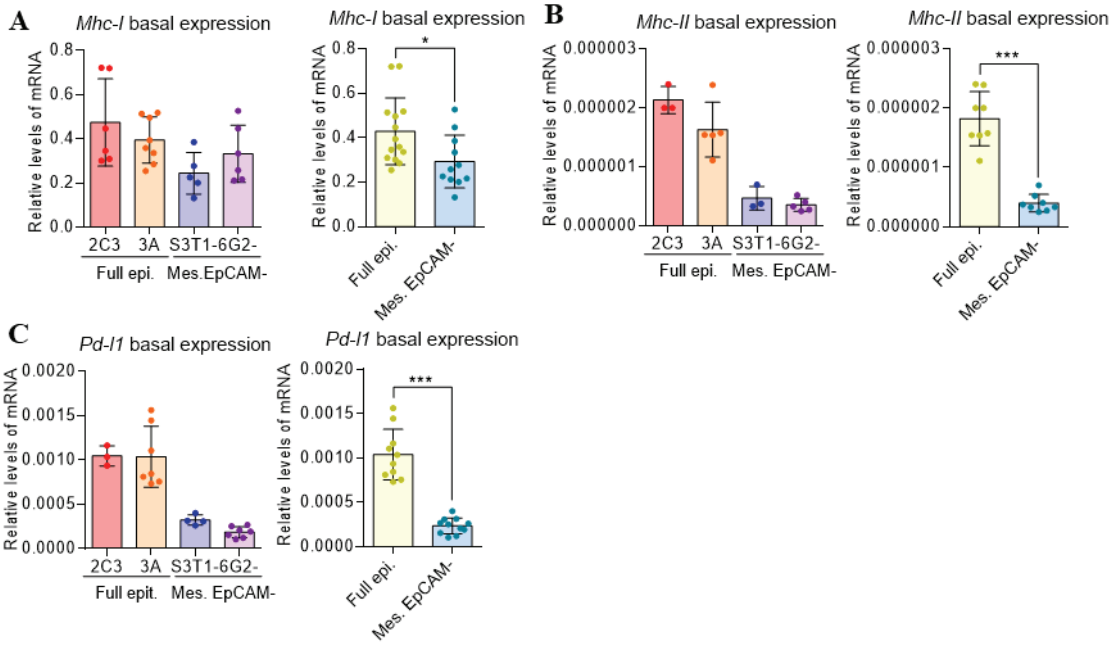

Figure 46. *Mhc-I*, *Mhc-II* and *Pd-l1* mRNA basal expressions are downregulated in mesenchymal EpCAM$^-$ SCC cells. Results show (mean ± SD) the basal mRNA levels normalized to *Ppia* of (**A**) *Mhc-I*, (**B**) *Mhc-II*, and (**C**) *Pd-l1* in the indicated tumor cells. Dots represent independent experiments (*n=3-8*). Grouped analysis were performed considering 2C3 and 3A full epithelial SCC cells and S3T1$^-$ and 6G2$^-$ mesenchymal EpCAM$^-$ SCC cells. Statistical significance of the differences observed between full epithelial and mesenchymal EpCAM$^-$ SCC cells was analyzed by unpaired two-tailed Student's T test. * p≤0.05; *** p≤0.001. Full epi.: full epithelial SCC cells; Mes. EpCAM$^-$: mesenchymal EpCAM$^-$ SCC cells.

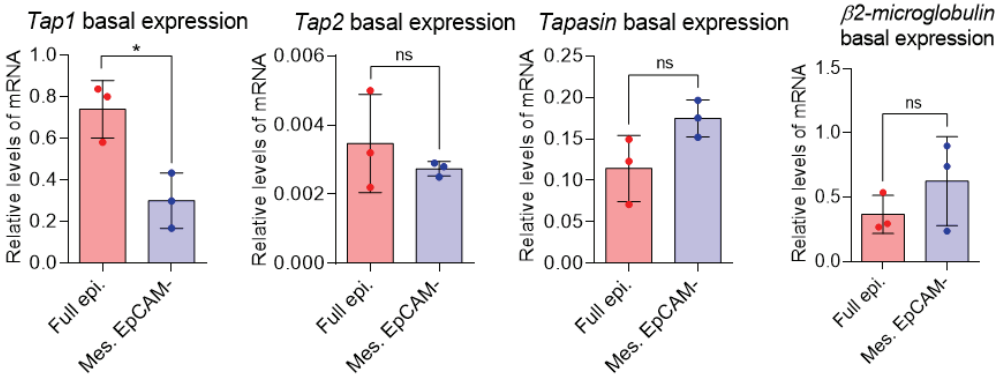

Figure 47. The basal expression of MHC-I antigen processing protein *Tap1* is downregulated in mesenchymal EpCAM$^-$ SCC cells. Results show (mean ± SD) the basal mRNA levels normalized to *Ppia* of *Tap1*, *Tap2*, *Tapasin*, and *β2-microglobulin* in full epithelial SCC cells (2C3 cells) and mesenchymal EpCAM$^-$ SCC cells (S3T1$^-$ cells). Dots represent independent experiments (*n=3*). Statistical significance of the differences observed between full epithelial and mesenchymal EpCAM$^-$ SCC cells was analyzed by unpaired two-tailed Student's T test. ns: p>0.05; * p≤0.05. Full epi.: full epithelial SCC cells; Mes. EpCAM$^-$: mesenchymal EpCAM$^-$ SCC cells.

Next, the cell surface expression of MHC-I, MHC-II, and PD-L1 was analyzed by flow cytometry in full epithelial and mesenchymal EpCAM$^-$ SCC cells. In accordance with the previous *in vivo* data from the group, full epithelial SCC cells expressed MHC-I, MHC-II, and PD-L1 while mesenchymal EpCAM$^-$ cells did not express these proteins on the cell surface (Figures 48A-48C). So, despite *Mhc-I*, *Mhc-II*, and *Pd-l1* mRNA being detectable in mesenchymal EpCAM$^-$ SCC cells, these cells did not express these proteins in the cell surface, indicating a further post-transcriptional control on the processing and cell surface location of these proteins.

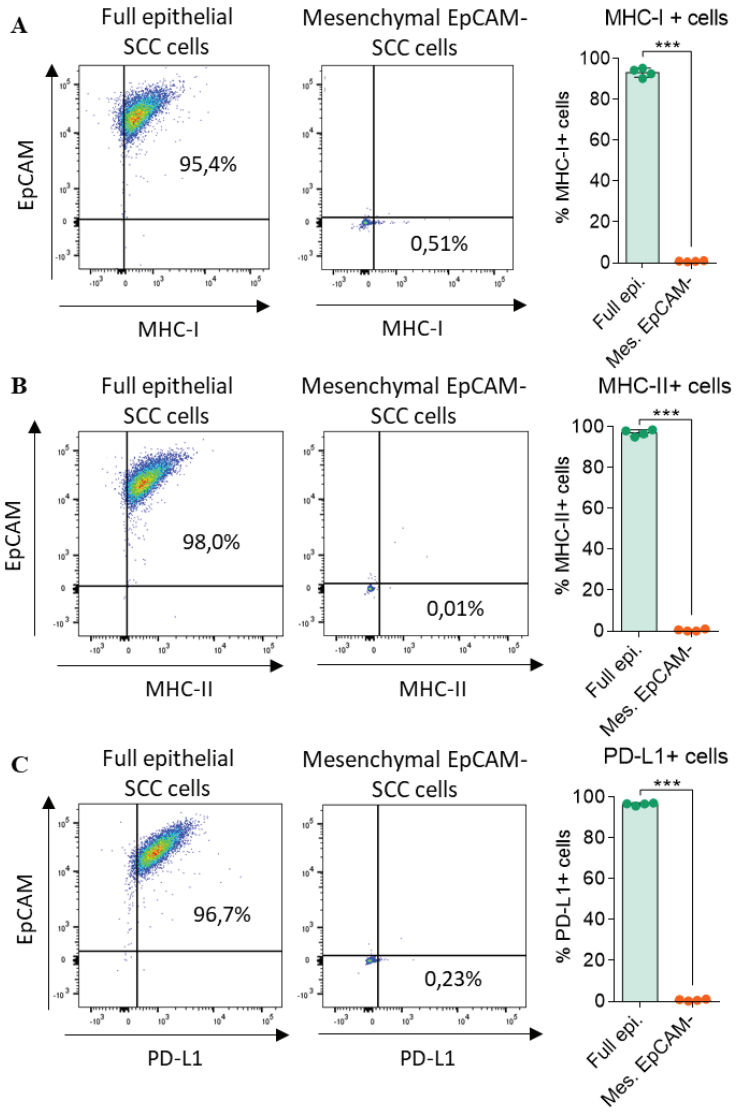

Figure 48. MHC-I, MHC-II and PD-L1 proteins are not detected in the cell surface of mesenchymal EpCAM$^-$ SCC cells. Representative flow cytometry dot plots and quantification of the percentage of cells (mean ± SD) expressing cell surface (**A**) MHC-I, (**B**) MHC-II, and (**C**) PD-L1, as determined by flow cytometry. Dots represent independent experiments (*n=4*). Grouped analysis were performed considering 2C3 and 3A full epithelial SCC cells and S3T1$^-$ and 6G2$^-$ mesenchymal EpCAM$^-$ SCC cells. Statistical significance of the differences observed between full epithelial and mesenchymal EpCAM$^-$ SCC cells was analyzed by unpaired two-tailed Student's T test. *** $p \leq 0.001$. Full epi.: full epithelial SCC cells; Mes. EpCAM$^-$: mesenchymal EpCAM$^-$ SCC cells.

Histone methylation is a conserved process, where the addition of methyl groups on certain amino acids of histones modifies the packaging and accessibility to DNA, ultimately resulting in gene expression control. Dysregulation of histone methylation has been extensively documented in aging and cancer states leading to altered gene expression regulation (Michalak et al., 2019). In this sense, the administration of GSK126, which is a selective EZH2 methyltransferase inhibitor, promotes antigen presentation and antitumor immunity in head and neck cancer cells by increasing *Mhc-I* transcription (L. Zhou et al., 2020). To determine if MHC-1 downregulation may be related to altered histone methylation in mesenchymal SCC cells, full epithelial SCC cells and mesenchymal EpCAM$^-$ SCC cells were treated with GSK126, following a previously established protocol in our laboratory, and the expression of *Mhc-I* and *Pd-l1* was analyzed. GSK126 treatment reduced histone H3 lysine 27 trimethylation, which is a target of EZH2 methyltransferase, indicating a correct function of the drug (Figure 49A). Despite blocking EZH2 function, *Mhc-I* and *Pd-l1* expression was not increased in full epithelial or mesenchymal EpCAM$^-$ SCC cells. Accordingly, *Mhc-I* and *Pd-l1* mRNA levels in mesenchymal EpCAM$^-$ SCC cells were not restored to the levels of full epithelial SCC cells with GSK126 treatment (Figures 49B-49C). The cell surface expression of MHC-I and PD-L1 also remained unaltered after GSK126 treatment (Figures 49D-49E). Thus, in advanced mesenchymal SCC cells, *Mhc-I* downregulation is not dependent on EZH2 methyltransferase activity on histones interacting with the *Mhc-I* promoter and gene region as observed in other tumor types.

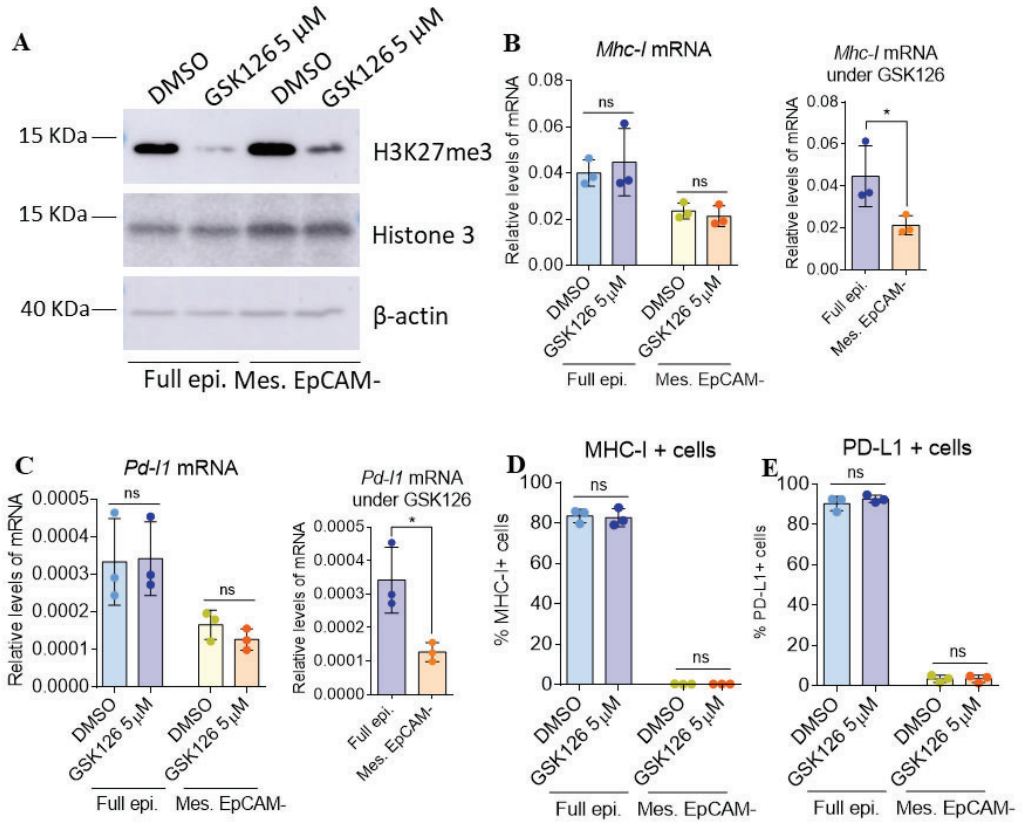

Figure 49. Figure legend on next page.

Figure 49. GSK126 treatment does not restore *Mhc-I* expression in mesenchymal EpCAM$^-$ SCC cells. (**A**) Representative image of histone 3 lysine 27 trimethylation levels in full epithelial SCC cells (2C3 cells) and mesenchymal EpCAM$^-$ SCC cells (S3T1$^-$ cells) upon DMSO or 5 μM GSK126 treatment during 72 hours, as determined by western blot. Results show (mean ± SD) the mRNA levels normalized to *Gadph* of (**B**) *Mhc-I* and (**C**) *Pd-l1* upon DMSO or 5 μM GSK126 treatment for 72 hours in the indicated tumor cells. Quantification (mean ± SD) of the percentage of cells expressing cell surface (**D**) MHC-I and (**E**) PD-L1 as determined by flow cytometry upon DMSO or 5 μM GSK126 treatment during 72 hours in the indicated tumor cells. Dots represent independent experiments (*n=3*). Statistical significance of the differences observed between compared groups was analyzed by unpaired two-tailed Student's T test. ns: $p>0.05$; * $p\leq0.05$. Full epi.: full epithelial SCC cells; Mes. EpCAM$^-$: mesenchymal EpCAM$^-$ SCC cells.

3.2 IFN-γ signaling pathway and MHC-I expression in cSCC cells

Given that *Mhc-I*, *Mhc-II*, *Pd-l1* and MHC-I antigen processing genes expression is controlled by IFN-γ signaling (F. Zhou, 2009)(Abiko et al., 2015), it was analyzed whether this pathway was altered in mesenchymal EpCAM$^-$ cells. The receptor of IFN-γ is a heterodimer composed of two subunits, IFNGR1 and IFNGR2, both needed for the correct transduction of the signal. The *Ifngr1* was expressed at higher levels in full epithelial SCC cells than in mesenchymal EpCAM$^-$ SCC cells (Figure 50A), while *Ifngr2* expression was higher in mesenchymal EpCAM$^-$ SCC cells (Figure 50B). Interestingly, when combining the data of both receptors, it was observed that mesenchymal EpCAM$^-$ SCC cells had balanced mRNA levels of both *Ifngr1* and *Ifngr2*, whereas full epithelial SCC cells presented an unbalanced transcriptional level of both receptors (Figure 50D). In addition, the basal expression of *Irf1*, which is a downstream effector of IFN-γ signaling was higher in mesenchymal EpCAM$^-$ SCC cells than in full epithelial SCC cells (Figure 50C). So, despite both full epithelial and mesenchymal EpCAM$^-$ SCC cells expressed *Ifngr1* and *Ifngr2* they might respond differently to IFN-γ given its different expression levels.

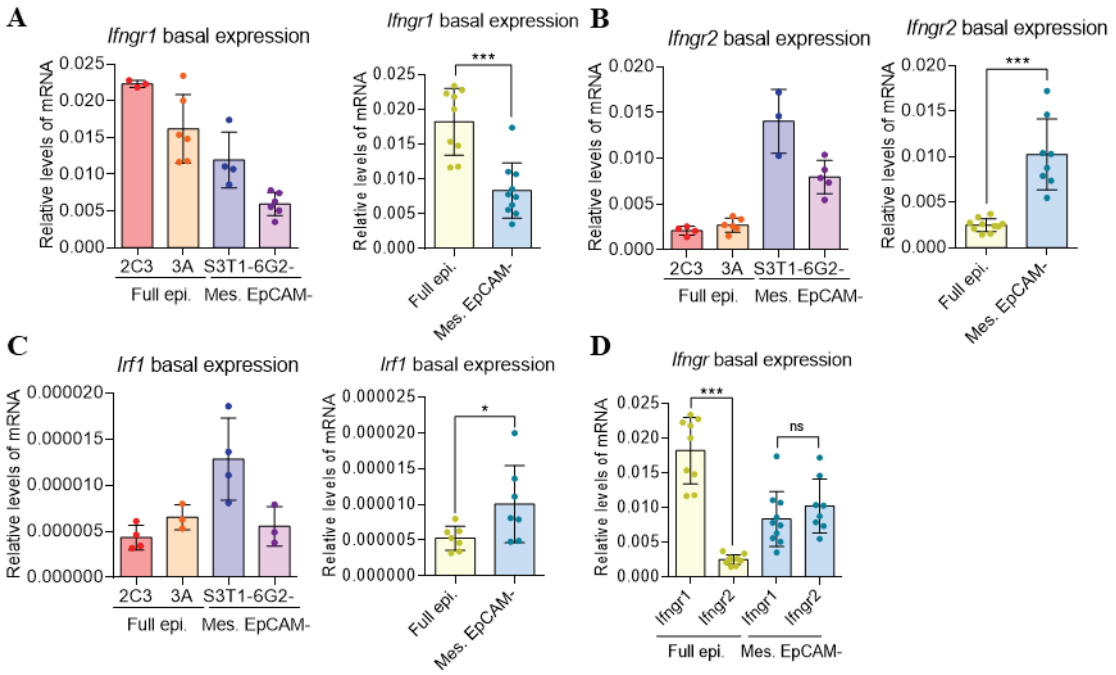

Figure 50. *Infgr1*, *Infgr2* and *Irf1* are differently expressed in full epithelial SCC cells and mesenchymal EpCAM$^-$ SCC cells. Results show (mean ± SD) the basal mRNA levels normalized to *Ppia* of (**A**) *Ifngr1*, (**B**) *Infgr2*, (**C**) *Irf1*, (**D**) *Ifngr1/2* in the indicated tumor cells. Dots represent independent experiments (*n=3-6*). Grouped analysis were performed considering 2C3 and 3A full epithelial SCC cells and S3T1$^-$ and 6G2$^-$ mesenchymal EpCAM$^-$ SCC cells. Statistical significance of the differences observed between full epithelial and mesenchymal EpCAM$^-$ SCC cells was analyzed by unpaired two-tailed Student's T test. * p≤0.05; *** p≤0.001. Full epi.: full epithelial SCC cells; Mes. EpCAM$^-$: mesenchymal EpCAM$^-$ SCC cells.

To test this hypothesis, full epithelial SCC cells and mesenchymal EpCAM$^-$ SCC cells were treated with recombinant murine IFN-γ for 48 hours and both upregulated STAT1 phosphorylation and *Irf1* expression, which are downstream effectors of IFN-γ signaling indicating that these SCC cells are sensible to IFN-γ and present a correct signal transduction of this pathway (Figures 51A-51C). Specifically, mesenchymal EpCAM$^-$ SCC cells treated with IFN-γ induced a higher phosphorylation state of STAT1 than full epithelial SCC cells (Figure 51B). In contrast, full epithelial SCC cells induced higher levels of *Irf1* upon IFN-γ stimulation in comparison to mesenchymal EpCAM- SCC cells (Figure 51C). So, despite presenting some differences, the IFN-γ signaling pathway is functional in both full epithelial SCC cells and mesenchymal EpCAM$^-$ SCC cells.

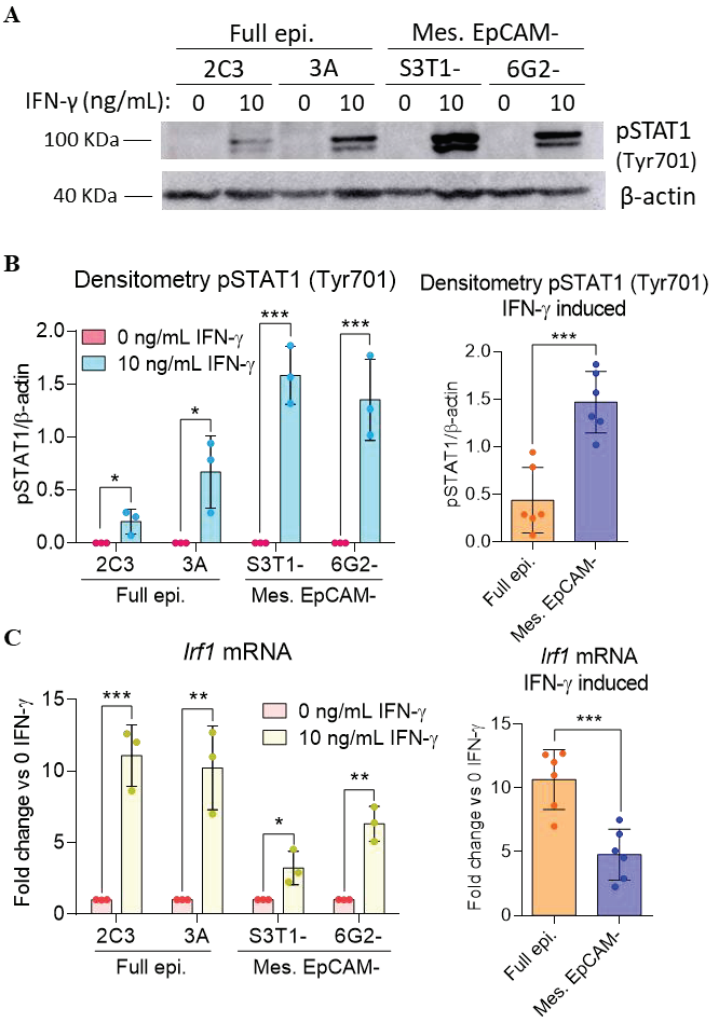

Figure 51. IFN-γ signalling is functional in full epithelial and mesenchymal EpCAM$^-$ SCC cells. (**A**) Representative image of Phospho-STAT1 (Tyr 701) levels in the indicated cell populations upon basal and 10 ng/mL IFN-γ treatment, as determined by western blot. (**B**) Quantification of phosphorylated STAT1 (Tyr-701) relative to β-actin levels (mean ± SD) in the indicated cell populations upon basal and 10 ng/mL IFN-γ treatment. Densitometry analysis was based on 3 different WB assays performed in the same conditions. (**C**) Results show the *Irf1* mRNA levels fold change (mean ± SD) of 10 ng/mL IFN-γ treated cells compared to its basal condition normalized to *Gapdh* and *Ppia* expression in the indicated cell populations. Dots represent independent experiments (*n=3*). Grouped analysis were performed considering 2C3 and 3A full epithelial SCC cells and S3T1$^-$ and 6G2$^-$ mesenchymal EpCAM$^-$ SCC cells. Statistical significance of the differences observed between compared groups was analyzed by unpaired two-tailed Student's T test. * p≤0.05; ** p≤0.01; *** p≤0.001. Full epi.: full epithelial SCC cells; Mes. EpCAM$^-$: mesenchymal EpCAM$^-$ SCC cells.

Once validated that full epithelial SCC cells and mesenchymal EpCAM- SCC cells were responding to IFN-γ, we studied the expression of *Mhc-I*, *Mhc-II*, *Pd-l1*, and MHC-I antigen processing genes upon IFN-γ stimulation. Full epithelial SCC cells and mesenchymal EpCAM$^-$ SCC cells treated with IFN-γ increased the mRNA expression of *Mhc-I*, *Mhc-II*, and *Pd-l1* (Figures 52A-52C). *Pd-l1* upregulated expression was higher in mesenchymal EpCAM- SCC cells than in full epithelial SCC cells treated with IFN-γ (Figure 52C), while the induction of *Mhc-I* and *Mhc-II* expression was slightly higher in IFN-γ stimulated full epithelial SCC cells than mesenchymal SCC cells (Figures 52A-52B). The expression of MHC-I antigen processing genes *Tap1*, *Tap2*, *Tapasin*, and *β2-microglobulin* was increased in both full epithelial and mesenchymal EpCAM$^-$ SCC cells upon IFN-γ treatment (Figures 53A-53D). INF-γ induced expression of *Tap2* was higher in full epithelial SCC cells than in mesenchymal EpCAM$^-$ SCC cells (Figure 53B) while *β2-microglobulin* and *Tapasin* expression was slightly more induced in mesenchymal EpCAM$^-$ SCC cells (Figures 53C-53D). So, the expression of *Mhc-I*, *Mhc-II*, *Pd-l1*, and MHC-I antigen processing genes was increased in full epithelial SCC cells and mesenchymal EpCAM$^-$ cells upon IFN-γ stimulation indicating that IFN-γ signaling pathway is not altered in SCC cells and correctly induces the mRNA expression of MHC-I related genes as reported in the bibliography.

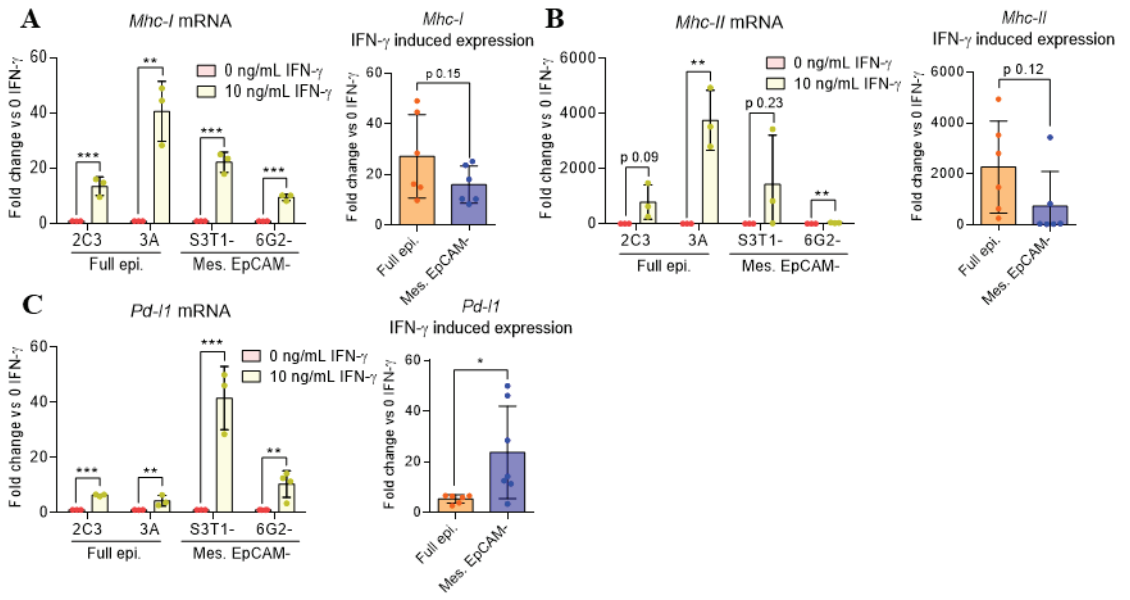

Figure 52. *Mhc-I*, *Mhc-II*, and *Pd-l1* mRNA levels are increased upon IFN-γ treatment in full epithelial and mesenchymal EpCAM$^-$ SCC cells. Results show (mean ± SD) the mRNA level fold change of 10 ng/mL IFN-γ treated cells compared to its basal condition normalized to *Gapdh* and *Ppia* expression of (**A**) *Mhc-I*, (**B**) *Mhc-II*, and (**C**) *Pd-l1* in the indicated cell populations. Dots represent independent experiments (*n=3-4*). Grouped analysis were performed considering 2C3 and 3A full epithelial SCC cells and S3T1$^-$ and 6G2$^-$ mesenchymal EpCAM$^-$ SCC cells. Statistical significance of the differences observed between compared groups was analyzed by unpaired two-tailed Student's T test. ns: p>0.05; * p≤0.05. Full epi.: full epithelial SCC cells; Mes. EpCAM$^-$: mesenchymal EpCAM$^-$ SCC cells.

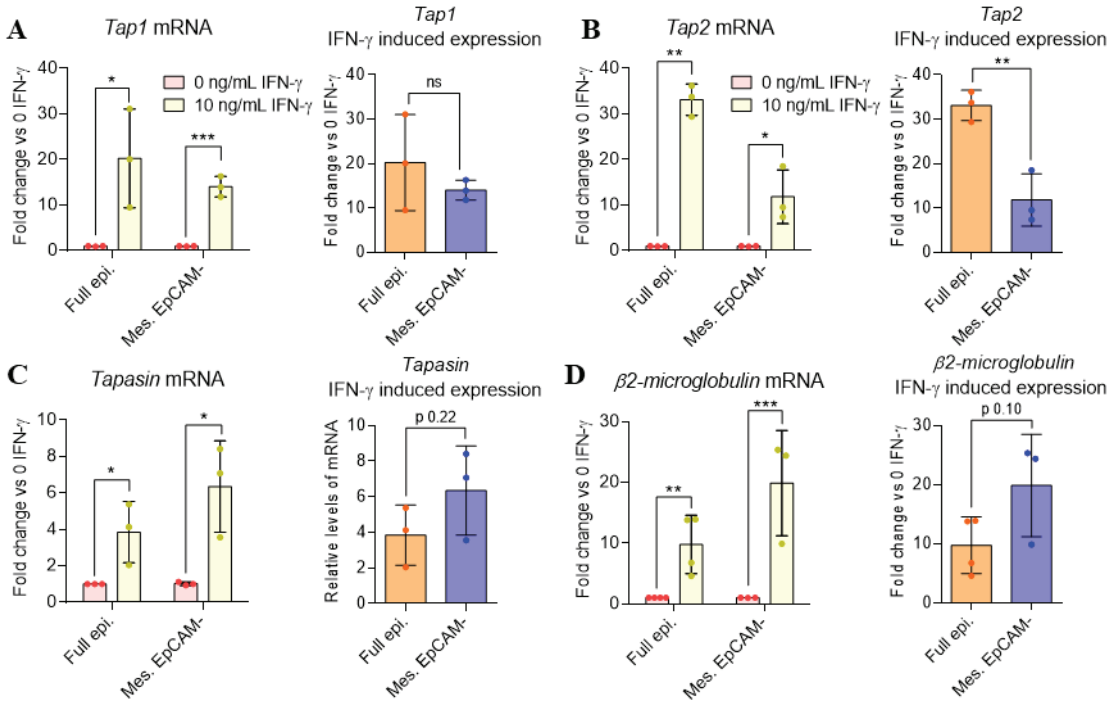

Figure 53. mRNA levels of MHC-I antigen processing proteins are increased upon IFN-γ treatment in full epithelial and mesenchymal EpCAM$^-$ SCC cells. Results show (mean ± SD) the mRNA levels fold change of 10 ng/mL IFN-γ treated cells compared to its basal condition normalized to *Gapdh* and *Ppia* expression of (**A**) *Tap1*, (**B**) *Tap2*, (**C**) *Tapasin*, and (**D**) *β2-microglobulin* in full epithelial SCC cells (2C3 cells) and mesenchymal EpCAM$^-$ SCC cells (S3T1$^-$ cells). Dots represent independent experiments (*n=3*). Statistical significance of the differences observed between compared groups was analyzed by unpaired two-tailed Student's T test. ns: $p>0.05$; * $p\leq0.05$; ** $p\leq0.01$; *** $p\leq0.001$. Full epi.: full epithelial SCC cells; Mes. EpCAM$^-$: mesenchymal EpCAM$^-$ SCC cells.

Next, the total amount of MHC-I expressed by full epithelial SCC cells and mesenchymal EpCAM$^-$ SCC cells were analyzed via WB analysis. Interestingly, a similar level of MHC-I protein was detected in both full epithelial and mesenchymal EpCAM$^-$ SCC cells under basal conditions (Figure 54A). In addition, the total amount of MHC-I protein was increased in both cell types upon IFN-γ stimulation, although only in full epithelial SCC cells this induction was significant (Figure 54B). Hence, despite mesenchymal EpCAM$^-$ SCC cells did not express MHC-I in the cell surface, MHC-I was being translated into protein suggesting that mesenchymal EpCAM$^-$ SCC cells might present alterations in MHC-I processing and translocation to the cell membrane.

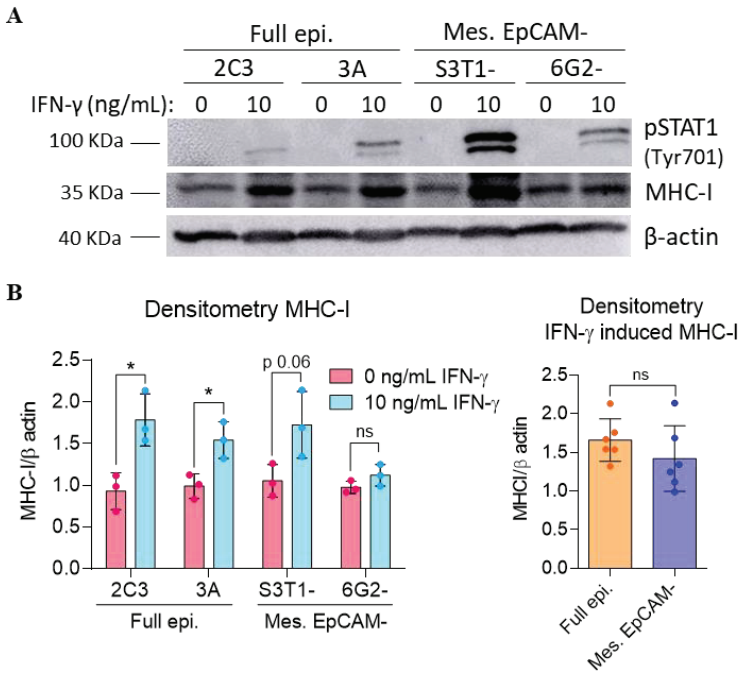

Figure 54. MHC-I protein levels are increased in full epithelial SCC cells upon IFN-γ stimulation. (**A**) Representative image of Phospho-STAT1 (Tyr 701) and MHC-I levels in the indicated cell populations upon basal and 10 ng/mL IFN-γ treatment, as determined by western blot. (**B**) Quantification of MHC-I relative to β-actin levels (mean ± SD) in the indicated cell populations upon basal and 10 ng/mL IFN-γ treatment. Densitometry analysis was made on 3 different WB assays performed in the same conditions. Dots represent independent experiments (*n=3*). Grouped analysis were performed considering 2C3 and 3A full epithelial SCC cells and S3T1$^-$ and 6G2$^-$ mesenchymal EpCAM$^-$ SCC cells. Statistical significance of the differences observed between compared groups was analyzed by unpaired two-tailed Student's T test. ns: $p>0.05$; * $p\leq0.05$. Full epi.: full epithelial SCC cells; Mes. EpCAM$^-$: mesenchymal EpCAM$^-$ SCC cells.

Next, MHC-I, MHC-II, and PD-L1 cell surface expression upon basal and IFN-γ treatment was analyzed by flow cytometry in full epithelial SCC cells and mesenchymal EpCAM$^-$ SCC cells. Full epithelial SCC cells treated with IFN-γ increased the cell surface expression of MHC-I. However, MHC-I was not detected in the mesenchymal EpCAM$^-$ SCC cell surface even after IFN-γ stimulation (Figures 55A-55C). MHC-II cell surface expression in full epithelial SCC cells was increased upon IFN-γ treatment, and mesenchymal EpCAM$^-$ SCC cells presented a slightly increased MHC-II cell surface expression upon IFN-γ stimulation (Figures 56A-56C). Interestingly, both full epithelial SCC cells and mesenchymal EpCAM$^-$ SCC cells upregulated the cell surface expression of PD-L1 upon IFN-γ treatment (Figures 57A-57C). This indicates that MHC-I, MHC-II, and PD-L1 proteins present an independent maturation process and translocation to the cell membrane in mesenchymal EpCAM$^-$ SCC cells. In addition, the lack of MHC-I cell surface detection despite its mRNA levels and the total amount of MHC-I protein being increased with IFN-γ stimulation suggests that there is a post-translational mechanism preventing the arrival of MHC-I to the cell membrane of advanced SCC cells.

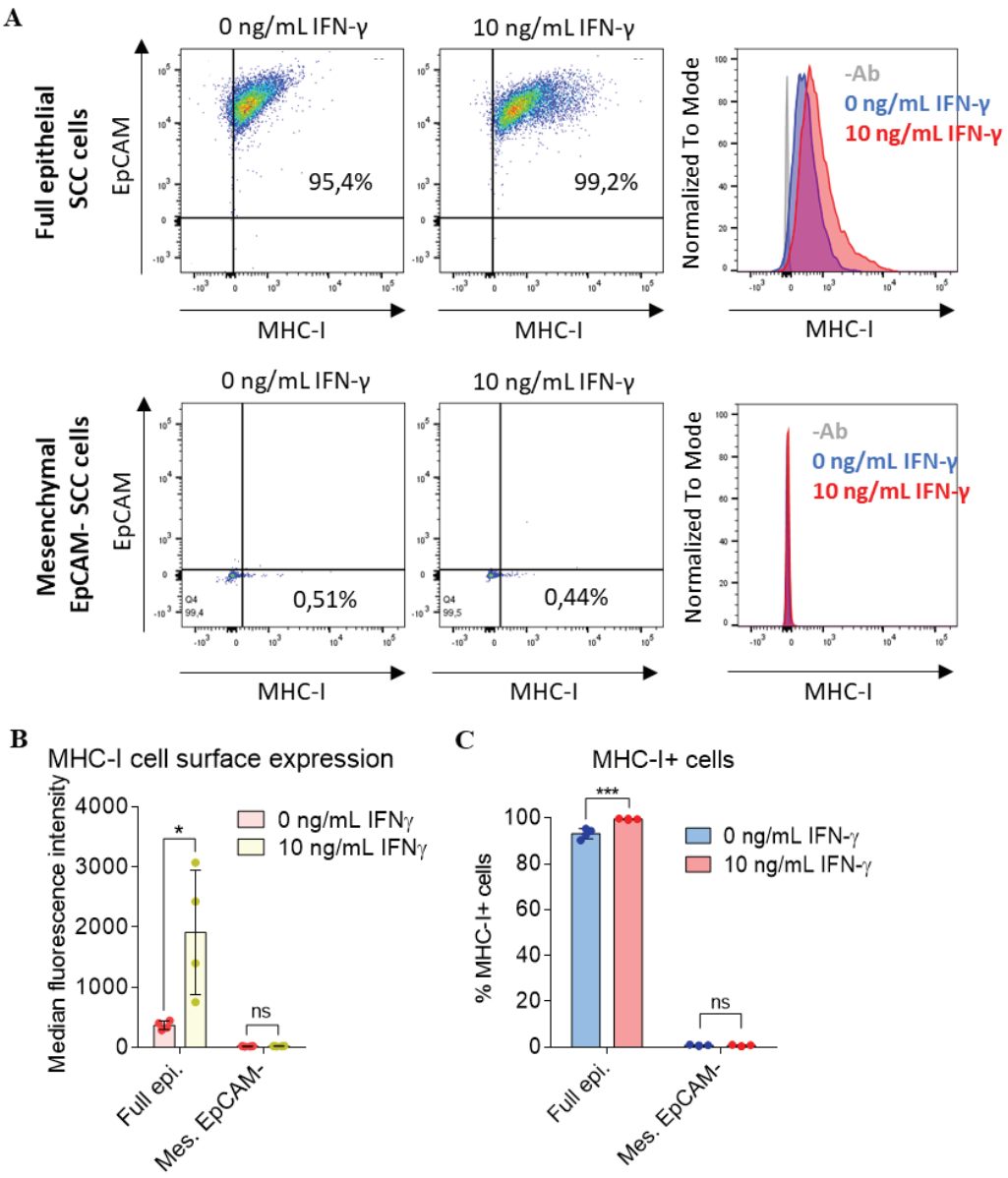

Figure 55. MHC-I is not detected in the cell surface of mesenchymal EpCAM$^-$ SCC cells despite IFN-γ stimulation. (**A**) Representative flow cytometry dot plots and intensity of cell surface expression of MHC-I in the indicated cell types upon basal and 10 ng/mL IFN-γ treatment (**B**) Quantification of the intensity (mean ± SD) of MHC-I expression at cell surface in full epithelial SCC cells (2C3 and 3A cells) and mesenchymal EpCAM$^-$ SCC cells (S3T1$^-$ and 6G2$^-$ cells) upon basal and 10 ng/mL IFN-γ treatment, as determined by flow cytometry. (**C**) Quantification of the percentage of cells (mean ± SD) expressing cell surface MHC-I in full epithelial SCC cells (2C3 and 3A cells) and mesenchymal EpCAM$^-$ SCC cells (S3T1$^-$ and 6G2$^-$ cells) upon basal and 10 ng/mL IFN-γ treatment, as determined by flow cytometry. Dots represent independent experiments (*n=4*). Grouped analysis were performed considering 2C3 and 3A full epithelial SCC cells and S3T1$^-$ and 6G2$^-$ mesenchymal EpCAM$^-$ SCC cells. Statistical significance of the differences observed between compared groups was analyzed by unpaired two-tailed Student's T test. ns: $p>0.05$; * $p\leq0.05$; *** $p\leq0.001$. Full epi.: full epithelial SCC cells; Mes. EpCAM$^-$: mesenchymal EpCAM$^-$ SCC cells.

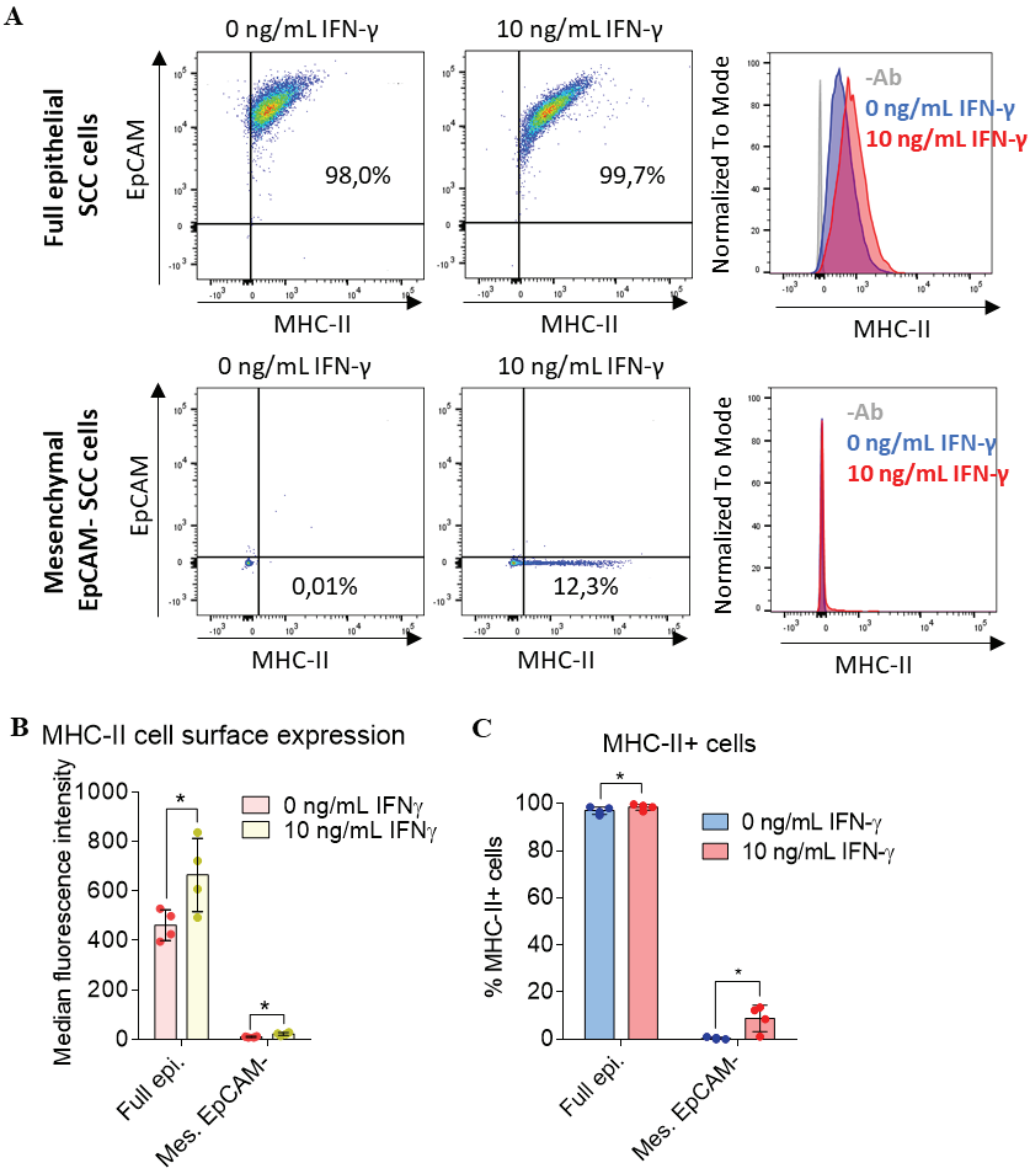

Figure 56. MHC-II cell surface expression is increased in mesenchymal EpCAM$^-$ SCC cells upon IFN-γ treatment. (**A**) Representative flow cytometry dot plots and intensity of cell surface expression of MHC-II in the indicated cell types upon basal and 10 ng/mL IFN-γ treatment. (**B**) Quantification of the intensity (mean ± SD) of MHC-II expression at cell surface in full epithelial SCC cells (2C3 and 3A cells) and mesenchymal EpCAM$^-$ SCC cells (S3T1$^-$ and 6G2$^-$ cells) upon basal and 10 ng/mL IFN-γ treatment, as determined by flow cytometry. (**C**) Quantification of the percentage of cells (mean ± SD) expressing cell surface MHC-II in full epithelial SCC cells (2C3 and 3A cells) and mesenchymal EpCAM$^-$ SCC cells (S3T1$^-$ and 6G2$^-$ cells) upon basal and 10 ng/mL IFN-γ treatment, as determined by flow cytometry. Dots represent independent experiments (*n=4*). Grouped analysis were performed considering 2C3 and 3A full epithelial SCC cells and S3T1$^-$ and 6G2$^-$ mesenchymal EpCAM$^-$ SCC cells. Statistical significance of the differences observed between compared groups was analyzed by unpaired two-tailed Student's T test. ns: $p>0.05$; * $p\leq0.05$; *** $p\leq0.001$. Full epi.: full epithelial SCC cells; Mes. EpCAM$^-$: mesenchymal EpCAM$^-$ SCC cells.

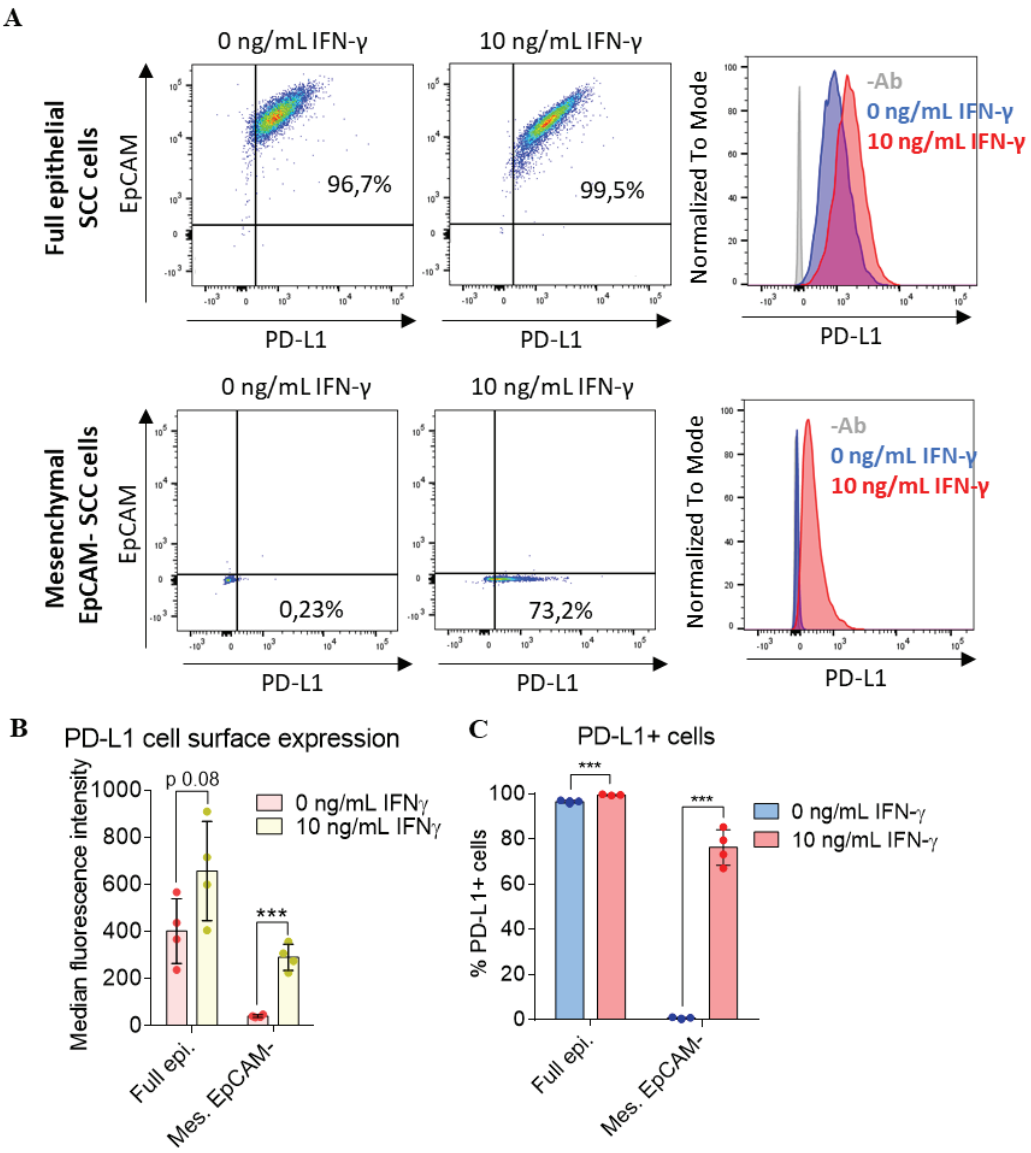

Figure 57. PD-L1 expression detected in the cell surface of mesenchymal EpCAM$^-$ SCC cells is increased upon IFN-γ treatment. (**A**) Representative flow cytometry dot plots and intensity of cell surface expression of PD-L1 in the indicated cell types upon basal and 10 ng/mL IFN-γ treatment. (**B**) Quantification of the intensity (mean ± SD) of cell surface expression of PD-L1 in full epithelial SCC cells (2C3 and 3A cells) and mesenchymal EpCAM$^-$ SCC cells (S3T1$^-$ and 6G2$^-$ cells) upon basal and 10 ng/mL IFN-γ treatment, as determined by flow cytometry. (**C**) Quantification of the percentage of cells (mean ± SD) expressing cell surface PD-L1 in full epithelial SCC cells (2C3 and 3A cells) and mesenchymal EpCAM$^-$ SCC cells (S3T1$^-$ and 6G2$^-$ cells) upon basal and 10 ng/mL IFN-γ treatment, as determined by flow cytometry. Dots represent independent experiments (*n=4*). Grouped analysis were performed considering 2C3 and 3A full epithelial SCC cells and S3T1$^-$ and 6G2$^-$ mesenchymal EpCAM$^-$ SCC cells. Statistical significance of the differences observed between compared groups was analyzed by unpaired two-tailed Student's T test. ns: $p>0.05$; * $p\leq0.05$; *** $p\leq0.001$. Full epi.: full epithelial SCC cells; Mes. EpCAM$^-$: mesenchymal EpCAM$^-$ SCC cells.

To further validate these observations, the cellular location of MHC-I was analyzed via an immunofluorescence assay on full epithelial SCC cells and mesenchymal EpCAM$^-$ SCC cells with or without IFN-γ stimulation. Accordingly with our previous data, full epithelial SCC cells expressed MHC-I in the cell membrane in basal conditions, and upon IFN-γ treatment MHC-I expression was increased in the cell membrane (Figure 58). By contrast, MHC-I was not detected in the cell membrane of mesenchymal EpCAM$^-$ cells in basal conditions or upon stimulation with IFN-γ. Importantly, MHC-I was detected in accumulations at perinuclear regions when mesenchymal EpCAM$^-$ SCC cells were stimulated with IFN-γ (Figure 58). Hence, *Mhc-I* was translated into protein in mesenchymal EpCAM$^-$ cells but its trafficking to the cell membrane was not functional. This goes in accordance with the fact that mesenchymal EpCAM$^-$ SCC cells were not expressing cell surface MHC-I despite IFN-γ upregulated *Mhc-I* mRNA expression. Thus, advanced SCC cells correctly respond to IFN-γ increasing the expression of *Mhc-I* mRNA, but the protein cannot reach the cell surface, preventing its antigen presenting function.

Finally, it has been described that autophagy directly causes immune evasion by degrading MHC-I in different tumor conditions, such as pancreatic ductal adenocarcinoma (Yamamoto et al., 2020). Given that our results indicate that MHC-I is being translated into protein in mesenchymal EpCAM$^-$ cells but cannot arrive at the cell membrane, we hypothesized that autophagy could be preventing the arrival of MHC-I at the cell membrane by degrading MHC-I. To test this hypothesis, mesenchymal EpCAM$^-$ SCC cells were treated with the inhibitor of autophagic flux Bafilomycin A1, which led to the accumulation of LC3 protein (Figure 59A) validating the function of the drug. However, Bafilomycin A1 treatment did not increase MHC-I trafficking to the cell surface membrane of mesenchymal EpCAM$^-$ SCC cells (Figure 59B). Increasingly concentrations of Bafilomycin A1 did not increase MHC-I and PD-L1 levels at the cell surface (Figure 59C). In addition, combinatory treatment of Bafilomycin A1 with IFN-γ did not further increase MHC-I or PD-L1 cell surface expression in mesenchymal EpCAM$^-$ SCC cells (Figure 59D). Hence, MHC-I is accumulated in perinuclear regions upon IFN-γ stimulation, and this process is not dependent on autophagy, unlike other reported tumor types.

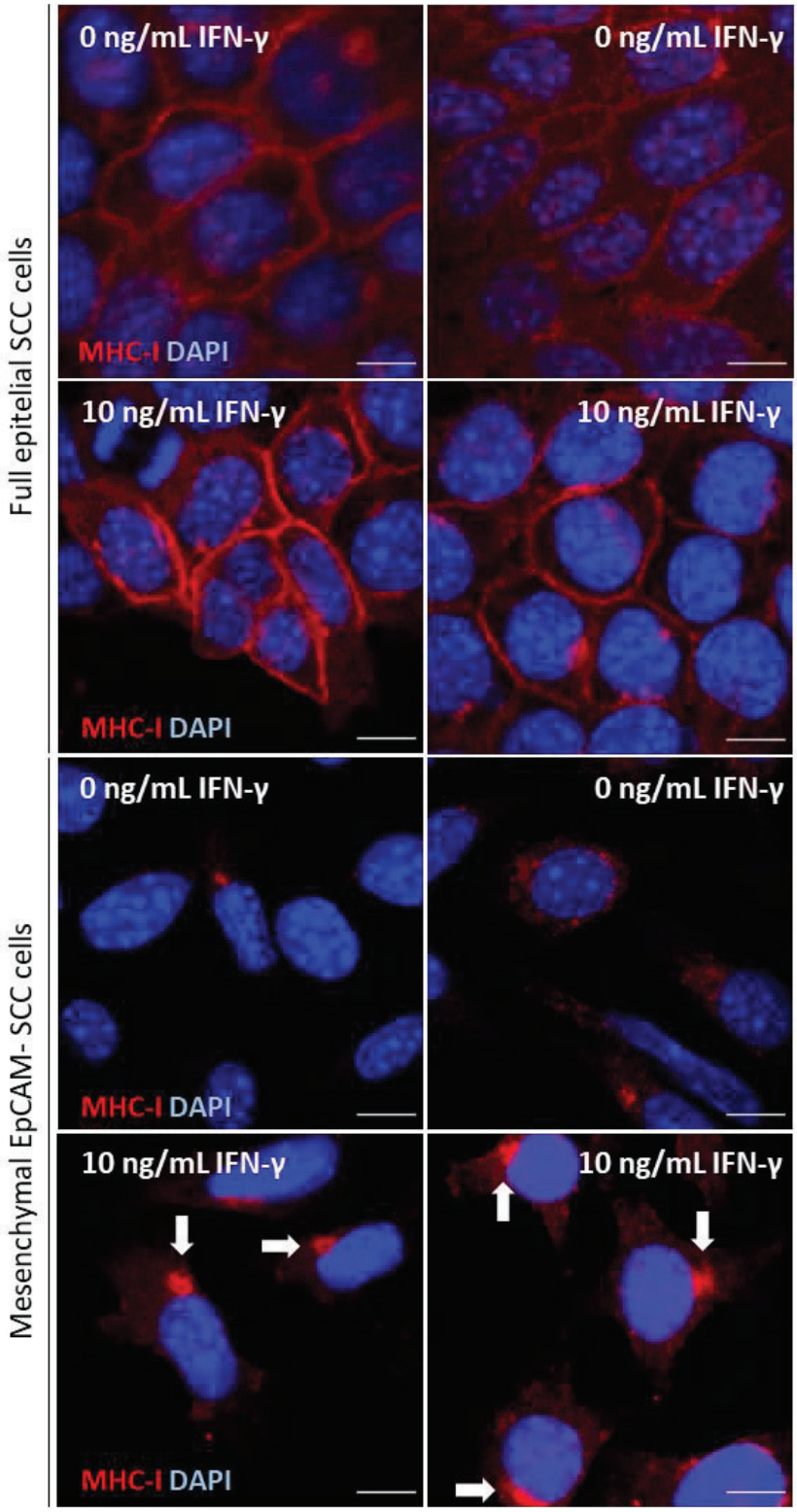

Figure 58. MHC-I is retained in perinuclear regions in mesenchymal EpCAM$^-$ SCC cells after IFN-γ stimulation. Representative immunofluorescence images of MHC-I (red) in full epithelial SCC cells (2C3 cells) and mesenchymal EpCAM$^-$ SCC cells (S3T1$^-$ cells) upon basal and 10 ng/mL IFN-γ treatment. Cell nuclei were stained with DAPI (blue). Images were obtained from 2 independent experiments in the same conditions (n=2). Arrows indicate MHC-I perinuclear accumulation. Scale bar: 10 μm.

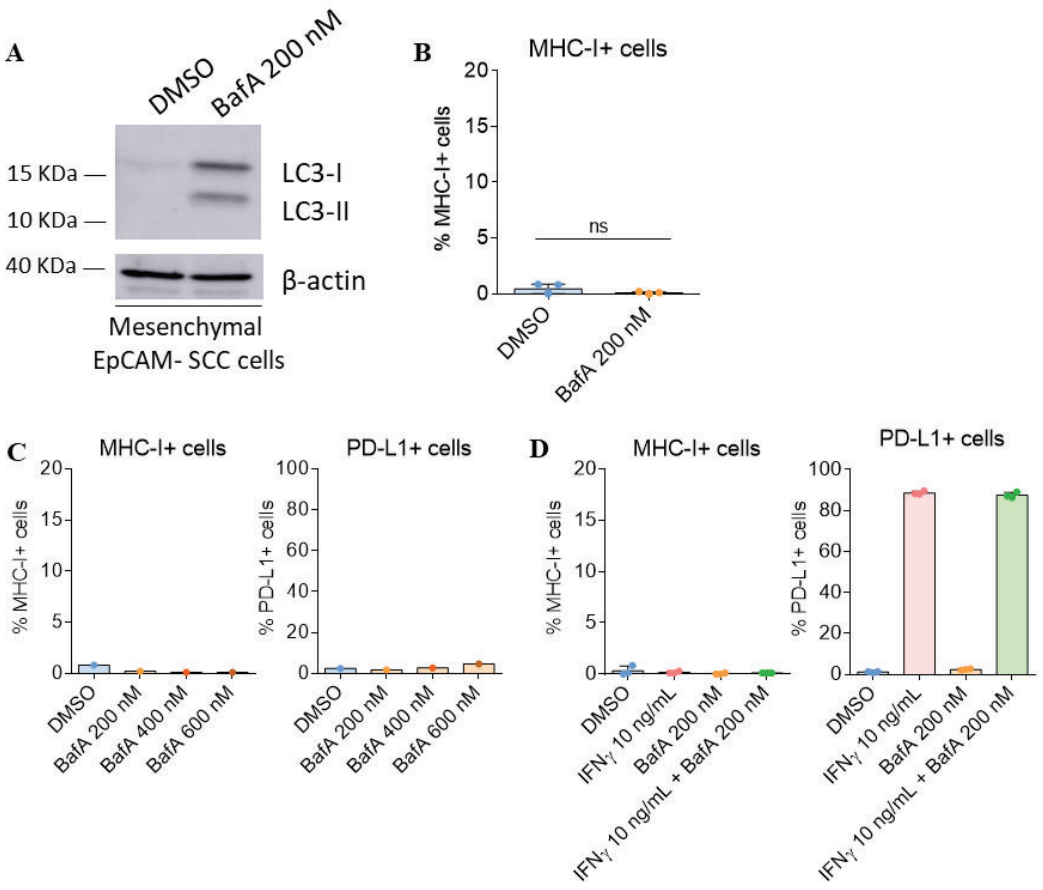

Figure 59. BafA treatment does not increase MHC-I expression in mesenchymal EpCAM$^-$ SCC cell surface. (**A**) Representative image of LC3 levels in mesenchymal EpCAM$^-$ SCC cells (S3T1$^-$ cells) upon DMSO or BafA 200 nM treatment, as determined by western blot. (**B**) Quantification of the percentage of cells (mean ± SD) expressing cell surface MHC-I upon DMSO or BafA 200 nM treatment in mesenchymal EpCAM$^-$ SCC cells (S3T1$^-$ cells), as determined by flow cytometry. Dots represent independent experiments (*n=3*). (**C**) Quantification of the percentage of cells expressing MHC-I and PD-L1 at the cell surface upon DMSO or increasing concentrations of BafA (200 nM – 400 nM – 600 nM) treatment in mesenchymal EpCAM$^-$ SCC cells (S3T1$^-$ cells), as determined by flow cytometry. Data obtained from 1 experiment (*n=1*). (**D**) Quantification of the percentage of mesenchymal EpCAM$^-$ SCC cells (S3T1$^-$ cells) (mean ± SD) expressing cell surface MHC-I and PD-L1 upon DMSO, IFN-γ 10 ng/mL, BafA 200 nM, or IFN-γ 10 ng/mL + BafA 200 nM treatment, as determined by flow cytometry. Dots represent independent experiments (*n=3*). Statistical significance of the differences observed between compared groups was analyzed by unpaired two-tailed Student's T test. ns: p>0.05.

CHAPTER 4: STUDY OF PATIENT cSCC AND HNSCC CELL CHARACTERISTICS ASSOCIATED WITH RESISTANCE TO ICI THERAPY

According to results from our group resistance to anti-PD-1/PD-L1 ICI therapy in cSCC may be a consequence of the plasticity of tumor cells, defined as the ability of cancer cells to progress from an epithelial state to a mesenchymal state. Our previous studies in mouse models of cSCC progression demonstrated that the emergency of mesenchymal tumor cells was associated with higher recruitment of immunosuppressive immune cells (Treg cells, M-MDSCs, and M2-like macrophages), which inactivate the antitumor activity of $CD8^+$ T lymphocytes (Lorenzo-Sanz et al., under-review manuscript). Additionally, mesenchymal SCC cells induce the expression of alternative ligands rather than PD-L1, which is mostly expressed by epithelial SCC cells. Specifically, murine mesenchymal SCC cells induced the expression of CD155 and CD80, which activate the IC receptors TIGIT, and CTLA-4, respectively. This would lead to the impairment of the anti-tumor immunity exerted by $CD8^+$ T cells even in the presence of anti-PD-1/PD-L1 inhibitors (Lorenzo-Sanz et al., under-review manuscript). Hence, we hypothesize that mesenchymal SCC cells activate evasion mechanisms of the anti-tumor immune response that are different from epithelial SCC cells. This scenario would prevent the correct response to immunotherapy based on anti-PD-1/PD-L1.

To determine if the presence of mesenchymal cancer cells may be associated with resistance to anti-PD-1 based therapy in patients, we compared cSCC and HNSCC samples from patients that showed response to treatment (responders) or those that exhibit resistance to ICI. Initially we aimed to identify 7 patients with advanced cSCC and 10 patients with recurrent and metastatic HNSCC who would have shown a response (sustainable response or stable disease for around one year) and a similar number of patients who would have shown resistance (lack of response or short-term response ending in disease progression). A retrospective study was performed with cSCC patients who had already been treated with this therapy and tumor samples (pre-treatment samples) were available. However, since immunotherapy based on anti-PD-1 was recently approved by the EMA for the treatment of advanced and cSCC, most of the patients who had been treated in our hospital center received this therapy for compassionate use, and we have been able to have samples from 5 patients, at the time of these assays. Given that immunotherapy based on anti-PD-1 was approved by the EMA a few years before to treat recurrent and metastatic HNSCC, we could obtain various samples of patients treated with anti-PD-1. However, most recurrent and metastatic HNSCC patients were resistant to anti-PD-1. To increase the number of responsive patients for this study, we have expanded the search to patients who had received anti-PD-L1 + anti-CTLA-4 combination therapies obtaining a total of 11 recurrent and metastatic HNSCC patient samples. The frequency of epithelial, hybrid, and mesenchymal cancer cells and the

expression of ICR in $CD8^+$ T cells were characterized by immunohistology analysis. This retrospective study was part of a project that we performed in collaboration with different members of the laboratory, and that was later validated in a higher cohort of cSCC patients (Lorenzo-Sanz et al., under-review manuscript).

4.1 Study of patient cSCC cell characteristics associated with resistance to ICI therapy

Six cSCC patient samples treated with anti-PD-1 therapy were studied in this initial retrospective study (Table 10). A complete response to this treatment (strong reduction in the size of the tumor or disappearance of the lesion) is rare in these patients and has been observed in ~7-13 % of advanced and metastatic cSCC patients (Migden et al., 2018) (Migden et al., 2020). Stabilization of the disease during a long period was considered a positive response, which indicated that the treatment prevented the progression of the disease, as the best response. The intra-treatment samples from PT 4 and PT 5 correspond to tumor biopsies obtained 6 months after the start of treatment, and therefore are samples with ongoing treatment. In contrast to the PT 4, the response of PT 5 was maintained for one year, therefore considering PT 5 as responder, even if disease progressed latter.

Some of the available pre-treatment samples correspond to tumor samples from several months before starting treatment with ICIs, and before to chemotherapy or radiotherapy treatments. The composition and characteristics of the tumor cells could change significantly after each treatment and subsequent recurrence. Thus, there could be important differences in the characteristics of the tumor cells between the biopsy analyzed (several months before starting treatment) and the time of starting treatment. Ideally, the tumor cell characteristics of the samples should be analyzed immediately before starting treatment, to establish a more precise relationship between the presence of hybrid or mesenchymal tumor cells and the response to ICI-based therapy.

Patient	Biopsy	Treatment lines prior to immunotherapy	Time from biopsy to start of ICI therapy	Response
PT 1	PT 1 PRE	Surg.1	11 months	Resistant[1]
PT 2	PT 2 PRE	Surg.1 Surg.2 + Rdt. Erbitux	> 24 months	Responder[2]
PT 3	PT 3 PRE	Surg.1 Surg.2	10 months	Resistant[3]
PT 4	PT 4 PRE	Surg.1 Surg.2 Surg.3	15 days	Resistant[5]
	PT 4 INTRA		6 months[4]	
PT 5	PT 5 INTRA	Surg.1 Chem. + Rdt.	6 months	Responder[6]

Table 10: Summary of the clinical information of skin SCC patients treated with anti-PD-1 immunotherapy included in this study. PT: patient; PRE: pretreatment sample; INTRA: intra-treatment sample; Surg.: surgery; Chem.: chemotherapy; Rdt.: radiotherapy; Erbitux: treatment of cisplatin and cetuximab (EGFR inhibitor). [1]No response was obtained and therapy was discontinued because the patient had an adverse reaction; [2]Treatment for a year and the best response was a stable disease for several months; [3]Treatment was interrupted before 6 months without response; [4]Time elapsed from the start of therapy based on ICIs and obtaining a tumor sample (in the course of treatment); [5]Treatment had an effect but failed to eliminate the tumor; [6]Treatment gave a sustained response for a year, but eventually the disease progressed.

Initially, other members of our group determined the epithelial and mesenchymal characteristics of tumor cells by analyzing the expression of E-cadherin (epithelial marker) and Vimentin (mesenchymal marker) by immunofluorescence (Figure 60), which allowed the quantification of the frequency of epithelial (E-cadherin$^+$/Vimentin$^-$), hybrid (E-cadherin$^+$/Vimentin$^+$) and mesenchymal (E-cadherin$^-$/Vimentin$^+$) tumor cells of cSCC samples (Figure 61A). Despite the high intra-tumor heterogeneity, it was observed that the tumors from PT 5 (responder) presented the highest frequency of E-cadherin$^+$/Vimentin$^-$ tumor cells (Figure 61A). The tumors from PT 2 (responder) and PT 1 and PT 3 (resistant) presented a similar composition of epithelial, hybrid, and mesenchymal cells (Figure 61A). Remarkably, PT 2 (responder) showed the highest E-cadherin expression (Figure 61C). In addition, PT 4 (resistant) presented the highest frequency of Vimentin$^+$ cancer cells (hybrid and mesenchymal cancer cells) (Figure 61B). We hypothesize that the presence of hybrid and mesenchymal tumor cells would be related to therapy resistance. However, given the low number of sensible and resistant cSCC patients to ICI included in this study, it is not possible to extract conclusions regarding the relationship between the ICI response and the E-cadherin/Vimentin expression of tumor cells.

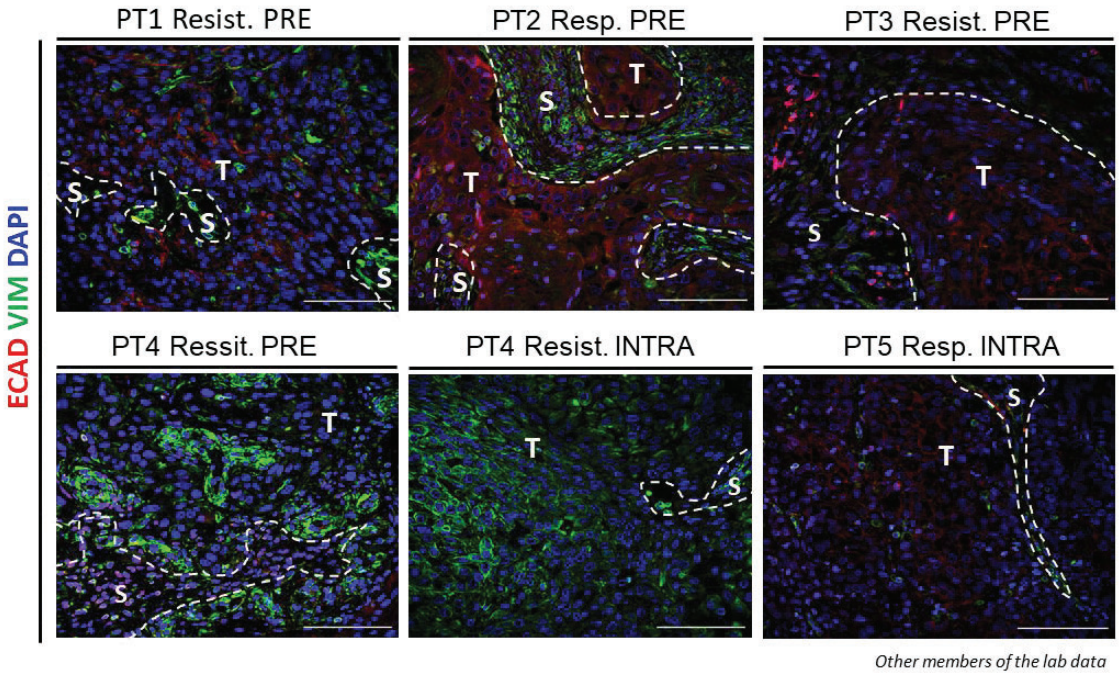

Figure 60. E-cadherin and vimentin expression in tumor cells from cSCC patients treated with ICIs. Representative images of the immunodetection of epithelial (E-cadherin^{+}/Vimentin^{-}), hybrid (E-cadherin^{+}/Vimentin^{+}), and mesenchymal (E-cadherin^{-}/Vimentin^{+}) tumor cells in the indicated cSCCs. Cell nuclei were stained with DAPI (blue). Scale bar: 100 µm. PT: patient; PRE: pretreatment sample; INTRA: intra-treatment sample; S: stroma region; T: tumor cell region; Resist.: resistant; Resp.: responder.

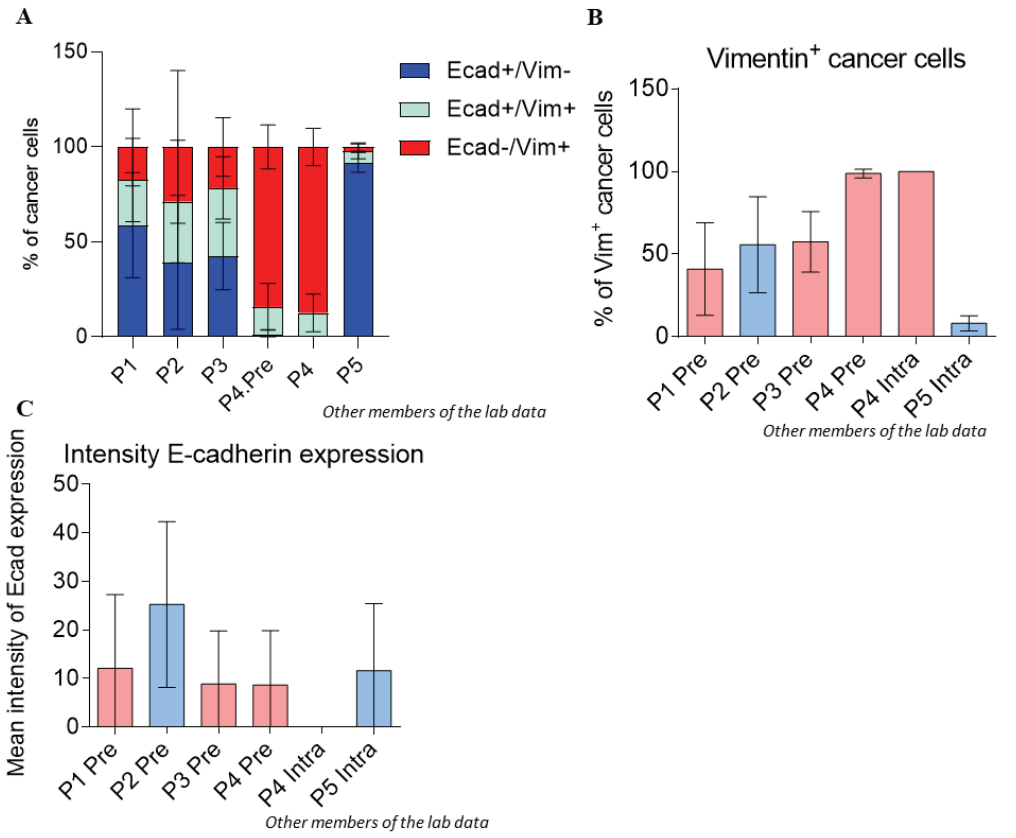

Figure 61. Quantification of the relative frequency of epithelial, hybrid or mesenchymal tumor cells in cSCCs treated with ICIs. (**A**) Quantification (mean ± SD; n= 10-14 images per tumor) of the frequency of epithelial (E-cadherin$^+$/Vimentin$^-$), hybrid (E-cadherin$^+$/Vimentin$^+$, and mesenchymal (E-cadherin$^-$/Vimentin$^+$) tumor cells per area of tumor region in the indicated samples. (**B**) Percentage (mean ± SD; n=10-14 images per tumor) of mesenchymal tumor cells (Vimentin$^+$) per area of tumor region in the indicated cSCCs. (**C**) Mean intensity (mean ± SD; n=10-14 images per tumor) of E-cadherin expression in the indicated cSCCs. PRE: pretreatment sample; INTRA: intra-treatment sample.

Exhausted CD8$^+$ T cells are characterized by an increased expression of various IC receptors including PD-1, CTLA-4, LAG-3, TIM-3, or TIGIT (W. Jiang et al., 2020) (Saleh et al., 2020). To study the presence of exhausted T cells in cSCC patient samples, the expression of the IC receptor PD-1 (Figure 62) and LAG-3 (analyzed by another member of the laboratory) in CD8$^+$ T cells was characterized by immunohistology analysis. Tumors from resistant cSCC patients to anti-PD-1 (PT 1 Pre, PT 3 Pre, and PT 4 Intra) presented a higher CD8$^+$ T cell infiltration compared to the responders (PT 2 Pre and PT 5 Intra) and the PT 4 Pre resistant tumors (Figure 63A). In addition, these T cells in resistant tumors showed a greater capacity to infiltrate the interior of resistant tumors in comparison to responder tumors (Figure 63B). Thus, favoring the contact of these immune cells with tumor cells. These apparently contradictory results suggest that the high infiltrate of CD8$^+$ T cells in resistant tumors could correspond to inactive or dysfunctional T cells that express IC receptors such as PD-1, LAG-3, and/or CTLA-4. In this

sense, our results showed that the frequency of $CD8^+/PD\text{-}1^+$ and $CD8^+/LAG\text{-}3^+$ cells was higher in resistant patients PT 1 and PT 3 than in responder patients PT 2 and PT 5 (Figures 63C-63D). Hence, despite more $CD8^+$ T cells were infiltrating resistant tumors, these $CD8^+$ T cells would be inactive and unable to attack tumor cells. These results indicate tumors from resistant patients to ICI accumulate a higher percentage of inactive $CD8^+$ cytotoxic cells than tumors from responder patients.

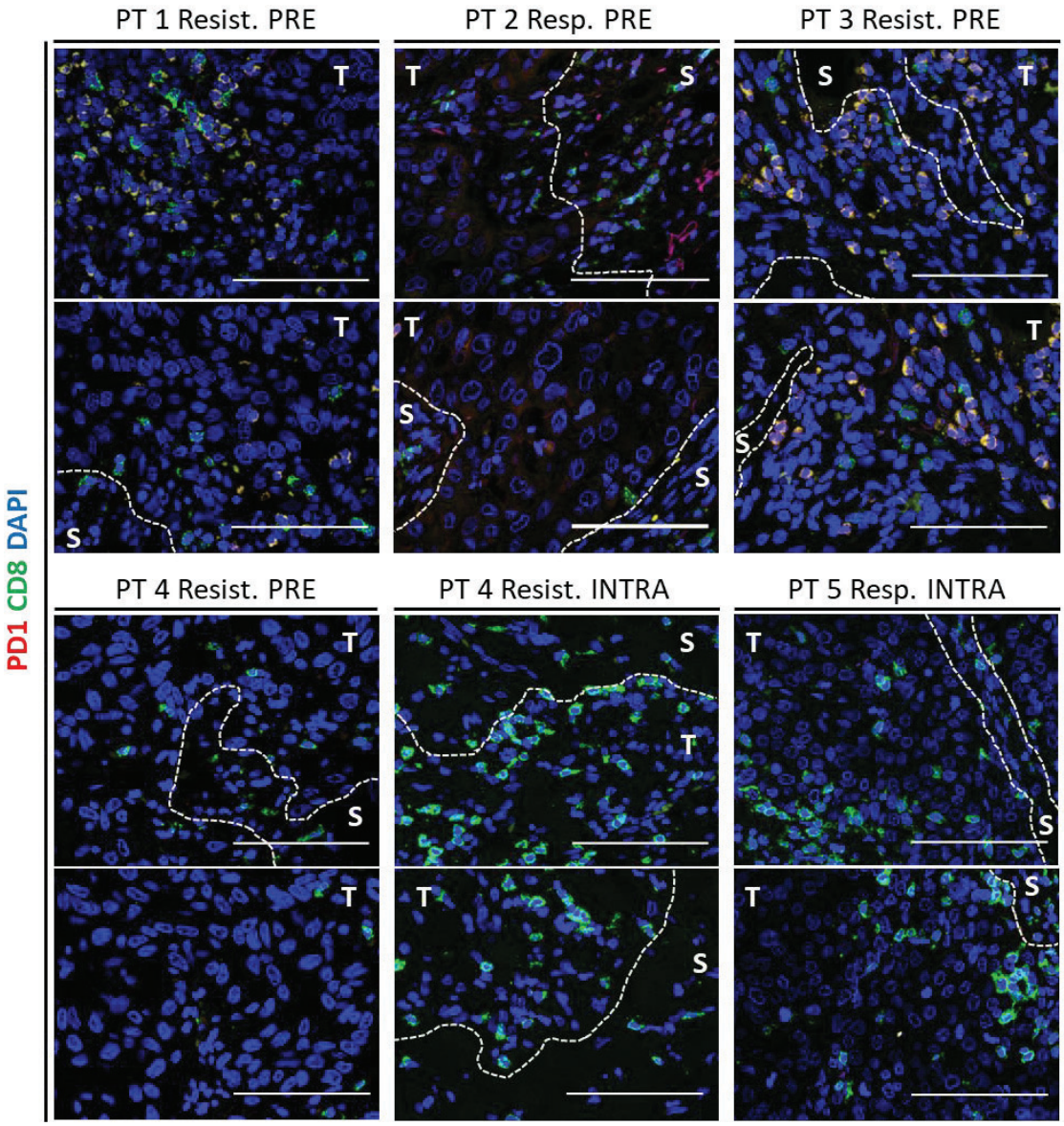

Figure 62. Immunodetection of $CD8^+$ T cells with or without PD-1 expression in cSCC patient samples treated with anti-PD-L1/PD-1. Representative immunofluorescence images of the immunodetection of $CD8^+$ cells (green) with expression of PD-1 (red) in the indicated cSCCs. Cell nuclei were stained with DAPI (blue). Scale bar: 100 µm. PT: patient; PRE: pretreatment sample; INTRA: intra-treatment sample; S: stroma region; T: tumor cell region; Resist.: resistant; Resp.: responder.

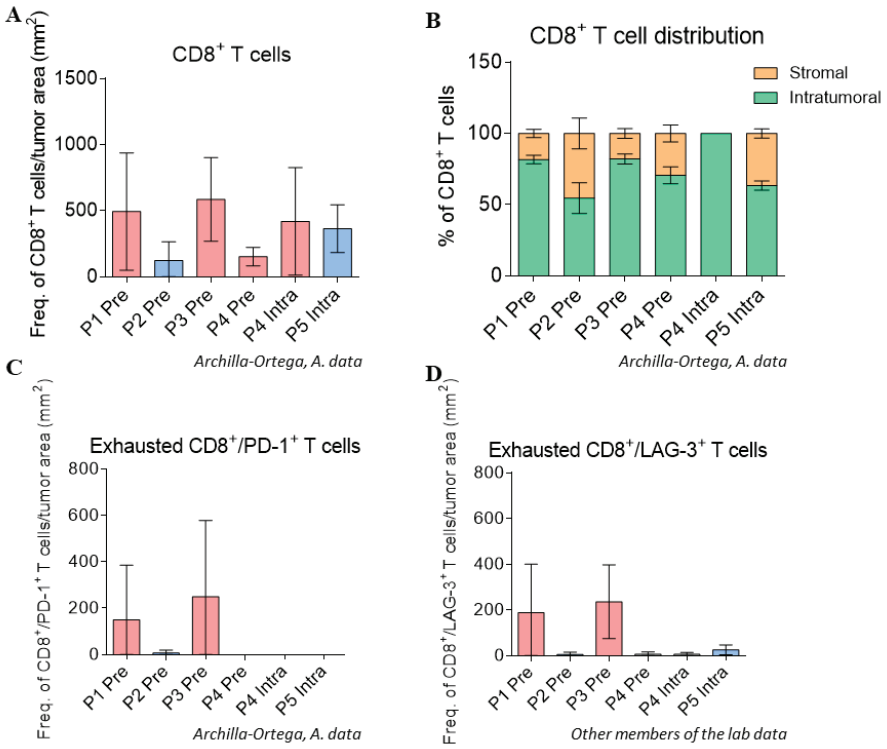

Figure 63. cSCC patients resistant to anti-PD-L1/PD-1 present increased infiltration of exhausted CD8$^+$ T cells. (**A**) Frequency (mean ± SD; *n=15-30* images per tumor) of CD8$^+$ T cells per area of tumor region in the indicated samples. (**B**) Percentage (mean ± SD; *n=10-14* images per tumor) of CD8$^+$ cells located in the stroma or infiltrating the interior of the tumor mass. Frequency (mean ± SD; *n=15-30* images per tumor) of (**C**) CD8$^+$/PD-1$^+$ and (**D**) CD8$^+$/LAG-3$^+$ T cells by tumor area in the indicated cSCCs. Statistical significance of the differences observed between responder *vs.* resistant groups was analyzed using unpaired two-tailed Student's T test. * p≤0.05; ** p≤0.01. Resist.: resistant; Resp.: responder.

Hence, these initial results suggest that tumors with a higher presence of epithelial tumor cells would respond to anti-PD-1/PD-L1 therapy while tumors with a lower presence of epithelial tumor cells and a higher presence of hybrid and mesenchymal tumors cells could be resistant to immunotherapy based on anti-PD-1/PD-L1. In addition, resistant tumors to ICI presented increased recruitment of exhausted T cells, which we hypothesize are linked to a higher presence of mesenchymal tumor cells. These initial observations were further validated in a larger cohort of cSCC patient samples in a posterior study conducted in our laboratory (Lorenzo-Sanz et al., under-review manuscript). In addition, results from our group further suggest that the infiltrate of immunosuppressive cells (Treg cells, MDSCs, and M2-like macrophages) is associated with the presence of mesenchymal tumor cells and could further contribute to the lack of response to therapy, as previously demonstrated by our group in cSCC progression mouse model.

4.2 Study of patient HNSCC cell characteristics associated with resistance to ICI therapy

Eleven advanced and metastatic HNSCC patients treated with anti-PD-L1/anti-PD-1 or the combination of anti-PD-L1 + anti-CTLA-4 therapy were studied (Table 11). A complete response to these immunotherapy treatments (strong reduction in the size of the tumor or disappearance of the lesion) is rare in these patients and is observed in around ~2 % of patients (Ferris et al., 2016) (Burtness et al., 2019). Stabilization of the disease or response maintained for 1 year has been considered a positive response, which indicated that the treatment prevented the progression of the disease, as the best response.

As done with cSCC patient samples, firstly a member of our group characterized the expression of E-cadherin and Vimentin by immunofluorescence assays in HNSCC samples (Figure 64) and quantified the presence of epithelial (E-cadherin^{+}/Vimentin^{-}), hybrid (E-cadherin^{+}/Vimentin^{+}) and mesenchymal (E-cadherin^{-}/Vimentin^{+}) cancer cells (Figure 65A). Similarly to what we observed in cSCC patients, we observed that advanced and metastatic HNSCCs showed strong heterogeneity. Thus, most of the samples analyzed had a variable content of hybrid tumor cells (E-cadherin^{+}/Vimentin^{+}) and mesenchymal cells (E-cadherin^{-}/Vimentin^{+}). When comparing the content of epithelial and mesenchymal cells between the samples of patients sensitive and resistant to ICIs, we observed that while the resistant PT 28 showed a high content of mesenchymal cells, the resistant PT 30 contained mostly epithelial cells and the percentage of epithelial cells was higher than that observed in the PT 66, which is sensitive to anti-PD-L1 (Figure 65A). Therefore, the hybrid and mesenchymal cell content varied markedly between patient samples. Nevertheless, when calculating the average number of Vimentin^{+} cancer cells (mesenchymal and hybrid cancer cells) it was observed that was significantly higher in tumors from non-responders than from responders treated with anti-PD-L1 + anti-CTLA-4 while this increase did not reach statistical significance in HNSCCs treated with anti-PD-1/PD-L1 (Figure 65B). These initial results suggest that a high content of mesenchymal cells would be associated with resistance to ICIs in advanced and metastatic HNSCCs. However, further analyses with a higher number of sensible and resistant advanced and metastatic HNSCC samples will be needed to reinforce and validate these results.

Patient	Biopsy	Treatment	Time of treatment (mo)	Time until disease progression (mo)	Time from biopsy to start of ICI therapy (mo)	Response
PT 24	PT 24 PRE	Anti-PD-L1	1,20	0,97	7,13	Resistant
PT 28	PT 28 PRE	Anti-PD-L1	1,90	1,80	21,5	Resistant
PT 30	PT 30 PRE	Anti-PD-L1	0,93	0,93	10,3	Resistant
PT 66	PT 66 PRE	Anti-PD-L1	14,87	20,77	9,5	Responder
PT 15	PT 15 PRE	Anti-PD-1	2,13	1,43	6,3	Resistant
PT 1	PT 1 PRE	Anti-PD-L1 + Anti-CTLA-4	1,50	1,37	0,8	Resistant
PT 6	PT 6 PRE	Anti-PD-L1 + Anti-CTLA-4	1,87	2,80	6,3	Resistant
PT 26	PT 26 PRE	Anti-PD-L1 + Anti-CTLA-4	1,20	1,20	9,9	Resistant
PT 42	PT 42 PRE	Anti-PD-L1 + Anti-CTLA-4	1,87	2,10	8,3	Resistant
PT 27	PT 27 PRE	Anti-PD-L1 + Anti-CTLA-4	11,87	21,17	9,8	Responder
PT 60	PT 60 PRE	Anti-PD-L1 + Anti-CTLA-4	14	14,10	8,9	Responder

Table 11: Summary of the clinical information of HNSCC patients treated with immunotherapy included in this study. PT: patient; PRE: pretreatment sample.

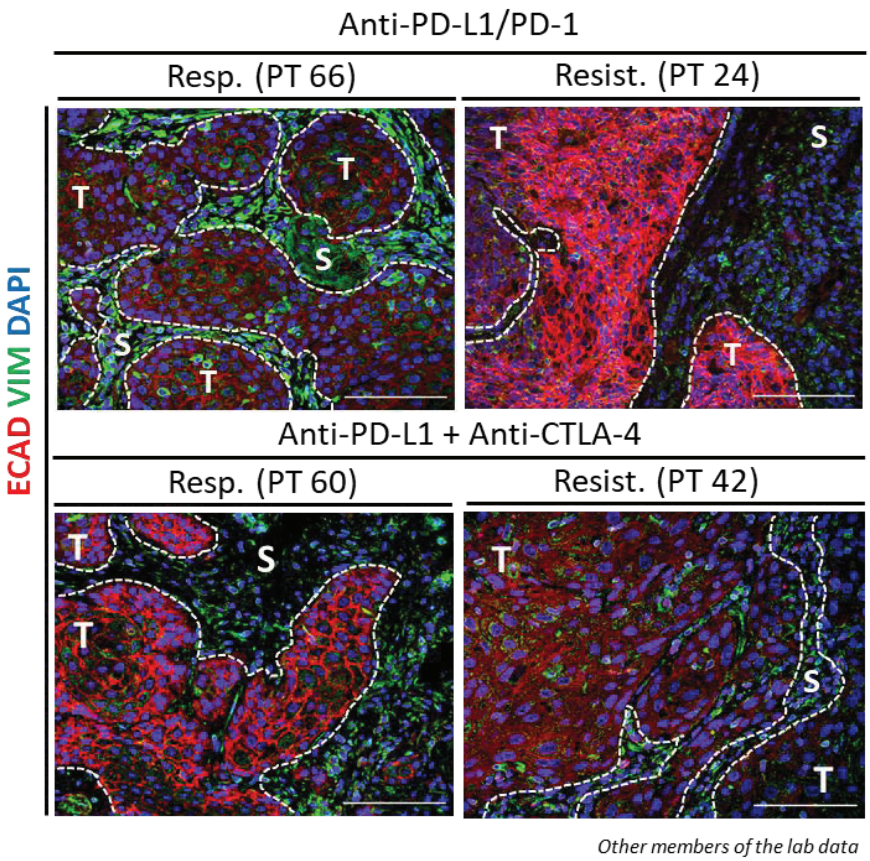

Figure 64. E-cadherin and vimentin expression in tumor cells from HNSCC patients treated with ICIs. Representative images of the immunodetection of epithelial (E-cadherin^{+}/Vimentin^{-}), hybrid (E-cadherin^{+}/Vimentin^{+}), and mesenchymal (E-cadherin^{-}/Vimentin^{+}) tumor cells in the indicated HNSCCs treated with anti-PD-1/PD-L1 or with anti-PD-L1 + anti-CTLA-4 therapy. Cell nuclei were stained with DAPI (blue). Scale bar: 100 µm. PT: patient; S: stroma region; T: tumor cell region; Resist.: resistant; Resp.: responder.

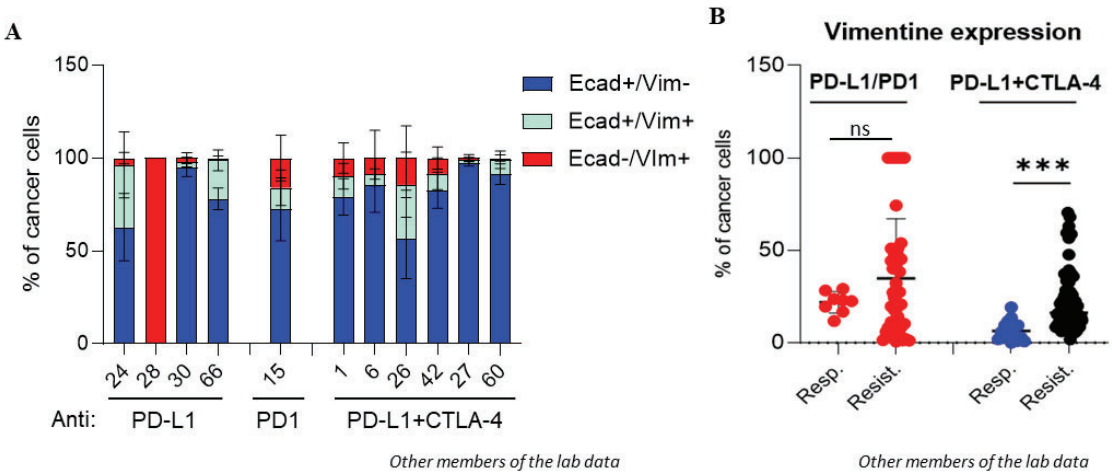

Figure 65. Figure legend on next page.

Figure 65. Quantification of the relative frequency of epithelial, hybrid or mesenchymal tumor cells in HNSCCs treated with ICIs. (**A**) Quantification (mean ± SD; n= 10-14 images per tumor) of the frequency of epithelial (E-cadherin^{+}/Vimentin^{-}), hybrid (E-cadherin^{+}/Vimentin^{+}, and mesenchymal (E-cadherin^{-}/Vimentin^{+}) tumor cells per area of tumor region in the indicated samples treated with the indicated ICIs. (**B**) Percentage (mean ± SD; n=10-14 images per tumor) of Vimentin^{+} tumor cells per area of tumor region in the indicated HNSCCs treated with the indicated ICIs. Statistical significance of the differences observed between compared groups was analyzed using unpaired two-tailed Student's T-test. ns: $p>0.05$; *** $p\leq0.001$.

To analyze the possible presence of exhausted T cells, the expression of the ICR PD-1 (Figure 66) and LAG-3 (analyzed by another member of the laboratory) in CD8^{+} T cells in patient HNSCC samples sensible or resistant to ICI treatment was analyzed by immunohistology analysis. This analysis showed that advanced and recurrent HNSCCs presented a lower CD8^{+} T cell infiltrate than cSCCs. In addition, we observed that the infiltrate of CD8^{+} T cells was higher in resistant tumors (anti-PD-L1 + anti-CTLA-4 therapy) than in tumors sensitive to this therapy (Figure 67A). These CD8^{+} T cells were distributed both in the stroma and inside the tumor in a similar proportion in responder and resistant tumors (Figure 67B). Unlike what was observed in anti-PD-1-treated cSCCs, only a small percentage of CD8^{+} T cells co-expressed PD-1 or LAG-3 in ICI-treated HNSCCs (Figures 67C-67D). However, and consistent with our previous results in advanced cSCC, those HNSCCs that showed a higher content of mesenchymal cells (resistant HNSCCs to anti-PD-L1 + anti-CTLA-4) had a higher percentage of inactive cytotoxic CD8^{+} cells that co-expressed LAG-3 (Figure 67D), but these differences were not significant.

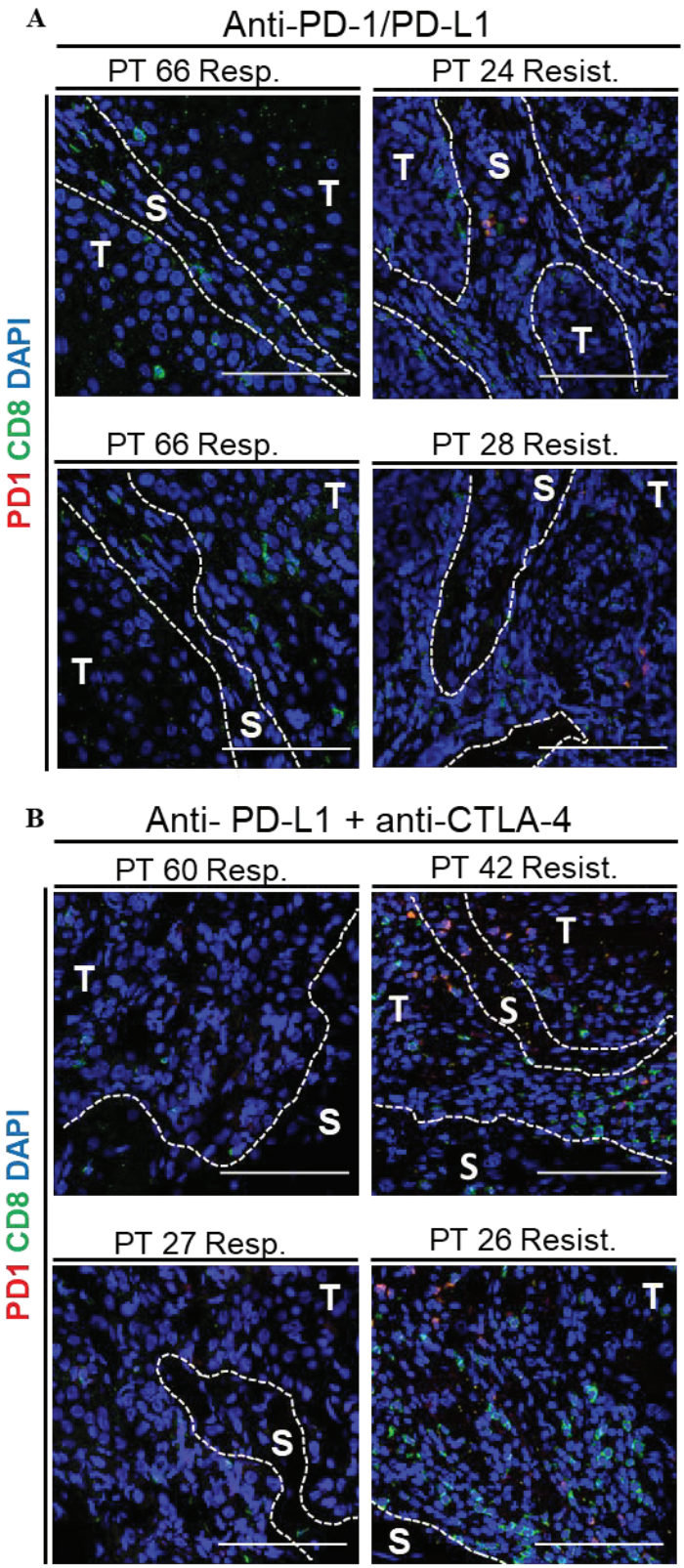

Figure 66. Immunodetection of CD8$^+$ T cells with or without PD-1 expression in advanced and metastatic HNSCC patient samples treated with IC inhibitors. Representative immunofluorescence images of the immunodetection of CD8$^+$ cells (green) with expression of PD-1 (red) in the indicated HNSCC treated with (**A**) anti-PD-1/PD-L1 or (**B**) anti-PD-L1 + anti-CTLA-4. Cell nuclei were stained with DAPI (blue). Scale bar: 100 µm. PT: patient; S: stroma region; T: tumor cell region; Resist.: resistant; Resp.: responder.

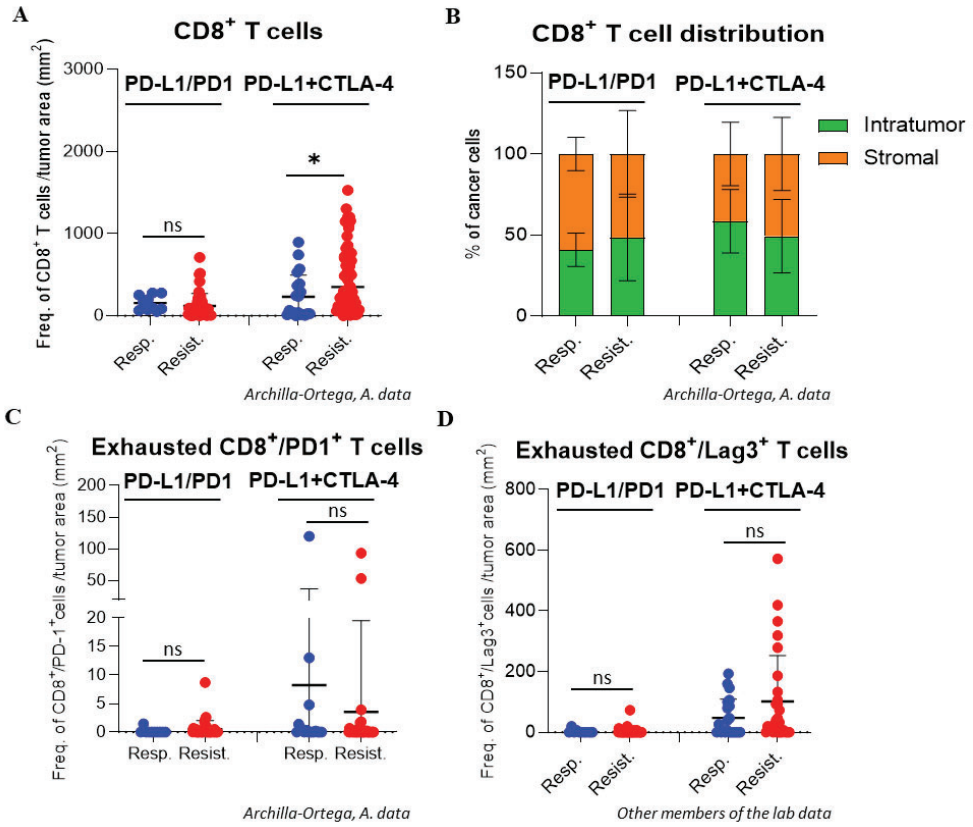

Figure 67. Increased infiltration of CD8$^+$ T cells is observed in advanced and metastatic HNSCCs from patients resistant to anti-PD-L1 + anti-CTLA-4 therapy. (**A**) Frequency (mean ± SD; *n=15-30* images per tumor) of CD8$^+$ T cells per area of tumor region in the indicated samples. (**B**) Percentage (mean ± SD; *n=10-14* images per tumor) of CD8$^+$ cells located in the stroma or infiltrating the interior of the tumor mass. Frequency (mean ± SD; *n=15-30* images per tumor) of (**C**) CD8$^+$/PD-1$^+$ and (**D**) CD8$^+$/LAG-3$^+$ T cells by tumor area in the indicated HNSCCs. Statistical significance of the differences observed between responder *vs.* resistant groups was analyzed using unpaired two-tailed Student's T test. ns: p>0.05; * p≤0.05. Resist.: resistant; Resp.: responder.

Considering these results, we hypothesize that advanced and recurrent HNSCCs with a higher content of mesenchymal cells could be resistant to immunotherapy based on ICI. Nevertheless, due to the limited number of HNSCC samples from responsive and resistant patients to ICI analyzed in this study, it is not possible to establish a correct correlation between the response to ICI and the expression of E-cadherin/Vimentin in tumor cells. In addition, we further hypothesize that resistant HNSCCs to ICI may present higher infiltration of exhausted CD8$^+$ T cells co-expressing various IC receptors. All these initial observations should be addressed in further experiments with a larger cohort of advanced and metastatic HNSCC patients sensible and resistant to ICI to further validate them.

DISCUSION

The TME plays a critical role in tumor progression and immunotherapy response (Binnewies et al., 2018). The presence of immunosuppressive cells is linked to poor ICI-based immunotherapy response leading to primary and acquired resistance against ICI (Jenkins et al., 2018). In addition, secreted factors by immunosuppressive cells can promote tumor progression and aggressiveness (F.-F. Qian & Han, 2020). Given the clinical relevance of the TME, it is crucial to unravel the reciprocal interplay and crosstalk between the TME and the tumor cells. More specific therapies can be designed by understanding how the TME becomes immunosuppressive and how tumors advance to more aggressive stages. This will help improve the clinical outcome of patients that do not benefit from actual ICI immunotherapies.

IDENTIFICATION OF TUMOR-INFILTRATING IMMUNE CELLS-DERIVED CYTOKINES RESPONSIBLE FOR PROMOTING THE MESENCHYMAL-LIKE STATE OF CANCER CELLS DURING MOUSE cSCC PROGRESSION

In the first objective of the present thesis, we aimed to characterize the cytokines released by immunosuppressive cells which can be responsible for promoting the acquisition of mesenchymal traits by cSCC cells. Previous data from our group demonstrated that PD-SCCs are enriched with immunosuppressive cells in comparison to WD-SCCs. The polarization profile of macrophages and MDSCs changes to a more immunosuppressive profile as cSCC progress. Specifically, M2-like macrophages and M-MDSCs express higher levels of immunosuppressive markers when infiltrating in PD-SCCs than when infiltrating WD-SCCs (Lorenzo-Sanz et al., under-review manuscript). In addition, the blockade of PMN-MDSCs recruitment into MD/PD-SCCs, which are characterized by containing plastic $EpCAM^{+}$ SCC cells with the ability to switch towards a mesenchymal-like phenotype, decreases the appearance of mesenchymal-like SCC cells (Lorenzo-Sanz et al., unpublished results). Remarkably, previous studies from our laboratory demonstrated that cSCC progression happens in athymic nude mice, which are deficient in T cells (including Treg cells), suggesting that Treg cells and their derived signals are not required to promote the acquisition of mesenchymal-like traits in cSCC. Therefore, we selected the immune cell populations of macrophages and MDSCs as candidates to release cytokines and soluble factors responsible for promoting the acquisition of mesenchymal-like traits by inducing the switch from epithelial-like states. Since macrophages and MDSCs tumor recruitment and polarization profile change during mouse cSCC progression (Lorenzo-Sanz et al., under-review manuscript), we aimed to isolate tumor-infiltrating macrophages and MDSCs from WD-SCCs and PD-SCCs to study which specific cytokines were releasing these immune cell populations. However, we could not establish primary cell cultures of tumor-infiltrating macrophages and MDSCs as others could (Schlecker et al., 2012) (Cassetta et al., 2016). An explanation to this could be that probably when cSCC tumors were enzymatically digested O/N tumor-infiltrating immune cells received cellular damage decreasing their short lifespan. We tested a shorter

enzymatic digestion of cSCC tumors before isolating tumor-infiltrating immune cells as described in the bibliography (Cassetta et al., 2016). However, isolated macrophages and MDSCs by cell sorting did not survive 48 hours *in vitro*. Given these initial technical issues, we decided to obtain alternative primary cell cultures of macrophages and MDSCs resembling the most to these immune cells when infiltrating into the tumor to study their derived cytokines, which we hypothesize could be inducing the switch from plastic EpCAM^{+} SCC cells to the mesenchymal state.

To study macrophages, we decided to isolate and culture BMDM from WD-SCC- and PD-SCC-bearing mice. Once isolated, BMDM cell cultures can be polarized into M1-like or M2-like profiles with soluble factors. In accordance with the bibliography, BMDM polarization with LPS increased the expression of M1-like markers (*Il-1b*, *Tnf-α*, *Il-6*, *Cxcl9*, and *Cxcl10*) while the polarization with IL-4 promoted the expression of M2-like markers (*Cd163*, *Arg1*, and *Pd-l2*) (Ying et al., 2013) (Jayasingam et al., 2019). Independently if BMDM were isolated from WD-SCC- or PD-SCC-bearing mice, BMDM differentiated into M1- and M2-like profiles indicating that these BMDM were able to shift to both polarization extremes upon soluble signals. Surprisingly, *Gas6* expression, which is a marker of an M2-like differentiation profile, was highly expressed in non-polarized BMDM growing in our culture medium (F12 B27). The expression of *Gas6* in macrophages is induced via STAT6, a downstream effector of IL-4 (Nepal et al., 2019). Hence, according to the bibliography, we would expect an increased expression of *Gas6* in IL-4 treated BMDM and this result would need further validation in our BMDM obtained from WD-SCC- and PD-SCC-bearing mice.

To obtain BMDM with a similar profile to tumor-infiltrating macrophages, we polarized the isolated BMDM with conditioned medium from full epithelial SCC cells (tumor cells from WD-SCCs) or mesenchymal EpCAM^{-} SCC cells (tumor cells from PD-SCCs). This approach to obtain BMDM with a similar profile to the one when infiltrating into the tumor has been used and validated in other tumor models such as melanoma (Al-Rayahi et al., 2017), lung carcinoma (Y. Zhang, Zhang, et al., 2022), and bladder cancer (Z. Jiang et al., 2021). We polarized the obtained BMDM with conditioned medium from *in vitro* culture of SCC cells. Secreted factors from full epithelial SCC cells slightly promoted the expression of certain M1-like markers while secreted factors from mesenchymal EpCAM^{-} SCC cells upregulated gene expression of specific M2-like markers. BMDM polarization profile with conditioned medium resembled that reported in the TME characterization during cSCC progression. In detail, M1-like macrophages were mainly infiltrating WD-SCCs while M2-like macrophages recruitment was induced in PD-SCCs (Lorenzo-Sanz et al., under-review manuscript). In addition, BMDM polarized with soluble factors from mesenchymal EpCAM^{-} SCC cells expressed slightly higher levels of the immunosuppressive marker *Arg1* suggesting that these BMDM would be more

immunosuppressive as described in M2-like macrophages infiltrating in PD-SCCs (Lorenzo-Sanz et al., under-review manuscript). So, despite not being able to establish primary cultures of tumor-infiltrating macrophages, we could obtain BMDM with a similar profile thanks to the polarization with conditioned medium from SCC tumor cells.

MDSCs are recruited into the spleen of tumor-bearing mice and can be isolated and used to study their derived signals (Youn et al., 2008) (Kumar et al., 2017). The isolation of splenic MDSCs can be performed either by magnetic-activated cell sorting or by FACS techniques (Y. Xu et al., 2014). We sorted splenic MDSCs by FACS given that this technique was routinely used in the laboratory. As described in the bibliography, we observed that the spleens of tumor-bearing mice were larger and MDSCs were more enriched in these spleens than in those from tumor-free mice (Beheshti et al., 2015). Additionally, MDSCs were increasingly more enriched as cSCC presented a more advanced profile and spleens were aberrantly bigger. Splenic MDSCs expressed higher immunosuppressive markers when isolated from spleens of PD-SCC-bearing mice than when isolated from spleens of WD-SCC-bearing mice. This goes in accordance with previous data from the group where M-MDSCs infiltrating PD-SCCs expressed high levels of immunosuppressive markers than M-MDSCs infiltrating WD-SCCs (Lorenzo-Sanz et al., under-review manuscript). Hence, MDSCs in contact with PD-SCCs derived signals expressed more immunosuppressive markers and we could establish primary cell cultures of splenic MDSCs with this characteristic. However, to completely validate the immunosuppressive capability of these immune cells a functional assay co-culturing splenic MDSCs with T cells would be needed. T cells in contact with immunosuppressive MDSCs stop proliferating and secrete lower levels of GzmB and IFN-γ (Bruger et al., 2019).

We obtained plastic $EpCAM^{+}$ SCC cells (from MD/PD-SCCs) with the ability to acquire mesenchymal-like traits. These primary cell cultures showed the ability to pass from $EpCAM^{high}$ to $EpCAM^{low}$ SCC cells but presented a little capacity to finally switch to $EpCAM^{-}$ SCC cells. A previous characterization from our group of plastic $EpCAM^{high}$ and plastic $EpCAM^{low}$ SCC cells revealed that the conversion of plastic $EpCAM^{high}$ SCC cells towards plastic $EpCAM^{low}$ SCC cells was the first step towards the acquisition of a mesenchymal phenotype. Plastic $EpCAM^{low}$ SCC cells induce the expression of mesenchymal markers and diminish the expression of epithelial markers despite do not completely lose the expression of these epithelial features (Lopez-Cerda et al., submitted manuscript). In addition, every plastic $EpCAM^{+}$ SCC primary cell culture can present a different capacity to acquire mesenchymal traits as observed previously in our laboratory (Lopez-Cerda et al., submitted manuscript). Therefore, the capacity of plastic $EpCAM^{+}$ SCC cells to acquire mesenchymal traits needs to be characterized before being used in these experiments. To this end, we cultured *in vitro* our derived plastic $EpCAM^{high}$ and $EpCAM^{low}$ SCC cells for 7-14 days with the control medium (F12 B27) and we analyzed its ability to generate mesenchymal

cells without external stimulus inducing the switch. Next, we compared these results with the acquisition of mesenchymal features when plastic EpCAM^{high} or EpCAM^{low} were cultured with the conditioned medium from immune cells and analyzed its ability to promote the generation of mesenchymal SCC cells.

To minimize the experimental variability from establishing a derived plastic EpCAM^{+} SCC cell culture, we used two different plastic EpCAM^{+} SCC primary cultures. These derived plastic EpCAM^{+} SCC cells were cultured with conditioned mediums from polarized BMDM or splenic MDSCs. Secreted factors from macrophages polarized with the conditioned medium of mesenchymal EpCAM^{-} SCC cells (BMDM PD) and splenic M-MDSCs from PD-SCC (M-MDSCs PD) showed the greatest capacity to induce the acquisition of mesenchymal traits in plastic EpCAM^{+} SCC cells by promoting the switch from plastic EpCAM^{high} to plastic EpCAM^{low} SCC cells. Hence, derived signals from BMDM PD and splenic M-MDSCs PD, which present similarities to tumor-infiltrating M2-like macrophages and M-MDSCs in PD-SCCs, induced *in vitro* the acquisition of mesenchymal features of plastic EpCAM^{high} SCC cells. However, these secreted factors by polarized macrophages and MDSCs were not sufficient to induce the complete loss of the expression of the epithelial marker EpCAM. This could be attributed to a lack of complementary signaling that could further promote the complete acquisition of a mesenchymal phenotype such as TGF-β secreted by other cells from the TME such as CAFs (Papageorgis, 2015) (Yoon et al., 2021) (Lopez-Cerda et al., submitted manuscript). Revealing which cytokine signaling can activate the switch of plastic EpCAM^{+} SCC cells towards plastic EpCAM^{low} and EpCAM^{-} tumor cells and might contribute to the progression of tumor cells towards a mesenchymal phenotype in MD/PD-SCCs is of high interest.

The cytokines secreted by M-MDSCs from spleens of PD-SCC-bearing mice (M-MDSCs PD), which presented the greatest capacity to induce the acquisition of mesenchymal-like features in plastic EpCAM^{high} SCC cells, were identified using a proteome profiler cytokine array. We detected several cytokines upregulated by M-MDSCs PD that have been described to induce EMT in various tumor conditions. B cell-activating factor (BAFF) which promotes the proliferation and differentiation of B cells has been observed to also promote EMT in epithelial breast cancer (Pelekanou et al., 2018) and induce the expression of EMT-related genes in pancreatic cancer (Koizumi et al., 2013). IL-28 signaling which participates in antiviral immunity also promotes EMT in a mammary tumor model (Mucha et al., 2014). CCL20 which participates is a chemoattractant of lymphocytes also promotes EMT of tumor cells from lung adenocarcinoma (Fan et al., 2022), gastric cancer (G. Han et al., 2015), epithelial breast cancer (Marsigliante et al., 2016), colorectal cancer (X.-S. Cheng et al., 2014), and pancreatic cancer (B. Liu et al., 2016). CCL21 which also serves as a chemoattractant of T cells also triggers EMT in oral squamous cell carcinoma (Y. Chen et al., 2020), pancreatic cancer (L. Zhang et al., 2016), and breast carcinoma

(F. Li et al., 2014). Finally, IL-7 which stimulates the proliferation of lymphoid lineage cells also promotes EMT in prostate cancer (Seol et al., 2019) and breast carcinoma (J. Yang et al., 2014). However, C reactive protein (CRP) which is a marker of tissue damage and mediates inflammation, IL-2 which participates in the immune response against microbial infections, C1qR1 which participates in the cellular adhesion process, Angiopoietin-like 3 which modulates lipid metabolism and Complement factor D which participates in the alternative complement pathway of the complement system were also upregulated in M-MDSCs PD but have not been previously described to promote EMT to date according to the bibliography. Importantly, the role of BAFF, IL-28, CCL20, CCL21, and IL-7 has not been studied in cSCCs. The implication of these cytokines promoting the acquisition of mesenchymal features has not been analyzed and should be addressed in future experiments. As a workflow, it should be studied which receptors of these cytokines are expressed by plastic SCC cells with the ability to acquire mesenchymal traits and undergo EMT. These receptors are BAFF-R (receptor of BAFF), IL-28 receptor alpha chain plus IL-10 receptor beta chain (receptor of IL-28), CCR6 (receptor of CCL20), CCR7 (receptor of CCL21), and IL-7 receptor (receptor of IL-7). Next, plastic $EpCAM^+$ SCC cells should be treated *in vitro* with recombinant proteins of the cytokine candidates. If an effect inducing the acquisition of mesenchymal traits is observed, the depletion of the cytokine signaling should be analyzed in MD/PD-SCCs to further validate the role of these cytokines in the acquisition of mesenchymal features from plastic $EpCAM^+$ cells in the *in vivo* context. In addition, it should not be discarded the possible additive effects of different cytokines promoting EMT. Thus, we have identified five candidate cytokines secreted by M-MDSCs, which could be responsible for promoting the acquisition of mesenchymal-like state of SCC cancer cells.

DETERMINE CANCER CELL-DERIVED CYTOKINES AND MECHANISMS INVOLVED IN THE RECRUITMENT OF IMMUNOSUPPRESSIVE CELLS, WHICH CONTRIBUTE TO THE EXHAUSTION OF CYTOTOXIC T CELLS IN ADVANCED MOUSE cSCCS

A prior RNA microarray done in the laboratory permitted the identification of the gene signature of SCC cells during cSCC progression and the differently expressed genes in this process. We took advantage of this information to analyze which cytokines were upregulated in advanced SCC cells. Using the RNA microarray data we analyzed the two extreme populations: full epithelial SCC cells the major cell component of WD-SCCs and mesenchymal $EpCAM^-$ SCC cells which form the PD-SCCs. The analysis revealed that mesenchymal $EpCAM^-$ SCC cells upregulate the mRNA of several cytokines including *Cxcl2*, *Csf1*, and *Csf2* among others, which could be responsible for recruiting immunosuppressive cells. The data obtained by an RNA microarray needs to be validated by other techniques such as RT-qPCR to ensure the observed differences. However, according to our results, some upregulated cytokines in mesenchymal $EpCAM^-$ SCC

cells identified by the RNA microarray, such as *Cxcl2*, were not upregulated according to RT-qPCR data. These discrepancies could be attributed to technical differences but also to the fact that the microarray analysis was performed in FACS-isolated tumor cells growing *in vivo* while our RT-qPCR data was obtained from the same tumor cells but from growing *in vitro*. Next, we decided to detect released cytokines at the protein level using a cytokine proteome profiler array. We detected secreted cytokines of freshly established primary cell cultures of full epithelial SCC cells and mesenchymal EpCAM$^-$ SCC cells. This allows the identification of cytokines which might be secreted by tumor cells and be present in the TME. Mesenchymal EpCAM$^-$ SCC cells from PD-SCCs present a different cytokine secretion profile than full epithelial SCC cells from WD-SCCs. CXCL1, CSF3, CCL2, and TIMP1 were the most secreted cytokines by mesenchymal EpCAM$^-$ SCC cells while IL-1ra was highly secreted by full epithelial SCC cells. CXCL1, CSF3, and CCL2 were the identified cytokines released by mesenchymal cells which have been linked to the establishment of an immunosuppressive TME in various tumor types by recruiting immunosuppressive cells. Specifically, CXCL1 promotes an immunosuppressive TME profile and CD8$^+$ T cell exhaustion by recruiting PMN-MDSCs in gastric cancer (X. Zhou et al., 2022) and pancreatic cancer (Kemp et al., 2021). CSF3 contributes to the establishment of an immunosuppressive TME by recruiting granulocytic MDSCs (PMN-MDSCs) in pancreatic cancer (J. Li et al., 2018) and both PMN-MDSCs and M-MDSCs in breast cancer (H.-W. Sun et al., 2020). Lastly, CCL2 recruits M-MDSCs and Treg cells to form an immunosuppressive microenvironment in glioma (Chang et al., 2016) and M2-like macrophages in lung adenocarcinoma (Hartwig et al., 2017). Given these reports, we hypothesized that CXCL1, CSF3, and CCL2 could be actively recruiting immunosuppressive cells into PD-SCCs and, consequently, preventing anti-tumoral immunity. To test this, we blocked pharmacologically the signaling of these cytokines in PD-SCCs and analyzed the derived TME profile.

CXCL1 is a small peptide belonging to the CXC chemokine family that acts as a chemoattractant for several immune cells, especially neutrophils (Moser et al., 1990). CXCL1 binds to the chemokine receptor CXCR2, which is also the receptor for CXCL2. CXCL1 mobilizes neutrophils (Jablonska et al., 2014), PMN-MDSCs (Varikuti et al., 2017) (Gibson et al., 2020), M-MDSCs (X. Han et al., 2019), and Treg cells (Lv et al., 2014b) to the tumor site. Inhibiting CXCR2 signaling reduces MDSCs trafficking to the tumor site improving anti-PD1 efficacy in rhabdomyosarcoma (Highfill et al., 2014). This pinpoints the role of CXCL1 modulating immune cell infiltration to the tumor core establishing an immunosuppressive TME. Despite CXCR2 signaling mobilizes MDSCs to the tumor site, the blockade of CXCR2 signaling using the small molecule SB225002 did not reduce MDSCs trafficking into PD-SCCs. This might be explained by cytokine redundancy, referred to the fact that many different cytokines can induce similar signals involved in the tumor recruitment of these immunosuppressive cells (C. Liu et al., 2021).

Hence, other signals beyond CXCR2 might be inducing MDSCs recruitment into PD-SCCs. Treg cells have been shown to express CXCR2 and its reduced infiltration on PD-SCCs treated with SB225002 might be a direct effect of CXCR2 signaling inhibition. Oppositely, $CD8^+$ T cells do not express CXCR2 (Kershaw et al., 2002). Thus, the increased presence of $CD8^+$ T cells and cytotoxic $GzmB^+$ cells in SB225002 treated tumors we hypothesize might be a secondary effect of Treg cells reduced presence. Hence, blockade of CXCR2, impairing CXCL1 and CXCL2 derived signaling in PD-SCCs, finally resulted in increased tumor presence of more active cytotoxic effector cells.

CSF3 is a cytokine that stimulates the production of bone marrow-derived granulocytes and hematopoietic stem cells and their release into the bloodstream (Tay et al., 2017). CSF3 binds specifically to the G-CSF-R, which is present in precursor cells in the bone marrow. CSF3 signaling induces neutrophils (Mouchemore et al., 2018) and MDSCs (W.-C. Wu et al., 2014) trafficking to the tumor site in breast cancer. In addition, MDSCs recruitment by CSF3 is linked to anti-tumoral therapy resistance in uterine cervical cancer (Kawano et al., 2015). Given the granulocytic characteristics of PMN-MDSCs, this specific cell population is highly recruited by CSF3 (Pelosi et al., 2021). Anti-CSF3 decreased the recruitment of PMN-MDSCs into PD-SCCs, while slightly increased M-MDSCs recruitment. This might be explained by the fact that PMN-MDSCs are granulocytic cells while M-MDSCs are not. We detected increased recruitment of $GzmB^+$ cells. The receptor of CSF3, G-CSF-R, has not been described in lymphocytes (Reyes et al., 1999). Hence, the increased recruitment of active cytotoxic cells ($GzmB^+$ cells) might be explained by indirect immunoregulatory effects such as the reduced presence of PMN-MDSCs or by the effect of other immune cells not analyzed in the present work such as TANs (which express G-CSF-R). So, the blockade of CSF3 signaling in PD-SCCs, decreased the tumor recruitment of PMN-MDSCs and resulted in an increased presence of cytotoxic $GzmB^+$ cells despite not increasing the tumor infiltration of $CD8^+$ T cells.

CCL2 is a cytokine that belongs to the CC chemokine family and participates in the inflammatory response produced by tissue injury or infection. CCL2 binds to the CCR2 cell surface receptor and serves as a strong chemoattractant involved in macrophage recruitment and as a powerful initiator of inflammation (Carson et al., 2017). Neutrophils are also recruited by CCL2 into the TME and can amplify the inflammatory response (Granot et al., 2011). In addition, the CCL2–CCR2 axe participates in Treg cells recruitment (Mondini et al., 2019), which is explained by the fact that Treg cells express CCR2 (Brühl et al., 2004). CCL2 mainly promotes tumor growth because of the accumulation of immunosuppressive cell subtypes, specifically TAMs (Wei et al., 2019). As expected, the blockade of CCL2 signaling reduced total macrophage recruitment in PD-SCCs. Specifically, M1-like macrophage infiltration was reduced while M2-like macrophage presence was slightly reduced despite not achieving statistical significance. In addition, the

blockade of CCL2 also reduced the TME recruitment of Treg cells as previously described (Kadomoto et al., 2021). Despite CCR2 can be expressed by T cells as serves as a tissue homing signal (Fei et al., 2021), the blockade of its signaling did not decrease $CD8^+$ T cells tumor recruitment. An increased presence of $GzmB^+$ cells was also detected in anti-CCL2 treated PD-SCCs and we suggest it could be attributed to a direct effect on $CCR2^+$ T cells or to an indirect effect of CCL2 reducing macrophages and Treg cells infiltration, which may also increase the cytotoxic activity of NK cells. In all, blocking CCL2 signaling in PD-SCCs reduced the immunosuppressive component of the TME and activated cytotoxic effector cells.

Single blockade of cytokine signaling is not sufficient to drastically reduce immunosuppression and achieve potent anti-tumor effects in PD-SCCs. This has been attributed to the redundancy of the cytokine network (C. Liu et al., 2021). Despite this, combinatory treatments blocking cytokines signaling are a promising approach to target tumors by increasing the efficacy of single treatment options (Berraondo et al., 2019). In addition to the immunosuppressive effect of immune cells, tumor cells, through the expression of IC ligands, activate IC receptors and block the function of $CD8^+$ and NK cells. Therefore, we probably have not seen a net effect of the tested inhibitors on tumor growth, because PD-L1 and other IC ligands are still operative. In this sense, combining the blockade of cytokine signaling with ICI has shown an increased anti-tumoral efficacy without increased adverse events in melanoma and CRC (Hailemichael et al., 2022) (Mortezaee & Majidpoor, 2022). The blockade of CXCL1, CSF3, and CCL2 derived signaling has shown benefits, and their blockade simultaneously to ICI might improve anti-tumor effects in PD-SCCs. In that regard, future experiments should combine the blockade of CXCL1, CSF3, or CCL2 signaling concomitantly with anti-ICs such as anti-PD-1/PD-L1, anti-CTLA-4, or anti-TIGIT and analyze if an anti-tumor synergic effect is observed.

A previous study of the group identified CXCL12 as a highly secreted cytokine in PD/S-SCCs, which are composed of full mesenchymal SCC cells. Specifically, CXCL12 binds to CXCR4 in PD/S-SCCS and the blockade of its signaling pathway by AMD3100 significantly decreases the presence of metastatic lesions in PD/S-SCCs (Bernat-Peguera et al., 2019). Accordingly, our data indicated that full mesenchymal SCC cells, which form PD/S-SCCs, expressed high levels of *Cxcl12*, while mesenchymal $EpCAM^-$ SCC cells, which are the main components of PD-SCCs, did not express *Cxcl12*. In addition, we observed that total WD-SCCs and PD-SCCs tumor lysates expressed higher levels of *Cxcl12* compared to their tumoral cells. This goes in accordance with the fact that other cells from the TME such as fibroblasts also express *Cxcl12* as demonstrated previously by our group (Bernat-Peguera et al., 2019). Importantly, the blockade of CXCL12 signaling with AMD3100 synergized with anti-PD-1 treatment reducing the immunosuppressive TME component in a mouse ovarian tumor model (Zeng et al., 2019). Considering this, we analyzed the TME of PD-S/SCCs treated with AMD3100. Our results demonstrated that the

blockade of CXCL12 signaling using AMD3100 reduced the immunosuppressive TME of PD/S-SCCs. CXCR4 is expressed on Treg cells and blockade of CXCR4 signaling with AMD3100 reduced their tumor infiltration (Santagata et al., 2017). AMD3100 treatment also decreased $CD8^+$ T cell recruitment. This may be explained by the fact that T cells express CXCR4 and CXCL12-CXCR4 signaling serves as a chemoattractant homing factor for T cells to infiltrate in peripheral lymph nodes (Scimone et al., 2004). Hence, blocking CXCL12-derived signaling in PD/S-SCCs with AMD3100 treatment would prevent the tumor infiltration of T cells by the CXCL12-CXCR4 signaling. Despite the decreased presence of $CD8^+$ T cells, the ratio of $CD8^+$ cells *vs*. Treg cells was higher in tumors treated with AMD3100 indicating that those $CD8^+$ T cells might be more active since proportionally fewer Treg cells are present in the TME of PD/S-SCCs. In addition, M2-like macrophages presence was reduced upon AMD3100 treatment. Macrophages express CXCR4, and blockade of CXCR4 signaling promotes M2-to-M1 polarization (Zeng et al., 2019). AMD3100 also increased the tumoral presence of cytotoxic $GzmB^+$ cells, which we hypothesize is probably an effect of Treg cells and M2-like macrophages decreased recruitment. Despite AMD3100 treatment reduced the immunosuppressive TME profile, this was not sufficient to induce strong anti-tumor effects delaying tumor growth or increasing necrotic regions in PD/S-SCCs. As observed in PD-SCCs, the single blockade of one cytokine signaling helps diminish the immunosuppression but probably should be combined with ICI agents to see an anti-tumor response. The fact that IC receptors keep being active in the TME is probably preventing stronger effects of single cytokine blockade therapies. Hence, the blockade of CXCL12 signaling could synergize with ICI treatments in PD/S-SCCs and this should be addressed in future experiments in dual blockade *in vivo* experiments.

STUDY ALTERNATIVE STRATEGIES TO PROMOTE ANTI-TUMOR RESPONSE OF ICI THERAPIES IN ADVANCED cSCCS

To evade the immune response, tumor cells adopt various mechanisms including defective antigen presentation. Tumor cells downregulating MHC-I have been described in 40-90% of human tumors and often correlate with worse prognosis (Cornel et al., 2020). Remarkably, MHC-I downregulated expression has been described to be a mechanism of intrinsic and acquired resistance to ICI immunotherapy (Taylor & Balko, 2022). Depending on the downregulation mechanism, MHC-I expression can be therapeutically restored to participate in anti-tumor immunity and improve ICI interventions. Specifically, the molecular mechanisms by which cancer cells can downregulate MHC-I expression at the cell surface have been previously described for many cancers (Cornel et al., 2020) (Dhatchinamoorthy et al., 2021). Those include loss of MHC-I expression in tumor cells through mutation or deletion of structural genes, transcriptional regulation, post-transcriptional/pre-translational regulation, post-translational mechanisms, and TME-derived extrinsic stimuli. Because tumor cells can avoid the expression of

MHC-I through a large variety of mechanisms, downregulation of MHC-I can be the result of various processes and might not be attributed to a single cause. We firstly validated in our primary *in vitro* SCC cells the previous results from our group indicating that full epithelial SCC cells from WD-SCCs expressed cell surface MHC-I and PD-L1 while mesenchymal EpCAM$^-$ SCC cells from PD-SCCs did not express these proteins in the *in vivo* context. Oppositely to cSCC, PD-L1 expression has been observed to be upregulated during EMT and in mesenchymal-like tumor cells in breast cancer (Noman et al., 2017), non-small cell lung cancer (Manjunath et al., 2019), and various sarcomas (Kösemehmetoğlu et al., 2017). Hence, cSCC specific characteristics might alter MHC-I and PD-L1 expression in mesenchymal EpCAM$^-$ SCC cells avoiding their cell surface presence and leading to poor responsiveness to IC blockade therapies.

We observed a decreased expression of *Mhc-I, Mhc-II, Pd-l1* and *Tap1* in mesenchymal EpCAM$^-$ SCC cells compared to full epithelial SCC cells, which indicates that there is a specific transcriptional downregulation of these genes. Transcriptional silencing of *Mhc-I* and antigen processing genes has been described in numerous tumor types (Burr et al., 2019) (Dhatchinamoorthy et al., 2021). *Mhc-I* expression can be dysregulated through alterations and impairment of the transcription factors NF-κB, IRF1, and NLRC5 (Lorenzi et al., 2012) (Yoshihama et al., 2016). Genetic defects in the antigen-presenting pathway have been documented in various tumor types resulting in decreased MHC-I antigen presentation. It has been reported that MHC-I expression is reduced by ~30-70% in TAP genetic deletions, by ~90% in Tapasin loss, and by ~50% in genetic defects affecting the immunoproteasomes (Dhatchinamoorthy et al., 2021). Reduced expression of *Tap1* and *Tap2* has been documented in melanoma (Vitale et al., 1998), colorectal cancer (Kaklamanis et al., 1994), and renal cell carcinoma (Seliger et al., 1996) resulting in defective peptide presentation. Hence, the downregulation of *Tap1* in mesenchymal EpCAM$^-$ SCC cells could be partially responsible for the decreased expression of cell surface MHC-I in mesenchymal EpCAM$^-$ SCC cells. Upregulation of specific miRNAs has been also reported to repress the expression of antigen processing genes (Colangelo et al., 2016) (Mari et al., 2018). *Tap1* transcripts decay has been associated to the binding of miR-200a-5p in melanomas (Lazaridou et al., 2020). Furthermore, mutations in K-RAS can downregulate TAP1 and Tapasin expression levels in colorectal carcinoma (Atkins et al., 2004). Somatic mutations, loss of heterozygosis, or complete loss of the β2-microglobulin gene leads to a decreased presence of MHC-I in tumor cells (Toth et al., 2013). However, according to our results, *β2-microglobulin*, *Tap2*, and *Tapasin* expression was not altered in mesenchymal EpCAM$^-$ SCC cells. Hence, in mesenchymal EpCAM$^-$ SCC cells there is a specific transcriptional downregulation specifically affecting *Mhc-I*, *Mhc-II*, *Pd-l1*, and *Tap1*.

Histone methylation is a conserved mechanism in which methyl groups are added to specific amino acids on histones. This process modifies the arrangement and availability of DNA,

ultimately influencing the control of gene expression. Alterations of histone methylation have been widely observed in aging and cancer conditions, causing changes in the regulation of gene expression (Michalak et al., 2019). The enzyme EZH2, which is a histone-lysine N-methyltransferase enzyme forming part of the Polycomb repressive complex 2, prevents *Mhc-I* expression causing cancer immune evasion in small cell lung cancer (Burr et al., 2019) and human lymphomas (Dersh et al., 2021). Targeting the methyltransferase EZH2 with the GSK126 inhibitor restores the expression of *Mhc-I* overcoming anti-PD-1 resistance in HNSCC (L. Zhou et al., 2020). Given the similar physiopathology of HNSCCs and cSCC, we hypothesized that the inhibition of EZH2 methyltransferase activity in cSCC by using GSK126 could restore *Mhc-I* expression in mesenchymal EpCAM$^-$ SCC cells. However, GSK126 treatment did not increase *Mhc-I* expression either in full epithelial or mesenchymal EpCAM$^-$ SCC cells. So, the downregulation of *Mhc-I* in mesenchymal EpCAM$^-$ SCC cells is not dependent on EZH2 histone-lysine N-methyltransferase activity.

Other epigenetic mechanisms could be involved in the *Mhc-I* downregulation, like DNA methylation of the MHC-I locus. Hypermethylation of the MHC-I locus and NLRC5 promoter region impairs *Mhc-I* expression as observed in esophageal squamous cell carcinoma (Nie et al., 2001), gastric cancer (Ye et al., 2010) and other tumor types (Yoshihama et al., 2016). MHC-I locus DNA hypermethylation can be reversed by IFN-γ stimulation (Vlková et al., 2014) or by DNA methyltransferases (DNMT) inhibitors like 5-aza-2'-deoxycytidine in melanoma (Fonsatti et al., 2007), 5-azacytidine in HPV16-associated tumors (Šímová et al., 2011), or guadecitabine in breast cancer (N. Luo et al., 2018). The treatment with DNMT inhibitors such as 5-aza-2'-deoxycytidine, 5-Azacytidine, or guadecitabine could restore *Mhc-I* expression levels of mesenchymal EpCAM$^-$ SCC cells and this should be addressed in future experiments.

To assess the functionality of the regulation of MHC-I gene expression and related proteins in full epithelial and mesenchymal EpCAM$^-$ SCC cells, we induced their expression by treating them with IFN-γ, as it has previously been shown to promote MHC-I mRNA expression in other tumor types (Jorgovanovic et al., 2020). In contrast to the abnormal functionality of the IFN-γ pathway that has been observed in different tumor types (Gao et al., 2016), full epithelial SCC cells and mesenchymal EpCAM$^-$ SCC cells correctly responded to IFN-γ indicating that this pathway was functional in SCC primary cells. We observed that IFN-γ induced levels of *Irf1* were significantly lower in mesenchymal EpCAM$^-$ SCC cells than those observed in full epithelial SCC cells, despite mesenchymal EpCAM$^-$ SCC cells showed increased phosphorylation levels of STAT1. IFN-γ binds an heterodimer of IFNGR1 and IFNGR2 in a relationship 1:1 (Alspach et al., 2019). Mesenchymal EpCAM$^-$ cells expressed balanced levels of both receptors while full epithelial SCC cells may present restricted IFNGR availability because of low expression of *Ifngr2*. Basal and induced *Irf1* mRNA levels were lower in mesenchymal EpCAM$^-$ SCC cells suggesting that IFN-

γ signaling transduction could be altered, resulting in a downregulation of *Irf1*. In this sense, it has been described that *Irf1* expression is downregulated in melanoma (Lowney et al., 1999), breast cancer (Connett et al., 2005), and pancreatic cancer (Sakai et al., 2014), among other tumors, leading to increased tumor growth. In contrast to our observations in mesenchymal EpCAM$^-$ SCC cells, IRF1 expression negatively correlates with the tumor differentiation stage in colorectal cancer cells (Ohsugi et al., 2019). Despite this reduced *Irf1* induction upon IFN-γ treatment, mesenchymal-SCC cells upregulated *Mhc-I*, *Mhc-II*, *Pd-l1,* and antigen-presenting genes expression. Hence, full epithelial SCC cells and mesenchymal EpCAM- SCC cells were not resistant to IFN-γ and correctly responded to its stimulation.

It has been extensively shown that IFN-γ derived signaling promotes the expression of MHC-I (F. Zhou, 2009), MHC-II (Steimle et al., 1994), and PD-L1 (Garcia-Diaz et al., 2017). Upon IFN-γ stimulation, full epithelial SCC cells and mesenchymal EpCAM$^-$ SCC cells expressed higher levels of *Mhc-I*, *Mhc-II*, and *Pd-l1*. Concretely, *Mhc-I* and *Mhc-II* were slightly more increased in full epithelial SCC cells, while *Pd-l1* was more induced in mesenchymal EpCAM$^-$ SCC cells upon IFN-γ stimulation. The distinct transcription factors that upregulate the expression of *Mhc-I*, *Mhc-II*, and *Pd-l1* may explain the differences in the upregulated mRNA levels. *Mhc-I* transcript levels are upregulated by NLRC5, IRF1, and NF-kβ pathway activation (Jongsma et al., 2021). *Mhc-II* expression is regulated by the master regulator CIITA, inducible by IRF1 (Choi et al., 2011). In contrast, *Pd-l1* expression can be induced by IRF1, STAT proteins, NF-kβ, AP-1, MYC, and JUN transcription factors (Ju et al., 2020). The expression of antigen-presenting genes including β2-microglobulin, TAP proteins, Tapasin, ERAP1, and immunoproteasome subunits are mainly coordinated under the transcription factors NF-kβ, IRF1, and NLRC5 (Kelly & Trowsdale, 2019) (Jongsma et al., 2019). Hence, their expression is also controlled by IFN-γ signaling. In this sense, *β2-microglobulin*, *Tap1*, *Tap2*, and *Tapasin* expression was upregulated upon IFN-γ stimulation. Interestingly, *Tap2* transcript levels were more upregulated in full epithelial SCC cells, *β2-microglobulin* expression was slightly more increased in mesenchymal EpCAM$^-$ SCC cells, and the other antigen processing genes were upregulated in a similar way in both compared SCC cells. This could be explained by the different affinity of transcription factors to bind to promoter regions of the indicated genes. A study reported that NLRC5 specifically binds to the promoter regions of MHC-I heavy chains, β2-microglobulin, and TAP1 while did not bind to the TAP2 promoter (Ludigs et al., 2015). Hence, the expression of *Mhc-I*, *Mhc-II*, *Pd-l1*, and antigen processing genes was upregulated upon IFN-γ stimulation supporting the proper functionality of the regulation of MHC-I transcription in both full epithelial SCC cells and mesenchymal EpCAM$^-$ SCC cells.

Upon IFN-γ stimulation, we detected an increase in the total amount of MHC-I protein via WB assays in full epithelial and mesenchymal EpCAM$^-$ SCC cells. Of note, MHC-I needs to arrive at

the cell membrane to present antigens. In full epithelial SCC cells, we observed an induced cell surface expression of MHC-I, MHC-II, and PD-L1 upon IFN-γ signaling stimulation, accordingly to the upregulated transcript levels of these proteins. However, mesenchymal EpCAM$^-$ cells treated with IFN-γ, did not express cell surface MHC-I, but upregulated the cell surface expression of PD-L1 and, to a lesser degree, MHC-II. Hence, *Mhc-I, Mhc-II,* and *Pd-l1* mRNA expression was upregulated upon IFN-γ treatment in mesenchymal EpCAM$^-$ cells, and the total amount of MHC-I protein could be detected, but only PD-L1 and MHC-II were translocated and detected in the cell membrane of mesenchymal EpCAM$^-$ cells. Our results indicate that specific post-translational alterations may prevent MHC-I translocation to the cell surface of mesenchymal EpCAM$^-$ SCC cells and consequently make mesenchymal EpCAM$^-$ SCC cells invisible to CD8$^+$ T cells. To further validate this, we analyzed the cellular location of MHC-I in full epithelial SCC cells and mesenchymal EpCAM- SCC cells upon IFN- γ stimulation by immunocytochemistry. According to our data, we observed that full epithelial SCC cells upregulated the cell surface expression of MHC-I upon IFN-γ stimulation, while MHC-I presented a perinuclear accumulation, and no cell surface expression was detected in stimulated mesenchymal EpCAM$^-$ cells. This indicates that MHC-I could not mature and translocate to the cell surface of mesenchymal EpCAM$^-$ SCC cells and consequently presents a mislocation.

Several mechanisms have been described as responsible for downregulating MHC-I at the protein level through post-translational mechanisms (Dhatchinamoorthy et al., 2021) (Blander, 2023). SND1 oncoprotein, which is highly expressed in various cancers, binds to MHC-I in the ER and promotes endoplasmic reticulum-associated degradation (ERAD) interrupting antigen presentation. Genetic silencing of SND1 increases MHC-I expression and arrival on the cell surface of melanoma and adenocarcinoma cells (Y. Wang et al., 2020). However, SND1 MHC-I degradation it is unlikely to happen in our SCC model given that we observed a perinuclear accumulation of MHC-I in mesenchymal EpCAM$^-$ SCC cells rather than a total absence due to increased degradation. In breast cancer, the MAL2 transmembrane protein participating in endocytosis causes the accumulation and turnover of cell surface MHC-I by regulating the interaction between MHC-I and RAB7, which is a protein implicated in the transport of late endosomes and lysosomes controlling the autophagic flux (Fang et al., 2021). In pancreatic cancer, it was described that MHC-I was not being translocated to the cell membrane of cancer cells because lysosomes were selectively degrading MHC-I by an autophagy-dependent mechanism. Blockade of autophagy using clinically available chloroquine and Bafilomycin A increased MHC-I cell surface levels and anti-tumor T cell response when combined with immunotherapy based on dual blockade of PD-1 and CTLA-4 (Yamamoto et al., 2020). So, different post-translational mechanisms could be impairing the arrival of MHC-I to the cell surface of mesenchymal EpCAM$^-$ SCC cells. We focused on inhibiting lysosomal degradation

given that the availability of drugs impairing the autophagic flux. Nevertheless, the blockade of autophagic flux with Bafilomycin A in mesenchymal EpCAM$^-$ SCC cells did not restore MHC-I cell surface expression. Other post-translational mechanisms, as the increased MAL2 activity should be analyzed in further experiments given that autophagy inhibition did not enhance the arrival of MHC-I to the cell membrane of mesenchymal EpCAM$^-$ SCC cells. In addition, other mechanisms can affect MHC-I/TCR interaction once MHC-I has arrived at the cell membrane and cannot be discarded to also happen in advanced SCC tumors. Lack of MHC-I cell surface expression in mesenchymal EpCAM$^-$ SCC cells can be considered as a combination of *Mhc-I* transcription inhibition altogether with post-translational mechanisms preventing the correct processing and arrival of MHC-I to the cell membrane of mesenchymal-like SCC cells. Further investigation in this subject is needed, so that elucidating the molecular mechanisms that regulate MHC-I cell surface expression in tumor cells may allow advanced SCC patients to increase their response to immunotherapy.

STUDY OF PATIENT cSCC AND HNSCC CELL CHARACTERISTICS ASSOCIATED WITH RESISTANCE TO ICI THERAPY

Failure of ICI therapy can result from defects in any step of the formation of tumor-reactive T cells, activation of effector T cells, and formation of effector memory T cells (Jenkins et al., 2018). For instance, lack of neo-antigens, impaired processing and presentation of tumor antigens by alterations on MHC-I antigen-presenting pathway, or impaired intratumor immune infiltration can impair the generation of newly tumor-reactive T cells. In addition, the presence of immunosuppressive cells and activation of alternate ICs pathways prevent the activation and function of effector T cells. Finally, severe T cell exhaustion and epigenetic changes prevent the formation of effector memory T cells, which hinders long-term duration effects of ICI therapy. These resistance mechanisms are poorly understood in cSCC (García-Sancha et al., 2021) and HNSCC (Dos Santos et al., 2021) and their relevance in patient response to anti-PD-1/PD-L1 immunotherapy has not been completely elucidated.

According to previous data from our group, the resistance to ICI based on anti-PD-1/PD-L1 immunotherapy may be a consequence of tumor cell plasticity leading to the acquisition of mesenchymal-like features. In a mouse model of cSCC progression, our group determined that mesenchymal tumor cells could induce the expression of alternative IC ligands leading to the activation of the various IC receptors such as CTLA-4 and TIGIT (Lorenzo-Sanz et al., under-review manuscript). In addition, the presence of mesenchymal tumor cells was accompanied by a higher presence of immunosuppressive cells (Treg cells, M-MDSCs, and M2-like macrophages) (Lorenzo-Sanz et al., under-review manuscript). All these events would be impairing the antitumor immunity exerted by CD8$^+$ T cells upon anti-PD-1/PD-L1 interventions. Given these

results, we were interested in analyzing whether the presence of mesenchymal tumor cells may be associated with resistance to anti-PD-1/PD-L1 immunotherapy in advanced and metastatic cSCC and HNSCC patients. We conducted a retrospective study analyzing six cSCC patient samples and eleven HNSCC patient samples that were treated with anti-PD-1/PD-L1 immunotherapy. A strong reduction in the size of the tumor or disappearance of the tumors is rare in these patients and has been observed in ~7-13 % of advanced and metastatic cSCC patients (Migden et al., 2018) (Migden et al., 2020) and in ~2 % of recurrent and metastatic HNSCC patients (Ferris et al., 2016) (Burtness et al., 2019). Hence, patients were classified as responders when presented an objective response (complete or partial response) or stabilization of the disease for 1 year, indicating in this last case that the treatment stopped the progression of the disease as the best response. This initial study was conducted by different members of the laboratory and the results were afterward confirmed in a larger cohort of advanced and metastatic cSCC patients (Lorenzo-Sanz et al., under-review manuscript).

Firstly, the epithelial and mesenchymal characteristics of tumor cells in human cSCC samples sensible and resistant to ICI were analyzed by other members of the group. Despite the high intratumor heterogeneity observed, which has also been documented in patient samples suffering from melanoma (Grzywa et al., 2017), esophageal SCC (L. Lin & Lin, 2019), and oral cavity SCC (Zandberg et al., 2019), we could initially observe that responder patients presented a higher epithelial tumor cell component. This was later validated in a larger cohort of cSCC patients where it was observed that non-responder patients to ICI were composed of more hybrid (E-cadherin^{+}/Vimentin^{+}) and mesenchymal (E-cadherin^{-}/Vimentin^{+}) tumor cells. Importantly, this has not been previously documented in cSCC patients according to the bibliography. The induction of EMT, which leads to the appearance of mesenchymal tumor cells, has been observed in a chemically induced squamous cell carcinoma mouse model leading to resistance to anti-PD-1 therapy (Dodagatta-Marri et al., 2019). In this sense, in metastatic melanoma patients, the expression of genes related to EMT in tumor cells has also been associated with innate anti-PD-1 resistance (Hugo et al., 2016). Hence, there is growing evidence that epithelial/mesenchymal plasticity in tumors leads to the appearance of mesenchymal tumor cells and is linked to resistance to therapeutic blockade of the PD-1 axe (L. A. Horn et al., 2020).

Exhausted CD8^{+} T cells exhibit elevated expression of multiple IC receptors (W. Jiang et al., 2020). The expression of IC receptors was characterized in CD8^{+} T cells to investigate the presence of exhausted T cells in cSCC samples. An increased presence of CD8^{+} T cells expressing PD-1 and LAG-3, which might be exhausted, were detected in pre-treatment samples of cSCC patients resistant to anti-PD-1/PD-L1 immunotherapy. Different responses to anti-PD-1/PD-L1 therapies have been observed between different subsets of PD-1^{+} CD8^{+} T cells (Blackburn et al., 2008). Partially exhausted PD-1^{+} CTLA-4^{+} CD8 T cells infiltrating tumors have been correlated

with a correct PD-1 response in melanoma (Daud et al., 2016). However, PD-1$^+$ CD8$^+$ T cells co-expressing various ICs receptors such as CTLA-4, TIM-3, LAG-3, or VISTA have been linked to resistance to anti-PD-1 immunotherapy in lung cancer (Thommen et al., 2015) (Koyama et al., 2016). The combination of anti-IC antibodies has shown improved anti-tumor response overcoming CD8$^+$ T cell exhaustion in preclinical models. Simultaneous blockade of LAG-3 and PD-1 improves anti-tumor response against melanoma and colon adenocarcinoma (Woo et al., 2012) while co-blockade of TIM-3 and PD-1 enhanced anti-tumor immunity against colon and mammary adenocarcinomas (Sakuishi et al., 2010). Indeed, results from our group indicate that mesenchymal tumor cells could be activating other IC apart from PD-1, which would maintain the exhaustion state of CD8+ T cells despite applying anti-PD-1 treatment (Lorenzo-Sanz et al., under-review manuscript). Hence in cSCC patients, the activation of various IC pathways in tumor-infiltrating CD8$^+$ T cells would lead to an exhausted state of CD8$^+$ T cells that probably cannot be reversed by the single blockade of the PD-1 axe.

Therefore, these initial results suggest that cSCC from patients resistant to anti-PD-1/PD-L1 therapies are composed of more hybrid and mesenchymal tumors cells accompanied by an increased presence of exhausted CD8$^+$ T cells. These initial observations were recently validated by other members of the lab in posterior studies using a larger cohort of sensible and resistant cSCC patients treated with ICI (Lorenzo-Sanz et al., unpublished results).

Given that HNSCCs present histopathological similarities with cSCCs, and anti-PD-1 therapy was approved before to treat advanced and metastatic HNSCC patients, we also analyzed molecular and cellular characteristics of HNSCCs of resistant patients to ICI treatment. A similar analysis was done as with cSCC samples. Firstly, the epithelial and mesenchymal characteristics of tumor cells of HNSCCs were determined by other members of the group. Despite observing a high intratumor heterogeneity, which has been observed in multiple tumor types, resistant HNSCC tumors to anti-PD-L1 + anti-CTLA-4 therapy had a higher presence of Vimentin$^+$ cancer cells (hybrid and mesenchymal cancer cells expressing Vimentin). To date, no other studies have linked an increased presence of mesenchymal tumor cells in human HNSCCs resistant to anti-PD-1 immunotherapies. In accordance with our observations, a bioinformatic study analyzing human HNSCCs found that tumors containing mesenchymal cells correlated with poor patient prognosis and presented higher IC signaling than those tumors mainly composed by epithelial cells (Jung et al., 2020). Another study correlated the presence of mesenchymal cells in HNSCC with increased tumor growth accompanied by decreased T-cell proliferation (Liotta et al., 2015). Hence, the presence of mesenchymal tumor cells in advanced and metastatic HNSCC could be actively disrupting antitumor immunity upon ICI treatment. To fully validate these preliminary observations, it is essential to address them through additional experiments involving a larger cohort of advanced and metastatic HNSCC patients sensitive and resistant to ICI therapy.

In contrast to resistant cSCC patients, HNSCC patients resistant to ICI did not present a significant increase presence of $CD8^+$ T cells co-expressing different IC receptors. A slightly increased presence of cytotoxic $CD8^+$ cells that expressed LAG-3 was detected in resistant tumors to anti-PD-1 + anti-CTLA-4 but not in resistant tumors to anti-PD-1/PD-L1. These differences might be explained by the low number of biological samples that were analyzed. Importantly, the presence of exhausted $CD8^+$ T cells in HNSCC, characterized by the co-expression of various IC receptors, has been linked to poor patient prognosis (Y. Zhang, Li, et al., 2022). Next studies should address a similar analysis in a larger cohort of sensible and resistant HNSCCs to ICI to corroborate this hypothesis.

Hence, resistant HNSCC to ICI may present higher frequency of hybrid and mesenchymal tumor cells that could go accompanied by an increased presence of exhausted T cells expressing various IC receptors. These prelaminar results in advanced and metastatic HNSCC patients would need to be further validated by increasing the sample size of patients and performing bioinformatic analysis correlating the presence of mesenchymal-like tumor cells and exhausted T cells with ICI outcome.

CONCLUSIONS

Based on the results obtained in this doctoral thesis, we conclude:

1. Secreted factors from BMDM polarized with the conditioned medium of mesenchymal EpCAM^{-} SCC cells and splenic MDSCs from PD-SCC-bearing mice, which present similar characteristics to tumor-infiltrating macrophages and M-MDSCs in PD-SCCs, promote the acquisition of mesenchymal traits of plastic EpCAM^{high} SCC cells.

2. Splenic M-MDSCs from PD-SCC-bearing mice upregulate the secretion of several cytokines including BAFF, IL28, CCL20, CCL21, and IL-7 which are candidates to promote the acquisition of mesenchymal-like features of plastic EpCAM^{high} SCC cells.

3. Mesenchymal EpCAM^{-} SCC cells from PD-SCCs present a different cytokine secretion profile than full epithelial SCC cells from WD-SCCs, being CXCL1, CSF3, CCL2, and TIMP1 the most secrete cytokines by mesenchymal EpCAM^{-} SCC cells.

4. Blockade of CXCL1 and CXCL2 signaling in PD-SCCs upon SB225002 treatment reduces immunosuppression by decreasing Treg cells recruitment and increasing the presence of GzmB^{+} cytotoxic cells.

5. CSF3 signaling inhibition in PD-SCCs enhances cytotoxic activity by effector immune cells despite not decreasing the recruitment of immunosuppressive M-MDSCs, macrophages, and Treg cells.

6. Anti-CCL2 treatment in PD-SCCs decreases the immunosuppressive TME of PD-SCCs by reducing Treg cells and macrophages recruitment and enhancing the presence of active GzmB^{+} cytotoxic cells.

7. Blockade of CXCL12 signaling in PD/S-SCCs reduces immunosuppression by reducing Treg cells and M2-like macrophages recruitment and increasing CD8 *vs.* FoxP3 ratio and the frequency of active GzmB^{+} cytotoxic cells.

8. Single blockade of cytokines signaling is not sufficient to drastically reduce immunosuppression and block the growth of advanced SCCs.

9. Mesenchymal EpCAM^{-} SCC cells present a decreased expression of *Mhc-I*, *Pd-l1*, and *Tap1* in comparison to full epithelial SCC cells indicating the existence of a specific transcriptional downregulation of these proteins in mesenchymal EpCAM^{-} SCC cells.

10. In contrast to PD-L1, MHC-I cell surface expression is not increased in response to IFN-γ treatment in mesenchymal EpCAM$^-$ SCC cells despite the transcript and protein levels are increased upon IFN-γ stimulation.

11. MHC-I accumulates in perinuclear regions under IFN-γ stimulation in mesenchymal EpCAM$^-$SCC cells indicating the existence of post-translational alterations in the MHC-I processing and arrival to the cell membrane of mesenchymal EpCAM$^-$SCC cells.

12. The frequency of CD8$^+$/PD-1$^+$ and CD8$^+$/LAG-3$^+$ cells was higher in cSCCs of resistant patients, indicating the exhausted state of these tumor infiltrating CD8$^+$ T cells in resistant cSCCs.

13. Characterization of cancer cell features in HNSCC samples from patients resistant to anti-PD-1/PD-L1 or anti-PD-1 + anti-CTLA-4 therapy indicates that a high content of mesenchymal tumor cells would be associated with resistance to ICIs in advanced and metastatic HNSCCs. Further analyses with a higher number of sensible and resistant advanced and metastatic HNSCC samples will be needed to further validate these results.

BIBLIOGRAPHY

Abiko, K., Matsumura, N., Hamanishi, J., Horikawa, N., Murakami, R., Yamaguchi, K., Yoshioka, Y., Baba, T., Konishi, I., & Mandai, M. (2015). IFN-γ from lymphocytes induces PD-L1 expression and promotes progression of ovarian cancer. *British Journal of Cancer*, *112*(9), 1501–1509. https://doi.org/10.1038/bjc.2015.101

Aboul-Fettouh, N., Morse, D., Patel, J., & Migden, M. R. (2021). Immunotherapy and Systemic Treatment of Cutaneous Squamous Cell Carcinoma. *Dermatology Practical & Conceptual*, *11*(Suppl 2), e2021169S. https://doi.org/10.5826/dpc.11S2a169S

Ademmer, K., Ebert, M., Müller-Ostermeyer, F., Friess, H., Büchler, M. W., Schubert, W., & Malfertheiner, P. (1998). Effector T lymphocyte subsets in human pancreatic cancer: Detection of CD8+CD18+ cells and CD8+CD103+ cells by multi-epitope imaging. *Clinical and Experimental Immunology*, *112*(1), 21–26. https://doi.org/10.1046/j.1365-2249.1998.00546.x

Ahmadzadeh, M., Johnson, L. A., Heemskerk, B., Wunderlich, J. R., Dudley, M. E., White, D. E., & Rosenberg, S. A. (2009). Tumor antigen-specific CD8 T cells infiltrating the tumor express high levels of PD-1 and are functionally impaired. *Blood*, *114*(8), 1537–1544. https://doi.org/10.1182/blood-2008-12-195792

Alam, M., & Ratner, D. (2001). Cutaneous squamous-cell carcinoma. *The New England Journal of Medicine*, *344*(13), 975–983. https://doi.org/10.1056/NEJM200103293441306

Alberti, A., & Bossi, P. (2021). Immunotherapy for Cutaneous Squamous Cell Carcinoma: Results and Perspectives. *Frontiers in Oncology*, *11*, 727027. https://doi.org/10.3389/fonc.2021.727027

Al-Rayahi, I. A. M., Browning, M. J., & Stover, C. (2017). Tumour cell conditioned medium reveals greater M2 skewing of macrophages in the absence of properdin. *Immunity, Inflammation and Disease*, *5*(1), 68–77. https://doi.org/10.1002/iid3.142

Alspach, E., Lussier, D. M., & Schreiber, R. D. (2019). Interferon γ and Its Important Roles in Promoting and Inhibiting Spontaneous and Therapeutic Cancer Immunity. *Cold Spring Harbor Perspectives in Biology*, *11*(3), a028480. https://doi.org/10.1101/cshperspect.a028480

Anderson, A. C., Joller, N., & Kuchroo, V. K. (2016). Lag-3, Tim-3, and TIGIT: Co-inhibitory Receptors with Specialized Functions in Immune Regulation. *Immunity*, *44*(5), 989–1004. https://doi.org/10.1016/j.immuni.2016.05.001

Archilla-Ortega, A., Domuro, C., Martin-Liberal, J., & Muñoz, P. (2022). Blockade of novel immune checkpoints and new therapeutic combinations to boost antitumor immunity. *Journal of Experimental & Clinical Cancer Research: CR*, *41*(1), 62. https://doi.org/10.1186/s13046-022-02264-x

Asada, N., Kunisaki, Y., Pierce, H., Wang, Z., Fernandez, N. F., Birbrair, A., Ma'ayan, A., & Frenette, P. S. (2017). Differential cytokine contributions of perivascular haematopoietic stem cell niches. *Nature Cell Biology*, *19*(3), 214–223. https://doi.org/10.1038/ncb3475

Aslan, K., Turco, V., Blobner, J., Sonner, J. K., Liuzzi, A. R., Núñez, N. G., De Feo, D., Kickingereder, P., Fischer, M., Green, E., Sadik, A., Friedrich, M., Sanghvi, K., Kilian, M., Cichon, F., Wolf, L., Jähne, K., von Landenberg, A., Bunse, L., … Platten, M. (2020). Heterogeneity of response to immune checkpoint blockade in hypermutated experimental gliomas. *Nature Communications*, *11*(1), 931. https://doi.org/10.1038/s41467-020-14642-0

Atkins, D., Breuckmann, A., Schmahl, G. E., Binner, P., Ferrone, S., Krummenauer, F., Störkel, S., & Seliger, B. (2004). MHC class I antigen processing pathway defects, ras mutations and disease stage in colorectal carcinoma. *International Journal of Cancer*, *109*(2), 265–273. https://doi.org/10.1002/ijc.11681

Baba, A. B., Rah, B., Bhat, Gh. R., Mushtaq, I., Parveen, S., Hassan, R., Hameed Zargar, M., & Afroze, D. (2022). Transforming Growth Factor-Beta (TGF-β) Signaling in Cancer-A Betrayal Within. *Frontiers in Pharmacology*, *13*. https://www.frontiersin.org/articles/10.3389/fphar.2022.791272

Bachmann, M. F., & Oxenius, A. (2007). Interleukin 2: From immunostimulation to immunoregulation and back again. *EMBO Reports*, *8*(12), 1142–1148. https://doi.org/10.1038/sj.embor.7401099

Baghban, R., Roshangar, L., Jahanban-Esfahlan, R., Seidi, K., Ebrahimi-Kalan, A., Jaymand, M., Kolahian, S., Javaheri, T., & Zare, P. (2020). Tumor microenvironment complexity and therapeutic implications at a glance. *Cell Communication and Signaling: CCS*, *18*(1), 59. https://doi.org/10.1186/s12964-020-0530-4

Barrientos, S., Stojadinovic, O., Golinko, M. S., Brem, H., & Tomic-Canic, M. (2008). PERSPECTIVE ARTICLE: Growth factors and cytokines in wound healing. *Wound Repair and Regeneration*, *16*(5), 585–601. https://doi.org/10.1111/j.1524-475X.2008.00410.x

Basu, A., Ramamoorthi, G., Albert, G., Gallen, C., Beyer, A., Snyder, C., Koski, G., Disis, M. L., Czerniecki, B. J., & Kodumudi, K. (2021). Differentiation and Regulation of TH Cells: A Balancing Act for Cancer Immunotherapy. *Frontiers in Immunology*, *12*, 669474. https://doi.org/10.3389/fimmu.2021.669474

Beatty, G. L., Winograd, R., Evans, R. A., Long, K. B., Luque, S. L., Lee, J. W., Clendenin, C., Gladney, W. L., Knoblock, D. M., Guirnalda, P. D., & Vonderheide, R. H. (2015). Exclusion of T Cells From Pancreatic Carcinomas in Mice Is Regulated by Ly6C(low) F4/80(+) Extratumoral Macrophages. *Gastroenterology*, *149*(1), 201–210. https://doi.org/10.1053/j.gastro.2015.04.010

Beheshti, A., Wage, J., McDonald, J. T., Lamont, C., Peluso, M., Hahnfeldt, P., & Hlatky, L. (2015). Tumor-host signaling interaction reveals a systemic, age-dependent splenic immune influence on tumor development. *Oncotarget*, *6*(34), 35419–35432.

Bejarano, L., Jordão, M. J. C., & Joyce, J. A. (2021). Therapeutic Targeting of the Tumor Microenvironment. *Cancer Discovery*, *11*(4), 933–959. https://doi.org/10.1158/2159-8290.CD-20-1808

Benci, J. L., Xu, B., Qiu, Y., Wu, T. J., Dada, H., Twyman-Saint Victor, C., Cucolo, L., Lee, D. S. M., Pauken, K. E., Huang, A. C., Gangadhar, T. C., Amaravadi, R. K., Schuchter, L. M., Feldman, M. D., Ishwaran, H., Vonderheide, R. H., Maity, A., Wherry, E. J., & Minn, A. J. (2016). Tumor Interferon Signaling Regulates a Multigenic Resistance Program to Immune Checkpoint Blockade. *Cell*, *167*(6), 1540-1554.e12. https://doi.org/10.1016/j.cell.2016.11.022

Berg, D., & Otley, C. C. (2002). Skin cancer in organ transplant recipients: Epidemiology, pathogenesis, and management. *Journal of the American Academy of Dermatology*, *47*(1), 1–17; quiz 18–20. https://doi.org/10.1067/mjd.2002.125579

Bernat-Peguera, A., Simón-Extremera, P., da Silva-Diz, V., López de Munain, M., Díaz-Gil, L., Penin, R. M., González-Suárez, E., Pérez Sidelnikova, D., Bermejo, O., Viñals, J. M., Viñals, F., & Muñoz, P. (2019). PDGFR-induced autocrine SDF-1 signaling in cancer cells promotes metastasis in advanced skin carcinoma. *Oncogene*, *38*(25), 5021–5037. https://doi.org/10.1038/s41388-019-0773-y

Berraondo, P., Sanmamed, M. F., Ochoa, M. C., Etxeberria, I., Aznar, M. A., Pérez-Gracia, J. L., Rodríguez-Ruiz, M. E., Ponz-Sarvise, M., Castañón, E., & Melero, I. (2019). Cytokines in clinical cancer immunotherapy. *British Journal of Cancer*, *120*(1), 6–15. https://doi.org/10.1038/s41416-018-0328-y

Bindea, G., Mlecnik, B., Tosolini, M., Kirilovsky, A., Waldner, M., Obenauf, A. C., Angell, H., Fredriksen, T., Lafontaine, L., Berger, A., Bruneval, P., Fridman, W. H., Becker, C., Pagès, F., Speicher, M. R., Trajanoski, Z., & Galon, J. (2013). Spatiotemporal dynamics of intratumoral immune cells reveal the immune landscape in human cancer. *Immunity*, *39*(4), 782–795. https://doi.org/10.1016/j.immuni.2013.10.003

Binnewies, M., Roberts, E. W., Kersten, K., Chan, V., Fearon, D. F., Merad, M., Coussens, L. M., Gabrilovich, D. I., Ostrand-Rosenberg, S., Hedrick, C. C., Vonderheide, R. H., Pittet, M. J., Jain, R. K., Zou, W., Howcroft, T. K., Woodhouse, E. C., Weinberg, R. A., & Krummel, M. F. (2018). Understanding the tumor immune microenvironment (TIME) for effective therapy. *Nature Medicine*, *24*(5), 541–550. https://doi.org/10.1038/s41591-018-0014-x

Biswas, A., Meissner, T. B., Kawai, T., & Kobayashi, K. S. (2012). Cutting edge: Impaired MHC class I expression in mice deficient for Nlrc5/class I transactivator. *Journal of Immunology (Baltimore, Md.: 1950)*, *189*(2), 516–520. https://doi.org/10.4049/jimmunol.1200064

Biswas, S. K., & Mantovani, A. (2010). Macrophage plasticity and interaction with lymphocyte subsets: Cancer as a paradigm. *Nature Immunology*, *11*(10), 889–896. https://doi.org/10.1038/ni.1937

Blackburn, S. D., Shin, H., Freeman, G. J., & Wherry, E. J. (2008). Selective expansion of a subset of exhausted CD8 T cells by alphaPD-L1 blockade. *Proceedings of the National Academy of Sciences of the United States of America*, *105*(39), 15016–15021. https://doi.org/10.1073/pnas.0801497105

Blander, J. M. (2023). Different routes of MHC-I delivery to phagosomes and their consequences to CD8 T cell immunity. *Seminars in Immunology*, *66*, 101713. https://doi.org/10.1016/j.smim.2023.101713

Blanpain, C., & Fuchs, E. (2009). Epidermal homeostasis: A balancing act of stem cells in the skin. *Nature Reviews. Molecular Cell Biology*, *10*(3), 207–217. https://doi.org/10.1038/nrm2636

Bocanegra, A., Fernandez-Hinojal, G., Zuazo-Ibarra, M., Arasanz, H., Garcia-Granda, M. J., Hernandez, C., Ibañez, M., Hernandez-Marin, B., Martinez-Aguillo, M., Lecumberri, M. J., Fernandez de Lascoiti, A., Teijeira, L., Morilla, I., Vera, R., Escors, D., & Kochan, G. (2019). PD-L1 Expression in Systemic Immune Cell Populations as a Potential Predictive Biomarker of Responses to PD-L1/PD-1 Blockade Therapy in Lung Cancer. *International Journal of Molecular Sciences*, *20*(7), 1631. https://doi.org/10.3390/ijms20071631

Boedtkjer, E., & Pedersen, S. F. (2020). The Acidic Tumor Microenvironment as a Driver of Cancer. *Annual Review of Physiology*, *82*, 103–126. https://doi.org/10.1146/annurev-physiol-021119-034627

Brantsch, K. D., Meisner, C., Schönfisch, B., Trilling, B., Wehner-Caroli, J., Röcken, M., & Breuninger, H. (2008). Analysis of risk factors determining prognosis of cutaneous squamous-cell carcinoma: A prospective study. *The Lancet. Oncology*, *9*(8), 713–720. https://doi.org/10.1016/S1470-2045(08)70178-5

Brinkman, J. N., Hajder, E., van der Holt, B., Den Bakker, M. A., Hovius, S. E. R., & Mureau, M. A. M. (2015). The Effect of Differentiation Grade of Cutaneous Squamous Cell Carcinoma on Excision Margins, Local Recurrence, Metastasis, and Patient Survival: A Retrospective Follow-Up Study. *Annals of Plastic Surgery*, *75*(3), 323–326. https://doi.org/10.1097/SAP.0000000000000110

Briukhovetska, D., Dörr, J., Endres, S., Libby, P., Dinarello, C. A., & Kobold, S. (2021). Interleukins in cancer: From biology to therapy. *Nature Reviews. Cancer*, *21*(8), 481–499. https://doi.org/10.1038/s41568-021-00363-z

Brougham, N. D. L. S., Dennett, E. R., Cameron, R., & Tan, S. T. (2012). The incidence of metastasis from cutaneous squamous cell carcinoma and the impact of its risk factors. *Journal of Surgical Oncology*, *106*(7), 811–815. https://doi.org/10.1002/jso.23155

Bruger, A. M., Dorhoi, A., Esendagli, G., Barczyk-Kahlert, K., van der Bruggen, P., Lipoldova, M., Perecko, T., Santibanez, J., Saraiva, M., Van Ginderachter, J. A., & Brandau, S. (2019). How to measure the immunosuppressive activity of MDSC: Assays, problems and potential solutions. *Cancer Immunology, Immunotherapy: CII*, *68*(4), 631–644. https://doi.org/10.1007/s00262-018-2170-8

Brühl, H., Cihak, J., Schneider, M. A., Plachý, J., Rupp, T., Wenzel, I., Shakarami, M., Milz, S., Ellwart, J. W., Stangassinger, M., Schlöndorff, D., & Mack, M. (2004). Dual role of CCR2 during initiation and progression of collagen-induced arthritis: Evidence for regulatory activity of CCR2+ T cells. *Journal of Immunology (Baltimore, Md.: 1950)*, *172*(2), 890–898. https://doi.org/10.4049/jimmunol.172.2.890

Burova, E., Hermann, A., Dai, J., Ullman, E., Halasz, G., Potocky, T., Hong, S., Liu, M., Allbritton, O., Woodruff, A., Pei, J., Rafique, A., Poueymirou, W., Martin, J., MacDonald, D., Olson, W. C., Murphy, A., Ioffe, E., Thurston, G., & Mohrs, M. (2019). Preclinical Development of the Anti-LAG-3 Antibody REGN3767: Characterization and Activity in Combination with the Anti-PD-1 Antibody Cemiplimab in Human PD-1xLAG-3-Knockin Mice. *Molecular Cancer Therapeutics*, *18*(11), 2051–2062. https://doi.org/10.1158/1535-7163.MCT-18-1376

Burr, M. L., Sparbier, C. E., Chan, K. L., Chan, Y.-C., Kersbergen, A., Lam, E. Y. N., Azidis-Yates, E., Vassiliadis, D., Bell, C. C., Gilan, O., Jackson, S., Tan, L., Wong, S. Q., Hollizeck, S., Michalak, E. M., Siddle, H. V., McCabe, M. T., Prinjha, R. K., Guerra, G. R., … Dawson, M. A. (2019). An Evolutionarily Conserved Function of Polycomb Silences the MHC Class I Antigen Presentation Pathway and Enables Immune Evasion in Cancer. *Cancer Cell*, *36*(4), 385-401.e8. https://doi.org/10.1016/j.ccell.2019.08.008

Burtness, B., Harrington, K. J., Greil, R., Soulières, D., Tahara, M., de Castro, G., Psyrri, A., Basté, N., Neupane, P., Bratland, Å., Fuereder, T., Hughes, B. G. M., Mesía, R., Ngamphaiboon, N., Rordorf, T., Wan Ishak, W. Z., Hong, R.-L., González Mendoza, R., Roy, A., … KEYNOTE-048 Investigators. (2019). Pembrolizumab alone or with chemotherapy versus cetuximab with chemotherapy for recurrent or metastatic squamous cell carcinoma of the head and neck (KEYNOTE-048): A randomised, open-label, phase 3 study. *Lancet (London, England)*, *394*(10212), 1915–1928. https://doi.org/10.1016/S0140-6736(19)32591-7

Carson, W. F., Salter-Green, S. E., Scola, M. M., Joshi, A., Gallagher, K. A., & Kunkel, S. L. (2017). Enhancement of macrophage inflammatory responses by CCL2 is correlated with increased miR-9 expression and downregulation of the ERK1/2 phosphatase Dusp6. *Cellular Immunology*, *314*, 63–72. https://doi.org/10.1016/j.cellimm.2017.02.005

Cassetta, L., Noy, R., Swierczak, A., Sugano, G., Smith, H., Wiechmann, L., & Pollard, J. W. (2016). Isolation of Mouse and Human Tumor-Associated Macrophages. *Advances in Experimental Medicine and Biology*, *899*, 211–229. https://doi.org/10.1007/978-3-319-26666-4_12

Chaffer, C. L., San Juan, B. P., Lim, E., & Weinberg, R. A. (2016). EMT, cell plasticity and metastasis. *Cancer Metastasis Reviews*, *35*(4), 645–654. https://doi.org/10.1007/s10555-016-9648-7

Chambers, E. S., & Vukmanovic-Stejic, M. (2020). Skin barrier immunity and ageing. *Immunology*, *160*(2), 116–125. https://doi.org/10.1111/imm.13152

Chan, T. A., Yarchoan, M., Jaffee, E., Swanton, C., Quezada, S. A., Stenzinger, A., & Peters, S. (2019). Development of tumor mutation burden as an immunotherapy biomarker: Utility for the oncology clinic. *Annals of Oncology: Official Journal of the European Society for Medical Oncology*, *30*(1), 44–56. https://doi.org/10.1093/annonc/mdy495

Chang, A. L., Miska, J., Wainwright, D. A., Dey, M., Rivetta, C. V., Yu, D., Kanojia, D., Pituch, K. C., Qiao, J., Pytel, P., Han, Y., Wu, M., Zhang, L., Horbinski, C. M., Ahmed, A. U., & Lesniak, M. S. (2016). CCL2 Produced by the Glioma Microenvironment Is Essential for the Recruitment of Regulatory T Cells and Myeloid-Derived Suppressor Cells. *Cancer Research*, *76*(19), 5671–5682. https://doi.org/10.1158/0008-5472.CAN-16-0144

Chanmee, T., Ontong, P., Konno, K., & Itano, N. (2014). Tumor-associated macrophages as major players in the tumor microenvironment. *Cancers*, *6*(3), 1670–1690. https://doi.org/10.3390/cancers6031670

Chemokine. (2009). *British Journal of Pharmacology*, *158*(Suppl 1), S35–S37. https://doi.org/10.1111/j.1476-5381.2009.00501_19.x

Chen, D. S., & Mellman, I. (2013). Oncology meets immunology: The cancer-immunity cycle. *Immunity*, *39*(1), 1–10. https://doi.org/10.1016/j.immuni.2013.07.012

Chen, Y., Shao, Z., Jiang, E., Zhou, X., Wang, L., Wang, H., Luo, X., Chen, Q., Liu, K., & Shang, Z. (2020). CCL21/CCR7 interaction promotes EMT and enhances the stemness of OSCC via a JAK2/STAT3 signaling pathway. *Journal of Cellular Physiology*, *235*(9), 5995–6009. https://doi.org/10.1002/jcp.29525

Cheng, S., Li, Z., Gao, R., Xing, B., Gao, Y., Yang, Y., Qin, S., Zhang, L., Ouyang, H., Du, P., Jiang, L., Zhang, B., Yang, Y., Wang, X., Ren, X., Bei, J.-X., Hu, X., Bu, Z., Ji, J., & Zhang, Z. (2021). A pan-cancer single-cell transcriptional atlas of tumor infiltrating myeloid cells. *Cell*, *184*(3), 792-809.e23. https://doi.org/10.1016/j.cell.2021.01.010

Cheng, X.-S., Li, Y.-F., Tan, J., Sun, B., Xiao, Y.-C., Fang, X.-B., Zhang, X.-F., Li, Q., Dong, J.-H., Li, M., Qian, H., Yin, Z.-F., & Yang, Z.-B. (2014). CCL20 and CXCL8 synergize to promote progression and poor survival outcome in patients with colorectal cancer by collaborative induction of the epithelial-mesenchymal transition. *Cancer Letters*, *348*(1–2), 77–87. https://doi.org/10.1016/j.canlet.2014.03.008

Choi, N. M., Majumder, P., & Boss, J. M. (2011). Regulation of major histocompatibility complex class II genes. *Current Opinion in Immunology*, *23*(1), 81–87. https://doi.org/10.1016/j.coi.2010.09.007

Chu, W.-M. (2013). Tumor necrosis factor. *Cancer Letters*, *328*(2), 222–225. https://doi.org/10.1016/j.canlet.2012.10.014

Cohen, E. E. W., Soulières, D., Le Tourneau, C., Dinis, J., Licitra, L., Ahn, M.-J., Soria, A., Machiels, J.-P., Mach, N., Mehra, R., Burtness, B., Zhang, P., Cheng, J., Swaby, R. F., Harrington, K. J., & KEYNOTE-040 investigators. (2019). Pembrolizumab versus methotrexate, docetaxel, or cetuximab for recurrent or metastatic head-and-neck squamous cell carcinoma (KEYNOTE-040): A randomised, open-label, phase 3 study. *Lancet (London, England)*, *393*(10167), 156–167. https://doi.org/10.1016/S0140-6736(18)31999-8

Colangelo, T., Polcaro, G., Ziccardi, P., Pucci, B., Muccillo, L., Galgani, M., Fucci, A., Milone, M. R., Budillon, A., Santopaolo, M., Votino, C., Pancione, M., Piepoli, A., Mazzoccoli, G., Binaschi, M., Bigioni, M., Maggi, C. A., Fassan, M., Laudanna, C., … Colantuoni, V. (2016). Proteomic screening identifies calreticulin as a miR-27a direct target

repressing MHC class I cell surface exposure in colorectal cancer. *Cell Death & Disease*, *7*(2), e2120. https://doi.org/10.1038/cddis.2016.28

Connett, J. M., Badri, L., Giordano, T. J., Connett, W. C., & Doherty, G. M. (2005). Interferon regulatory factor 1 (IRF-1) and IRF-2 expression in breast cancer tissue microarrays. *Journal of Interferon & Cytokine Research: The Official Journal of the International Society for Interferon and Cytokine Research*, *25*(10), 587–594. https://doi.org/10.1089/jir.2005.25.587

Cornel, A. M., Mimpen, I. L., & Nierkens, S. (2020). MHC Class I Downregulation in Cancer: Underlying Mechanisms and Potential Targets for Cancer Immunotherapy. *Cancers*, *12*(7), 1760. https://doi.org/10.3390/cancers12071760

Coussens, L. M., Hanahan, D., & Arbeit, J. M. (1996). Genetic predisposition and parameters of malignant progression in K14-HPV16 transgenic mice. *The American Journal of Pathology*, *149*(6), 1899–1917.

Cretella, D., Digiacomo, G., Giovannetti, E., & Cavazzoni, A. (2019). PTEN Alterations as a Potential Mechanism for Tumor Cell Escape from PD-1/PD-L1 Inhibition. *Cancers*, *11*(9), 1318. https://doi.org/10.3390/cancers11091318

Criscione, V. D., Weinstock, M. A., Naylor, M. F., Luque, C., Eide, M. J., Bingham, S. F., & Department of Veteran Affairs Topical Tretinoin Chemoprevention Trial Group. (2009). Actinic keratoses: Natural history and risk of malignant transformation in the Veterans Affairs Topical Tretinoin Chemoprevention Trial. *Cancer*, *115*(11), 2523–2530. https://doi.org/10.1002/cncr.24284

Cui, C., Xu, C., Yang, W., Chi, Z., Sheng, X., Si, L., Xie, Y., Yu, J., Wang, S., Yu, R., Guo, J., & Kong, Y. (2021). Ratio of the interferon-γ signature to the immunosuppression signature predicts anti-PD-1 therapy response in melanoma. *NPJ Genomic Medicine*, *6*(1), 7. https://doi.org/10.1038/s41525-021-00169-w

Curigliano, G., Gelderblom, H., Mach, N., Doi, T., Tai, D., Forde, P. M., Sarantopoulos, J., Bedard, P. L., Lin, C.-C., Hodi, F. S., Wilgenhof, S., Santoro, A., Sabatos-Peyton, C. A., Longmire, T. A., Xyrafas, A., Sun, H., Gutzwiller, S., Manenti, L., & Naing, A. (2021). Phase I/Ib Clinical Trial of Sabatolimab, an Anti-TIM-3 Antibody, Alone and in Combination with Spartalizumab, an Anti-PD-1 Antibody, in Advanced Solid Tumors. *Clinical Cancer Research: An Official Journal of the American Association for Cancer Research*, *27*(13), 3620–3629. https://doi.org/10.1158/1078-0432.CCR-20-4746

da Silva-Diz, V., Lorenzo-Sanz, L., Bernat-Peguera, A., Lopez-Cerda, M., & Muñoz, P. (2018). Cancer cell plasticity: Impact on tumor progression and therapy response. *Seminars in Cancer Biology*, *53*, 48–58. https://doi.org/10.1016/j.semcancer.2018.08.009

da Silva-Diz, V., Simón-Extremera, P., Bernat-Peguera, A., de Sostoa, J., Urpí, M., Penín, R. M., Sidelnikova, D. P., Bermejo, O., Viñals, J. M., Rodolosse, A., González-Suárez, E., Moruno, A. G., Pujana, M. Á., Esteller, M., Villanueva, A., Viñals, F., & Muñoz, P. (2016). Cancer Stem-like Cells Act via Distinct Signaling Pathways in Promoting Late Stages of Malignant Progression. *Cancer Research*, *76*(5), 1245–1259. https://doi.org/10.1158/0008-5472.CAN-15-1631

Daud, A. I., Loo, K., Pauli, M. L., Sanchez-Rodriguez, R., Sandoval, P. M., Taravati, K., Tsai, K., Nosrati, A., Nardo, L., Alvarado, M. D., Algazi, A. P., Pampaloni, M. H., Lobach, I. V., Hwang, J., Pierce, R. H., Gratz, I. K., Krummel, M. F., & Rosenblum, M. D. (2016). Tumor immune profiling predicts response to anti-PD-1 therapy in human melanoma. *The Journal of Clinical Investigation*, *126*(9), 3447–3452. https://doi.org/10.1172/JCI87324

Davidson, D., Schraven, B., & Veillette, A. (2007). PAG-associated FynT regulates calcium signaling and promotes anergy in T lymphocytes. *Molecular and Cellular Biology*, *27*(5), 1960–1973. https://doi.org/10.1128/MCB.01983-06

Day, F., Kumar, M., Fenton, L., & Gedye, C. (2017). Durable Response of Metastatic Squamous Cell Carcinoma of the Skin to Ipilimumab Immunotherapy. *Journal of Immunotherapy (Hagerstown, Md.: 1997)*, *40*(1), 36–38. https://doi.org/10.1097/CJI.0000000000000146

de Vries, E., Trakatelli, M., Kalabalikis, D., Ferrandiz, L., Ruiz-de-Casas, A., Moreno-Ramirez, D., Sotiriadis, D., Ioannides, D., Aquilina, S., Apap, C., Micallef, R., Scerri, L., Ulrich, M., Pitkänen, S., Saksela, O., Altsitsiadis, E., Hinrichs, B., Magnoni, C., Fiorentini, C., … EPIDERM Group. (2012). Known and potential new risk factors for skin cancer in European populations: A multicentre case-control study. *The British Journal of Dermatology*, *167 Suppl 2*, 1–13. https://doi.org/10.1111/j.1365-2133.2012.11081.x

Deng, W.-W., Mao, L., Yu, G.-T., Bu, L.-L., Ma, S.-R., Liu, B., Gutkind, J. S., Kulkarni, A. B., Zhang, W.-F., & Sun, Z.-J. (2016). LAG-3 confers poor prognosis and its blockade reshapes antitumor response in head and neck squamous cell carcinoma. *Oncoimmunology*, *5*(11), e1239005. https://doi.org/10.1080/2162402X.2016.1239005

Der, S. D., Zhou, A., Williams, B. R., & Silverman, R. H. (1998). Identification of genes differentially regulated by interferon alpha, beta, or gamma using oligonucleotide arrays. *Proceedings of the National Academy of Sciences of the United States of America*, *95*(26), 15623–15628. https://doi.org/10.1073/pnas.95.26.15623

Dersh, D., Phelan, J. D., Gumina, M. E., Wang, B., Arbuckle, J. H., Holly, J., Kishton, R. J., Markowitz, T. E., Seedhom, M. O., Fridlyand, N., Wright, G. W., Huang, D. W., Ceribelli, M., Thomas, C. J., Lack, J. B., Restifo, N. P., Kristie, T. M., Staudt, L. M., & Yewdell, J. W. (2021). Genome-wide Screens Identify Lineage- and Tumor-Specific Genes Modulating MHC-I- and MHC-II-Restricted Immunosurveillance of Human Lymphomas. *Immunity*, *54*(1), 116-131.e10. https://doi.org/10.1016/j.immuni.2020.11.002

Dhatchinamoorthy, K., Colbert, J. D., & Rock, K. L. (2021). Cancer Immune Evasion Through Loss of MHC Class I Antigen Presentation. *Frontiers in Immunology*, *12*, 636568. https://doi.org/10.3389/fimmu.2021.636568

Didona, D., Paolino, G., Bottoni, U., & Cantisani, C. (2018). Non Melanoma Skin Cancer Pathogenesis Overview. *Biomedicines*, *6*(1), 6. https://doi.org/10.3390/biomedicines6010006

DiGiovanni, J. (1992). Multistage carcinogenesis in mouse skin. *Pharmacology & Therapeutics*, *54*(1), 63–128. https://doi.org/10.1016/0163-7258(92)90051-z

Dodagatta-Marri, E., Meyer, D. S., Reeves, M. Q., Paniagua, R., To, M. D., Binnewies, M., Broz, M. L., Mori, H., Wu, D., Adoumie, M., Del Rosario, R., Li, O., Buchmann, T., Liang, B., Malato, J., Arce Vargus, F., Sheppard, D., Hann, B. C., Mirza, A., … Akhurst, R. J. (2019). α-PD-1 therapy elevates Treg/Th balance and increases tumor cell pSmad3 that are both targeted by α-TGFβ antibody to promote durable rejection and immunity in squamous cell carcinomas. *Journal for Immunotherapy of Cancer*, *7*(1), 62. https://doi.org/10.1186/s40425-018-0493-9

Dos Santos, L. V., Abrahão, C. M., & William, W. N. (2021). Overcoming Resistance to Immune Checkpoint Inhibitors in Head and Neck Squamous Cell Carcinomas. *Frontiers in Oncology*, *11*, 596290. https://doi.org/10.3389/fonc.2021.596290

Dougan, M., Luoma, A. M., Dougan, S. K., & Wucherpfennig, K. W. (2021). Understanding and treating the inflammatory adverse events of cancer immunotherapy. *Cell*, *184*(6), 1575–1588. https://doi.org/10.1016/j.cell.2021.02.011

Duan, Q., Zhang, H., Zheng, J., & Zhang, L. (2020). Turning Cold into Hot: Firing up the Tumor Microenvironment. *Trends in Cancer*, *6*(7), 605–618. https://doi.org/10.1016/j.trecan.2020.02.022

Engelhard, V., Conejo-Garcia, J. R., Ahmed, R., Nelson, B. H., Willard-Gallo, K., Bruno, T. C., & Fridman, W. H. (2021). B cells and cancer. *Cancer Cell*, *39*(10), 1293–1296. https://doi.org/10.1016/j.ccell.2021.09.007

Evans, H. L., & Smith, J. L. (1980). Spindle cell squamous carcinomas and sarcoma-like tumors of the skin: A comparative study of 38 cases. *Cancer*, *45*(10), 2687–2697. https://doi.org/10.1002/1097-0142(19800515)45:10<2687::aid-cncr2820451034>3.0.co;2-r

Fan, T., Li, S., Xiao, C., Tian, H., Zheng, Y., Liu, Y., Li, C., & He, J. (2022). CCL20 promotes lung adenocarcinoma progression by driving epithelial-mesenchymal transition. *International Journal of Biological Sciences*, *18*(11), 4275–4288. https://doi.org/10.7150/ijbs.73275

Fang, Y., Wang, L., Wan, C., Sun, Y., Van der Jeught, K., Zhou, Z., Dong, T., So, K. M., Yu, T., Li, Y., Eyvani, H., Colter, A. B., Dong, E., Cao, S., Wang, J., Schneider, B. P., Sandusky, G. E., Liu, Y., Zhang, C., … Zhang, X. (2021). MAL2 drives immune evasion in breast cancer by suppressing tumor antigen presentation. *The Journal of Clinical Investigation*, *131*(1), e140837, 140837. https://doi.org/10.1172/JCI140837

Fania, L., Didona, D., Di Pietro, F. R., Verkhovskaia, S., Morese, R., Paolino, G., Donati, M., Ricci, F., Coco, V., Ricci, F., Candi, E., Abeni, D., & Dellambra, E. (2021). Cutaneous Squamous Cell Carcinoma: From Pathophysiology to Novel Therapeutic Approaches. *Biomedicines*, *9*(2), 171. https://doi.org/10.3390/biomedicines9020171

Fares, C. M., Van Allen, E. M., Drake, C. G., Allison, J. P., & Hu-Lieskovan, S. (2019). Mechanisms of Resistance to Immune Checkpoint Blockade: Why Does Checkpoint Inhibitor Immunotherapy Not Work for All Patients? *American Society of Clinical Oncology Educational Book. American Society of Clinical Oncology. Annual Meeting*, *39*, 147–164. https://doi.org/10.1200/EDBK_240837

Fei, L., Ren, X., Yu, H., & Zhan, Y. (2021). Targeting the CCL2/CCR2 Axis in Cancer Immunotherapy: One Stone, Three Birds? *Frontiers in Immunology*, *12*, 771210. https://doi.org/10.3389/fimmu.2021.771210

Feig, C., Jones, J. O., Kraman, M., Wells, R. J. B., Deonarine, A., Chan, D. S., Connell, C. M., Roberts, E. W., Zhao, Q., Caballero, O. L., Teichmann, S. A., Janowitz, T., Jodrell, D. I., Tuveson, D. A., & Fearon, D. T. (2013). Targeting CXCL12 from FAP-expressing carcinoma-associated fibroblasts synergizes with anti-PD-L1 immunotherapy in pancreatic cancer. *Proceedings of the National Academy of Sciences of the United States of America*, *110*(50), 20212–20217. https://doi.org/10.1073/pnas.1320318110

Ferlay, J., Colombet, M., Soerjomataram, I., Mathers, C., Parkin, D. M., Piñeros, M., Znaor, A., & Bray, F. (2019). Estimating the global cancer incidence and mortality in 2018: GLOBOCAN sources and methods. *International Journal of Cancer*, *144*(8), 1941–1953. https://doi.org/10.1002/ijc.31937

Ferrarotto, R., Bell, D., Rubin, M. L., Hutcheson, K. A., Johnson, J. M., Goepfert, R. P., Phan, J., Elamin, Y., Torman, D. K., Warneke, C. L., Hessel, A. C., Garden, A. S., Myers, J. N., Johnson, F. M., Lee, J. J., Sikora, A. G., Gillison, M. L., Glisson, B. S., & Gross, N. D. (2020). Impact of neoadjuvant durvalumab with or without tremelimumab on CD8+ tumor lymphocyte density, safety, and efficacy in patients with oropharynx cancer: CIAO trial results. *Clinical Cancer Research : An Official Journal of the American Association*

for Cancer Research, *26*(13), 3211–3219. https://doi.org/10.1158/1078-0432.CCR-19-3977

Ferris, R. L., Blumenschein, G., Fayette, J., Guigay, J., Colevas, A. D., Licitra, L., Harrington, K., Kasper, S., Vokes, E. E., Even, C., Worden, F., Saba, N. F., Iglesias Docampo, L. C., Haddad, R., Rordorf, T., Kiyota, N., Tahara, M., Monga, M., Lynch, M., … Gillison, M. L. (2016). Nivolumab for Recurrent Squamous-Cell Carcinoma of the Head and Neck. *The New England Journal of Medicine*, *375*(19), 1856–1867. https://doi.org/10.1056/NEJMoa1602252

Ferris, R. L., Haddad, R., Even, C., Tahara, M., Dvorkin, M., Ciuleanu, T. E., Clement, P. M., Mesia, R., Kutukova, S., Zholudeva, L., Daste, A., Caballero-Daroqui, J., Keam, B., Vynnychenko, I., Lafond, C., Shetty, J., Mann, H., Fan, J., Wildsmith, S., … Licitra, L. (2020). Durvalumab with or without tremelimumab in patients with recurrent or metastatic head and neck squamous cell carcinoma: EAGLE, a randomized, open-label phase III study. *Annals of Oncology: Official Journal of the European Society for Medical Oncology*, *31*(7), 942–950. https://doi.org/10.1016/j.annonc.2020.04.001

Ferris, R. L., Moskovitz, J., Kunning, S., Ruffin, A. T., Reeder, C., Ohr, J., Gooding, W. E., Kim, S., Karlovits, B. J., Vignali, D. A. A., Duvvuri, U., Johnson, J. T., Petro, D., Heron, D. E., Clump, D. A., Bruno, T. C., & Bauman, J. E. (2022). Phase I Trial of Cetuximab, Radiotherapy, and Ipilimumab in Locally Advanced Head and Neck Cancer. *Clinical Cancer Research: An Official Journal of the American Association for Cancer Research*, *28*(7), 1335–1344. https://doi.org/10.1158/1078-0432.CCR-21-0426

Ferris, R. L., Spanos, W. C., Leidner, R., Gonçalves, A., Martens, U. M., Kyi, C., Sharfman, W., Chung, C. H., Devriese, L. A., Gauthier, H., Chiosea, S. I., Vujanovic, L., Taube, J. M., Stein, J. E., Li, J., Li, B., Chen, T., Barrows, A., & Topalian, S. L. (2021). Neoadjuvant nivolumab for patients with resectable HPV-positive and HPV-negative squamous cell carcinomas of the head and neck in the CheckMate 358 trial. *Journal for Immunotherapy of Cancer*, *9*(6), e002568. https://doi.org/10.1136/jitc-2021-002568

Fonsatti, E., Nicolay, H. J. M., Sigalotti, L., Calabrò, L., Pezzani, L., Colizzi, F., Altomonte, M., Guidoboni, M., Marincola, F. M., & Maio, M. (2007). Functional up-regulation of human leukocyte antigen class I antigens expression by 5-aza-2'-deoxycytidine in cutaneous melanoma: Immunotherapeutic implications. *Clinical Cancer Research: An Official Journal of the American Association for Cancer Research*, *13*(11), 3333–3338. https://doi.org/10.1158/1078-0432.CCR-06-3091

Foster, J. R. (2001). The functions of cytokines and their uses in toxicology. *International Journal of Experimental Pathology*, *82*(3), 171–192. https://doi.org/10.1046/j.1365-2613.2001.iep0082-0171-x

Franco, R., Nicoletti, G., Lombardi, A., Di Domenico, M., Botti, G., Zito Marino, F., & Caraglia, M. (2013). Current treatment of cutaneous squamous cancer and molecular strategies for its sensitization to new target-based drugs. *Expert Opinion on Biological Therapy*, *13*(1), 51–66. https://doi.org/10.1517/14712598.2012.725720

Freeman, G. J., Long, A. J., Iwai, Y., Bourque, K., Chernova, T., Nishimura, H., Fitz, L. J., Malenkovich, N., Okazaki, T., Byrne, M. C., Horton, H. F., Fouser, L., Carter, L., Ling, V., Bowman, M. R., Carreno, B. M., Collins, M., Wood, C. R., & Honjo, T. (2000). Engagement of the PD-1 immunoinhibitory receptor by a novel B7 family member leads to negative regulation of lymphocyte activation. *The Journal of Experimental Medicine*, *192*(7), 1027–1034. https://doi.org/10.1084/jem.192.7.1027

Fridlender, Z. G., Sun, J., Kim, S., Kapoor, V., Cheng, G., Ling, L., Worthen, G. S., & Albelda, S. M. (2009). Polarization of tumor-associated neutrophil phenotype by TGF-beta: "N1"

versus "N2" TAN. *Cancer Cell*, *16*(3), 183–194. https://doi.org/10.1016/j.ccr.2009.06.017

Gabrilovich, D. I., & Nagaraj, S. (2009). Myeloid-derived-suppressor cells as regulators of the immune system. *Nature Reviews. Immunology*, *9*(3), 162–174. https://doi.org/10.1038/nri2506

Gabrilovich, D. I., Ostrand-Rosenberg, S., & Bronte, V. (2012). Coordinated regulation of myeloid cells by tumours. *Nature Reviews. Immunology*, *12*(4), 253–268. https://doi.org/10.1038/nri3175

Galon, J., & Bruni, D. (2019). Approaches to treat immune hot, altered and cold tumours with combination immunotherapies. *Nature Reviews. Drug Discovery*, *18*(3), 197–218. https://doi.org/10.1038/s41573-018-0007-y

Gao, J., Shi, L. Z., Zhao, H., Chen, J., Xiong, L., He, Q., Chen, T., Roszik, J., Bernatchez, C., Woodman, S. E., Chen, P.-L., Hwu, P., Allison, J. P., Futreal, A., Wargo, J. A., & Sharma, P. (2016). Loss of IFN-γ Pathway Genes in Tumor Cells as a Mechanism of Resistance to Anti-CTLA-4 Therapy. *Cell*, *167*(2), 397-404.e9. https://doi.org/10.1016/j.cell.2016.08.069

Garcia-Diaz, A., Shin, D. S., Moreno, B. H., Saco, J., Escuin-Ordinas, H., Rodriguez, G. A., Zaretsky, J. M., Sun, L., Hugo, W., Wang, X., Parisi, G., Saus, C. P., Torrejon, D. Y., Graeber, T. G., Comin-Anduix, B., Hu-Lieskovan, S., Damoiseaux, R., Lo, R. S., & Ribas, A. (2017). Interferon Receptor Signaling Pathways Regulating PD-L1 and PD-L2 Expression. *Cell Reports*, *19*(6), 1189–1201. https://doi.org/10.1016/j.celrep.2017.04.031

García-Sancha, N., Corchado-Cobos, R., Bellido-Hernández, L., Román-Curto, C., Cardeñoso-Álvarez, E., Pérez-Losada, J., Orfao, A., & Cañueto, J. (2021). Overcoming Resistance to Immunotherapy in Advanced Cutaneous Squamous Cell Carcinoma. *Cancers*, *13*(20), 5134. https://doi.org/10.3390/cancers13205134

Gardner, A., & Ruffell, B. (2016). Dendritic Cells and Cancer Immunity. *Trends in Immunology*, *37*(12), 855–865. https://doi.org/10.1016/j.it.2016.09.006

Gibson, J. T., Orlandella, R. M., Turbitt, W. J., Behring, M., Manne, U., Sorge, R. E., & Norian, L. A. (2020). Obesity-Associated Myeloid-Derived Suppressor Cells Promote Apoptosis of Tumor-Infiltrating CD8 T Cells and Immunotherapy Resistance in Breast Cancer. *Frontiers in Immunology*, *11*, 590794. https://doi.org/10.3389/fimmu.2020.590794

Giese, M. A., Hind, L. E., & Huttenlocher, A. (2019). Neutrophil plasticity in the tumor microenvironment. *Blood*, *133*(20), 2159–2167. https://doi.org/10.1182/blood-2018-11-844548

Gillison, M. L., Chaturvedi, A. K., & Lowy, D. R. (2008). HPV prophylactic vaccines and the potential prevention of noncervical cancers in both men and women. *Cancer*, *113*(10 Suppl), 3036–3046. https://doi.org/10.1002/cncr.23764

Granot, Z., Henke, E., Comen, E. A., King, T. A., Norton, L., & Benezra, R. (2011). Tumor entrained neutrophils inhibit seeding in the premetastatic lung. *Cancer Cell*, *20*(3), 300–314. https://doi.org/10.1016/j.ccr.2011.08.012

Grasso, C. S., Tsoi, J., Onyshchenko, M., Abril-Rodriguez, G., Ross-Macdonald, P., Wind-Rotolo, M., Champhekar, A., Medina, E., Torrejon, D. Y., Shin, D. S., Tran, P., Kim, Y. J., Puig-Saus, C., Campbell, K., Vega-Crespo, A., Quist, M., Martignier, C., Luke, J. J., Wolchok, J. D., … Ribas, A. (2020). Conserved Interferon-γ Signaling Drives Clinical Response to Immune Checkpoint Blockade Therapy in Melanoma. *Cancer Cell*, *38*(4), 500-515.e3. https://doi.org/10.1016/j.ccell.2020.08.005

Griffith, J. W., Sokol, C. L., & Luster, A. D. (2014). Chemokines and chemokine receptors: Positioning cells for host defense and immunity. *Annual Review of Immunology*, *32*, 659–702. https://doi.org/10.1146/annurev-immunol-032713-120145

Grob, J.-J., Gonzalez, R., Basset-Seguin, N., Vornicova, O., Schachter, J., Joshi, A., Meyer, N., Grange, F., Piulats, J. M., Bauman, J. R., Zhang, P., Gumuscu, B., Swaby, R. F., & Hughes, B. G. M. (2020). Pembrolizumab Monotherapy for Recurrent or Metastatic Cutaneous Squamous Cell Carcinoma: A Single-Arm Phase II Trial (KEYNOTE-629). *Journal of Clinical Oncology: Official Journal of the American Society of Clinical Oncology*, *38*(25), 2916–2925. https://doi.org/10.1200/JCO.19.03054

Groth, C., Hu, X., Weber, R., Fleming, V., Altevogt, P., Utikal, J., & Umansky, V. (2019). Immunosuppression mediated by myeloid-derived suppressor cells (MDSCs) during tumour progression. *British Journal of Cancer*, *120*(1), 16–25. https://doi.org/10.1038/s41416-018-0333-1

Grzywa, T. M., Paskal, W., & Włodarski, P. K. (2017). Intratumor and Intertumor Heterogeneity in Melanoma. *Translational Oncology*, *10*(6), 956–975. https://doi.org/10.1016/j.tranon.2017.09.007

Hailemichael, Y., Johnson, D. H., Abdel-Wahab, N., Foo, W. C., Bentebibel, S.-E., Daher, M., Haymaker, C., Wani, K., Saberian, C., Ogata, D., Kim, S. T., Nurieva, R., Lazar, A. J., Abu-Sbeih, H., Fa'ak, F., Mathew, A., Wang, Y., Falohun, A., Trinh, V., … Diab, A. (2022). Interleukin-6 blockade abrogates immunotherapy toxicity and promotes tumor immunity. *Cancer Cell*, *40*(5), 509-523.e6. https://doi.org/10.1016/j.ccell.2022.04.004

Hamilton, J. A. (2008). Colony-stimulating factors in inflammation and autoimmunity. *Nature Reviews Immunology*, *8*(7), Article 7. https://doi.org/10.1038/nri2356

Han, G., Wu, D., Yang, Y., Li, Z., Zhang, J., & Li, C. (2015). CrkL meditates CCL20/CCR6-induced EMT in gastric cancer. *Cytokine*, *76*(2), 163–169. https://doi.org/10.1016/j.cyto.2015.05.009

Han, X., Shi, H., Sun, Y., Shang, C., Luan, T., Wang, D., Ba, X., & Zeng, X. (2019). CXCR2 expression on granulocyte and macrophage progenitors under tumor conditions contributes to mo-MDSC generation via SAP18/ERK/STAT3. *Cell Death & Disease*, *10*(8), 598. https://doi.org/10.1038/s41419-019-1837-1

Han, Y., Liu, D., & Li, L. (2020). PD-1/PD-L1 pathway: Current researches in cancer. *American Journal of Cancer Research*, *10*(3), 727–742.

Hartwig, T., Montinaro, A., von Karstedt, S., Sevko, A., Surinova, S., Chakravarthy, A., Taraborrelli, L., Draber, P., Lafont, E., Arce Vargas, F., El-Bahrawy, M. A., Quezada, S. A., & Walczak, H. (2017). The TRAIL-Induced Cancer Secretome Promotes a Tumor-Supportive Immune Microenvironment via CCR2. *Molecular Cell*, *65*(4), 730-742.e5. https://doi.org/10.1016/j.molcel.2017.01.021

Harwood, C. A., Surentheran, T., McGregor, J. M., Spink, P. J., Leigh, I. M., Breuer, J., & Proby, C. M. (2000). Human papillomavirus infection and non-melanoma skin cancer in immunosuppressed and immunocompetent individuals. *Journal of Medical Virology*, *61*(3), 289–297. https://doi.org/10.1002/1096-9071(200007)61:3<289::aid-jmv2>3.0.co;2-z

Herbst, R. S., Soria, J.-C., Kowanetz, M., Fine, G. D., Hamid, O., Gordon, M. S., Sosman, J. A., McDermott, D. F., Powderly, J. D., Gettinger, S. N., Kohrt, H. E. K., Horn, L., Lawrence, D. P., Rost, S., Leabman, M., Xiao, Y., Mokatrin, A., Koeppen, H., Hegde, P. S., … Hodi, F. S. (2014). Predictive correlates of response to the anti-PD-L1 antibody MPDL3280A in cancer patients. *Nature*, *515*(7528), 563–567. https://doi.org/10.1038/nature14011

Highfill, S. L., Cui, Y., Giles, A. J., Smith, J. P., Zhang, H., Morse, E., Kaplan, R. N., & Mackall, C. L. (2014). Disruption of CXCR2-mediated MDSC tumor trafficking enhances anti-PD1 efficacy. *Science Translational Medicine*, *6*(237), 237ra67. https://doi.org/10.1126/scitranslmed.3007974

Hinshaw, D. C., & Shevde, L. A. (2019). The Tumor Microenvironment Innately Modulates Cancer Progression. *Cancer Research*, *79*(18), 4557–4566. https://doi.org/10.1158/0008-5472.CAN-18-3962

Hong, C.-C., Yao, S., McCann, S. E., Dolnick, R. Y., Wallace, P. K., Gong, Z., Quan, L., Lee, K. P., Evans, S. S., Repasky, E. A., Edge, S. B., & Ambrosone, C. B. (2013). Pretreatment levels of circulating Th1 and Th2 cytokines, and their ratios, are associated with ER-negative and triple negative breast cancers. *Breast Cancer Research and Treatment*, *139*(2), 477–488. https://doi.org/10.1007/s10549-013-2549-3

Horn, L. A., Fousek, K., & Palena, C. (2020). Tumor plasticity and resistance to immunotherapy. *Trends in Cancer*, *6*(5), 432–441. https://doi.org/10.1016/j.trecan.2020.02.001

Horn, L., Spigel, D. R., Vokes, E. E., Holgado, E., Ready, N., Steins, M., Poddubskaya, E., Borghaei, H., Felip, E., Paz-Ares, L., Pluzanski, A., Reckamp, K. L., Burgio, M. A., Kohlhäeufl, M., Waterhouse, D., Barlesi, F., Antonia, S., Arrieta, O., Fayette, J., … Eberhardt, W. E. E. (2017). Nivolumab Versus Docetaxel in Previously Treated Patients With Advanced Non-Small-Cell Lung Cancer: Two-Year Outcomes From Two Randomized, Open-Label, Phase III Trials (CheckMate 017 and CheckMate 057). *Journal of Clinical Oncology: Official Journal of the American Society of Clinical Oncology*, *35*(35), 3924–3933. https://doi.org/10.1200/JCO.2017.74.3062

Huang, A. C., Postow, M. A., Orlowski, R. J., Mick, R., Bengsch, B., Manne, S., Xu, W., Harmon, S., Giles, J. R., Wenz, B., Adamow, M., Kuk, D., Panageas, K. S., Carrera, C., Wong, P., Quagliarello, F., Wubbenhorst, B., D'Andrea, K., Pauken, K. E., … Wherry, E. J. (2017). T-cell invigoration to tumour burden ratio associated with anti-PD-1 response. *Nature*, *545*(7652), 60–65. https://doi.org/10.1038/nature22079

Huang, B., Huang, M., & Li, Q. (2019). Cancer-Associated Fibroblasts Promote Angiogenesis of Hepatocellular Carcinoma by VEGF-Mediated EZH2/VASH1 Pathway. *Technology in Cancer Research & Treatment*, *18*, 1533033819879905. https://doi.org/10.1177/1533033819879905

Huang, P. Y., & Balmain, A. (2014). Modeling cutaneous squamous carcinoma development in the mouse. *Cold Spring Harbor Perspectives in Medicine*, *4*(9), a013623. https://doi.org/10.1101/cshperspect.a013623

Huang, W., Luo, S., Burgess, R., Yi, Y.-H., Huang, G. F., & Huang, R.-P. (2018). New Insights into the Tumor Microenvironment Utilizing Protein Array Technology. *International Journal of Molecular Sciences*, *19*(2), 559. https://doi.org/10.3390/ijms19020559

Huang, Y.-H., Yang, H.-Y., Huang, S.-W., Ou, G., Hsu, Y.-F., & Hsu, M.-J. (2016). Interleukin-6 Induces Vascular Endothelial Growth Factor-C Expression via Src-FAK-STAT3 Signaling in Lymphatic Endothelial Cells. *PLoS ONE*, *11*(7), e0158839. https://doi.org/10.1371/journal.pone.0158839

Hugo, W., Zaretsky, J. M., Sun, L., Song, C., Moreno, B. H., Hu-Lieskovan, S., Berent-Maoz, B., Pang, J., Chmielowski, B., Cherry, G., Seja, E., Lomeli, S., Kong, X., Kelley, M. C., Sosman, J. A., Johnson, D. B., Ribas, A., & Lo, R. S. (2016). Genomic and Transcriptomic Features of Response to Anti-PD-1 Therapy in Metastatic Melanoma. *Cell*, *165*(1), 35–44. https://doi.org/10.1016/j.cell.2016.02.065

Huntington, N. D., Cursons, J., & Rautela, J. (2020). The cancer-natural killer cell immunity cycle. *Nature Reviews. Cancer*, *20*(8), 437–454. https://doi.org/10.1038/s41568-020-0272-z

In, G. K., Vaidya, P., Filkins, A., Hermel, D. J., King, K. G., Ragab, O., Tseng, W. W., Swanson, M., Kokot, N., Lang, J. E., Menendez, L., DeClerck, B., Kim, G., Hu, J. C., Terando, A., Jadvar, H., Ricker, C., Miller, K. A., Peng, D. H., & Wysong, A. (2021). PD-1 inhibition therapy for advanced cutaneous squamous cell carcinoma: A retrospective analysis from the University of Southern California. *Journal of Cancer Research and Clinical Oncology*, *147*(6), 1803–1811. https://doi.org/10.1007/s00432-020-03458-6

Jablonska, J., Wu, C.-F., Andzinski, L., Leschner, S., & Weiss, S. (2014). CXCR2-mediated tumor-associated neutrophil recruitment is regulated by IFN-β. *International Journal of Cancer*, *134*(6), 1346–1358. https://doi.org/10.1002/ijc.28551

Jayasingam, S. D., Citartan, M., Thang, T. H., Mat Zin, A. A., Ang, K. C., & Ch'ng, E. S. (2019). Evaluating the Polarization of Tumor-Associated Macrophages Into M1 and M2 Phenotypes in Human Cancer Tissue: Technicalities and Challenges in Routine Clinical Practice. *Frontiers in Oncology*, *9*, 1512. https://doi.org/10.3389/fonc.2019.01512

Jenkins, R. W., Barbie, D. A., & Flaherty, K. T. (2018). Mechanisms of resistance to immune checkpoint inhibitors. *British Journal of Cancer*, *118*(1), 9–16. https://doi.org/10.1038/bjc.2017.434

Jiang, W., He, Y., He, W., Wu, G., Zhou, X., Sheng, Q., Zhong, W., Lu, Y., Ding, Y., Lu, Q., Ye, F., & Hua, H. (2020). Exhausted CD8+T Cells in the Tumor Immune Microenvironment: New Pathways to Therapy. *Frontiers in Immunology*, *11*, 622509. https://doi.org/10.3389/fimmu.2020.622509

Jiang, Y., Li, Y., & Zhu, B. (2015). T-cell exhaustion in the tumor microenvironment. *Cell Death & Disease*, *6*(6), e1792. https://doi.org/10.1038/cddis.2015.162

Jiang, Z., Zhang, Y., Zhang, Y., Jia, Z., Zhang, Z., & Yang, J. (2021). Cancer derived exosomes induce macrophages immunosuppressive polarization to promote bladder cancer progression. *Cell Communication and Signaling : CCS*, *19*, 93. https://doi.org/10.1186/s12964-021-00768-1

Johnson, D. E., Burtness, B., Leemans, C. R., Lui, V. W. Y., Bauman, J. E., & Grandis, J. R. (2020). Head and neck squamous cell carcinoma. *Nature Reviews. Disease Primers*, *6*(1), 92. https://doi.org/10.1038/s41572-020-00224-3

Joller, N., Hafler, J. P., Brynedal, B., Kassam, N., Spoerl, S., Levin, S. D., Sharpe, A. H., & Kuchroo, V. K. (2011). Cutting edge: TIGIT has T cell-intrinsic inhibitory functions. *Journal of Immunology (Baltimore, Md.: 1950)*, *186*(3), 1338–1342. https://doi.org/10.4049/jimmunol.1003081

Jongsma, M. L. M., Guarda, G., & Spaapen, R. M. (2019). The regulatory network behind MHC class I expression. *Molecular Immunology*, *113*, 16–21. https://doi.org/10.1016/j.molimm.2017.12.005

Jongsma, M. L. M., Neefjes, J., & Spaapen, R. M. (2021). Playing hide and seek: Tumor cells in control of MHC class I antigen presentation. *Molecular Immunology*, *136*, 36–44. https://doi.org/10.1016/j.molimm.2021.05.009

Jorgovanovic, D., Song, M., Wang, L., & Zhang, Y. (2020). Roles of IFN-γ in tumor progression and regression: A review. *Biomarker Research*, *8*, 49. https://doi.org/10.1186/s40364-020-00228-x

Joyce, J. A., & Fearon, D. T. (2015). T cell exclusion, immune privilege, and the tumor microenvironment. *Science (New York, N.Y.)*, *348*(6230), 74–80. https://doi.org/10.1126/science.aaa6204

Joyce, J. A., & Pollard, J. W. (2009). Microenvironmental regulation of metastasis. *Nature Reviews. Cancer*, *9*(4), 239–252. https://doi.org/10.1038/nrc2618

Ju, X., Zhang, H., Zhou, Z., & Wang, Q. (2020). Regulation of PD-L1 expression in cancer and clinical implications in immunotherapy. *American Journal of Cancer Research*, *10*(1), 1–11.

Jung, A. R., Jung, C.-H., Noh, J. K., Lee, Y. C., & Eun, Y.-G. (2020). Epithelial-mesenchymal transition gene signature is associated with prognosis and tumor microenvironment in head and neck squamous cell carcinoma. *Scientific Reports*, *10*(1), 3652. https://doi.org/10.1038/s41598-020-60707-x

Kadomoto, S., Izumi, K., & Mizokami, A. (2021). Roles of CCL2-CCR2 Axis in the Tumor Microenvironment. *International Journal of Molecular Sciences*, *22*(16), 8530. https://doi.org/10.3390/ijms22168530

Kaklamanis, L., Townsend, A., Doussis-Anagnostopoulou, I. A., Mortensen, N., Harris, A. L., & Gatter, K. C. (1994). Loss of major histocompatibility complex-encoded transporter associated with antigen presentation (TAP) in colorectal cancer. *The American Journal of Pathology*, *145*(3), 505–509.

Kalbasi, A., & Ribas, A. (2020). Tumour-intrinsic resistance to immune checkpoint blockade. *Nature Reviews. Immunology*, *20*(1), 25–39. https://doi.org/10.1038/s41577-019-0218-4

Kalluri, R., & Weinberg, R. A. (2009). The basics of epithelial-mesenchymal transition. *The Journal of Clinical Investigation*, *119*(6), 1420–1428. https://doi.org/10.1172/JCI39104

Kaplan, D. H., Shankaran, V., Dighe, A. S., Stockert, E., Aguet, M., Old, L. J., & Schreiber, R. D. (1998). Demonstration of an interferon gamma-dependent tumor surveillance system in immunocompetent mice. *Proceedings of the National Academy of Sciences of the United States of America*, *95*(13), 7556–7561. https://doi.org/10.1073/pnas.95.13.7556

Karagas, M. R., Nelson, H. H., Zens, M. S., Linet, M., Stukel, T. A., Spencer, S., Applebaum, K. M., Mott, L., & Mabuchi, K. (2007). Squamous cell and basal cell carcinoma of the skin in relation to radiation therapy and potential modification of risk by sun exposure. *Epidemiology (Cambridge, Mass.)*, *18*(6), 776–784. https://doi.org/10.1097/EDE.0b013e3181567ebe

Katoh, H., Wang, D., Daikoku, T., Sun, H., Dey, S. K., & DuBois, R. N. (2013). CXCR2-expressing myeloid-derived suppressor cells are essential to promote colitis-associated tumorigenesis. *Cancer Cell*, *24*(5), 631–644. https://doi.org/10.1016/j.ccr.2013.10.009

Kawano, M., Mabuchi, S., Matsumoto, Y., Sasano, T., Takahashi, R., Kuroda, H., Kozasa, K., Hashimoto, K., Isobe, A., Sawada, K., Hamasaki, T., Morii, E., & Kimura, T. (2015). The significance of G-CSF expression and myeloid-derived suppressor cells in the chemoresistance of uterine cervical cancer. *Scientific Reports*, *5*, 18217. https://doi.org/10.1038/srep18217

Kelly, A., & Trowsdale, J. (2019). Genetics of antigen processing and presentation. *Immunogenetics*, *71*(3), 161–170. https://doi.org/10.1007/s00251-018-1082-2

Kemp, S. B., Carpenter, E. S., Steele, N. G., Donahue, K. L., Nwosu, Z. C., Pacheco, A., Velez-Delgado, A., Menjivar, R. E., Lima, F., The, S., Espinoza, C. E., Brown, K., Long, D., Lyssiotis, C. A., Rao, A., Zhang, Y., Pasca di Magliano, M., & Crawford, H. C. (2021). Apolipoprotein E Promotes Immune Suppression in Pancreatic Cancer through NF-κB-Mediated Production of CXCL1. *Cancer Research*, *81*(16), 4305–4318. https://doi.org/10.1158/0008-5472.CAN-20-3929

Kershaw, M. H., Wang, G., Westwood, J. A., Pachynski, R. K., Tiffany, H. L., Marincola, F. M., Wang, E., Young, H. A., Murphy, P. M., & Hwu, P. (2002). Redirecting migration of T

cells to chemokine secreted from tumors by genetic modification with CXCR2. *Human Gene Therapy*, *13*(16), 1971–1980. https://doi.org/10.1089/10430340260355374

Kessenbrock, K., Plaks, V., & Werb, Z. (2010). Matrix Metalloproteinases: Regulators of the Tumor Microenvironment. *Cell*, *141*(1), 52–67. https://doi.org/10.1016/j.cell.2010.03.015

Khalaf, K., Hana, D., Chou, J. T.-T., Singh, C., Mackiewicz, A., & Kaczmarek, M. (2021). Aspects of the Tumor Microenvironment Involved in Immune Resistance and Drug Resistance. *Frontiers in Immunology*, *12*, 656364. https://doi.org/10.3389/fimmu.2021.656364

Khan, W. A. (2019). *Autoantibodies and Cytokines*. BoD – Books on Demand.

Kim, E. S., Kim, J. E., Patel, M. A., Mangraviti, A., Ruzevick, J., & Lim, M. (2016). Immune Checkpoint Modulators: An Emerging Antiglioma Armamentarium. *Journal of Immunology Research*, *2016*, 4683607. https://doi.org/10.1155/2016/4683607

Kim, J. E., Patel, M. A., Mangraviti, A., Kim, E. S., Theodros, D., Velarde, E., Liu, A., Sankey, E. W., Tam, A., Xu, H., Mathios, D., Jackson, C. M., Harris-Bookman, S., Garzon-Muvdi, T., Sheu, M., Martin, A. M., Tyler, B. M., Tran, P. T., Ye, X., … Lim, M. (2017). Combination Therapy with Anti-PD-1, Anti-TIM-3, and Focal Radiation Results in Regression of Murine Gliomas. *Clinical Cancer Research: An Official Journal of the American Association for Cancer Research*, *23*(1), 124–136. https://doi.org/10.1158/1078-0432.CCR-15-1535

Kim, R., Emi, M., & Tanabe, K. (2006). Cancer immunosuppression and autoimmune disease: Beyond immunosuppressive networks for tumour immunity. *Immunology*, *119*(2), 254–264. https://doi.org/10.1111/j.1365-2567.2006.02430.x

Klemm, F., & Joyce, J. A. (2015). Microenvironmental regulation of therapeutic response in cancer. *Trends in Cell Biology*, *25*(4), 198–213. https://doi.org/10.1016/j.tcb.2014.11.006

Koizumi, M., Hiasa, Y., Kumagi, T., Yamanishi, H., Azemoto, N., Kobata, T., Matsuura, B., Abe, M., & Onji, M. (2013). Increased B Cell-Activating Factor Promotes Tumor Invasion and Metastasis in Human Pancreatic Cancer. *PLoS ONE*, *8*(8), e71367. https://doi.org/10.1371/journal.pone.0071367

Kösemehmetoğlu, K., Özoğul, E., Babaoğlu, B., Tezel, G., & Gedikoğlu, G. (2017). Programmed Death Ligand 1 (PD-L1) Expression in Malignant Mesenchymal Tumors. *Turk Patoloji Dergisi*, *1*(1). https://doi.org/10.5146/tjpath.2017.01395

Koyama, S., Akbay, E. A., Li, Y. Y., Herter-Sprie, G. S., Buczkowski, K. A., Richards, W. G., Gandhi, L., Redig, A. J., Rodig, S. J., Asahina, H., Jones, R. E., Kulkarni, M. M., Kuraguchi, M., Palakurthi, S., Fecci, P. E., Johnson, B. E., Janne, P. A., Engelman, J. A., Gangadharan, S. P., … Hammerman, P. S. (2016). Adaptive resistance to therapeutic PD-1 blockade is associated with upregulation of alternative immune checkpoints. *Nature Communications*, *7*, 10501. https://doi.org/10.1038/ncomms10501

Kumar, V., Donthireddy, L., Marvel, D., Condamine, T., Wang, F., Lavilla-Alonso, S., Hashimoto, A., Vonteddu, P., Behera, R., Goins, M. A., Mulligan, C., Nam, B., Hockstein, N., Denstman, F., Shakamuri, S., Speicher, D. W., Weeraratna, A. T., Chao, T., Vonderheide, R. H., … Gabrilovich, D. I. (2017). Cancer-Associated Fibroblasts Neutralize the Anti-tumor Effect of CSF1 Receptor Blockade by Inducing PMN-MDSC Infiltration of Tumors. *Cancer Cell*, *32*(5), 654-668.e5. https://doi.org/10.1016/j.ccell.2017.10.005

Kumar, V., Patel, S., Tcyganov, E., & Gabrilovich, D. I. (2016). The Nature of Myeloid-Derived Suppressor Cells in the Tumor Microenvironment. *Trends in Immunology*, *37*(3), 208–220. https://doi.org/10.1016/j.it.2016.01.004

Labani-Motlagh, A., Ashja-Mahdavi, M., & Loskog, A. (2020). The Tumor Microenvironment: A Milieu Hindering and Obstructing Antitumor Immune Responses. *Frontiers in Immunology*, *11*, 940. https://doi.org/10.3389/fimmu.2020.00940

Lazaridou, M.-F., Gonschorek, E., Massa, C., Friedrich, M., Handke, D., Mueller, A., Jasinski-Bergner, S., Dummer, R., Koelblinger, P., & Seliger, B. (2020). Identification of miR-200a-5p targeting the peptide transporter TAP1 and its association with the clinical outcome of melanoma patients. *Oncoimmunology*, *9*(1), 1774323. https://doi.org/10.1080/2162402X.2020.1774323

Lee, S., & Margolin, K. (2011). Cytokines in Cancer Immunotherapy. *Cancers*, *3*(4), 3856–3893. https://doi.org/10.3390/cancers3043856

Lee, Y. S., & Radford, K. J. (2019). The role of dendritic cells in cancer. *International Review of Cell and Molecular Biology*, *348*, 123–178. https://doi.org/10.1016/bs.ircmb.2019.07.006

Li, F., Zou, Z., Suo, N., Zhang, Z., Wan, F., Zhong, G., Qu, Y., Ntaka, K. S., & Tian, H. (2014). CCL21/CCR7 axis activating chemotaxis accompanied with epithelial-mesenchymal transition in human breast carcinoma. *Medical Oncology (Northwood, London, England)*, *31*(9), 180. https://doi.org/10.1007/s12032-014-0180-8

Li, J., Byrne, K. T., Yan, F., Yamazoe, T., Chen, Z., Baslan, T., Richman, L. P., Lin, J., Sun, Y. H., Rech, A. J., Balli, D., Hay, C. A., Sela, Y., Merrell, A. J., Liudahl, S. M., Gordon, N., Norgard, R. J., Yuan, S., Yu, S., … Stanger, B. Z. (2018). Tumor cell-intrinsic factors underlie heterogeneity of immune cell infiltration and response to immunotherapy. *Immunity*, *49*(1), 178-193.e7. https://doi.org/10.1016/j.immuni.2018.06.006

Li, W., Zhang, X., Wu, F., Zhou, Y., Bao, Z., Li, H., Zheng, P., & Zhao, S. (2019). Gastric cancer-derived mesenchymal stromal cells trigger M2 macrophage polarization that promotes metastasis and EMT in gastric cancer. *Cell Death & Disease*, *10*(12), 918. https://doi.org/10.1038/s41419-019-2131-y

Li, Y., Xiang, S., Pan, W., Wang, J., Zhan, H., & Liu, S. (2023). Targeting tumor immunosuppressive microenvironment for pancreatic cancer immunotherapy: Current research and future perspective. *Frontiers in Oncology*, *13*. https://www.frontiersin.org/articles/10.3389/fonc.2023.1166860

Li, Z.-L., Ye, S.-B., OuYang, L.-Y., Zhang, H., Chen, Y.-S., He, J., Chen, Q.-Y., Qian, C.-N., Zhang, X.-S., Cui, J., Zeng, Y.-X., & Li, J. (2015). COX-2 promotes metastasis in nasopharyngeal carcinoma by mediating interactions between cancer cells and myeloid-derived suppressor cells. *Oncoimmunology*, *4*(11), e1044712. https://doi.org/10.1080/2162402X.2015.1044712

Liao, C., Wang, Q., An, J., Long, Q., Wang, H., Xiang, M., Xiang, M., Zhao, Y., Liu, Y., Liu, J., & Guan, X. (2021). Partial EMT in Squamous Cell Carcinoma: A Snapshot. *International Journal of Biological Sciences*, *17*(12), 3036. https://doi.org/10.7150/ijbs.61566

Lim, W., Ma, W., Gee, K., Aucoin, S., Nandan, D., Diaz-Mitoma, F., Kozlowski, M., & Kumar, A. (2002). Distinct role of p38 and c-Jun N-terminal kinases in IL-10-dependent and IL-10-independent regulation of the costimulatory molecule B7.2 in lipopolysaccharide-stimulated human monocytic cells. *Journal of Immunology (Baltimore, Md.: 1950)*, *168*(4), 1759–1769. https://doi.org/10.4049/jimmunol.168.4.1759

Lin, L., & Lin, D.-C. (2019). Biological Significance of Tumor Heterogeneity in Esophageal Squamous Cell Carcinoma. *Cancers*, *11*(8), 1156. https://doi.org/10.3390/cancers11081156

Lin, W., Zhang, H., Niu, Z., Wang, Z., Kong, Y., Yang, X., & Yuan, F. (2020). The disease stage-associated imbalance of Th1/Th2 and Th17/Treg in uterine cervical cancer patients and

their recovery with the reduction of tumor burden. *BMC Women's Health*, *20*, 126. https://doi.org/10.1186/s12905-020-00972-0

Liotta, F., Querci, V., Mannelli, G., Santarlasci, V., Maggi, L., Capone, M., Rossi, M. C., Mazzoni, A., Cosmi, L., Romagnani, S., Maggi, E., Gallo, O., & Annunziato, F. (2015). Mesenchymal stem cells are enriched in head neck squamous cell carcinoma, correlates with tumour size and inhibit T-cell proliferation. *British Journal of Cancer*, *112*(4), 745–754. https://doi.org/10.1038/bjc.2015.15

Lipski, D. A., Dewispelaere, R., Foucart, V., Caspers, L. E., Defrance, M., Bruyns, C., & Willermain, F. (2017). MHC class II expression and potential antigen-presenting cells in the retina during experimental autoimmune uveitis. *Journal of Neuroinflammation*, *14*(1), 136. https://doi.org/10.1186/s12974-017-0915-5

Liu, B., Jia, Y., Ma, J., Wu, S., Jiang, H., Cao, Y., Sun, X., Yin, X., Yan, S., Shang, M., & Mao, A. (2016). Tumor-associated macrophage-derived CCL20 enhances the growth and metastasis of pancreatic cancer. *Acta Biochimica Et Biophysica Sinica*, *48*(12), 1067–1074. https://doi.org/10.1093/abbs/gmw101

Liu, C., Chu, D., Kalantar-Zadeh, K., George, J., Young, H. A., & Liu, G. (2021). Cytokines: From Clinical Significance to Quantification. *Advanced Science (Weinheim, Baden-Wurttemberg, Germany)*, *8*(15), e2004433. https://doi.org/10.1002/advs.202004433

Liu, C., Yu, S., Kappes, J., Wang, J., Grizzle, W. E., Zinn, K. R., & Zhang, H.-G. (2007). Expansion of spleen myeloid suppressor cells represses NK cell cytotoxicity in tumor-bearing host. *Blood*, *109*(10), 4336–4342. https://doi.org/10.1182/blood-2006-09-046201

Liu, D., Jenkins, R. W., & Sullivan, R. J. (2019). Mechanisms of Resistance to Immune Checkpoint Blockade. *American Journal of Clinical Dermatology*, *20*(1), 41–54. https://doi.org/10.1007/s40257-018-0389-y

Liu, J., Geng, X., Hou, J., & Wu, G. (2021). New insights into M1/M2 macrophages: Key modulators in cancer progression. *Cancer Cell International*, *21*(1), 389. https://doi.org/10.1186/s12935-021-02089-2

Liu, Y., Zugazagoitia, J., Ahmed, F. S., Henick, B. S., Gettinger, S. N., Herbst, R. S., Schalper, K. A., & Rimm, D. L. (2020). Immune Cell PD-L1 Colocalizes with Macrophages and Is Associated with Outcome in PD-1 Pathway Blockade Therapy. *Clinical Cancer Research: An Official Journal of the American Association for Cancer Research*, *26*(4), 970–977. https://doi.org/10.1158/1078-0432.CCR-19-1040

Liu, Y.-T., & Sun, Z.-J. (2021). Turning cold tumors into hot tumors by improving T-cell infiltration. *Theranostics*, *11*(11), 5365–5386. https://doi.org/10.7150/thno.58390

Lomas, A., Leonardi-Bee, J., & Bath-Hextall, F. (2012). A systematic review of worldwide incidence of nonmelanoma skin cancer. *The British Journal of Dermatology*, *166*(5), 1069–1080. https://doi.org/10.1111/j.1365-2133.2012.10830.x

Lorenzi, S., Forloni, M., Cifaldi, L., Antonucci, C., Citti, A., Boldrini, R., Pezzullo, M., Castellano, A., Russo, V., van der Bruggen, P., Giacomini, P., Locatelli, F., & Fruci, D. (2012). IRF1 and NF-kB Restore MHC Class I-Restricted Tumor Antigen Processing and Presentation to Cytotoxic T Cells in Aggressive Neuroblastoma. *PLoS ONE*, *7*(10), e46928. https://doi.org/10.1371/journal.pone.0046928

Lorenzo-Sanz, L., & Muñoz, P. (2019). Tumor-Infiltrating Immunosuppressive Cells in Cancer-Cell Plasticity, Tumor Progression and Therapy Response. *Cancer Microenvironment: Official Journal of the International Cancer Microenvironment Society*, *12*(2–3), 119–132. https://doi.org/10.1007/s12307-019-00232-2

Lowney, J. K., Boucher, L. D., Swanson, P. E., & Doherty, G. M. (1999). Interferon regulatory factor-1 and -2 expression in human melanoma specimens. *Annals of Surgical Oncology*, *6*(6), 604–608. https://doi.org/10.1007/s10434-999-0604-4

Lowy, D. R., Kirnbauer, R., & Schiller, J. T. (1994). Genital human papillomavirus infection. *Proceedings of the National Academy of Sciences of the United States of America*, *91*(7), 2436–2440.

Luckheeram, R. V., Zhou, R., Verma, A. D., & Xia, B. (2012). $CD4^+$T cells: Differentiation and functions. *Clinical & Developmental Immunology*, *2012*, 925135. https://doi.org/10.1155/2012/925135

Ludigs, K., Seguín-Estévez, Q., Lemeille, S., Ferrero, I., Rota, G., Chelbi, S., Mattmann, C., MacDonald, H. R., Reith, W., & Guarda, G. (2015). NLRC5 exclusively transactivates MHC class I and related genes through a distinctive SXY module. *PLoS Genetics*, *11*(3), e1005088. https://doi.org/10.1371/journal.pgen.1005088

Luo, H., Xia, X., Huang, L.-B., An, H., Cao, M., Kim, G. D., Chen, H.-N., Zhang, W.-H., Shu, Y., Kong, X., Ren, Z., Li, P.-H., Liu, Y., Tang, H., Sun, R., Li, C., Bai, B., Jia, W., Liu, Y., … Xu, H. (2022). Pan-cancer single-cell analysis reveals the heterogeneity and plasticity of cancer-associated fibroblasts in the tumor microenvironment. *Nature Communications*, *13*(1), 6619. https://doi.org/10.1038/s41467-022-34395-2

Luo, N., Nixon, M. J., Gonzalez-Ericsson, P. I., Sanchez, V., Opalenik, S. R., Li, H., Zahnow, C. A., Nickels, M. L., Liu, F., Tantawy, M. N., Sanders, M. E., Manning, H. C., & Balko, J. M. (2018). DNA methyltransferase inhibition upregulates MHC-I to potentiate cytotoxic T lymphocyte responses in breast cancer. *Nature Communications*, *9*(1), 248. https://doi.org/10.1038/s41467-017-02630-w

Lv, M., Xu, Y., Tang, R., Ren, J., Shen, S., Chen, Y., Liu, B., Hou, Y., & Wang, T. (2014a). MiR141-CXCL1-CXCR2 signaling-induced Treg recruitment regulates metastases and survival of non-small cell lung cancer. *Molecular Cancer Therapeutics*, *13*(12), 3152–3162. https://doi.org/10.1158/1535-7163.MCT-14-0448

Lv, M., Xu, Y., Tang, R., Ren, J., Shen, S., Chen, Y., Liu, B., Hou, Y., & Wang, T. (2014b). MiR141-CXCL1-CXCR2 signaling-induced Treg recruitment regulates metastases and survival of non-small cell lung cancer. *Molecular Cancer Therapeutics*, *13*(12), 3152–3162. https://doi.org/10.1158/1535-7163.MCT-14-0448

Manjunath, Y., Upparahalli, S. V., Avella, D. M., Deroche, C. B., Kimchi, E. T., Staveley-O'Carroll, K. F., Smith, C. J., Li, G., & Kaifi, J. T. (2019). PD-L1 Expression with Epithelial Mesenchymal Transition of Circulating Tumor Cells Is Associated with Poor Survival in Curatively Resected Non-Small Cell Lung Cancer. *Cancers*, *11*(6). https://doi.org/10.3390/cancers11060806

Mari, L., Hoefnagel, S. J. M., Zito, D., van de Meent, M., van Endert, P., Calpe, S., Sancho Serra, M. D. C., Heemskerk, M. H. M., van Laarhoven, H. W. M., Hulshof, M. C. C. M., Gisbertz, S. S., Medema, J. P., van Berge Henegouwen, M. I., Meijer, S. L., Bergman, J. J. G. H. M., Milano, F., & Krishnadath, K. K. (2018). MicroRNA 125a Regulates MHC-I Expression on Esophageal Adenocarcinoma Cells, Associated With Suppression of Antitumor Immune Response and Poor Outcomes of Patients. *Gastroenterology*, *155*(3), 784–798. https://doi.org/10.1053/j.gastro.2018.06.030

Marin-Acevedo, J. A., Kimbrough, E. O., & Lou, Y. (2021). Next generation of immune checkpoint inhibitors and beyond. *Journal of Hematology & Oncology*, *14*(1), 45. https://doi.org/10.1186/s13045-021-01056-8

Marks, R., Rennie, G., & Selwood, T. S. (1988). Malignant transformation of solar keratoses to squamous cell carcinoma. *Lancet (London, England)*, *1*(8589), 795–797. https://doi.org/10.1016/s0140-6736(88)91658-3

Marsigliante, S., Vetrugno, C., & Muscella, A. (2016). Paracrine CCL20 loop induces epithelial-mesenchymal transition in breast epithelial cells. *Molecular Carcinogenesis*, *55*(7), 1175–1186. https://doi.org/10.1002/mc.22360

Martinez, F. O., & Gordon, S. (2014). The M1 and M2 paradigm of macrophage activation: Time for reassessment. *F1000Prime Reports*, *6*, 13. https://doi.org/10.12703/P6-13

Matsuyama, T., Kimura, T., Kitagawa, M., Pfeffer, K., Kawakami, T., Watanabe, N., Kündig, T. M., Amakawa, R., Kishihara, K., & Wakeham, A. (1993). Targeted disruption of IRF-1 or IRF-2 results in abnormal type I IFN gene induction and aberrant lymphocyte development. *Cell*, *75*(1), 83–97.

Maubec, E., Boubaya, M., Petrow, P., Beylot-Barry, M., Basset-Seguin, N., Deschamps, L., Grob, J.-J., Dréno, B., Scheer-Senyarich, I., Bloch-Queyrat, C., Leccia, M.-T., Stefan, A., Saiag, P., Grange, F., Meyer, N., de Quatrebarbes, J., Dinulescu, M., Legoupil, D., Machet, L., … Groupe de Cancérologie Cutanée30. (2020). Phase II Study of Pembrolizumab As First-Line, Single-Drug Therapy for Patients With Unresectable Cutaneous Squamous Cell Carcinomas. *Journal of Clinical Oncology: Official Journal of the American Society of Clinical Oncology*, *38*(26), 3051–3061. https://doi.org/10.1200/JCO.19.03357

Michalak, E. M., Burr, M. L., Bannister, A. J., & Dawson, M. A. (2019). The roles of DNA, RNA and histone methylation in ageing and cancer. *Nature Reviews. Molecular Cell Biology*, *20*(10), 573–589. https://doi.org/10.1038/s41580-019-0143-1

Migden, M. R., Khushalani, N. I., Chang, A. L. S., Lewis, K. D., Schmults, C. D., Hernandez-Aya, L., Meier, F., Schadendorf, D., Guminski, A., Hauschild, A., Wong, D. J., Daniels, G. A., Berking, C., Jankovic, V., Stankevich, E., Booth, J., Li, S., Weinreich, D. M., Yancopoulos, G. D., … Rischin, D. (2020). Cemiplimab in locally advanced cutaneous squamous cell carcinoma: Results from an open-label, phase 2, single-arm trial. *The Lancet. Oncology*, *21*(2), 294–305. https://doi.org/10.1016/S1470-2045(19)30728-4

Migden, M. R., Rischin, D., Schmults, C. D., Guminski, A., Hauschild, A., Lewis, K. D., Chung, C. H., Hernandez-Aya, L., Lim, A. M., Chang, A. L. S., Rabinowits, G., Thai, A. A., Dunn, L. A., Hughes, B. G. M., Khushalani, N. I., Modi, B., Schadendorf, D., Gao, B., Seebach, F., … Fury, M. G. (2018). PD-1 Blockade with Cemiplimab in Advanced Cutaneous Squamous-Cell Carcinoma. *The New England Journal of Medicine*, *379*(4), 341–351. https://doi.org/10.1056/NEJMoa1805131

Miller, D. M., Faulkner-Jones, B. E., Stone, J. R., & Drews, R. E. (2017). Complete pathologic response of metastatic cutaneous squamous cell carcinoma and allograft rejection after treatment with combination immune checkpoint blockade. *JAAD Case Reports*, *3*(5), 412–415. https://doi.org/10.1016/j.jdcr.2017.06.005

Mirlekar, B. (2022). Tumor promoting roles of IL-10, TGF-β, IL-4, and IL-35: Its implications in cancer immunotherapy. *SAGE Open Medicine*, *10*, 20503121211069012. https://doi.org/10.1177/20503121211069012

Mizukami, Y., Kono, K., Kawaguchi, Y., Akaike, H., Kamimura, K., Sugai, H., & Fujii, H. (2008). CCL17 and CCL22 chemokines within tumor microenvironment are related to accumulation of Foxp3+ regulatory T cells in gastric cancer. *International Journal of Cancer*, *122*(10), 2286–2293. https://doi.org/10.1002/ijc.23392

Mlecnik, B., Bindea, G., Angell, H. K., Maby, P., Angelova, M., Tougeron, D., Church, S. E., Lafontaine, L., Fischer, M., Fredriksen, T., Sasso, M., Bilocq, A. M., Kirilovsky, A., Obenauf, A. C., Hamieh, M., Berger, A., Bruneval, P., Tuech, J.-J., Sabourin, J.-C., …

Galon, J. (2016). Integrative Analyses of Colorectal Cancer Show Immunoscore Is a Stronger Predictor of Patient Survival Than Microsatellite Instability. *Immunity*, *44*(3), 698–711. https://doi.org/10.1016/j.immuni.2016.02.025

Molon, B., Ugel, S., Del Pozzo, F., Soldani, C., Zilio, S., Avella, D., De Palma, A., Mauri, P., Monegal, A., Rescigno, M., Savino, B., Colombo, P., Jonjic, N., Pecanic, S., Lazzarato, L., Fruttero, R., Gasco, A., Bronte, V., & Viola, A. (2011). Chemokine nitration prevents intratumoral infiltration of antigen-specific T cells. *The Journal of Experimental Medicine*, *208*(10), 1949–1962. https://doi.org/10.1084/jem.20101956

Mondini, M., Loyher, P.-L., Hamon, P., Gerbé de Thoré, M., Laviron, M., Berthelot, K., Clémenson, C., Salomon, B. L., Combadière, C., Deutsch, E., & Boissonnas, A. (2019). CCR2-Dependent Recruitment of Tregs and Monocytes Following Radiotherapy Is Associated with TNFα-Mediated Resistance. *Cancer Immunology Research*, *7*(3), 376–387. https://doi.org/10.1158/2326-6066.CIR-18-0633

Moon, J., Oh, Y. M., & Ha, S.-J. (2021). Perspectives on immune checkpoint ligands: Expression, regulation, and clinical implications. *BMB Reports*, *54*(8), 403–412. https://doi.org/10.5483/BMBRep.2021.54.8.054

Morad, G., Helmink, B. A., Sharma, P., & Wargo, J. A. (2021). Hallmarks of response, resistance, and toxicity to immune checkpoint blockade. *Cell*, *184*(21), 5309–5337. https://doi.org/10.1016/j.cell.2021.09.020

Morris, R. J., Liu, Y., Marles, L., Yang, Z., Trempus, C., Li, S., Lin, J. S., Sawicki, J. A., & Cotsarelis, G. (2004). Capturing and profiling adult hair follicle stem cells. *Nature Biotechnology*, *22*(4), 411–417. https://doi.org/10.1038/nbt950

Morris, R. M., Mortimer, T. O., & O'Neill, K. L. (2022). Cytokines: Can Cancer Get the Message? *Cancers*, *14*(9), 2178. https://doi.org/10.3390/cancers14092178

Mortezaee, K., & Majidpoor, J. (2022). Checkpoint inhibitor/interleukin-based combination therapy of cancer. *Cancer Medicine*, *11*(15), 2934–2943. https://doi.org/10.1002/cam4.4659

Moser, B., Clark-Lewis, I., Zwahlen, R., & Baggiolini, M. (1990). Neutrophil-activating properties of the melanoma growth-stimulatory activity. *The Journal of Experimental Medicine*, *171*(5), 1797–1802. https://doi.org/10.1084/jem.171.5.1797

Mouchemore, K. A., Anderson, R. L., & Hamilton, J. A. (2018). Neutrophils, G-CSF and their contribution to breast cancer metastasis. *The FEBS Journal*, *285*(4), 665–679. https://doi.org/10.1111/febs.14206

Mucha, J., Majchrzak, K., Taciak, B., Hellmén, E., & Król, M. (2014). MDSCs mediate angiogenesis and predispose canine mammary tumor cells for metastasis via IL-28/IL-28RA (IFN-λ) signaling. *PloS One*, *9*(7), e103249. https://doi.org/10.1371/journal.pone.0103249

Muhlethaler-Mottet, A., Di Berardino, W., Otten, L. A., & Mach, B. (1998). Activation of the MHC class II transactivator CIITA by interferon-gamma requires cooperative interaction between Stat1 and USF-1. *Immunity*, *8*(2), 157–166. https://doi.org/10.1016/s1074-7613(00)80468-9

Myers, J. A., & Miller, J. S. (2021). Exploring the NK cell platform for cancer immunotherapy. *Nature Reviews. Clinical Oncology*, *18*(2), 85–100. https://doi.org/10.1038/s41571-020-0426-7

Nagarsheth, N., Wicha, M. S., & Zou, W. (2017). Chemokines in the cancer microenvironment and their relevance in cancer immunotherapy. *Nature Reviews. Immunology*, *17*(9), 559–572. https://doi.org/10.1038/nri.2017.49

Nahrendorf, M., & Swirski, F. K. (2016). Abandoning M1/M2 for a Network Model of Macrophage Function. *Circulation Research*, *119*(3), 414–417. https://doi.org/10.1161/CIRCRESAHA.116.309194

Nakamura, K., & Smyth, M. (2020). Myeloid immunosuppression and immune checkpoints in the tumor microenvironment. *Cellular & Molecular Immunology*, *17*(1), 1–12. https://doi.org/10.1038/s41423-019-0306-1

Nauseef, W. M., & Borregaard, N. (2014). Neutrophils at work. *Nature Immunology*, *15*(7), 602–611. https://doi.org/10.1038/ni.2921

Nepal, S., Tiruppathi, C., Tsukasaki, Y., Farahany, J., Mittal, M., Rehman, J., Prockop, D. J., & Malik, A. B. (2019). STAT6 induces expression of Gas6 in macrophages to clear apoptotic neutrophils and resolve inflammation. *Proceedings of the National Academy of Sciences of the United States of America*, *116*(33), 16513–16518. https://doi.org/10.1073/pnas.1821601116

Nie, Y., Yang, G., Song, Y., Zhao, X., So, C., Liao, J., Wang, L. D., & Yang, C. S. (2001). DNA hypermethylation is a mechanism for loss of expression of the HLA class I genes in human esophageal squamous cell carcinomas. *Carcinogenesis*, *22*(10), 1615–1623. https://doi.org/10.1093/carcin/22.10.1615

Nishikawa, H., & Koyama, S. (2021). Mechanisms of regulatory T cell infiltration in tumors: Implications for innovative immune precision therapies. *Journal for Immunotherapy of Cancer*, *9*(7), e002591. https://doi.org/10.1136/jitc-2021-002591

Noman, M. Z., Janji, B., Abdou, A., Hasmim, M., Terry, S., Tan, T. Z., Mami-Chouaib, F., Thiery, J. P., & Chouaib, S. (2017). The immune checkpoint ligand PD-L1 is upregulated in EMT-activated human breast cancer cells by a mechanism involving ZEB-1 and miR-200. *Oncoimmunology*, *6*(1), e1263412. https://doi.org/10.1080/2162402X.2016.1263412

Ohsugi, T., Yamaguchi, K., Zhu, C., Ikenoue, T., Takane, K., Shinozaki, M., Tsurita, G., Yano, H., & Furukawa, Y. (2019). Anti-apoptotic effect by the suppression of IRF1 as a downstream of Wnt/β-catenin signaling in colorectal cancer cells. *Oncogene*, *38*(32), 6051–6064. https://doi.org/10.1038/s41388-019-0856-9

Oka, N., Markova, T., Tsuzuki, K., Li, W., El-Darawish, Y., Pencheva-Demireva, M., Yamanishi, K., Yamanishi, H., Sakagami, M., Tanaka, Y., & Okamura, H. (2020). IL-12 regulates the expansion, phenotype, and function of murine NK cells activated by IL-15 and IL-18. *Cancer Immunology, Immunotherapy: CII*, *69*(9), 1699–1712. https://doi.org/10.1007/s00262-020-02553-4

O'Shea, J. J., Gadina, M., & Siegel, R. M. (2019). 9—Cytokines and Cytokine Receptors. In R. R. Rich, T. A. Fleisher, W. T. Shearer, H. W. Schroeder, A. J. Frew, & C. M. Weyand (Eds.), *Clinical Immunology (Fifth Edition)* (pp. 127-155.e1). Elsevier. https://doi.org/10.1016/B978-0-7020-6896-6.00009-0

Ouzounova, M., Lee, E., Piranlioglu, R., El Andaloussi, A., Kolhe, R., Demirci, M. F., Marasco, D., Asm, I., Chadli, A., Hassan, K. A., Thangaraju, M., Zhou, G., Arbab, A. S., Cowell, J. K., & Korkaya, H. (2017). Monocytic and granulocytic myeloid derived suppressor cells differentially regulate spatiotemporal tumour plasticity during metastatic cascade. *Nature Communications*, *8*, 14979. https://doi.org/10.1038/ncomms14979

Ozga, A. J., Chow, M. T., & Luster, A. D. (2021). Chemokines and the immune response to cancer. *Immunity*, *54*(5), 859–874. https://doi.org/10.1016/j.immuni.2021.01.012

Pai, S. I., & Westra, W. H. (2009). Molecular pathology of head and neck cancer: Implications for diagnosis, prognosis, and treatment. *Annual Review of Pathology*, *4*, 49–70. https://doi.org/10.1146/annurev.pathol.4.110807.092158

Pal, A., Barrett, T. F., Paolini, R., Parikh, A., & Puram, S. V. (2021). Partial EMT in head and neck cancer biology: A spectrum instead of a switch. *Oncogene*, *40*(32), 5049–5065. https://doi.org/10.1038/s41388-021-01868-5

Pandey, P., Khan, F., Qari, H. A., Upadhyay, T. K., Alkhateeb, A. F., & Oves, M. (2022). Revolutionization in Cancer Therapeutics via Targeting Major Immune Checkpoints PD-1, PD-L1 and CTLA-4. *Pharmaceuticals (Basel, Switzerland)*, *15*(3), 335. https://doi.org/10.3390/ph15030335

Papageorgis, P. (2015). TGFβ Signaling in Tumor Initiation, Epithelial-to-Mesenchymal Transition, and Metastasis. *Journal of Oncology*, *2015*, 587193. https://doi.org/10.1155/2015/587193

Pardoll, D. M. (2012). The blockade of immune checkpoints in cancer immunotherapy. *Nature Reviews. Cancer*, *12*(4), 252–264. https://doi.org/10.1038/nrc3239

Pauken, K. E., Sammons, M. A., Odorizzi, P. M., Manne, S., Godec, J., Khan, O., Drake, A. M., Chen, Z., Sen, D. R., Kurachi, M., Barnitz, R. A., Bartman, C., Bengsch, B., Huang, A. C., Schenkel, J. M., Vahedi, G., Haining, W. N., Berger, S. L., & Wherry, E. J. (2016). Epigenetic stability of exhausted T cells limits durability of reinvigoration by PD-1 blockade. *Science (New York, N.Y.)*, *354*(6316), 1160–1165. https://doi.org/10.1126/science.aaf2807

Pelekanou, V., Notas, G., Athanasouli, P., Alexakis, K., Kiagiadaki, F., Peroulis, N., Kalyvianaki, K., Kampouri, E., Polioudaki, H., Theodoropoulos, P., Tsapis, A., Castanas, E., & Kampa, M. (2018). BCMA (TNFRSF17) Induces APRIL and BAFF Mediated Breast Cancer Cell Stemness. *Frontiers in Oncology*, *8*, 301. https://doi.org/10.3389/fonc.2018.00301

Pelosi, A., Besi, F., Tumino, N., Merli, P., Quatrini, L., Li Pira, G., Algeri, M., Moretta, L., & Vacca, P. (2021). NK Cells and PMN-MDSCs in the Graft From G-CSF Mobilized Haploidentical Donors Display Distinct Gene Expression Profiles From Those of the Non-Mobilized Counterpart. *Frontiers in Immunology*, *12*, 657329. https://doi.org/10.3389/fimmu.2021.657329

Pennock, N. D., White, J. T., Cross, E. W., Cheney, E. E., Tamburini, B. A., & Kedl, R. M. (2013). T cell responses: Naïve to memory and everything in between. *Advances in Physiology Education*, *37*(4), 273–283. https://doi.org/10.1152/advan.00066.2013

Pesce, S., Greppi, M., Tabellini, G., Rampinelli, F., Parolini, S., Olive, D., Moretta, L., Moretta, A., & Marcenaro, E. (2017). Identification of a subset of human natural killer cells expressing high levels of programmed death 1: A phenotypic and functional characterization. *The Journal of Allergy and Clinical Immunology*, *139*(1), 335-346.e3. https://doi.org/10.1016/j.jaci.2016.04.025

Pestka, S., Krause, C. D., & Walter, M. R. (2004). Interferons, interferon-like cytokines, and their receptors. *Immunological Reviews*, *202*(1), 8–32. https://doi.org/10.1111/j.0105-2896.2004.00204.x

Philip, M., Fairchild, L., Sun, L., Horste, E. L., Camara, S., Shakiba, M., Scott, A. C., Viale, A., Lauer, P., Merghoub, T., Hellmann, M. D., Wolchok, J. D., Leslie, C. S., & Schietinger, A. (2017). Chromatin states define tumour-specific T cell dysfunction and reprogramming. *Nature*, *545*(7655), 452–456. https://doi.org/10.1038/nature22367

Ping, Q., Yan, R., Cheng, X., Wang, W., Zhong, Y., Hou, Z., Shi, Y., Wang, C., & Li, R. (2021). Cancer-associated fibroblasts: Overview, progress, challenges, and directions. *Cancer Gene Therapy*, *28*(9), 984–999. https://doi.org/10.1038/s41417-021-00318-4

Pio, R., Ajona, D., Ortiz-Espinosa, S., Mantovani, A., & Lambris, J. D. (2019). Complementing the Cancer-Immunity Cycle. *Frontiers in Immunology*, *10*, 774. https://doi.org/10.3389/fimmu.2019.00774

Potenta, S., Zeisberg, E., & Kalluri, R. (2008). The role of endothelial-to-mesenchymal transition in cancer progression. *British Journal of Cancer*, *99*(9), 1375–1379. https://doi.org/10.1038/sj.bjc.6604662

Propper, D. J., & Balkwill, F. R. (2022). Harnessing cytokines and chemokines for cancer therapy. *Nature Reviews. Clinical Oncology*, *19*(4), 237–253. https://doi.org/10.1038/s41571-021-00588-9

Pulte, D., & Brenner, H. (2010). Changes in survival in head and neck cancers in the late 20th and early 21st century: A period analysis. *The Oncologist*, *15*(9), 994–1001. https://doi.org/10.1634/theoncologist.2009-0289

Qian, B.-Z., Li, J., Zhang, H., Kitamura, T., Zhang, J., Campion, L. R., Kaiser, E. A., Snyder, L. A., & Pollard, J. W. (2011). CCL2 recruits inflammatory monocytes to facilitate breast-tumour metastasis. *Nature*, *475*(7355), 222–225. https://doi.org/10.1038/nature10138

Qian, B.-Z., & Pollard, J. W. (2010). Macrophage diversity enhances tumor progression and metastasis. *Cell*, *141*(1), 39–51. https://doi.org/10.1016/j.cell.2010.03.014

Qian, F.-F., & Han, B.-H. (2020). Mechanisms of resistance to immune checkpoint inhibitors and strategies to reverse drug resistance in lung cancer. *Chinese Medical Journal*, *133*(20), 2444–2455. https://doi.org/10.1097/CM9.0000000000001124

Qingjun, L., Zhongjie, S., & Ligong, C. (2020). Memory T cells: Strategies for optimizing tumor immunotherapy. *Protein & Cell*, *11*(8). https://doi.org/10.1007/s13238-020-00707-9

Quail, D. F., & Joyce, J. A. (2013). Microenvironmental regulation of tumor progression and metastasis. *Nature Medicine*, *19*(11), 1423–1437. https://doi.org/10.1038/nm.3394

Que, H., Fu, Q., Lan, T., Tian, X., & Wei, X. (2022). Tumor-associated neutrophils and neutrophil-targeted cancer therapies. *Biochimica Et Biophysica Acta. Reviews on Cancer*, *1877*(5), 188762. https://doi.org/10.1016/j.bbcan.2022.188762

Raftopoulou, S., Valadez-Cosmes, P., Mihalic, Z. N., Schicho, R., & Kargl, J. (2022). Tumor-Mediated Neutrophil Polarization and Therapeutic Implications. *International Journal of Molecular Sciences*, *23*(6), 3218. https://doi.org/10.3390/ijms23063218

Raskov, H., Orhan, A., Christensen, J. P., & Gögenur, I. (2021). Cytotoxic CD8+ T cells in cancer and cancer immunotherapy. *British Journal of Cancer*, *124*(2), 359–367. https://doi.org/10.1038/s41416-020-01048-4

Ratushny, V., Gober, M. D., Hick, R., Ridky, T. W., & Seykora, J. T. (2012). From keratinocyte to cancer: The pathogenesis and modeling of cutaneous squamous cell carcinoma. *The Journal of Clinical Investigation*, *122*(2), 464–472. https://doi.org/10.1172/JCI57415

Rébé, C., & Ghiringhelli, F. (2020). Interleukin-1β and Cancer. *Cancers*, *12*(7), 1791. https://doi.org/10.3390/cancers12071791

Reeves, E., & James, E. (2017). Antigen processing and immune regulation in the response to tumours. *Immunology*, *150*(1), 16–24. https://doi.org/10.1111/imm.12675

Reyes, E., García-Castro, I., Esquivel, F., Hornedo, J., Cortes-Funes, H., Solovera, J., & Alvarez-Mon, M. (1999). Granulocyte colony-stimulating factor (G-CSF) transiently suppresses mitogen-stimulated T-cell proliferative response. *British Journal of Cancer*, *80*(1–2), 229–235. https://doi.org/10.1038/sj.bjc.6690344

Rischin, D., Migden, M. R., Lim, A. M., Schmults, C. D., Khushalani, N. I., Hughes, B. G. M., Schadendorf, D., Dunn, L. A., Hernandez-Aya, L., Chang, A. L. S., Modi, B., Hauschild, A., Ulrich, C., Eigentler, T., Stein, B., Pavlick, A. C., Geiger, J. L., Gutzmer, R., Alam, M., … Guminski, A. (2020). Phase 2 study of cemiplimab in patients with metastatic

cutaneous squamous cell carcinoma: Primary analysis of fixed-dosing, long-term outcome of weight-based dosing. *Journal for Immunotherapy of Cancer*, *8*(1), e000775. https://doi.org/10.1136/jitc-2020-000775

Rizvi, N. A., Hellmann, M. D., Snyder, A., Kvistborg, P., Makarov, V., Havel, J. J., Lee, W., Yuan, J., Wong, P., Ho, T. S., Miller, M. L., Rekhtman, N., Moreira, A. L., Ibrahim, F., Bruggeman, C., Gasmi, B., Zappasodi, R., Maeda, Y., Sander, C., … Chan, T. A. (2015). Mutational landscape determines sensitivity to PD-1 blockade in non–small cell lung cancer. *Science (New York, N.Y.)*, *348*(6230), 124–128. https://doi.org/10.1126/science.aaa1348

Roma-Rodrigues, C., Mendes, R., Baptista, P. V., & Fernandes, A. R. (2019). Targeting Tumor Microenvironment for Cancer Therapy. *International Journal of Molecular Sciences*, *20*(4), 840. https://doi.org/10.3390/ijms20040840

Rosenberg, J. E., Hoffman-Censits, J., Powles, T., van der Heijden, M. S., Balar, A. V., Necchi, A., Dawson, N., O'Donnell, P. H., Balmanoukian, A., Loriot, Y., Srinivas, S., Retz, M. M., Grivas, P., Joseph, R. W., Galsky, M. D., Fleming, M. T., Petrylak, D. P., Perez-Gracia, J. L., Burris, H. A., … Dreicer, R. (2016). Atezolizumab in patients with locally advanced and metastatic urothelial carcinoma who have progressed following treatment with platinum-based chemotherapy: A single-arm, multicentre, phase 2 trial. *Lancet (London, England)*, *387*(10031), 1909–1920. https://doi.org/10.1016/S0140-6736(16)00561-4

Rowshanravan, B., Halliday, N., & Sansom, D. M. (2018). CTLA-4: A moving target in immunotherapy. *Blood*, *131*(1), 58–67. https://doi.org/10.1182/blood-2017-06-741033

Rudensky, A. Y. (2011). Regulatory T Cells and Foxp3. *Immunological Reviews*, *241*(1), 260–268. https://doi.org/10.1111/j.1600-065X.2011.01018.x

Ruffell, B., Chang-Strachan, D., Chan, V., Rosenbusch, A., Ho, C. M. T., Pryer, N., Daniel, D., Hwang, E. S., Rugo, H. S., & Coussens, L. M. (2014). Macrophage IL-10 blocks CD8+ T cell-dependent responses to chemotherapy by suppressing IL-12 expression in intratumoral dendritic cells. *Cancer Cell*, *26*(5), 623–637. https://doi.org/10.1016/j.ccell.2014.09.006

Russo, M., & Nastasi, C. (2022). Targeting the Tumor Microenvironment: A Close Up of Tumor-Associated Macrophages and Neutrophils. *Frontiers in Oncology*, *12*(871513). https://doi.org/10.3389/fonc.2022.871513

Sahai, E., Astsaturov, I., Cukierman, E., DeNardo, D. G., Egeblad, M., Evans, R. M., Fearon, D., Greten, F. R., Hingorani, S. R., Hunter, T., Hynes, R. O., Jain, R. K., Janowitz, T., Jorgensen, C., Kimmelman, A. C., Kolonin, M. G., Maki, R. G., Powers, R. S., Puré, E., … Werb, Z. (2020). A framework for advancing our understanding of cancer-associated fibroblasts. *Nature Reviews. Cancer*, *20*(3), 174–186. https://doi.org/10.1038/s41568-019-0238-1

Sakai, T., Mashima, H., Yamada, Y., Goto, T., Sato, W., Dohmen, T., Kamada, K., Yoshioka, M., Uchinami, H., Yamamoto, Y., & Ohnishi, H. (2014). The roles of interferon regulatory factors 1 and 2 in the progression of human pancreatic cancer. *Pancreas*, *43*(6), 909–916. https://doi.org/10.1097/MPA.0000000000000116

Sakuishi, K., Apetoh, L., Sullivan, J. M., Blazar, B. R., Kuchroo, V. K., & Anderson, A. C. (2010). Targeting Tim-3 and PD-1 pathways to reverse T cell exhaustion and restore anti-tumor immunity. *The Journal of Experimental Medicine*, *207*(10), 2187–2194. https://doi.org/10.1084/jem.20100643

Saleh, R., & Elkord, E. (2019). Treg-mediated acquired resistance to immune checkpoint inhibitors. *Cancer Letters*, *457*(10), 168–179. https://doi.org/10.1016/j.canlet.2019.05.003

Saleh, R., Taha, R. Z., Toor, S. M., Sasidharan Nair, V., Murshed, K., Khawar, M., Al-Dhaheri, M., Petkar, M. A., Abu Nada, M., & Elkord, E. (2020). Expression of immune checkpoints and T cell exhaustion markers in early and advanced stages of colorectal cancer. *Cancer Immunology, Immunotherapy: CII*, *69*(10), 1989–1999. https://doi.org/10.1007/s00262-020-02593-w

Salmon, H., Remark, R., Gnjatic, S., & Merad, M. (2019). Host tissue determinants of tumour immunity. *Nature Reviews. Cancer*, *19*(4), 215–227. https://doi.org/10.1038/s41568-019-0125-9

Salzmann, M., Leiter, U., Loquai, C., Zimmer, L., Ugurel, S., Gutzmer, R., Thoms, K.-M., Enk, A. H., & Hassel, J. C. (2020). Programmed cell death protein 1 inhibitors in advanced cutaneous squamous cell carcinoma: Real-world data of a retrospective, multicenter study. *European Journal of Cancer (Oxford, England: 1990)*, *138*, 125–132. https://doi.org/10.1016/j.ejca.2020.07.029

Sanchez-Correa, B., Valhondo, I., Hassouneh, F., Lopez-Sejas, N., Pera, A., Bergua, J. M., Arcos, M. J., Bañas, H., Casas-Avilés, I., Durán, E., Alonso, C., Solana, R., & Tarazona, R. (2019). DNAM-1 and the TIGIT/PVRIG/TACTILE Axis: Novel Immune Checkpoints for Natural Killer Cell-Based Cancer Immunotherapy. *Cancers*, *11*(6), 877. https://doi.org/10.3390/cancers11060877

Santagata, S., Napolitano, M., D'Alterio, C., Desicato, S., Maro, S. D., Marinelli, L., Fragale, A., Buoncervello, M., Persico, F., Gabriele, L., Novellino, E., Longo, N., Pignata, S., Perdonà, S., & Scala, S. (2017). Targeting CXCR4 reverts the suppressive activity of T-regulatory cells in renal cancer. *Oncotarget*, *8*(44), 77110–77120. https://doi.org/10.18632/oncotarget.20363

Saxton, R. A., Glassman, C. R., & Garcia, K. C. (2023). Emerging principles of cytokine pharmacology and therapeutics. *Nature Reviews. Drug Discovery*, *22*(1), 21–37. https://doi.org/10.1038/s41573-022-00557-6

Schlecker, E., Stojanovic, A., Eisen, C., Quack, C., Falk, C. S., Umansky, V., & Cerwenka, A. (2012). Tumor-infiltrating monocytic myeloid-derived suppressor cells mediate CCR5-dependent recruitment of regulatory T cells favoring tumor growth. *Journal of Immunology (Baltimore, Md.: 1950)*, *189*(12), 5602–5611. https://doi.org/10.4049/jimmunol.1201018

Schmults, C. D., Karia, P. S., Carter, J. B., Han, J., & Qureshi, A. A. (2013). Factors predictive of recurrence and death from cutaneous squamous cell carcinoma: A 10-year, single-institution cohort study. *JAMA Dermatology*, *149*(5), 541–547. https://doi.org/10.1001/jamadermatol.2013.2139

Schoenfeld, A. J., & Hellmann, M. D. (2020). Acquired Resistance to Immune Checkpoint Inhibitors. *Cancer Cell*, *37*(4), 443–455. https://doi.org/10.1016/j.ccell.2020.03.017

Scimone, M. L., Felbinger, T. W., Mazo, I. B., Stein, J. V., von Andrian, U. H., & Weninger, W. (2004). CXCL12 Mediates CCR7-independent Homing of Central Memory Cells, But Not Naive T Cells, in Peripheral Lymph Nodes. *The Journal of Experimental Medicine*, *199*(8), 1113–1120. https://doi.org/10.1084/jem.20031645

Seliger, B., Höhne, A., Knuth, A., Bernhard, H., Ehring, B., Tampé, R., & Huber, C. (1996). Reduced membrane major histocompatibility complex class I density and stability in a subset of human renal cell carcinomas with low TAP and LMP expression. *Clinical*

Cancer Research: An Official Journal of the American Association for Cancer Research, *2*(8), 1427–1433.

Seol, M. A., Kim, J.-H., Oh, K., Kim, G., Seo, M. W., Shin, Y.-K., Sim, J. H., Shin, H. M., Seo, B. Y., Lee, D.-S., Ku, J.-L., Han, I., Kang, I., Park, S. I., & Kim, H.-R. (2019). Interleukin-7 Contributes to the Invasiveness of Prostate Cancer Cells by Promoting Epithelial-Mesenchymal Transition. *Scientific Reports*, *9*(1), 6917. https://doi.org/10.1038/s41598-019-43294-4

Sharma, P., Hu-Lieskovan, S., Wargo, J. A., & Ribas, A. (2017). Primary, Adaptive, and Acquired Resistance to Cancer Immunotherapy. *Cell*, *168*(4), 707–723. https://doi.org/10.1016/j.cell.2017.01.017

Sharonov, G. V., Serebrovskaya, E. O., Yuzhakova, D. V., Britanova, O. V., & Chudakov, D. M. (2020). B cells, plasma cells and antibody repertoires in the tumour microenvironment. *Nature Reviews. Immunology*, *20*(5), 294–307. https://doi.org/10.1038/s41577-019-0257-x

Shi, Y. (2018). Regulatory mechanisms of PD-L1 expression in cancer cells. *Cancer Immunology, Immunotherapy: CII*, *67*(10), 1481–1489. https://doi.org/10.1007/s00262-018-2226-9

Shibata, H., Saito, S., & Uppaluri, R. (2021). Immunotherapy for Head and Neck Cancer: A Paradigm Shift From Induction Chemotherapy to Neoadjuvant Immunotherapy. *Frontiers in Oncology*, *11*, 727433. https://doi.org/10.3389/fonc.2021.727433

Shimasaki, N., Jain, A., & Campana, D. (2020). NK cells for cancer immunotherapy. *Nature Reviews. Drug Discovery*, *19*(3), 200–218. https://doi.org/10.1038/s41573-019-0052-1

Šímová, J., Polláková, V., Indrová, M., Mikyšková, R., Bieblová, J., Štěpánek, I., Bubeník, J., & Reiniš, M. (2011). Immunotherapy augments the effect of 5-azacytidine on HPV16-associated tumours with different MHC class I-expression status. *British Journal of Cancer*, *105*(10), 1533–1541. https://doi.org/10.1038/bjc.2011.428

Singh, S., Ramani, P., Jayakumar, N. D., Pannu, S. J., Sharma, R. K., & Gill, S. S. (2022). Role of Pro-inflammatory and Anti-inflammatory Cytokines in Pathophysiology of Psoriasis. *Current Oral Health Reports*, *9*(4), 132–145. https://doi.org/10.1007/s40496-022-00320-1

Siu, L. L., Even, C., Mesía, R., Remenar, E., Daste, A., Delord, J.-P., Krauss, J., Saba, N. F., Nabell, L., Ready, N. E., Braña, I., Kotecki, N., Zandberg, D. P., Gilbert, J., Mehanna, H., Bonomi, M., Jarkowski, A., Melillo, G., Armstrong, J. M., … Fayette, J. (2019). Safety and Efficacy of Durvalumab With or Without Tremelimumab in Patients With PD-L1-Low/Negative Recurrent or Metastatic HNSCC: The Phase 2 CONDOR Randomized Clinical Trial. *JAMA Oncology*, *5*(2), 195–203. https://doi.org/10.1001/jamaoncol.2018.4628

Sobierajska, K., Ciszewski, W. M., Sacewicz-Hofman, I., & Niewiarowska, J. (2020). Endothelial Cells in the Tumor Microenvironment. *Advances in Experimental Medicine and Biology*, *1234*, 71–86. https://doi.org/10.1007/978-3-030-37184-5_6

Solanas, G., & Benitah, S. A. (2013). Regenerating the skin: A task for the heterogeneous stem cell pool and surrounding niche. *Nature Reviews. Molecular Cell Biology*, *14*(11), 737–748. https://doi.org/10.1038/nrm3675

Steimle, V., Siegrist, C. A., Mottet, A., Lisowska-Grospierre, B., & Mach, B. (1994). Regulation of MHC class II expression by interferon-gamma mediated by the transactivator gene CIITA. *Science (New York, N.Y.)*, *265*(5168), 106–109. https://doi.org/10.1126/science.8016643

Stratigos, A., Garbe, C., Lebbe, C., Malvehy, J., del Marmol, V., Pehamberger, H., Peris, K., Becker, J. C., Zalaudek, I., Saiag, P., Middleton, M. R., Bastholt, L., Testori, A., Grob,

J.-J., European Dermatology Forum (EDF), European Association of Dermato-Oncology (EADO), & European Organization for Research and Treatment of Cancer (EORTC). (2015). Diagnosis and treatment of invasive squamous cell carcinoma of the skin: European consensus-based interdisciplinary guideline. *European Journal of Cancer (Oxford, England: 1990)*, *51*(14), 1989–2007. https://doi.org/10.1016/j.ejca.2015.06.110

Su, K., Guo, L., He, K., Rao, M., Zhang, J., Yang, X., Huang, W., Gu, T., Xu, K., Liu, Y., Wang, J., Chen, J., Wu, Z., Hu, L., Zeng, H., Li, H., Tong, J., Li, X., Yang, Y., … Han, Y. (2022). PD-L1 expression on circulating tumor cells can be a predictive biomarker to PD-1 inhibitors combined with radiotherapy and antiangiogenic therapy in advanced hepatocellular carcinoma. *Frontiers in Oncology*, *12*, 873830. https://doi.org/10.3389/fonc.2022.873830

Sun, C., Mezzadra, R., & Schumacher, T. N. (2018). Regulation and Function of the PD-L1 Checkpoint. *Immunity*, *48*(3), 434–452. https://doi.org/10.1016/j.immuni.2018.03.014

Sun, H.-W., Wu, W.-C., Chen, H.-T., Xu, Y.-T., Yang, Y.-Y., Chen, J., Yu, X.-J., Wang, Z., Shuang, Z.-Y., & Zheng, L. (2020). Glutamine Deprivation Promotes the Generation and Mobilization of MDSCs by Enhancing Expression of G-CSF and GM-CSF. *Frontiers in Immunology*, *11*, 616367. https://doi.org/10.3389/fimmu.2020.616367

Sun, R., Kong, X., Qiu, X., Huang, C., & Wong, P.-P. (2021). The Emerging Roles of Pericytes in Modulating Tumor Microenvironment. *Frontiers in Cell and Developmental Biology*, *9*, 676342. https://doi.org/10.3389/fcell.2021.676342

Tanaka, K. (2009). The proteasome: Overview of structure and functions. *Proceedings of the Japan Academy. Series B, Physical and Biological Sciences*, *85*(1), 12–36. https://doi.org/10.2183/pjab.85.12

Tay, J., Levesque, J.-P., & Winkler, I. G. (2017). Cellular players of hematopoietic stem cell mobilization in the bone marrow niche. *International Journal of Hematology*, *105*(2), 129–140. https://doi.org/10.1007/s12185-016-2162-4

Taylor, B., & Balko, J. (2022). Mechanisms of MHC-I Downregulation and Role in Immunotherapy Response. *Frontiers in Immunology*, *13*. https://doi.org/10.3389/fimmu.2022.844866

Techasen, A., Loilome, W., Namwat, N., Dokduang, H., Jongthawin, J., & Yongvanit, P. (2012). Cytokines released from activated human macrophages induce epithelial mesenchymal transition markers of cholangiocarcinoma cells. *Asian Pacific Journal of Cancer Prevention: APJCP*, *13 Suppl*, 115–118.

Thiery, J. P., Acloque, H., Huang, R. Y. J., & Nieto, M. A. (2009). Epithelial-mesenchymal transitions in development and disease. *Cell*, *139*(5), 871–890. https://doi.org/10.1016/j.cell.2009.11.007

Thommen, D. S., Schreiner, J., Müller, P., Herzig, P., Roller, A., Belousov, A., Umana, P., Pisa, P., Klein, C., Bacac, M., Fischer, O. S., Moersig, W., Savic Prince, S., Levitsky, V., Karanikas, V., Lardinois, D., & Zippelius, A. (2015). Progression of Lung Cancer Is Associated with Increased Dysfunction of T Cells Defined by Coexpression of Multiple Inhibitory Receptors. *Cancer Immunology Research*, *3*(12), 1344–1355. https://doi.org/10.1158/2326-6066.CIR-15-0097

Togashi, Y., Shitara, K., & Nishikawa, H. (2019). Regulatory T cells in cancer immunosuppression—Implications for anticancer therapy. *Nature Reviews. Clinical Oncology*, *16*(6), 356–371. https://doi.org/10.1038/s41571-019-0175-7

Toth, D. F., Raderer, M., Wadsak, W., & Karanikas, G. (2013). Beta-2 microglobulin as a diagnostic parameter in non-Hodgkin lymphoma: A comparative study with FDG-PET. *Anticancer Research*, *33*(8), 3341–3345.

Tough, D. F., Rioja, I., Modis, L. K., & Prinjha, R. K. (2020). Epigenetic Regulation of T Cell Memory: Recalling Therapeutic Implications. *Trends in Immunology*, *41*(1), 29–45. https://doi.org/10.1016/j.it.2019.11.008

Tsai, J. H., Donaher, J. L., Murphy, D. A., Chau, S., & Yang, J. (2012). Spatiotemporal regulation of epithelial-mesenchymal transition is essential for squamous cell carcinoma metastasis. *Cancer Cell*, *22*(6), 725–736. https://doi.org/10.1016/j.ccr.2012.09.022

Van Allen, E. M., Miao, D., Schilling, B., Shukla, S. A., Blank, C., Zimmer, L., Sucker, A., Hillen, U., Foppen, M. H. G., Goldinger, S. M., Utikal, J., Hassel, J. C., Weide, B., Kaehler, K. C., Loquai, C., Mohr, P., Gutzmer, R., Dummer, R., Gabriel, S., … Garraway, L. A. (2015). Genomic correlates of response to CTLA-4 blockade in metastatic melanoma. *Science (New York, N.Y.)*, *350*(6257), 207–211. https://doi.org/10.1126/science.aad0095

van Meeteren, L. A., & ten Dijke, P. (2012). Regulation of endothelial cell plasticity by TGF-β. *Cell and Tissue Research*, *347*(1), 177–186. https://doi.org/10.1007/s00441-011-1222-6

Vandercappellen, J., Van Damme, J., & Struyf, S. (2008). The role of CXC chemokines and their receptors in cancer. *Cancer Letters*, *267*(2), 226–244. https://doi.org/10.1016/j.canlet.2008.04.050

Varikuti, S., Oghumu, S., Elbaz, M., Volpedo, G., Ahirwar, D. K., Alarcon, P. C., Sperling, R. H., Moretti, E., Pioso, M. S., Kimble, J., Nasser, M. W., Ganju, R. K., Terrazas, C., & Satoskar, A. R. (2017). STAT1 gene deficient mice develop accelerated breast cancer growth and metastasis which is reduced by IL-17 blockade. *Oncoimmunology*, *6*(11), e1361088. https://doi.org/10.1080/2162402X.2017.1361088

Veglia, F., Sanseviero, E., & Gabrilovich, D. I. (2021). Myeloid-derived suppressor cells in the era of increasing myeloid cell diversity. *Nature Reviews. Immunology*, *21*(8), 485–498. https://doi.org/10.1038/s41577-020-00490-y

Vitale, M., Rezzani, R., Rodella, L., Zauli, G., Grigolato, P., Cadei, M., Hicklin, D. J., & Ferrone, S. (1998). HLA class I antigen and transporter associated with antigen processing (TAP1 and TAP2) down-regulation in high-grade primary breast carcinoma lesions. *Cancer Research*, *58*(4), 737–742.

Vlková, V., Štěpánek, I., Hrušková, V., Šenigl, F., Mayerová, V., Šrámek, M., Šímová, J., Bieblová, J., Indrová, M., Hejhal, T., Dérian, N., Klatzmann, D., Six, A., & Reiniš, M. (2014). Epigenetic regulations in the IFNγ signalling pathway: IFNγ-mediated MHC class I upregulation on tumour cells is associated with DNA demethylation of antigen-presenting machinery genes. *Oncotarget*, *5*(16), 6923–6935.

von Boehmer, H., & Daniel, C. (2013). Therapeutic opportunities for manipulating T(Reg) cells in autoimmunity and cancer. *Nature Reviews. Drug Discovery*, *12*(1), 51–63. https://doi.org/10.1038/nrd3683

Walter, U., & Santamaria, P. (2005). CD8+ T cells in autoimmunity. *Current Opinion in Immunology*, *17*(6), 624–631. https://doi.org/10.1016/j.coi.2005.09.014

Wang, M., Zhao, J., Zhang, L., Wei, F., Lian, Y., Wu, Y., Gong, Z., Zhang, S., Zhou, J., Cao, K., Li, X., Xiong, W., Li, G., Zeng, Z., & Guo, C. (2017). Role of tumor microenvironment in tumorigenesis. *Journal of Cancer*, *8*(5), 761–773. https://doi.org/10.7150/jca.17648

Wang, M., Zhou, Z., Wang, X., Zhang, C., & Jiang, X. (2022). Natural killer cell awakening: Unleash cancer-immunity cycle against glioblastoma. *Cell Death & Disease*, *13*(7), 588. https://doi.org/10.1038/s41419-022-05041-y

Wang, N., Liang, H., & Zen, K. (2014). Molecular Mechanisms That Influence the Macrophage M1–M2 Polarization Balance. *Frontiers in Immunology*, *5*, 614. https://doi.org/10.3389/fimmu.2014.00614

Wang, Q., Shao, X., Zhang, Y., Zhu, M., Wang, F. X. C., Mu, J., Li, J., Yao, H., & Chen, K. (2023). Role of tumor microenvironment in cancer progression and therapeutic strategy. *Cancer Medicine*. https://doi.org/10.1002/cam4.5698

Wang, Y., Wang, X., Cui, X., Zhuo, Y., Li, H., Ha, C., Xin, L., Ren, Y., Zhang, W., Sun, X., Ge, L., Liu, X., He, J., Zhang, T., Zhang, K., Yao, Z., Yang, X., & Yang, J. (2020). Oncoprotein SND1 hijacks nascent MHC-I heavy chain to ER-associated degradation, leading to impaired CD8+ T cell response in tumor. *Science Advances*, *6*(22), eaba5412. https://doi.org/10.1126/sciadv.aba5412

Warren, M. K., & Vogel, S. N. (1985). Bone marrow-derived macrophages: Development and regulation of differentiation markers by colony-stimulating factor and interferons. *Journal of Immunology (Baltimore, Md.: 1950)*, *134*(2), 982–989.

Wculek, S. K., Cueto, F. J., Mujal, A. M., Melero, I., Krummel, M. F., & Sancho, D. (2020). Dendritic cells in cancer immunology and immunotherapy. *Nature Reviews. Immunology*, *20*(1), 7–24. https://doi.org/10.1038/s41577-019-0210-z

Wei, C., Yang, C., Wang, S., Shi, D., Zhang, C., Lin, X., Liu, Q., Dou, R., & Xiong, B. (2019). Crosstalk between cancer cells and tumor associated macrophages is required for mesenchymal circulating tumor cell-mediated colorectal cancer metastasis. *Molecular Cancer*, *18*(1), 64. https://doi.org/10.1186/s12943-019-0976-4

Wermuth, P. J., Carney, K. R., Mendoza, F. A., Piera-Velazquez, S., & Jimenez, S. A. (2017). Endothelial cell-specific activation of transforming growth factor-β signaling in mice induces cutaneous, visceral, and microvascular fibrosis. *Laboratory Investigation; a Journal of Technical Methods and Pathology*, *97*(7), 806–818. https://doi.org/10.1038/labinvest.2017.23

Wherry, E. J., & Kurachi, M. (2015). Molecular and cellular insights into T cell exhaustion. *Nature Reviews. Immunology*, *15*(8), 486–499. https://doi.org/10.1038/nri3862

Windon, M. J., D'Souza, G., Rettig, E. M., Westra, W. H., van Zante, A., Wang, S. J., Ryan, W. R., Mydlarz, W. K., Ha, P. K., Miles, B. A., Koch, W., Gourin, C., Eisele, D. W., & Fakhry, C. (2018). Increasing prevalence of human papillomavirus-positive oropharyngeal cancers among older adults. *Cancer*, *124*(14), 2993–2999. https://doi.org/10.1002/cncr.31385

Wing, K., Onishi, Y., Prieto-Martin, P., Yamaguchi, T., Miyara, M., Fehervari, Z., Nomura, T., & Sakaguchi, S. (2008). CTLA-4 control over Foxp3+ regulatory T cell function. *Science (New York, N.Y.)*, *322*(5899), 271–275. https://doi.org/10.1126/science.1160062

Wojdasiewicz, P., Poniatowski, Ł. A., & Szukiewicz, D. (2014). The Role of Inflammatory and Anti-Inflammatory Cytokines in the Pathogenesis of Osteoarthritis. *Mediators of Inflammation*, *2014*, e561459. https://doi.org/10.1155/2014/561459

Wong, S. S., Tan, K. C., & Goh, C. L. (1998). Cutaneous manifestations of chronic arsenicism: Review of seventeen cases. *Journal of the American Academy of Dermatology*, *38*(2 Pt 1), 179–185. https://doi.org/10.1016/s0190-9622(98)70596-1

Woo, S.-R., Turnis, M. E., Goldberg, M. V., Bankoti, J., Selby, M., Nirschl, C. J., Bettini, M. L., Gravano, D. M., Vogel, P., Liu, C. L., Tangsombatvisit, S., Grosso, J. F., Netto, G., Smeltzer, M. P., Chaux, A., Utz, P. J., Workman, C. J., Pardoll, D. M., Korman, A. J., … Vignali, D. A. A. (2012). Immune inhibitory molecules LAG-3 and PD-1 synergistically regulate T-cell function to promote tumoral immune escape. *Cancer Research*, *72*(4), 917–927. https://doi.org/10.1158/0008-5472.CAN-11-1620

Wu, S., Slater, N. A., Sayed, C. J., & Googe, P. B. (2020). PD-L1 and LAG-3 expression in advanced cutaneous squamous cell carcinomas. *Journal of Cutaneous Pathology*, *47*(10), 882–887. https://doi.org/10.1111/cup.13709

Wu, W.-C., Sun, H.-W., Chen, H.-T., Liang, J., Yu, X.-J., Wu, C., Wang, Z., & Zheng, L. (2014). Circulating hematopoietic stem and progenitor cells are myeloid-biased in cancer patients. *Proceedings of the National Academy of Sciences of the United States of America*, *111*(11), 4221–4226. https://doi.org/10.1073/pnas.1320753111

Xiang, X., Niu, Y.-R., Wang, Z.-H., Ye, L.-L., Peng, W.-B., & Zhou, Q. (2022). Cancer-associated fibroblasts: Vital suppressors of the immune response in the tumor microenvironment. *Cytokine & Growth Factor Reviews*, *67*, 35–48. https://doi.org/10.1016/j.cytogfr.2022.07.006

Xiao, Y., & Yu, D. (2021). Tumor microenvironment as a therapeutic target in cancer. *Pharmacology & Therapeutics*, *221*, 107753. https://doi.org/10.1016/j.pharmthera.2020.107753

Xing, F., Saidou, J., & Watabe, K. (2010). Cancer associated fibroblasts (CAFs) in tumor microenvironment. *Frontiers in Bioscience : A Journal and Virtual Library*, *15*, 166–179.

Xu, S., Xu, H., Wang, W., Li, S., Li, H., Li, T., Zhang, W., Yu, X., & Liu, L. (2019). The role of collagen in cancer: From bench to bedside. *Journal of Translational Medicine*, *17*(1), 309. https://doi.org/10.1186/s12967-019-2058-1

Xu, Y., Zhao, W., Wu, D., Xu, J., Lin, S., Tang, K., Yin, Z., & Wang, X. (2014). Isolation of myeloid-derived suppressor cells subsets from spleens of orthotopic liver cancer-bearing mice by fluorescent-activated and magnetic-activated cell sorting: Similarities and differences. *International Journal of Clinical and Experimental Pathology*, *7*(11), 7545–7553.

Yamamoto, K., Venida, A., Yano, J., Biancur, D. E., Kakiuchi, M., Gupta, S., Sohn, A. S. W., Mukhopadhyay, S., Lin, E. Y., Parker, S. J., Banh, R. S., Paulo, J. A., Wen, K. W., Debnath, J., Kim, G. E., Mancias, J. D., Fearon, D. T., Perera, R. M., & Kimmelman, A. C. (2020). Autophagy promotes immune evasion of pancreatic cancer by degrading MHC-I. *Nature*, *581*(7806), 100–105. https://doi.org/10.1038/s41586-020-2229-5

Yamashita, N., Tokunaga, E., Iimori, M., Inoue, Y., Tanaka, K., Kitao, H., Saeki, H., Oki, E., & Maehara, Y. (2018). Epithelial Paradox: Clinical Significance of Coexpression of E-cadherin and Vimentin With Regard to Invasion and Metastasis of Breast Cancer. *Clinical Breast Cancer*, *18*(5), e1003–e1009. https://doi.org/10.1016/j.clbc.2018.02.002

Yang, F., Wang, J. F., Wang, Y., Liu, B., & Molina, J. R. (2021). Comparative Analysis of Predictive Biomarkers for PD-1/PD-L1 Inhibitors in Cancers: Developments and Challenges. *Cancers*, *14*(1), 109. https://doi.org/10.3390/cancers14010109

Yang, H., Zhang, Q., Xu, M., Wang, L., Chen, X., Feng, Y., Li, Y., Zhang, X., Cui, W., & Jia, X. (2020). CCL2-CCR2 axis recruits tumor associated macrophages to induce immune evasion through PD-1 signaling in esophageal carcinogenesis. *Molecular Cancer*, *19*(1), 41. https://doi.org/10.1186/s12943-020-01165-x

Yang, J., Zeng, Z., Peng, Y., Chen, J., Pan, L., & Pan, D. (2014). IL-7 splicing variant IL-7δ5 induces EMT and metastasis of human breast cancer cell lines MCF-7 and BT-20 through activation of PI3K/Akt pathway. *Histochemistry and Cell Biology*, *142*(4), 401–410. https://doi.org/10.1007/s00418-014-1222-1

Yang, Y., Andersson, P., Hosaka, K., Zhang, Y., Cao, R., Iwamoto, H., Yang, X., Nakamura, M., Wang, J., Zhuang, R., Morikawa, H., Xue, Y., Braun, H., Beyaert, R., Samani, N., Nakae, S., Hams, E., Dissing, S., Fallon, P. G., … Cao, Y. (2016). The PDGF-BB-SOX7 axis-modulated IL-33 in pericytes and stromal cells promotes metastasis through tumour-associated macrophages. *Nature Communications*, *7*, 11385. https://doi.org/10.1038/ncomms11385

Yanofsky, V. R., Mercer, S. E., & Phelps, R. G. (2011). Histopathological Variants of Cutaneous Squamous Cell Carcinoma: A Review. *Journal of Skin Cancer*, *2011*, 210813. https://doi.org/10.1155/2011/210813

Yarchoan, M., Hopkins, A., & Jaffee, E. M. (2017). Tumor Mutational Burden and Response Rate to PD-1 Inhibition. *The New England Journal of Medicine*, *377*(25), 2500–2501. https://doi.org/10.1056/NEJMc1713444

Ye, Q., Shen, Y., Wang, X., Yang, J., Miao, F., Shen, C., & Zhang, J. (2010). Hypermethylation of HLA class I gene is associated with HLA class I down-regulation in human gastric cancer. *Tissue Antigens*, *75*(1), 30–39. https://doi.org/10.1111/j.1399-0039.2009.01390.x

Ying, W., Cheruku, P. S., Bazer, F. W., Safe, S. H., & Zhou, B. (2013). Investigation of macrophage polarization using bone marrow derived macrophages. *Journal of Visualized Experiments: JoVE*, *76*, 50323. https://doi.org/10.3791/50323

Yoon, H., Tang, C.-M., Banerjee, S., Delgado, A. L., Yebra, M., Davis, J., & Sicklick, J. K. (2021). TGF-β1-mediated transition of resident fibroblasts to cancer-associated fibroblasts promotes cancer metastasis in gastrointestinal stromal tumor. *Oncogenesis*, *10*(2), 13. https://doi.org/10.1038/s41389-021-00302-5

Yoshihama, S., Roszik, J., Downs, I., Meissner, T. B., Vijayan, S., Chapuy, B., Sidiq, T., Shipp, M. A., Lizee, G. A., & Kobayashi, K. S. (2016). NLRC5/MHC class I transactivator is a target for immune evasion in cancer. *Proceedings of the National Academy of Sciences of the United States of America*, *113*(21), 5999–6004. https://doi.org/10.1073/pnas.1602069113

Youn, J.-I., Nagaraj, S., Collazo, M., & Gabrilovich, D. I. (2008). Subsets of myeloid-derived suppressor cells in tumor-bearing mice. *Journal of Immunology (Baltimore, Md.: 1950)*, *181*(8), 5791–5802. https://doi.org/10.4049/jimmunol.181.8.5791

Yunna, C., Mengru, H., Lei, W., & Weidong, C. (2020). Macrophage M1/M2 polarization. *European Journal of Pharmacology*, *877*, 173090. https://doi.org/10.1016/j.ejphar.2020.173090

Zandberg, D. P., Tallon, L. J., Nagaraj, S., Sadzewicz, L. K., Zhang, Y., Strome, M. B., Zhao, X. E., Vavikolanu, K., Zhang, X., Papadimitriou, J. C., Hubbard, F. A., Bentzen, S. M., Strome, S. E., & Fraser, C. M. (2019). Intratumor genetic heterogeneity in squamous cell carcinoma of the oral cavity. *Head & Neck*, *41*(8), 2514–2524. https://doi.org/10.1002/hed.25719

Zeisberg, E. M., Potenta, S., Xie, L., Zeisberg, M., & Kalluri, R. (2007). Discovery of endothelial to mesenchymal transition as a source for carcinoma-associated fibroblasts. *Cancer Research*, *67*(21), 10123–10128. https://doi.org/10.1158/0008-5472.CAN-07-3127

Zeng, Y., Li, B., Liang, Y., Reeves, P. M., Qu, X., Ran, C., Liu, Q., Callahan, M. V., Sluder, A. E., Gelfand, J. A., Chen, H., & Poznansky, M. C. (2019). Dual blockade of CXCL12-CXCR4 and PD-1-PD-L1 pathways prolongs survival of ovarian tumor-bearing mice by prevention of immunosuppression in the tumor microenvironment. *FASEB Journal: Official Publication of the Federation of American Societies for Experimental Biology*, *33*(5), 6596–6608. https://doi.org/10.1096/fj.201802067RR

Zhang, L., Wang, D., Li, Y., Liu, Y., Xie, X., Wu, Y., Zhou, Y., Ren, J., Zhang, J., Zhu, H., & Su, Z. (2016). CCL21/CCR7 Axis Contributed to CD133+ Pancreatic Cancer Stem-Like Cell Metastasis via EMT and Erk/NF-κB Pathway. *PloS One*, *11*(8), e0158529. https://doi.org/10.1371/journal.pone.0158529

Zhang, Y., Guan, X.-Y., & Jiang, P. (2020). Cytokine and Chemokine Signals of T-Cell Exclusion in Tumors. *Frontiers in Immunology*, *11*, 594609. https://doi.org/10.3389/fimmu.2020.594609

Zhang, Y., Li, L., Zheng, W., Zhang, L., & Yao, N. (2022). CD8+ T-cell exhaustion in the tumor microenvironment of head and neck squamous cell carcinoma determines poor prognosis. *Annals of Translational Medicine*, *10*(6), 273. https://doi.org/10.21037/atm-22-867

Zhang, Y., Zhang, Z., Chen, L., & Zhang, X. (2022). Tumor cells-derived conditioned medium induced pro-tumoral phenotypes in macrophages through calcium-nuclear factor κB interaction. *BMC Cancer*, *22*(1), 1327. https://doi.org/10.1186/s12885-022-10431-8

Zheng, L. (2017). PD-L1 Expression in Pancreatic Cancer. *JNCI Journal of the National Cancer Institute*, *109*(6), djw304. https://doi.org/10.1093/jnci/djw304

Zheng, L., Qin, S., Si, W., Wang, A., Xing, B., Gao, R., Ren, X., Wang, L., Wu, X., Zhang, J., Wu, N., Zhang, N., Zheng, H., Ouyang, H., Chen, K., Bu, Z., Hu, X., Ji, J., & Zhang, Z. (2021). Pan-cancer single-cell landscape of tumor-infiltrating T cells. *Science (New York, N.Y.)*, *374*(6574), abe6474. https://doi.org/10.1126/science.abe6474

Zhou, F. (2009). Molecular mechanisms of IFN-gamma to up-regulate MHC class I antigen processing and presentation. *International Reviews of Immunology*, *28*(3–4), 239–260. https://doi.org/10.1080/08830180902978120

Zhou, L., Mudianto, T., Ma, X., Riley, R., & Uppaluri, R. (2020). Targeting EZH2 enhances antigen presentation, antitumor immunity and circumvents anti-PD-1 resistance in head and neck cancer. *Clinical Cancer Research : An Official Journal of the American Association for Cancer Research*, *26*(1), 290–300. https://doi.org/10.1158/1078-0432.CCR-19-1351

Zhou, X., Fang, D., Liu, H., Ou, X., Zhang, C., Zhao, Z., Zhao, S., Peng, J., Cai, S., He, Y., & Xu, J. (2022). PMN-MDSCs accumulation induced by CXCL1 promotes CD8+ T cells exhaustion in gastric cancer. *Cancer Letters*, *532*, 215598. https://doi.org/10.1016/j.canlet.2022.215598

Zhouhong, G., Peppelenbosch, M. P., Sprengers, D., & Kwekkeboom, J. (2021). TIGIT, the Next Step Towards Successful Combination Immune Checkpoint Therapy in Cancer. *Frontiers in Immunology*, *12*, 699895. https://doi.org/10.3389/fimmu.2021.699895

Zhu, C., Chrifi, I., Mustafa, D., van der Weiden, M., Leenen, P. J. M., Duncker, D. J., Kros, J. M., & Cheng, C. (2017). CECR1-mediated cross talk between macrophages and vascular mural cells promotes neovascularization in malignant glioma. *Oncogene*, *36*(38), 5356–5368. https://doi.org/10.1038/onc.2017.145

Zhu, H., Gu, Y., Xue, Y., Yuan, M., Cao, X., & Liu, Q. (2017). CXCR2+ MDSCs promote breast cancer progression by inducing EMT and activated T cell exhaustion. *Oncotarget*, *8*(70), 114554–114567. https://doi.org/10.18632/oncotarget.23020

Zitti, B., & Bryceson, Y. T. (2018). Natural killer cells in inflammation and autoimmunity. *Cytokine & Growth Factor Reviews*, *42*, 37–46. https://doi.org/10.1016/j.cytogfr.2018.08.001

ANNEX

Journal of Experimental & Clinical Cancer Research

REVIEW

Open Access

Blockade of novel immune checkpoints and new therapeutic combinations to boost antitumor immunity

Adrià Archilla-Ortega[1], Carla Domuro[1], Juan Martin-Liberal[2] and Purificación Muñoz[1*]

Abstract

Immunotherapy has emerged as a promising strategy for boosting antitumoral immunity. Blockade of immune checkpoints (ICs), which regulate the activity of cytotoxic T lymphocytes (CTLs) and natural killer (NK) cells has proven clinical benefits. Antibodies targeting CTLA-4, PD-1, and PD-L1 are IC-blockade drugs approved for the treatment of various solid and hematological malignancies. However, a large subset of patients does not respond to current anti-IC immunotherapy. An integrative understanding of tumor-immune infiltrate, and IC expression and function in immune cell populations is fundamental to the design of effective therapies. The simultaneous blockade of newly identified ICs, as well as of previously described ICs, could improve antitumor response. We review the potential for novel combinatory blockade strategies as antitumoral therapy, and their effects on immune cells expressing the targeted ICs. Preclinical evidence and clinical trials involving the blockade of the various ICs are reported. We finally discuss the rationale of IC co-blockade strategy with respect to its downstream signaling in order to improve effective antitumoral immunity and prevent an increased risk of immune-related adverse events (irAEs).

Keywords: Immunotherapy, Immune checkpoint, Cytotoxic T lymphocytes, NK cells, Tumor microenvironment

Background

Tumor growth involves a complex interplay between tumor, immune, and stromal cells, and extracellular matrix components. In the last decade, the relevance of the tumor-immune microenvironment and its direct impact on patients' clinical outcome has become widely acknowledged [1]. The host immune system is primed to identify and kill malignantly transformed cells to prevent tumorigenesis and tumor growth. Cytotoxic T lymphocytes (CTLs) and natural killer (NK) cells are immune cell populations responsible for immunosurveillance and, when required, for eliminating target cells. Tumor cells can be identified by CTLs as altered cells by the expression of neoantigens displayed by the major histocompatibility complex (MHC) [2]. Tumor cells expressing low levels of MHC molecules can become invisible to T cells and may escape T-cell immune control. In these cases, NK cells can identify and target cancer cells that lack MHC expression. However, tumor immune evasion, defined as the ability of tumor cells to evade the host's immune response, happens during tumorigenesis and tumor growth. Multiple activating and inhibiting mechanisms tightly regulate the effector function of CTLs and NK cells to prevent autoimmune events and preserve tissue homeostasis. In this regard, immune checkpoints (ICs) are signaling pathways that modulate the immune response. CTLs and NK cells can express IC receptors that, when interacting with IC ligands, activate IC signaling pathways, blocking their cytotoxic activity [3]. These IC ligands can be expressed by immunosuppressive cells, including M2-like macrophages, myeloid-derived

*Correspondence: p.munoz@idibell.cat
[1] Aging and Cancer Group, Oncobell Program, Bellvitge Biomedical Research Institute (IDIBELL), Av. Gran Vía de L'Hospitalet 199-203, 08907 Barcelona, Spain
Full list of author information is available at the end of the article

suppressor cells (MDSCs), and T-regulatory (Treg) cells, as well as cancer cells. The continuous interaction between IC ligands and their respective IC receptors expressed by CTLs and NK, help produce a dysfunctional state in these immune cells known as exhaustion. Tumors avoid antitumoral immunity by upregulating the expression of IC ligands and recruiting immunosuppressive cells, which give rise to an immunosuppressive tumor microenvironment (TME). Tumors with a strong immunosuppressive TME have been associated with impaired immune cytotoxicity, are more aggressive, and have a poor prognosis [4].

Immunotherapy is based on stimulating the host immune system to elicit a response against cancer cells. Pharmacological blockade of the interaction between ICs and their ligands with IC inhibitors has been identified as a promising strategy for restoring immune cytotoxic activity [5]. In recent years, T cell-mediated cytolysis has been the focus of major efforts to modulate antitumor cytotoxicity as therapy. However, NK cells are another immunotherapy target for boosting antitumor response. Importantly, the IC receptors expressed by NK and T cells can be expressed by other immune cell populations, and their blockade may also modulate the function of those populations. Here, we describe the various IC receptors expressed by T, NK, and other immune cells, and their biological function. We also analyze the antitumoral activity of IC blockade therapies, as single agents or in combination, for cancer treatment.

Main text

Effector cells: cytotoxic T lymphocytes and natural killer cells

CTLs and NK cells are the two major immune populations that are able to eliminate malignant cells. CTLs participate in the adaptive immune response while NK cells are part of the innate immune system. Cytotoxicity arises by two pathways: Perforin/Granzyme B/Granulysin-related lysis, and death receptor-induced apoptosis. Although CTLs and NK cells act in a mechanistically similar fashion, the regulation of the activity of these immune cells, and the recognition of the targets differ. CTL cytotoxicity is acquired after T cell activation upon antigen presentation by antigen presenting cells (APCs) —mainly dendritic cells (DCs) — whereas NK cells lyse target cells without antigen presentation [6]. When activated, CTLs and NK cells both secrete interferon (IFN)-γ and tumor necrosis factor (TNF)-α, which stimulate a pro-inflammatory immune response. Antitumoral effects have been extensively ascribed to these two immune cell populations, highlighting the relevance of comprehensively understanding the activation and inhibition mechanisms that regulate their cytotoxic activity against cancer cells by pharmacological strategies.

CTLs are defined as activated effector $CD3^+$ $CD8^+$ T lymphocytes and recognize target cells via the interaction between polyclonally rearranged T-cell receptor (TCR) with a peptide/MHC class I complex. Naïve $CD8^+$ T cells interact with APCs and, upon the correct presentation of the peptide-MHC class I complex, TCR signaling causes the formation of a stabilization complex between T cells and the APC. To become fully activated, the co-stimulatory receptor CD28 must interact with its ligands, CD80 (B7.1) and CD86 (B7.2). The activity of T cells is determined by the balance of positive and negative signals from co-activator and co-inhibitory receptors when they recognize their target. To eliminate target cells, CTLs produce a stabilization complex, after which, lytic granules are secreted. Perforin forms pores in the extracellular membrane of the target cells, allowing Granzyme B and Granulysin to enter the cytosol and induce apoptosis, while membrane-bound FasL binds to its receptor Fas, inducing apoptosis in an independent manner [6].

Human NK cells are phenotypically defined as $CD3^-$ $CD56^+$ lymphocytes. Two functionally distinct subsets of NK cells have been defined on the basis of their levels of expression of CD56 and CD16 (also known as Fcγ receptor III). NK cells with high-density expression of CD56 ($CD56^{bright}$) and $CD16^-$ are mostly found in lymph nodes and have a great ability to release immune-modulating cytokines such as IFN-γ and TNF-α. On the other hand, low-density expression of CD56 ($CD56^{dim}$) $CD16^+$ NK cells mostly occurs in peripheral blood, where it presents a more cytotoxic phenotype characterized by high levels of Perforin and Granzyme B expression [7]. Cytotoxic NK cell activity is independent of foreign antigens presented by MHC molecules. The balance between activation and inhibition signals, which NK cells sense through multiple innate receptors, allows the cells to respond to alterations such as cellular stress, cellular transformation, and malignancy. When activated, NK cells form a stabilization complex similarly to CTLs and release cytotoxic granules.

CTL and NK-cell activity is tightly controlled to preserve antigenic self-tolerance. Autoreactive T-cell clones are eliminated in the thymus by a process known as central tolerance. Also, a peripheral regulation of the cytotoxic response is essential to avoid inappropriate responses to self-antigens. The release of immunosuppressive molecules by M2-like macrophages and Treg cells plays a key role in establishing immune self-tolerance [8]. Activated CTLs and NK cells upregulate the expression of multiple coinhibitory receptors, known as ICs receptors, which downregulate their cytotoxic activity when binding to their ligands, ensuring the precise

regulation of their effector function (Fig. 1). Although self-tolerance mechanisms are tightly regulated, T-cell exhaustion occurs and is often observed in tumors and chronic infections [9]. NK cells can present a similar exhausted phenotype that is characterized by stronger expression of coinhibitory receptors and weaker expression of activating receptors [10]. Tumor-infiltrating lymphocytes (TILs) and tumor-infiltrating NK cells exhibit enhanced expression of IC receptors [5, 10]. This has boosted interest in understanding how these coinhibitory receptors function in order to therapeutically block them. The best characterized IC receptors are the cytotoxic T-lymphocyte-associated molecule 4 (CTLA-4) and the programmed cell death protein 1 (PD-1), but many other ICs play key central roles in controlling CTL and NK cell effector functions (Table 1).

Approved IC inhibitors for cancer treatment

IC signaling inhibition can be exploited as a therapeutic strategy for treating cancer [11, 12]. CTLA-4 and PD-1 were the first ICs to be blocked in preclinical models addressing cancer therapy. Several IC blockade antibodies were approved by the US Food and Drug Administration (FDA) and the European Medicines Agency (EMA), and are currently used to treat a variety of tumor types (Table 2). However, we are far from fully exploiting the potential of this therapeutic strategy. CTLs and NK cells may be modulated by anti-IC drugs by direct mechanisms when the effector cells express the targeted IC, and/or by indirect mechanisms, when blockade of the IC alters the immunomodulatory functions of other immune cell populations. While the currently approved IC blockade drugs produce a good clinical response in some patients, a percentage of patients show short-duration response or even no response at all (Table 3). Furthermore, late relapses occur in subsets of patients who initially responded to IC blockade therapy [13], which has sparked interest in targeting other coinhibitory receptors to find new therapeutic combinations to treat non-responsive tumors.

CTLA-4 blockade

CTLA-4, which binds CD80 and CD86 ligands, was the first IC to be described in T cells [11]. CD80 and CD86

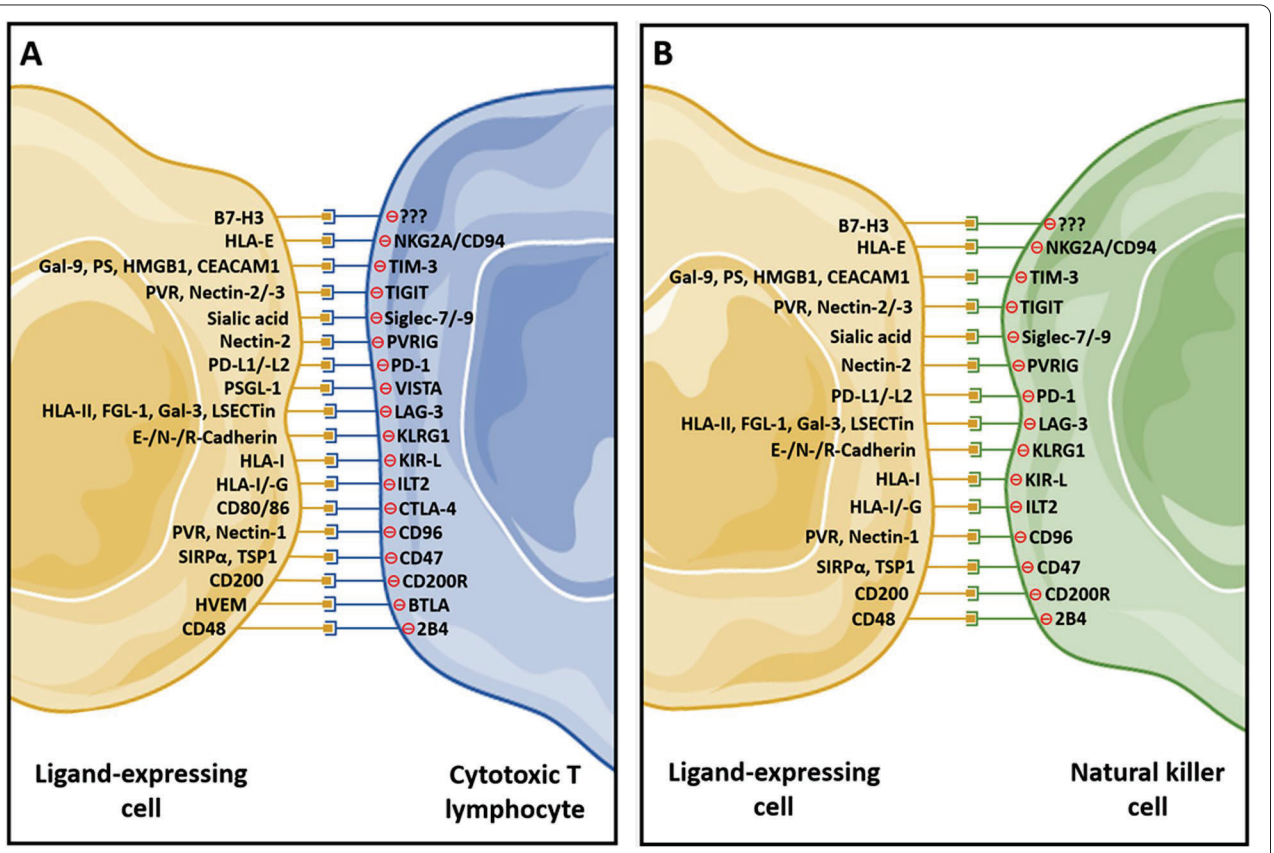

Fig. 1 Coinhibitory receptors expressed by cytotoxic T lymphocytes (**A**) and natural killer cells (**B**) and their ligands. Cytotoxic T lymphocytes and natural killer cells can express multiple coinhibitory receptors, known as immune checkpoints, that produce downstream inhibitory signals when activated upon binding to their ligands. Note that not all ICs are expressed simultaneously by cytotoxic T lymphocytes or NK cells

Table 1 Expression of coinhibitory receptors and their ligands in immune cell populations

Coinhibitory receptor	Expression in human CTLs	Expression in human NK cells	Expression in other immune cell populations	Ligand-expressing cells
2B4 (CD244, SLAMF4)	Subsets of CTLs and increased in tumor-infiltrating CTLs	Subsets of NK cells	DCs, monocytes, MDSCs and basophils	CD48 (SLAMF2): Lymphocytes, DCs, monocytes, macrophages, endothelial cells and tumor cells
BTLA	Subsets of CTLs and increased in tumor-infiltrating CTLs	Not expressed	B cells and DCs	HVEM: T cells, B cells, NK cells, DCs, monocytes and tumor cells
CD200R	Subsets of CTLs	Subsets of NK cells	Th cells, B cells, DCs, macrophages and neutrophils	CD200: T cells, B cells, DCs, endothelial cells and tumor cells
CD47 (IAP)	Subsets of CTLs	Subsets of NK cells	Expressed ubiquitously in human cells	SIRPα: DCs, macrophages, monocytes and granulocytes TSP1: Endothelial cells, monocytes, macrophages, granulocytes and cancer cells
CD96 (TACTILE)	Subsets of CTLs and increased in tumor-infiltrating CTLs	Subsets of NK cells and increased in tumor-infiltrating NK cells	Treg cells	PVR (CD155. Necl-5): DCs, neutrophils, macrophages and tumor cells Nectin-1 (PVRL1, CD111): DCs and tumor cells
CTLA-4	Subsets of CTLs and increased in tumor-infiltrating CTLs	Unclear	Th cells and Treg cells	CD80 (B7–1): B cells, T cells, DCs, macrophages and tumor cells CD86 (B7–2): B cells, T cells, DCs, macrophages and tumor cells
ILT2 (LIR1)	Subsets of CTLs and increased in tumor-infiltrating CTLs	Subsets of NK cells and increased in tumor-infiltrating NK cells	Th cells, B cells, DCs and MDSCs	HLA-G: Tumor cells HLA-I (A/B/C): Ubiquitously in human cells
KIR-L	Subsets of CTLs and increased in tumor-infiltrating CTLs	Subsets of NK cells and increased in tumor-infiltrating NK cells	Th cells	HLA-I (A/B/C): Ubiquitously in human cells
KLRG1	Subsets of CTLs and increased in tumor-infiltrating CTLs	Subsets of NK cells	Not expressed	E-cadherin: Epithelial cells and cancer cells N-cadherin: Mesenchymal cells and cancer cells R-cadherin: Neural tissue
LAG-3	Subsets of CTLs and increased in tumor-infiltrating CTLs	Subsets of NK cells	Th cells, Treg cells, B cells and DCs	HLA-II: DCs, macrophages, B cells, neutrophils, fibroblasts and tumor cells FGL-1: Tumor cells Gal-3: Fibroblasts LSECtin: Tumor cells
NKG2A/CD94	Subsets of CTLs and increased in tumor-infiltrating CTLs	Subsets of NK cells and increased in tumor-infiltrating NK cells	Not expressed	HLA-E: Ubiquitously in human cells and increased in tumor cells
PD-1	Subsets of CTLs and increased in tumor-infiltrating CTLs	Expressed in tumor-infiltrating NK cells	Th cells, Treg cells, B cells, macrophages and DCs	PD-L1 (B7-H1): Treg cells, B cells, DCs, macrophages, monocytes, MDSCs and tumor cells. PD-L2 (B7-DC): DCs, macrophages, B cells and tumor cells.

Table 1 (continued)

Coinhibitory receptor	Expression in human CTLs	Expression in human NK cells	Expression in other immune cell populations	Ligand-expressing cells
PVRIG (CD112R)	Subsets of CTLs and induced in tumor-infiltrating CTLs	Subsets of NK cells and increased in tumor-infiltrating NK cells	Not expressed	Nectin-2 (PVRL2, CD112): DCs, endothelial cells, and tumor cells
Siglec-7/−9	Siglec-7: Subsets of CTLs, Siglec-9: Subsets of CTLs and induced in tumor-infiltrating CTLs	Siglec-7: Subsets of NK cells, Siglec-9: Subsets of NK cells	Siglec-7: Macrophages, monocytes and mast cells Siglec-9: DCs, macrophages, monocytes and neutrophils	Sialic acid-containing ligands: Glycoproteins expressed by human cells. Hypersialylation, xenosialylation, and sialic acid alterations in tumor cells
TIGIT	Subsets of CTLs and increased in tumor-infiltrating CTLs	Subsets of NK cells and increased in tumor-infiltrating NK cells	Th cells and Treg cells	PVR (CD155, Necl-5): DCs, neutrophils, macrophages and tumor cells Nectin-2 (PVRL2, CD112): DCs, endothelial cells, and tumor cells Nectin-3 (PVRL3, CD113): DCs, endothelial cells, T cells and tumor cells
TIM-3	Subsets of CTLs and increased in tumor-infiltrating CTLs	Subsets of NK cells and increased in tumor-infiltrating NK cells	Th cells, Treg cells, DCs, macrophages and monocytes	Galectin-9: T cells, Treg cells, NK cells, B cells, macrophages, endothelial cells and mast cells and tumor cells. PS: Inner-cell membrane phospholipid of human cells. HMGB1: NK cells, DCs, macrophages and tumor cells CEACAM1: T cells, B cells, NK cells, neutrophils, monocytes and tumor cells
Undiscovered B7-H3 receptor	/	/	/	B7-H3: T cells, B cells, NK cells, monocytes and tumor cells
VISTA (PD-1H)	Subsets of CTLs and increased in tumor-infiltrating CTLs	Not expressed	Th cells, Treg cells, DCs, macrophages, monocytes, neutrophils and basophils	PSGL-1: T cells, B cells, DCs, macrophages, monocytes, endothelial cells, and neutrophils

CTLs cytotoxic T lymphocytes, *NK* natural killer, *DCs* dendritic cells, *MDSCs* myeloid-derived suppressor cells, *BTLA* B and T cell lymphocyte attenuator, *HVEM* herpesvirus entry mediator, *Th* T-helper, *SIRPα* signal regulatory protein alpha, *TSP1* thrombospondin-1, *Treg* T-regulatory, *ILT2* immunoglobulin-like transcript-2, *KIR-L* killer immunoglobulin-like receptor long cytoplasmic tail, *LAG3* lymphocyte activation gene-3, *FGL-1* fibrinogen-like protein 1, *Gal-3* galectin-3, *NKG2A* natural killer group 2A, *PD-1* programmed cell death protein 1, *PD-L1* programmed death-ligand 1, *PD-L2* programmed cell death 1 ligand 2, *TIGIT* T cell immunoglobulin and ITIM domain, *TIM-3* T-cell immunoglobulin and mucin-domain containing-3, *PS* phosphatidylserine (PS), *HMGB1* high-mobility group protein 1, *CEACAM1* carcinoembryonic antigen-related cell adhesion molecule 1, *VISTA* V-domain Ig suppressor of T cell activation, *PSGL-1* P-selectin glycoprotein ligand 1

Table 2 Immune checkpoint inhibitors approved for clinical use up to 2021, according to www.fda.gov

Target	Drug name	Indication	Brand name (company)
CTLA-4	Ipilimumab	Melanoma; metastatic melanoma	Yervoy (Bristol-Myers Squibb Co.)
CTLA-4 + PD-1	Ipilimumab + nivolumab	HCC; metastatic CRC; metastatic melanoma; metastatic RCC; metastatic NSCLC; malignant pleural mesothelioma	Yervoy + Opdivo (Bristol-Myers Squibb Co.)
PD-1	Nivolumab	HCC; Hodgkin lymphoma; metastatic CRC; metastatic melanoma; melanoma; metastatic RCC; metastatic urothelial carcinoma; metastatic HNSCC; metastatic SCLC; metastatic NSCLC; ESCC	Opdivo (Bristol-Myers Squibb Co.)
PD-1	Pembrolizumab	HCC; Merkel cell carcinoma; NSCLC; metastatic squamous NSCLC; RCC; melanoma; metastatic gastric cancer; metastatic gastroesophageal junction adenocarcinoma; metastatic urothelial carcinoma; metastatic cervical cancer; Hodgkin lymphoma; metastatic NSCLC; metastatic endometrial cancer; CRC; NMIBC; pancreatic cancer; primary mediastinal B-cell lymphoma; metastatic HNSCC; metastatic tumor mutational burden-high solid tumors; metastatic cSCC, metastatic TNBC	Keytruda (Merck & Co. Inc.)
PD-1	Cemiplimab	Metastatic cSCC	Libtayo (Regeneron Pharmaceuticals Inc. / Sanofi-Aventis SA)
PD-L1	Atezolizumab	Metastatic TNBC; metastatic NSCLC; SCLC; metastatic urothelial cancer; HCC; metastatic melanoma	Tecentriq (Genentech Inc. / Roche Registration Ltd.)
PD-L1	Durvalumab	SCLC; metastatic urothelial cancer; NSCLC	Imfinzi (AstraZeneca Pharmaceuticals LP)
PD-L1	Avelumab	Metastatic RCC; metastatic urothelial cancer; Merkel cell carcinoma	Bavencio (Merck KGaA / Pfizer Inc.)

HCC hepatocellular carcinoma, *CRC* colorectal cancer, *RCC* renal cell carcinoma, *NSCLC* non-small-cell lung cancer, *HNSCC* head and neck squamous cell carcinoma, *SCLC* small-cell lung cancer, *ESCC* esophageal squamous cell carcinoma, *NMIBC* non-muscle invasive bladder cancer, *cSCC* cutaneous squamous cell carcinoma, *TNBC* triple-negative breast cancer

are also ligands of the T cell co-activator receptor CD28. CTLA-4 has a high sequence similarity to that of CD28 and competes, with higher affinity, to bind CD80 and CD86. CTLA-4 regulates early stages of $CD8^+$ T cell activation, ensuring tolerance of self-antigens in the lymph nodes. Mechanistically, CTLA-4 indirectly limits CD28 signaling by capturing and sequestering CD80 and CD86 from ligand-expressing cells through a process named trans-endocytosis [14]. Genetic ablation of CTLA-4 increases early lethality in mice due to lymphoproliferation [5]. Blockade experiments demonstrated that in vitro and in vivo anti-CTLA-4 treatment enhance T-cell proliferation [15]. CTLA-4 is also expressed by Treg cells, and its signaling enhances their suppressive functions [16]. In addition, $CD4^+$ T cells expressing CTLA-4 exhibit lower rates of proliferation [17]. The role of CTLA-4 in NK cells remains to be elucidated. While some studies indicated that CTLA-4 is expressed in mouse and human NK cells, and that it regulates their effector functions, others reported that human NK cells are not affected by the CD28/CTLA-4 axis [18].

In vivo administration of anti-CTLA-4 antibody increases antitumor immunity, causing pre-established tumors to be rejected [11]. Further experiments demonstrated that blockade of CTLA-4 stimulates the $CD8^+$ T cell cytotoxic response against tumor cells [5]. Importantly, the complete antitumoral response provoked by CTLA-4 blockade requires Treg cells. CTLA-4 conditional knockout (KO) in Treg cells reduces tumor growth [15]. Blockade of CTLA-4 accelerates Th1 proliferation and increases interleukin (IL)-2 production. While no direct function of anti-CTLA-4 in NK cells has yet been clearly identified, in vivo blockade of CTLA-4 might enhance NK cell activity indirectly by inhibiting Treg immunosuppressive activity and enhancing Th1 pro-inflammatory function [18]. Finally, the concomitant blockade of CTLA-4 and PD-1 signaling enhances antitumor response and increases the cytotoxic activity of $CD8^+$ T cells in preclinical models [19].

CTLA-4 was the first IC receptor to be clinically targeted. In 2011, ipilimumab, an anti-CTLA-4 monoclonal antibody (mAb), was approved by the FDA and the EMA for treating patients with advanced melanoma. At present, ipilimumab is the only anti-CTLA-4 mAb approved for clinical use. It has value as a monotherapy for melanoma in adjuvant and metastatic settings, or combined with nivolumab, an anti-PD-1 antibody, for patients suffering several advanced cancer types (Table 2). Several clinical trials are testing the efficacy of anti-CTLA-4

Table 3 Summary of the differences in the application of immune checkpoint inhibitors against common tumors, according to FDA approval information

Condition	Drug	ORR (%)	mPFS (months)	mOS (months)	Grade 3–5 AE (%)	Approval time	Key trials
Melanoma	Ipilimumab	16.8	2.70	11.2	11	03/2011	NCT00324155
	Ipilimumab + nivolumab	60	8.50	Not reached	62	10/2015	CheckMate-067
	Pembrolizumab	37	5.00	> 24	< 10	09/2014	KeyNote-001
	Nivolumab	32	4.70	17.3	9	12/2014	CheckMate-037
	Atezolizumab	60	15.10	16.1	33.5	07/2020	IMspire150
NSCLC	Nivolumab	20	3.50	9.2	7	03/2015	CheckMate-063; CheckMate-017
	Ipilimumab + nivolumab	36	5.1	17.1	58	05/2020	CheckMate-227
	Pembrolizumab	19.4	4.00	12.7	< 10	10/2015	KeyNote-001; KeyNote-010
	Atezolizumab	17	2.70	12.6	11	10/2016	Poplar (NCT01903993)
	Durvalumab	28.4	16.80	23.2	29.9	02/2018	NCT02125461
	Cemiplimab	39	8.20	Not reached	28	02/2021	NCT03088540
RCC	Nivolumab	25	4.60	25	19	11/2015	CheckMate-025
	Ipilimumab + nivolumab	41.6	11.6	Not reached	65	04/2018	CheckMate-214
	Pembrolizumab	59.3	15.10	Not reached	75.8	04/2019	KeyNote-426
	Avelumab	51.4	13.80	11.6	71.2	05/2019	JAVELIN Renal 101
HCC	Nivolumab	14.3	4.00	15	25	09/2017	CheckMate-040
	Ipilimumab + nivolumab	33	8.3	17.5	37	03/2020	Checkmate-040
	Pembrolizumab	17	4.9	12.9	26	11/2018	KeyNote-224
	Atezolizumab	65	6.80	Not evaluated	56.5	05/2020	IMbrave150
SCLC	Nivolumab	12	1.4	5.6	45	08/2018	CheckMate-032
	Atezolizumab	60.2	5.20	12.3	37	03/2019	Impower133
	Pembrolizumab	19	2.0	8.7	31	06/2019	KeyNote-158; KeyNote-028
	Durvalumab	68	5.10	13	62	03/2020	CASPIAN (NCT03043872)
CRC	Nivolumab	32	14.30	5.6	45	08/2017	CheckMate-142
	Ipilimumab + nivolumab	55	12	Not evaluated	20	07/2018	CheckMate-8HW
	Pembrolizumab	43.8	16.50	13.7	22	06/2020	KeyNote-177

ORR overall rate response, *mPFS* median progression free survival, *mOS* median overall survival, *AE* adverse events, *NSCLC* non-small-cell lung cancer, *RCC* renal cell carcinoma, *HCC* hepatocellular carcinoma, *SCLC* small-cell lung cancer, *CRC* colorectal cancer

combined with other anti-ICs in a variety of tumor types (Table 4).

PD-1 and PD-L1 blockade

PD-1 promotes inhibitory signals upon binding to its ligands, programmed death-ligand 1 (PD-L1) and programmed cell death 1 ligand 2 (PD-L2), in T cells [12]. PD-1 is expressed in distinct immune cell populations, including those of B, Treg, and myeloid cells. While PD-L1 may be expressed in hematopoietic and non-hematopoietic cells, physiological expression of PD-L2 is restricted to DCs, macrophages, and B cells. Notably, PD-L1 and PD-L2 expression is upregulated in many tumor types and is usually associated with poor patient outcome. PD-1 regulates activated T cell function in the later stages of the immune response in peripheral tissues [15]. Activated T cells induce PD-1 expression, and its signaling, upon binding to PD-L1/−L2, decreases T cell proliferation and cytokine secretion. PD-1 cytoplasmic tail contains classic inhibitory motifs ITIM and ITSM which recruit SHP-2 phosphatases resulting in reduced TCR downstream phosphorylation and signaling [20] (Fig. 2B). High PD-1 levels, concomitantly with other ICs, can be detected in TILs and in association with an exhausted phenotype [21]. PD-1 signaling in Treg cells enhances their proliferative and suppressive functions [5]. In NK cells, PD-1 expression has only been identified under pathological conditions [22]. PD-1 is upregulated in tumor-infiltrating NK cells and PD-1^{+} NK cells are known to be functionally exhausted [23]. Although PD-1 downstream mechanisms leading to NK exhaustion have not been completely elucidated, SHP-2 recruitment might participate in the process, given its role damping NK cell function [24]. An interaction between PD-L1 and CD80 expressed in T cells was also characterized, which led

Table 4 Clinical-stage development of monotherapies and combinatory therapies with immune checkpoint inhibitors in 2021, according to www.clinicaltrials.gov

Target	Drug name	Indication	Status
CTLA-4 + PD-1	Ipilimumab + nivolumab	NSCLC (NCT03351361) (NCT02864251) (NCT02477826) (NCT02869789) (NCT03391869) (NCT04026412) (NCT02998528) (NCT03215706); gastric cancer; GEJ cancer (NCT02872116) (NCT03604991); HNSCC (NCT03700905); metastatic HNSCC (NCT02741570); melanoma (NCT02905266) (NCT02599402) (NCT03068455) (NCT02388906); SCLC (NCT02538666); RCC (NCT03793166) (NCT03873402) (NCT03937219) (NCT03138512) (NCT04513522); esophageal cancer (NCT03143153); sarcoma (NCT04741438); glioblastoma (NCT02017717) (NCT04396860); squamous cell lung cancer (NCT02785952); metastatic urothelial cancer (NCT03036098); metastatic prostate cancer (NCT03879122)	Phase III
CTLA-4 + PD-1	Ipilimumab + pembrolizumab	Metastatic NSCLC (NCT03302234); metastatic melanoma (NCT01866319); solid tumors (NCT03755739)	Phase III
CTLA-4 + PD-1	Ipilimumab + REGN2810	NSCLC (NCT03515629) (NCT03409614)	Phase III
CTLA-4 + PD-L1	Tremelimumab + durvalumab	Advanced solid tumors (NCT03084471); HNSCC (NCT02369874); NSCLC (NCT02453282); SCLC (NCT03703297); metastatic NSCLC (NCT02542293) (NCT02352948) (NCT03164616); metastatic urothelial cancer (NCT03682068); urothelial cancer (NCT02516241); metastatic HNSCC (NCT02551159); HCC (NCT03298451); squamous cell lung cancer (NCT02154490); RCC (NCT03288532); SCLC (NCT03043872)	Phase III
PD-1 + LAG-3	Nivolumab + relatlimab	Metastatic melanoma (NCT03470922)	Phase III
PD-1 + LAG-3 + B7-H3	MGD013 + enoblituzumab	Gastric cancer; GEJ cancer (NCT04082364), metastatic HNSCC (NCT04129320)	Phase III
PD-1 + TIGIT	Tislelizumab + BGB-A1217	NSCLC (NCT04746924)	Phase III
PD-1 + TIGIT	Zimberelimab + AB154	Metastatic NSCLC (NCT04736173)	Phase III
PD-1 + B7-H3	MGA012 + enoblituzumab	Metastatic HNSCC (NCT04129320)	Phase III
PD-L1 + TIGIT	Atezolizumab + tiragolumab	NSCLC (NCT04294810) (NCT04513925); SCLC (NCT04256421) (NCT04665856); esophageal squamous cell carcinoma (NCT04540211) (NCT04543617);	Phase III
LAG-3 + PD-1	Relatlimab + nivolumab	Multiple solid tumors (NCT01968109); CRC (NCT03642067); metastatic soft-tissue sarcoma (NCT04095208); HNSCC (NCT04080804); NSCLC (NCT04205552) (NCT02750514); RCC (NCT02996110); gastric cancer (NCT02935634); metastatic melanoma (NCT04552223) (NCT03743766) (NCT03724968); solid tumors (NCT03607890); HCC (NCT04567615); metastatic basal cell carcinoma (NCT03521830); HNSCC (NCT04326257); metastatic NSCLC (NCT04623775); metastatic CRC (NCT03867799); GEJ adenocarcinoma (NCT03704077) (NCT03662659) (NCT03610711) (NCT04062656); advanced cancers (NCT03459222) (NCT02488759); metastatic ovarian cancer (NCT046111269); melanoma (NCT02519322); multiple myeloma (NCT04150965)	Phase II

Table 4 (continued)

Target	Drug name	Indication	Status
LAG-3 + PD-1	BI-754111 + BI-754091	Metastatic solid tumors (NCT03697304)	Phase II
LAG-3 + PD-1	REGN3767 + cemiplimab	Breast cancer (NCT01042379); metastatic solid tumors (NCT04706715)	Phase II
LAG-3 + PD-1	LAG525 + spartalizumab	TNBC (NCT03499899); advanced malignancies (NCT03365791) (NCT02460224); melanoma (NCT03484923)	Phase II
LAG-3 + PD-1 + TIM-3	INCAGN02385 + INCMGA00012 + INCAGN02390	Advanced malignancies (NCT04370704)	Phase II
LAG-3 + PD-1	MK-4280 + pembrolizumab	Hodgkin lymphoma; non-Hodgkin lymphoma (NCT03598608); advanced NSCLC (NCT03516981)	Phase II
TIM-3	MBG453	Myelodysplastic syndromes; chronic myelomonocytic leukemia (NCT04266301)	Phase III
TIM-3	MBG453	AML (NCT04150029) (NCT04623216); advanced solid tumors (NCT02608268); myelofibrosis (NCT04097821)	Phase II
TIM-3 + PD-1	BMS-986258 + nivolumab	Solid tumors (NCT03446040)	Phase II
TIM-3 + PD-1	BGB-A425 + tislelizumab	Solid tumors (NCT03744468)	Phase II
TIM-3 + PD-1	TSR-022 + TSR-042	Liver cancer (NCT03680508); melanoma (NCT04139902)	Phase II
TIGIT + PD-L1	Tiragolumab + atezolizumab	Cervical cancer (NCT04300647); gastric adenocarcinoma; GEJ adenocarcinoma; esophageal carcinoma (NCT03281369); urothelial carcinoma (NCT03869190); pancreatic adenocarcinoma (NCT03193190); NSCLC (NCT03563716); metastatic NSCLC (NCT04619797); metastatic HNSCC (NCT04665843); SCLC (NCT04308785); HNSCC (NCT03708224); liver cancer (NCT04524871)	Phase II
TIGIT + PD-1	AB154 + zimberelimab	NSCLC (NCT04262856)	Phase II
TIGIT	BMS-986207	Multiple myeloma (NCT04150965)	Phase II
TIGIT + PD-1	BMS-986207 + nivolumab	Solid tumors (NCT02913313) (NCT04570839)	Phase II
PVRIG + PD-1	COM701 + nivolumab	Advanced solid tumors (NCT03667716) (NCT04570839)	Phase I
KIR2DL1 + KIR2DL2 + KIR2DL3	Lirilumab	AML (NCT01687387); chronic lymphocytic leukemia (NCT02481297); refractory AML (NCT02399917)	Phase II
KIR2DL1 + KIR2DL2 + KIR2DL3 + PD-1	Lirilumab + nivolumab	HNSCC (NCT03341936); metastatic malignancies (NCT03347123); multiple myeloma (NCT01592370); refractory tumors (NCT02813135)	Phase II
KIR2DL1 + KIR2DL2 + KIR2DL3 + PD-1 + CTLA-4	Lirilumab + nivolumab + ipilimumab	Advanced solid tumors (NCT01714739)	Phase II
KIR3DL2	IPH4102	Advanced T cell lymphoma (NCT03902184).	Phase II
NKG2A	Monalizumab	Metastatic HNSCC (NCT04590963)	Phase III
NKG2A	Monalizumab	Metastatic HNSCC (NCT02643550) (NCT03088059); breast cancer (NCT04307329); chronic lymphoid leukemia (NCT02557516)	Phase II
NKG2A + PD-L1	Monalizumab + durvalumab	CRC (NCT04145193); solid tumors (NCT02671435); NSCLC (NCT03822351) (NCT038223519) (NCT03833440)	Phase II
CD200	Samalizumab	AML (NCT03013998), multiple myeloma (NCT00648739)	Phase II

Table 4 (continued)

Target	Drug name	Indication	Status
CD47	Magrolimab	Myelodysplastic syndrome (NCT04313881); AML (NCT04778397)	Phase III
CD47 + PD-L1	Magrolimab + atezolizumab	Metastatic urothelial carcinoma (NCT03869190)	Phase II
CD47	Magrolimab	Solid tumors (NCT02953782); refractory B-cell non-Hodgkin lymphoma (NCT02953509); myeloid malignancies (NCT04778410)	Phase II
CD47	RRX-001	SCLC (NCT03699956)	Phase III
CD47	RRX-001	Solid tumors (NCT02489903); metastatic CRC (NCT02096354)	Phase II
BTLA	JS004	Advanced solid tumors (NCT04278859)	Phase I
BTLA	TAB004	Advanced solid malignancies (NCT04137900)	Phase I
VISTA	JNJ-61610588	Advanced solid tumors (NCT02671955)	Phase I
VISTA + PD-L1	CA170	Advanced solid tumors and lymphomas (NCT02812875)	Phase I
B7-H3	Enoblituzumab	Metastatic HNSCC (NCT04129320)	Phase III
B7-H3	Enoblituzumab	Prostate cancer (NCT02923180)	Phase II
B7-H3	131I-omburtamab	Neuroblastoma; central nervous system metastases; leptomeningeal metastases (NCT03275402)	Phase III
B7-H3	177Lu-DTPA-omburtamab	Medulloblastoma (NCT04167618); solid tumors (NCT04315246)	Phase II
B7-H3	DS-7300a	Advanced solid tumors (NCT04145622)	Phase II
B7-H3 + PD-1	MGC018 + MGC012	Advanced solid tumors (NCT03729596)	Phase II

NSCLC non-small-cell lung cancer, *GEJ* gastroesophageal junction, *HNSCC* head and neck squamous cell carcinoma, *SCLC* small-cell lung cancer, *RCC* renal cell carcinoma, *HCC* hepatocellular carcinoma, *MIBC* muscle invasive bladder cancer, *ESCC* esophageal squamous cell carcinoma, *TNBC* triple-negative breast cancer, *CRC* colorectal cancer, *NMIBC* non-muscle invasive bladder cancer, *AML* acute myeloid leukemia

to inhibition of T cell function in vitro [25]. However, other studies suggest that the PD-L1 interaction with CD80 could cause T cell expansion without promoting exhaustion. Specifically, it has been reported that in bone marrow transplantations, the interaction of CD80 from donor $CD8^+$ T cells with PD-L1 in lymphoid tissues from recipient patients, promotes T cell expansion, resulting in increased graft-versus-leukemia activity [26]. According to these findings, the blockade of PD-L1 signaling could reduce the antitumoral activity of T cells in specific tissue environments.

PD-1 signaling blockade increases antitumor immunity and decreases tumor growth. Specifically, PD-L1 transgenic expression in tumor cells enhances tumorigenesis, which can be reversed with anti-PD-L1 antibodies. PD-L1 mAb blockade enhances DC-mediated T cell activation and antitumor function. Tumor-infiltrating exhausted NK cells express PD-1 and its blockade partially restores NK antitumoral activity [23]. Although PD-1 signaling in Treg cells enhances immunosuppressive functions, in vivo PD-1 blockade in Treg cells leads to different tumor-dependent responses [27]. Moreover, a complete anti-PD-1 antitumoral effect requires DC stimulation and function [28]. A bispecific anti-PD-1/PD-L1 antibody gave rise to greater antitumoral efficacy relative to monospecific therapies in a high-grade serous ovarian

(See figure on next page.)

Fig. 2 Immune checkpoint downstream inhibitory signaling in $CD8^+$ T cells. Immune checkpoint pathways initiated after binding of ligands to their respective IC receptors (blue boxes) interfere with TCR signaling by a variety of mechanisms. ICs have inhibitory motifs in their cytoplasmic tail that can recruit (blue arrows) protein tyrosine phosphatases SHP1 and/or SHP2, which are responsible for dephosphorylating (red inhibitory arrows) TCR downstream signaling proteins. This is the case for PVRIG, 2B4, Siglec-7/−9, ILT2, BTLA, KIR-L, NKG2A, TIGIT, PD-1, and KLRG1. However, some ICs, such as CTLA-4, TIM-3, CD47, and CD200R1, present alternative downstream mechanisms, while other IC downstream signaling, such as that involving LAG-3, VISTA, CD96, CD160, and B7-H3, remains to be fully elucidated. Schematic representation of (**A**) SHP1-dependent inhibition of TCR signaling, (**B**) SHP2-dependent inhibition of TCR signaling, and (**C**) non-dependent SHP1 and SHP2 inhibition of TCR signaling. Dotted lines indicate indirect mechanisms (created with BioRender.com)

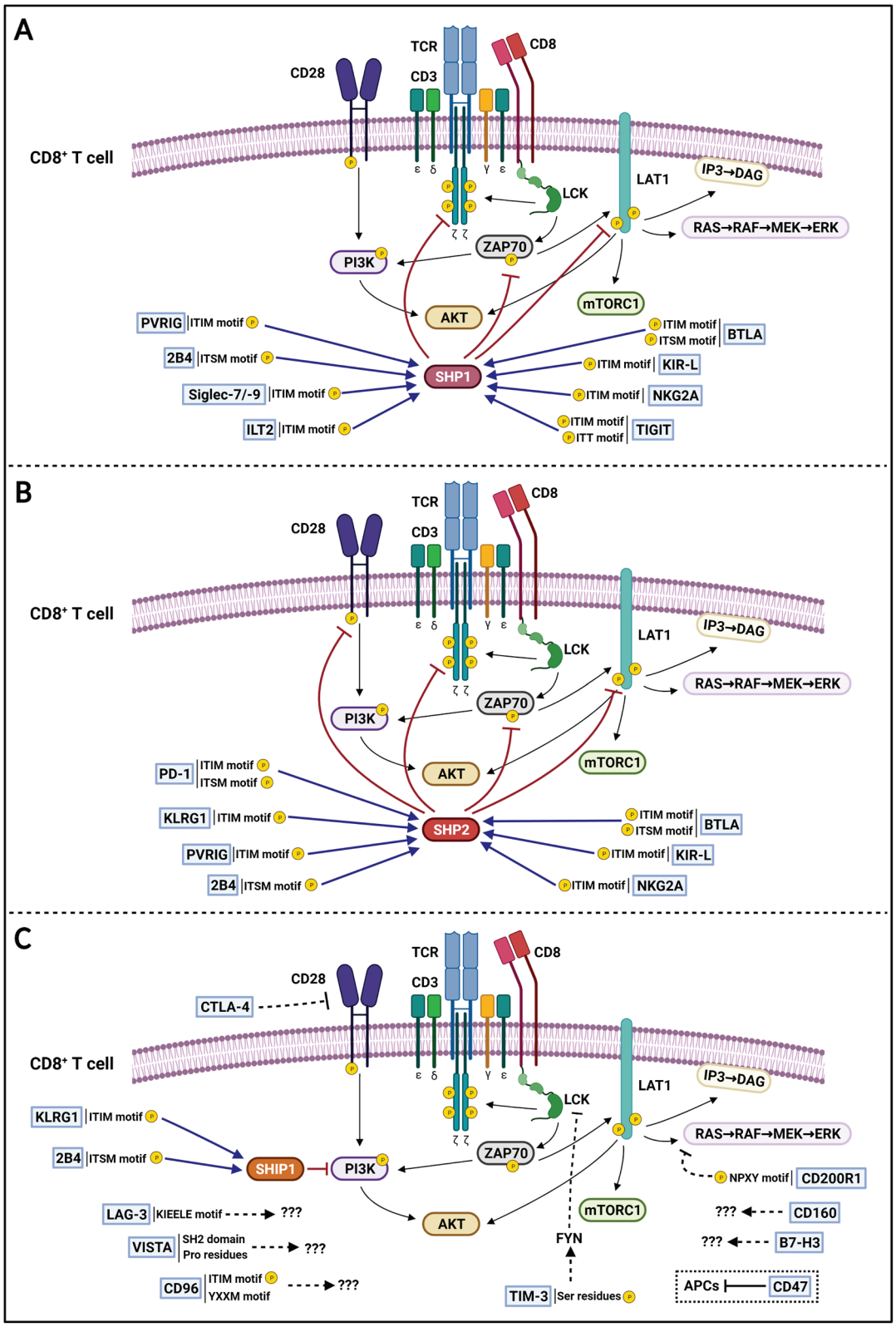

Fig. 2 (See legend on previous page.)

cancer model by inducing a superior cytotoxicity in both T and NK cells [29]. This suggests that PD-L1 could be involved in interactions other than those binding to PD-1. PD-1 blockade alongside other ICs has shown itself to increase T cell response [30] and to bestow therapeutic benefits, which will be further discussed in the corresponding IC blockade section.

Inhibition of the PD-1/PD-L1 axis is the most commonly applied IC blockade therapy. Nivolumab, pembrolizumab, and cemiplimab are PD-1-blocking mAbs that have proven therapeutic efficacy in treating patients suffering from different tumor types (Table 2). Multiple anti-PD-1 antibodies, including these three, are being tested either alone (Table S1) or in combination with other anti-IC antibodies in multiple cancers (Table 4). The anti-PD-L1 antibodies, atezolizumab, durvalumab, and avelumab, also have a therapeutic value in treating certain tumor types and have been approved for clinical use (Table 2). These three antibodies, among others, are being tested as treatments for a wide range of solid tumors in clinical trials, either as monotherapy (Table S1) or in combination with other IC blockade antibodies (Table 4).

IC inhibitors under clinical development

LAG-3 blockade

The coinhibitory receptor lymphocyte activation gene-3 (LAG-3) is an IC receptor expressed by $CD8^+$ T cells and NK cells that regulates peripheral tolerance. LAG-3 binds to HLA class II as well as to fibrinogen-like protein 1 (FGL-1), Galectin-3 (Gal-3), and LSECTin. LAG-3 ligands are expressed by tumor cells, and, notably, FGL-1 participates in immune evasion mechanisms that reduce the T cell response [31]. Mice deficient in LAG-3 have altered T cell proliferation. LAG-3 is expressed in Treg cells and its blockade disrupts Treg suppressor functions [32]. LAG-3 is also expressed in NK cells, but its function is not yet fully understood. Blockade of LAG-3 in human NK cells does not induce NK cytotoxicity against different tumor types [18]. Recent findings indicate that LAG-3 blockade in vitro increases cytokine production by NK cells without affecting their cytotoxicity [33]. The mechanism of action of LAG-3 remains largely unknown. LAG-3 cytoplasmic tail does not contain classical inhibitory motifs but presents a KIEELE motif that may mediate LAG-3 inhibitory functions [34] (Fig. 2C).

Anti-LAG-3 mAb administration was found to increase the proliferation and effector function of $CD8^+$ T cells and delay tumor growth in a prostate cancer mouse model. LAG-3 is co-expressed with PD-1 in $CD4^+$ and $CD8^+$ TILs in many mouse and human tumors [35]. Simultaneous blockade of PD-1 and LAG-3 synergizes to enhance anti-tumor CTLs activity and reduces tumor growth in a colon adenocarcinoma model [36], a chronic lymphocytic leukemia (CLL) model [37], and a malignant pleural mesothelioma model [38]. LAG-3 expression has been linked to a stronger suppressive function of Treg cells [39]. The role of NK cells in LAG-3 blockade therapy response, and the possible contribution of NK cells to the observed antitumoral effects remain largely unknown. A unique study determined that treatment of the 4T1 mouse model of metastatic breast cancer with IL-12, combined with anti-LAG-3 or anti-PD-1, recovered NK cell cytotoxicity and proliferation, which resulted in a reduced presence of pulmonary metastases [40]. LAG-3 blockade is currently being investigated in clinical trials, either as monotherapy or combined with the inhibition of other ICs, to treat multiple tumor types (Table 4).

TIM-3 blockade

T-cell immunoglobulin and mucin-domain containing-3 (TIM-3) acts as a coinhibitory receptor of T cells and is also expressed in Tregs, NK cells, DCs, and macrophages. TIM-3 expression is known to be increased in exhausted TILs [41]. The first TIM-3 ligand to be described was Galectin-9 (Gal-9), but TIM-3 also binds to phosphatidylserine (PS), carcinoembryonic antigen-related cell adhesion molecule 1 (CEACAM1), and high-mobility group protein 1 (HMGB1). The expression of TIM-3 ligands is upregulated by APCs, endothelial cells, and neutrophils, among other immune cells, and has been linked to carcinogenesis and tumor progression. Gal-9 interaction with TIM-3 negatively regulates T-helper function and can induce T-cell death [42]. TIM-3 blockade and gene depletion downregulate Th1 cell function and increase CTL proliferation and cytokine production [31]. $TIM\text{-}3^+$ Treg cells increase suppressor functions in vitro [43]. Blockade of TIM-3 reverses the exhausted phenotype of CTLs from patients with advanced tumors. TIM-3 interaction with its ligands leads to the phosphorylation of conserved tyrosine residues in its cytoplasmic tail by the tyrosine ITK [44]. Phosphorylation of the TIM-3 cytoplasmic tail leads to the release of BAT3 protein and the recruitment of the tyrosine kinase FYN, ultimately resulting in TCR downstream kinase LCK inhibition [45] (Fig. 2C). In NK cells, TIM-3 acts as a negative regulator of NK effector functions. Its expression is upregulated in cancer, and has been associated with NK exhaustion [18]. Additionally, TIM-3 ligand Gal-9 can also interact with PD-1 expressed by T cells, which dampens the $CD4^+$ and $CD8^+$ T cell response [42, 46]. Specifically, Gal-9 interacts with PD-1 through glycans without affecting the PD-1/PD-L1 interaction. Likewise, the Gal-9/PD-1 interaction enables the formation of PD-1 and TIM-3

heterodimers, which promotes T cell exhaustion but dampens Gal-9/TIM-3-induced T cell apoptosis [47]. It is of note that, human Treg cells express high levels of Gal-9, which induces Treg death upon interacting with TIM-3 expressed by tumor resident cells [47]. Hence, anti-Gal-9 therapy might promote Treg function, thereby limiting the antitumoral function of $CD8^+$ T cells. In this sense, the combination of anti-Gal-9 with Treg cell treatment depletion promotes synergistic antitumor activity in a breast tumor model by activating specific subsets of TILs [47].

In a TIM-3-overexpressing mouse model, anti-TIM-3 antibody reduces tumor growth by restoring T-cell activity [48]. Concomitant blockade of PD-1 and TIM-3 further improves T cell anti-tumor function and reduces tumor growth more effectively. Simultaneously targeting TIM-3 and PD-1 increases LAG-3 expression in TILs, suggesting a cross-regulation between IC receptors, and triple blockade of TIM-3, PD-1, and LAG-3 results in reduced tumor growth in a colon adenocarcinoma model [49]. Simultaneous blockade of TIM-3 and PD-L1 significantly reduces tumor growth in orthotopic models of HNSCC [50] whereas treatment with anti-TIM-3 concurrently with anti-PD-1 causes greater regression of murine glioma than is produced by a single checkpoint blockade [51]. TIM-3 blockade reverses exhausted NK cells isolated from lung adenocarcinoma patients [52], and advanced MHC class I-deficient tumors treated with IL-21 combined with anti-TIM-3 and anti-PD-1 reduce tumor progression by enhancing NK cell antitumoral immunity [53]. Hence, TIM-3 blockade also boosts NK cytotoxic activity in specific tumor settings. The presence of $TIM\text{-}3^+$ Treg cells is associated with poor prognosis in lung cancer, and pharmacological blockade of TIM-3 reduces the suppressive function of intratumoral Treg cells [41]. In vitro experiments indicated that TIM-3 signaling in DCs blocks DC activation and maturation [54]. A recent study concluded that the accumulation of $TIM\text{-}3^+$ $CD4^+$ T cells in tumoral regions favors TIM-3-mediated immunosuppressive functions in hepatocellular carcinoma (HCC) patients. Depletion of $CD4^+$ T cells abrogates the antitumoral effects of anti-TIM-3 therapy, indicating that $CD4^+$ T cells might be responsible for TIM-3-mediated immunosuppression [55]. The response of TIM-3 blockade-based therapy is currently being analyzed in clinical trials as monotherapy or in combination with anti-PD-1 antibodies (Table 4).

TIGIT blockade

The T cell immunoglobulin and ITIM domain (TIGIT) is a member of the immunoglobulin superfamily of paired receptors expressed by T cells and NK cells that interact with ligands of the nectin and nectin-like family. TIGIT acts as an inhibitor receptor when binding to its ligands PVR, nectin-2, and nectin-3 (CD113), all of which are expressed in APCs and a variety of non-hematopoietic cells, including tumor cells [56]. Specifically, TIGIT interacts with PVR with a higher affinity than with nectin-2, while the nectin-3/TIGIT interaction has a weak binding affinity. In addition, DNAM-1 is another co-stimulatory receptor expressed by NK and T cells that competes with TIGIT to bind PVR and nectin-2, which enables it to regulate T cell inhibition precisely [57]. In NK cells, TIGIT signaling reduces NK cytotoxicity and cytokine release, while in T cells it reduces T cell activation, proliferation, and effector functions. Specifically, the TIGIT intracellular cytoplasmic tail contains an ITIM and an ITT-like domain that recruit SHP-1 phosphatases, leading to the blockade of PI3K and MAPK pathways in NK cells [58], and decreased TCR downstream signaling [59] (Fig. 2A). $TIGIT^+$ Treg cells have greater suppressive capacities in vitro and selectively suppress the Th1 pro-inflammatory response in vivo [31]. TIGIT interaction with PRV expressed by DCs forces the DCs to be tolerogenic by increasing their production of immunosuppressive IL-10 cytokine [60].

TIGIT ligands are expressed by cancer cells and exhausted $TIGIT^+$ T and NK cells are detected in various human cancers. Antibody blockade of TIGIT enhances antitumor $CD8^+$ T cell response and prompts tumor regression in a colorectal cancer (CRC) mouse model. TIGIT dual blockade with PD-1, PD-L1, or TIM-3 has a synergistic action that produces enhanced $CD8^+$ T cell activity and tumor regression in a colorectal carcinoma model [61]. Dual blockade of PD-1 and TIGIT enhances antitumor response and increases survival in a mouse glioblastoma model [62]. Conditional TIGIT KO in Treg cells reduces tumor growth in a melanoma mouse model, proving that the TIGIT blockade effect is also mediated by Treg cells [31]. Recently, it was demonstrated that TIGIT blockade elicits NK-mediated antitumoral immunity in tumor-bearing mouse models [63]. Antibodies targeting TIGIT are currently being investigated in clinical trials to treat patients with different tumor types (Table 4).

PVRIG blockade

PVRIG, also known as CD112R, is another member of the immunoglobulin superfamily of paired receptors. It has recently been identified in human T and NK cells. PVRIG binds to nectin-2 but does not recognize PVR. In T cells, PVRIG signaling inhibits the TCR-mediated signal dampening T cell response by recruiting SHP-1 and SHP-2 phosphatases to its ITIM-like domains [64] (Fig. 2B). Human NK cells expressing PVRIG present

reduced proliferation and cytokine release [56]. Recent results suggest that PVRIG expression is reduced during human NK-cell activation [65], while exhausted tumor-infiltrating NK cells express high levels of PVRIG [66]. Until now, expression of PVRIG has not been described in myeloid immune cell populations.

Targeting PVRIG with antibodies promoted T cell expansion in vitro, which was further increased by simultaneous blockade with TIGIT [64]. PVRIG blockade enhances in vitro NK cell antitumoral activity and increases IFN-γ release [67]. In AML patients, anti-PVRIG therapy promotes NK-cell cytotoxicity against AML blasts [65]. In mouse models of cancer, TILs show high PVRIG levels [68]. Ex vivo PVRIG blockade of patient-derived T cells upregulates T-cell function, an effect that is further enhanced when combined with anti-TIGIT or anti-PD-1 treatments [56]. Anti-PVRIG treatment delays tumor growth and prolongs survival of tumor-bearing mice by reversing exhaustion of NK and $CD8^+$ T cells of solid tumors. Dual blockade of PVRIG and PD-L1 enhances the antitumoral effects in comparison to single-blockade therapies in solid tumors [66, 68]. Notably, $PVRIG^{-/-}$ mice exhibit reduced tumor growth in a $CD8^+$ T cell-dependent manner, an effect that is synergistically enhanced by PD-L1 blockade. Finally, PVRIG is co-expressed with PD-1 and TIGIT in activated T cells and combinatory dual blockade of PVRIG with PD-1 or TIGIT additionally promoted T-cell activity [69]. An anti-PVRIG mAb is currently being tested in a clinical trial in patients with advanced solid tumors (Table 4).

KIR-L blockade

Killer immunoglobulin-like (KIRs) are a family of receptors that regulate self-tolerance and effector functions of NK cells by binding to classic HLA class I allotypes (HLA-A, HLA-B, and HLA-C). These receptors allow the identification and elimination of cells that fail to express a sufficient level of HLA, like many tumor cells, in a process called missing self-recognition. KIR receptors with a long cytoplasmic tail (KIR-L) mainly present NK coinhibitory capabilities, while short-tailed KIR receptors (KIR-S) enhance NK function [70]. The KIR-L cytoplasmic tail contains ITIM motifs that become phosphorylated upon binding with its ligand, and recruit tyrosine phosphatases such as SHP-1 and SHP-2, resulting in NK-cell inhibition [71] (Fig. 2A and B). KIRs were initially characterized as NK cell receptors, but they are also expressed in $CD8^+$ T-cell subsets. It has been proposed that KIR expression can be sustained by TCR engagement, and may participate in T-cell tolerance to self-antigens [72].

Initial evidence that the blockade of KIR signaling could be beneficial in treating cancer came with the observation that acute myeloid leukemia (AML) patients did not experience recurrence within 5 years if they received a bone marrow transplantation from a donor who presented NK with KIRs that mismatched the interaction with the HLA of the patients [73]. Thus, the lack of recognition of HLA class I molecules by KIRs enhances NK cell cytotoxic activity, causing the elimination of malignant cells. Additionally, tumor-infiltrating NK cells have a high level of expression of inhibitory KIRs that are correlated with poor clinical outcome in non-small-cell lung cancer (NSCLC) [74]. A unique mAb targeting KIR2DL1, KIR2DL2, and KIR2DL3 receptors increases NK-cell cytotoxicity against autologous AML blasts and multiple myeloma cells [18]. Hence, KIR blockade appears to enhance NK cell function in the tumors. Different KIR inhibitors are being tested in clinical trials as single agents or combined with anti-PD-1 or anti-CTLA-4 antibodies (Table 4).

NKG2A blockade

The natural killer group 2A (NKG2A) is a member of the NKG2 receptor group, which dimerizes with CD94 to bind to non-classic HLA-E class I molecules, which are ubiquitously expressed. Upon binding to its ligand, CD94/NKG2A signaling downregulates NK cell-mediated cytotoxicity. Tumor-infiltrating NK cells from patients with liver cancer express high levels of NKG2A and are functionally exhausted [75]. NKG2A and CD94 expression is restricted to a subset of $CD8^+$ T cells [76] and its expression in TILs generates negative regulatory signals. Mechanistically, NKG2A contains cytoplasmic ITIM motifs responsible for its inhibitory functions by recruiting the phosphatases SHP-1 and SHP-2 [77] (Fig. 2A and B).

Combined blockade of NKG2A and PD-1 or PD-L1 synergizes to reduce tumor growth in a mouse model of B-cell lymphoma by promoting NK and $CD8^+$ T cell cytotoxic activity [78]. Anti-NKG2A blockade enhances $NKG2A^+$ NK cells' cytotoxic function, eliminating human leukemia cells engrafted in mice [79]. Monalizumab is a humanized mAb that specifically blocks NKG2A and enhances NK and T cell effector function and promotes anti-tumor immunity [78]. Monalizumab is under analysis in clinical trials in which it is used either alone or in combination with anti-PD-L1 antibodies to treat a variety of tumor types (Table 4).

CD200 blockade

CD200 is a cell-surface glycoprotein that binds to the coinhibitory receptor CD200R1 expressed in subsets of

NK, T, B, and myeloid cells. CD200 expression is detected in various human tissues such as endothelium, central nervous system, retina, and in activated DCs, T, and B cells. It is of note that the interaction between CD200 and CD200R1 occurs between different cells expressing ligand and receptor (in *trans*), while the interaction in the same cell (in *cis*) is remote due to steric constraints [80]. CD200R1 signaling in NK cells inhibits their cytotoxic activity and cytokine release [18]. CD200R1 contains a NPXY motif in its cytoplasmic tail that when phosphorylated inhibits the Ras/MAPK signaling [81] (Fig. 2C). A direct effect of CD200R1 signaling on T cell activity is less clear. While one study in CD200R KO mice suggested greater T-cell cytotoxicity, another showed a normal T-cell response with a lack of CD200R1 signaling [82]. In DCs and macrophages, CD200R1 signaling reduces pro-inflammatory cytokine production, leading to a tolerogenic state [82]. CD200 may have indirect inhibitory effects on T-cell activity by modifying the cytokine landscape rather than a direct cell-intrinsic inhibitory signal. No direct effect of CD200R1 signaling in other CD200R-expressing immune populations has been reported.

$CD200^{-/-}$ mice displayed reduced rate of skin carcinogenesis [82]. $CD200^{+}$ leukemic cells from AML patients reduced NK cytotoxic activity relative to $CD200^{-}$ leukemic cells and NK function was recovered with anti-CD200 mAb [83]. CD200 blockade increased antitumoral response in a mammary carcinoma mouse model [84]. Finally, CD200 blockade stimulated T cell antitumoral response in CLL patients [85]. Samalizumab, an antibody that targets CD200, is being tested in clinical trials (Table 4). No anti-CD200R1 antibodies have been evaluated in preclinical or clinical contexts as antitumoral therapy.

CD47 blockade

CD47, originally called integrin-associated protein (IAP), is a transmembrane glycoprotein of the immunoglobulin superfamily that is expressed ubiquitously by human cells. When CD47 binds to its ligands, the signal regulatory protein alpha (SIRPα) and thrombospondin-1 (TSP1) can induce cell activation or apoptosis, depending on the cellular context. CD47 activation in immune cells has been linked to tumor immune evasion, decreased antigen-presentation cell function, and impaired effector functions of NK and T cells [86]. In vivo experiments have shown that CD47 signaling inhibits NK and T cell cytotoxicity indirectly through impaired APC functions [87, 88]. Notably, the best characterized function of CD47 serves as an antiphagocytic signal for macrophages upon binding to SIRPα [86].

CD47 blockade indirectly enhances anti-tumor cytotoxicity by stimulating macrophage phagocytosis and antigen presentation by APCs, which enhances $CD8^{+}$ T cell cytotoxicity. In this sense, the antitumoral effects of anti-CD47 treatment are abrogated in T cell-deficient mouse models [88]. Head and neck squamous cell carcinoma (HNSCC) cells with a high level of expression of CD47 show lower NK cytotoxicity, which is reversed upon anti-CD47 treatment [87]. Another strategy that has been developed involves the direct blockage of the SIRPα ligand. An anti-SIRPα antibody reduced tumor growth in an NK- and T cell-dependent manner [86]. A recent study in a mouse model of breast cancer demonstrated that the simultaneous blockade of CD47 and PD-L1 inhibits tumor growth by enhancing T- and NK-cell activity [89]. The targeting of CD47 is being tested in clinical trials for the treatment of various tumor types (Table 4).

BTLA blockade

B and T cell lymphocyte attenuator (BTLA) is a coinhibitory receptor expressed in T cells, DCs, and B cells, but not in NK cells. BTLA binds to the herpesvirus entry mediator (HVEM) protein, which is expressed by B cells, DCs, and T cells. In naïve T cells, BTLA-HVEM interaction in *cis* inhibits T-cell activation, ensuring a quiescent state [90]. At the signaling level, BTLA cytoplasmic tail contains ITIM and ITSM motifs responsible for recruiting the tyrosine phosphatases SHP-1 and SHP-2 which reduces TCR downstream phosphorylation [91] (Fig. 2A and B). TILs exhibit upregulated expression of BTLA, less proliferation, and less extensive cytokine production when they interact with HVEM expressed by cancer cells. Indeed, BTLA and PD-1 co-expression is detected in exhausted TILs from patients with advanced melanoma [92]. Finally, DCs expressing BTLA, when interacting with HVEM, promote the differentiation of peripheral Treg cells, and induce antigen tolerance [93].

Anti-BTLA therapy combined with chemotherapy reduces tumor growth, and increases the survival of tumor-bearing mice [94]. Recent proteomic studies have revealed a rationale for simultaneously blocking PD-1 and BTLA in order to increase the T-cell antitumoral response [95]. In this regard, BTLA blockade upon anti-PD-1 and anti-TIM-3 treatment further increases $CD8^{+}$ T cell proliferation [92]. Interestingly, in ovarian carcinomas BTLA expression was mainly identified in B lymphocytes rather than T or NK cells, and the BTLA blockade antitumoral effect was caused by inhibiting a specific subset of B lymphocytes rather than stimulating T or NK cell function [94]. Two mAbs targeting BTLA are currently being studied in early-phase clinical trials (Table 4).

VISTA blockade

V-domain Ig suppressor of T cell activation (VISTA), also known as programmed death-1 homolog (PD-1H), is an IC expressed by CTLs, Treg cells, DCs, macrophages, and neutrophils, but not NK cells. VISTA has been considered to be a ligand or a receptor in different studies. Here, we will consider it to be a receptor, since the interaction with its ligand leads to VISTA intracellular downstream signaling. VISTA is a functionally pH-selective receptor and interacts with the P-selectin glycoprotein ligand-1 (PSGL-1) under acid pH conditions [96]. PSGL-1 is expressed by different cell populations as T, B, endothelial cells, DCs, macrophages, monocytes, and neutrophils, and participates in leukocyte homing processes. VISTA signaling suppresses T-cell activation and proliferation in in vivo experiments [97]. The VISTA cytoplasmic tail contains conserved proline residues and an SH2 domain that may be responsible for its inhibitory functions [98] (Fig. 2C).

Anti-VISTA antibodies reduce tumor growth and increase T-cell tumor infiltration and effector functions in preclinical models. VISTA blockade decreases the suppressive functions of Treg cells, reduces the intratumoral presence of MDSCs, and increases tumor infiltration of activated DCs [99]. Dual blockade of PD-1 and VISTA synergistically enhance the antitumor T-cell response in various mouse models [100]. Finally, given that VISTA binds its ligand, PSGL-1, under low pH conditions, the possibility of using engineered pH-selective antibodies that bind its epitope in specific pH environments has arisen. The synergy between an acidic pH-selective VISTA-blocking antibody and an anti-PD-1 antibody has been shown to reduce tumor growth in a mouse model of colon adenocarcinoma [96]. VISTA blockade has been translated to the clinical milieu for testing as an anticancer therapy (Table 4).

B7-H3 blockade

The B7 homolog 3 protein (B7-H3) is a B7 family molecule that functions as a ligand, but its receptor remains to be discovered. T lymphocytes and NK cells respond to B7-H3, suggesting that the B7-H3 receptor is expressed in these immune cell types [18]. B7-H3 has been reported as playing a variety of roles in T cells. B7-H3 signaling increases T-cell proliferation, cytokine release, and enhances antitumor T cell activity in cancer mouse models [101]. Conversely, B7-H3 signaling in T cells is also able to inhibit them by blocking TCR signaling [102]. These contradictory effects might be due to specific TME features interfering with T-cell function. B7-H3 functions as an inhibitory ligand for NK cells, and anti-B7-H3 antibodies enhance NK-cell cytotoxicity in vitro. Various human cancer cells upregulate B7-H3 expression, and are related to impaired T-cell function, suppressed NK cytolytic activity, and tumor immune evasion [18].

Anti-B7-H3 treatment reduces tumor growth in cancer mouse models that express B7-H3. B7-H3 KO glioma-initiating cells show less invasiveness and higher susceptibility to NK cell-mediated cytolysis [103]. Other preclinical studies have indicated that higher levels of B7-H3 may be beneficial in the T-cell-mediated anti-tumor response against mastocytoma. A synergistic antitumoral response between anti-B7-H3 mAbs and chemotherapy has been observed in several preclinical models [104]. Thus, blockade of B7-H3 may be beneficial, boosting T and NK cell effector functions in specific tumor types and cellular contexts. Finally, the combination of anti-B7-H3 and anti-PD-L1 treatment promotes a synergistic antitumor response relative to single-agent blockades in a mouse model of NSCLC [105]. Antibodies blocking B7-H3 are being tested in clinical trials for the treatment of several tumor types (Table 4).

IC inhibitors under preclinical investigation

CD96 blockade

CD96, also known as T cell activation increased late expression protein (TACTILE), is a member of the immunoglobulin superfamily of paired receptors which contains intracellular inhibitory and activating motifs. The cytoplasmic tail of CD96 contains an inhibitory motif ITIM and a YXXM motif that is thought to mediate activating or inhibitory functions depending on the cell type [106] (Fig. 2C). CD96 binds to PVR and nectin-1 (CD111) and is expressed in T and NK cells. It has been reported that CD96 signaling in NK cells negatively controls cytokine release [56]. CD96's role in $CD8^+$ T cells is controversial. Cross-linking CD96 in $CD8^+$ T cells induces proliferation and effector cytokine production [107]. However, recent findings indicate that CD96 blockade inhibits primary tumor growth in various tumor mouse models, an effect that is dependent on $CD8^+$ T cell activity [108]. Further studies are needed to determine the role of CD96 in T cells under pathological conditions.

The presence of exhausted $CD96^+$ NK cells is associated with poor clinical prognosis in HCC patients. CD96 blockade increases NK cell-mediated lysis and synergizes with an anti-TIGIT antibody to produce an enhanced antitumoral effect. $CD96^{-/-}$ mice injected with B16 melanoma cells develop fewer lung metastases, this reduction being dependent on NK cells. Another study reported decreased metastasis development after anti-CD96 treatment in several preclinical models [18]. Dual blockade of CD96 with PD-1, PD-L1, TIGIT, or CTLA-4 increases antitumor response, and triple blockade of CD96, PD-1 and TIGIT yields the highest level of

antitumoral immunity in various mouse tumor models [108]. To date, antibodies blocking CD96 have not been evaluated in clinical trials.

ILT2 blockade

The immunoglobulin-like transcript-2 (ILT2), also known as leukocyte immunoglobulin-like receptor-1 (LIR1), is a coinhibitory receptor expressed by NK cells, subsets of T, B cells, and DCs. Non-classic HLA-G class I molecules are ILT2 ligands. HLA-G maintains fetal-maternal immune tolerance, and is expressed in adult tissues in cancer. ILT2 signaling inhibits NK-cell effector functions by decreasing cytotoxicity and IFN-γ release. ILT2 interaction with HLA-G inhibits T-cell proliferation and related cytolysis by recruiting SHP-1 phosphatase to its cytoplasmic ITIM domain [109] (Fig. 2A). In DCs, ILT2 signaling induces the development of tolerogenic DCs. Furthermore, exposure of HLA-G molecules to DCs induces anergy in $CD4^+$ and $CD8^+$ T cells, and impairs NK cytolytic functions [110].

Simultaneous blockade of ILT2 and NKG2A increases the cytotoxicity of NK cells to acute myelogenous leukemia and acute lymphoblastic leukemia human blasts. Moreover, ILT2 blockade increases NK-cell cytotoxicity, leading to the elimination of malignant cells from CLL patients [111]. At present, no ILT2 blockade antibodies have been reported in clinical trials.

Siglec-7 and Siglec-9 blockade

Sialic acid-binding immunoglobulin type lectins (Siglecs) are cell-surface receptors of the I-type lectin family that bind sialic acid-containing glycans present on glycoproteins and glycolipids. Siglec-7 and Siglec-9 are expressed by human NK cells, negatively regulating NK effector function [18]. $CD8^+$ T cell subsets expressing Siglec-7 and Siglec-9 receptors present reduced activity. Specifically, Siglec-7 and Siglec-9 contain cytosolic inhibitory ITIM motifs responsible for recruiting the phosphatase SHP-1 [112] (Fig. 2A). In monocytes, Siglec-7 signaling induces the release of pro-inflammatory molecules upon pathogen recognition [113]. Siglec-9 signaling in macrophages reduces LPS-induced CCR7 expression, revealing a role in modulating innate immunity [114], while Siglec-9 ligand interaction with immature DCs reduces LPS-induced IL-12 release [115]. Finally, the presence of molecules containing sialic acid modifications, including hypersialylation and xenosialylation, has been linked to tumor progression [116].

Siglec-9 is co-expressed with PD-1 in TILs from patients with various cancer types [117]. Targeting Siglec signaling pathways enhances the antitumoral response, while genetically modified mice expressing Siglec-9 in T cells show accelerated growth of CRC tumors [117]. Isolated NK cells from cancer patients with upregulated Siglec-9 expression are less cytotoxic. Anti-Siglec-7 and anti-Siglec-9 antibodies strengthen the effector function of NK cells against cancer cell lines expressing Siglec-7 or Siglec-9 ligands [118]. At present, there are no reports of Siglec-7 or Siglec-9 antibodies being assessed in clinical trials.

KLRG1 blockade

KLRG1 is a coinhibitory receptor expressed exclusively in NK and T cells that binds to E-cadherin and N-cadherin. KLRG1 signaling inhibits NK-associated cytotoxicity and reduces IFN-γ production [119]. In T cells, KLRG1 signaling inhibits cell proliferation and cytotoxic activity [120]. Upon binding to its ligands, KLRG1 recruits SHIP-1 and SHP-2 phosphatases but not SHP-1 to its cytoplasmic ITIM domains resulting in interfered TCR signaling [121] (Fig. 2B and C).

Although KLRG1 KO mice do not display increased NK or T cell cytotoxic functions, pharmacological targeting of KLRG1 increases the effector functions of NK and T cells [122]. Antibody blockade of KLRG1 restores NK-cell cytotoxicity of genetically engineered KLRG1-expressing NK cells in vitro [123]. Administration of anti-KLRG1 antibody does not modify primary tumor growth but has been shown to reduce lung metastases in breast cancer mouse models [124]. Notably, dual blockade of KLRG1 and PD-1 has been shown to decrease primary tumor growth synergistically in melanoma and CRC mouse models [124]. No clinical trials involving anti-KLRG1 antibodies have so far been reported.

2B4 Blockade

2B4, also known as CD244, is a coinhibitory receptor expressed by myeloid cells, NK cells, and a subset of $CD8^+$ T cells. CD48, which is 2B4 ligand, is ubiquitously expressed by hematopoietic cells and upregulated in hematological malignancies [125, 126]. 2B4 receptors contains inhibitory ITSM motifs responsible of recruiting the tyrosine phosphatases SHP-1, SHP-2 and SHIP-1 [127] (Fig. 2). In human NK cell precursors, 2B4 presents inhibitory functions, whereas in mature NK cells, 2B4 signaling enhances their cytotoxic activity [128]. NK cells and $CD8^+$ T cells expressing 2B4 from human cancer patients present an exhausted phenotype that can be reversed by the blockade of the 2B4-CD48 interaction [129]. Furthermore, 2B4 expression levels in tumor-infiltrating DCs and MDSCs are correlated with tumor cell PD-L1 expression and MDSC production of immunosuppressive molecules [130].

In vitro blockade of 2B4 with mAbs increases NK-cell and T-cell functions in $2B4^+$-exhausted NK and T cells [129]. A 2B4 KO mouse model revealed increased

rejection of engrafted melanoma cells [131]. In addition, 2B4 KO mice presented impaired HNSCC growth in a preclinical model. Anti-2B4 mAb treatment phenocopies 2B4 KO mice, inhibiting tumor growth and increasing the presence of TILs [130]. No 2B4 blockade therapies have so far been tested in clinical trials.

Current challenges: improving efficacy without increasing adverse events

Although immunotherapy based on IC blockade has produced promising results in a fraction of patients, a large number of patients do not benefit from the existing approved drugs (Table 3). Tumor-infiltrating immune cells present in the TME play a fundamental role in therapy response. Tumors that are not likely to generate a robust immune response have been classified as poorly immunogenic or cold tumors. These tumors have low quantities of immune infiltrate [1]. On the other hand, hot tumors have high levels of T cell infiltration and are highly immunogenic. Targeting the TME to transform cold tumors into hot tumors before IC blockade therapies is being investigated as a strategy to increase the responsiveness to these therapies. The approaches promoting immunogenicity of cold tumors include enhancing antigen presentation by DCs, reducing the presence and function of immunosuppressive cells, and delivering immunomodulatory factors to boost inflammation [132].

Combining IC blockade drugs with other immunotherapeutic agents also produces promising enhanced antitumoral responses. Chimeric antigen receptor (CAR) T cells are engineered autologous T cells with an artificial TCR that recognize a specific antigen in an MHC-independent manner. CAR T cells achieve long-lasting responses in hematological malignancies, whereas the clinical activity observed so far in solid tumors has been more modest. This may occur because the immunosuppressive TME that present solid tumors can lead to CAR T cell exhaustion [133]. Hence, combining CAR T cells with anti-IC drugs and/or drugs targeting the immunosuppressive TME may ideally produce a synergistic effect, unleashing CAR T cell activity against tumoral cells. Combining anti-PD-1 antibodies with adoptive transfer of CAR T cells might overcome PD-1 dependent T cell exhaustion, thereby improving single-treatment responses [134, 135]. Another interesting strategy to overcome the exhaustion of CAR T cells in solid tumors is to use PD-1 KO CAR T cells, which have enhanced cytotoxic activity [136]. Given the crucial role of APCs in priming antigen-specific T cell immunity, the modulation of APC function has also been used as an antitumoral strategy. In this regard, several DC-based immunotherapies are being clinically studied, such as treatment with immunostimulatory molecules that promote DC activity or vaccine administration of tumor-associated antigens (TAAs) that can be processed and presented by endogenous DCs [137]. The use of DC vaccines consisting of ex vivo-amplified autologous DCs, tumor antigen load and reinfusion to patients, has also proven clinical benefits [137]. Combining dendritic cell vaccines with anti-PD-1 therapies may boost efficacy by improving T cell antitumoral function in mouse models [138, 139]. In addition, DC vaccination can overcome IC blockade-resistant murine lung cancers by eliciting an antitumoral response [140]. Hence, the appropriate combination of immunotherapeutic agents is a promising strategy for treating single-agent-resistant tumors. In addition, chemotherapy and radiotherapy are standard cancer therapies used in the clinic setting that produce immunostimulatory effects and that can be combined with IC blockade therapies to increase antitumoral immunity [141, 142].

Despite the positive results of IC blockade therapies as single agents or in combination, patients treated with IC inhibitors may suffer from secondary autoimmune events, also known as immune-related adverse events (irAEs) [143]. Immune cell exhaustion, promoted by the activation of IC pathways, among other mechanisms, prevents overactivation of effector immune cells and preserves normal homeostasis and self-tolerance. Genetic ablation of ICs leads to the development of autoimmune diseases in multiple mouse models. CTLA-4 KO leads to lymphoproliferative disorders and early lethality, and PD-1 gene abrogation promotes severe autoimmune diseases, while TIM-3 KO and TIGIT KO cause experimental autoimmune encephalomyelitis (EAE) [15]. Pharmacological blockade of IC receptors exacerbates autoimmune events in mouse models of autoimmune diseases [15]. Hence, IC blockade therapies in cancer patients can lead to the appearance of irAEs, which can be variable from person to person. Typically, these toxicities, which have recently been reviewed [144], affect barrier tissues such as the skin, gastrointestinal tract, liver, and respiratory epithelium.

The overall response rate (ORR) to IC blockade antibodies, as a measure of therapy response, varies between tumor types (Table 3). This variation may be due to tumor-specific biological differences. Tumor types with a higher mutation rate and that conserve the expression of HLA have more neo-antigens, and are more likely to be identified and attacked by T cells. Moreover, tumor types with an immunosuppressive TME, including the presence of M2 macrophages, MDSCs, Treg cells, and immunosuppressive soluble factors, are less responsive to anti-IC therapies [145]. In addition, differences in ORR within same tumor type between drugs targeting the same pathway also arise (Table 3), possibly as a consequence of the intertumoral heterogeneity observed in

patients with the same tumor type [146]. As previously described, IC blockade therapy response is affected by the TME profile, which also varies between patients [1].

To improve efficacy, the immune infiltrate and IC ligand expression in tumor and tumor-infiltrating immune cells could be characterized to determine the IC pathway most likely to be responsible for the attenuation of cytotoxic immune cell activity. Despite this, the overall response rates to single IC blockade therapies are generally low. Combining the blockade of multiple ICs is a strategy to increase the response of these therapies against certain tumor types but potentially increases the risk of irAE development. In order to minimize the risk of irAEs and maximize the response, the combinatory blockade of ICs with non-redundant downstream signaling could be a good strategy for enhancing antitumor immunity. Ideally, the blockade of an IC that recruits the phosphatases SHP-1 and/or SHP-2, such as PD-1, KLRG1, PVRIG, 2B4, Siglec-7/−9, ILT2, TIGIT, NKG2A, KIR-L, or BTLA, should be combined with the blockade of another IC that exhibits alternative downstream signaling, such as CTLA-4, TIM3, LAG-3, CD47, CD200R1, or VISTA. Non-redundant IC combinatory blockade therapies may have synergistic effects that boost antitumoral immunity. However, further studies should be carried out to address this hypothesis. In addition, it needs to be considered that combining the blockade of any IC with CTLA-4 might present stronger secondary events given the role of CTLA-4 in regulating central tolerance [147]. Moreover, combinatory treatments that promote T and NK cell function simultaneously to reduce the presence of immunosuppressive cells might also be of value. The use of novel small-molecule inhibitors of PD-1/PD-L1 currently under clinical development might be beneficial because of their reduced immunogenicity. Indeed, immune checkpoint antibodies have a longer pharmacokinetic half-life than small-molecule inhibitors, which manifests as sustained immune system activation and a greater quantity of derived irAEs [148]. Combining small-molecule inhibitors of ICs concomitantly with the blockade of antibodies for different ICs may result in increased effector cell function and reduced tumor growth without any more frequent occurrence of irAEs.

Finding the correct IC blockade combination for each tumor setting to ensure that efficacy is increased without raising the risk of irAEs occurring is a major challenge. Understanding the mechanisms leading to irAEs will allow biomarkers to be developed that can classify patients according to the administration of the most effective and safe IC blockade therapy. Some of the plausible biomarkers studied for this purpose include peripheral blood cell counts, circulating cytokines and chemokines, the presence of autoantibodies, and the composition of gut microbiota [149]. However, the predictive information of these biomarkers has been studied in very few tumor types. The study of genetic polymorphisms associated with autoimmune diseases may also be of importance in identifying patients who are more likely to develop irAEs. Omics studies are of particular interest when reliable biomarkers across multiple tumor types need to be established. The expression of the lymphocyte cytosolic protein 1 (LCP1) and the adenosine diphosphate- dependent glucokinase (ADPGK) have been proposed as biomarkers of irAEs [150]. Further prospective trials are needed to identify the probable combinations of biomarkers that will allow us to categorize patients with respect to the determining the therapy that is safest for them to receive.

Conclusions

The stimulation of antitumoral immunity through immunotherapy has revolutionized cancer treatment in recent years. Antibodies against CTLA-4, PD-1, and PD-L1 have been approved for the treatment of several types of tumors but have been of limited clinical benefit in some patients. This could be related to the existence of the many mechanisms that tumor cells use to evade the immune response, such as the expression of a long repertoire of IC ligands and the infiltration of several immunosuppressive immune cell populations. Blockade of novel ICs is being evaluated in clinical trials. Antibodies against LAG-3, TIM-3, TIGIT, CD47, and B7-H3 are the most advanced IC blockade drugs and may be approved for the treatment of specific tumor types in the near future, depending on the results of the trials. However, other challenges need to be overcome to fully exploit the therapeutic potential of blockade ICs, and thereby boost antitumoral immunity.

A full understanding of the crosstalk between cancer cells and the TME of every tumor type is needed to identify the specific immune-evasion mechanisms exploited by cancer cells and, subsequently, to apply proper therapy. Tumor cells can upregulate the expression of various IC ligands and promote the activation of multiple IC receptors of tumor-infiltrating immune cells. Hence, activation of alternative IC signals in the tumors may diminish the effect of single-blockade antibodies. Combinatory IC blockade treatments might present synergistic antitumoral responses in specific tumor types, and potentially increase the risk of secondary events such as irAEs. Hence, finding the best IC blockade combination to achieve increased effectiveness while minimizing the risk of irAEs should be a priority. Given that some IC receptors share downstream mechanisms to interfere with T and NK cell activation, the co-blockade of IC with non-redundant signaling to

improve antitumoral immunity and prevent overlapping signals could be a good strategy. Furthermore, the use of small-molecule IC inhibitors might be advantageous compared with blockade antibodies, given their reduced immunogenicity. Importantly, development and analysis of biomarkers that allow patients to be classified according to their specific pathology settings and IC activation status should improve response rates to IC blockade therapies. The rational blockade of ICs, based on the specific tumor characteristics of each patient, may represent a breakthrough in our pursuit of a more personalized medicine.

Abbreviations
ICs: Immune checkpoints; CTLs: Cytotoxic T lymphocytes; NK: Natural killer; CTLA-4: Cytotoxic T lymphocyte-associated molecule-4; PD-1: Programmed cell death receptor-1; PD-L1: Programmed death ligand-1; PD-L2: Programmed cell death 1 ligand 2; MHC: Major histocompatibility complex; MDSCs: Myeloid-derived suppressor cells; Treg: T regulatory; TME: Tumor microenvironment; CAR: Chimeric antigen receptor; IFN: Interferon; TNF: Tumor necrosis factor; TCR: T-cell receptor; HLA: Human leukocyte antigen; APCs: Antigen-presenting cells; DCs: Dendritic cells; Th: T-helper; Th1: T-helper 1; Th2: T-helper 2; GM-CSF: Granulocyte-macrophage colony-stimulating factor; TILs: Tumor-infiltrating lymphocytes; FDA: US Food and Drug Administration; EMA: European Medicines Agency; KO: Knockout; mAb: Monoclonal antibody; CRC: Colorectal cancer; RCC: Renal cell cancer; NSCLC: Non-small cell lung cancer; LAG-3: Lymphocyte activation gene-3; FGL-1: Fibrinogen-like protein 1; TIM-3: T cell immunoglobulin and mucin domain-containing protein 3; PS: Phosphatidylserine; CEACAM1: Carcinoembryonic antigen-related cell adhesion molecule 1; HMGB1: High-mobility group protein 1; TIM-3: T-cell immunoglobulin and mucin-domain containing-3; TIGIT: T cell immunoglobulin and ITIM domain; PVRIG: Poliovirus receptor-related immunoglobulin; PVR: Poliovirus receptor; TACTILE: T cell activation increased late expression protein; KIR: Killer immunoglobulin-like; NKG2A: Natural killer group 2A; ILT-2: Immunoglobulin-like transcript-2; KIR-L: Long-tailed KIR; KIR-S: Short-tailed KIR; AML: Acute myeloid leukemia; IAP: Integrin-associated protein; SIRPα: Signal regulatory protein alpha; TSP1: Thrombospodin-1; HNSCC: Head and neck squamous cell carcinoma; Siglecs: Sialic acid-binding immunoglobulin type lectins; LPS: Lipopolysaccharide; KLRG1: Killer cell lectin-like receptor subfamily G member 1; BTLA: B and T cell lymphocyte attenuator; HVEM: Herpesvirus entry mediator; VISTA: V-domain Ig suppressor of T cell activation; PD-1H: Programmed death.1 homolog; PSGL-1: P-selectin glycoprotein ligand-1; B7-H3: B7 homolog 3 protein; EAE: Experimental autoimmune encephalomyelitis; ORR: Overall response rate; mPFS: Median progression-free survival.

Supplementary Information

The online version contains supplementary material available at https://doi.org/10.1186/s13046-022-02264-x.

Additional file 1: Supplementary Table 1. Phase III clinical trials of single-blockade immune checkpoint inhibitors including CTLA-4, PD-1, and PD-L1 in 2021, according to www.clinicaltrials.gov.

Acknowledgements
We thank G. Jorba (SOM Innovation Biotech, S.A.) for exhaustively analyzing ongoing clinical trials.

Authors' contributions
AAO and PMM designed the study. AAO and CD reviewed the information. AAO wrote the manuscript. CD, JML, and PMM critically reviewed the manuscript. All authors read and approved the final manuscript.

Funding
AAO acknowledges the Government of Andorra for a predoctoral grant, ATC0XX - AND-2019/2020. P. Muñoz's laboratory is supported by the Spanish Ministry of Science and Innovation (PID2020-113495RB-I00; co-funded by FEDER funds/European Regional Development Fund (ERDF) – A way to make Europe) and by the Catalan Department of Health (CERCA; Generalitat de Catalunya, 2017/SGR565). JML acknowledges funding by Instituto de Salud Carlos III through the project "PI19/01210" (Co-funded by European Regional Development Fund, A way to make Europe).

Availability of data and materials
The datasets supporting the conclusions of this article are available in the Drug Approvals and Databases FDA repository, www.fda.gov and in the Data clinical trials repository, www.clinicaltrials.gov.

Declarations

Ethics approval and consent to participate
Not applicable.

Consent for publication
Not applicable.

Competing interests
JML has received advisory fees from Bristol-Myers Squibb, MSD, Novartis, Pierre Fabre, Roche, Sanofi; lecture fees from Astellas, Bristol-Myers Squibb, MSD, Novartis, Pierre Fabre, Pfizer, Roche; and travel grants from Bristol-Myers Squibb, MSD, Novartis, Pierre Fabre, Pfizer, Roche, Ipsen. All other authors declare no potential conflicts of interest.

Author details
[1]Aging and Cancer Group, Oncobell Program, Bellvitge Biomedical Research Institute (IDIBELL), Av. Gran Via de L'Hospitalet 199-203, 08907 Barcelona, Spain. [2]Medical Oncology Department, Catalan Institute of Oncology (ICO) Hospitalet, IDIBELL, Barcelona, Spain.

Received: 30 September 2021 Accepted: 18 January 2022
Published online: 14 February 2022

References

1. Binnewies M, Roberts EW, Kersten K, Chan V, Fearon DF, Merad M, et al. Understanding the tumor immune microenvironment (TIME) for effective therapy. Nat Med. 2018;24:541–50. https://doi.org/10.1038/s41591-018-0014-x Nature Publishing Group.
2. Schumacher TN, Schreiber RD. Neoantigens in cancer immunotherapy. Science (80-). 2015:69–74. https://doi.org/10.1126/science.aaa4971.
3. Kim ES, Kim JE, Patel MA, Mangraviti A, Ruzevick J, Lim M. Immune checkpoint modulators: an emerging antiglioma armamentarium. J Immunol Res. 2016;2016:4683607.
4. Wang M, Zhao J, Zhang L, Wei F, Lian Y, Wu Y, et al. Role of tumor microenvironment in tumorigenesis. J Cancer. 2017:761–73. https://doi.org/10.7150/jca.17648.
5. Pardoll DM. The blockade of immune checkpoints in cancer immunotherapy. Nat Rev Cancer. 2012;12:252–64.
6. Voskoboinik I, Whisstock JC, Trapani JA. Perforin and granzymes: function, dysfunction and human pathology. Nat Rev Immunol. 2015;15:388–400.
7. Moretta A, Marcenaro E, Parolini S, Ferlazzo G, Moretta L. NK cells at the interface between innate and adaptive immunity. Cell Death Differ. 2008;15:226–33.
8. Kim R, Emi M, Tanabe K. Cancer immunosuppression and autoimmune disease: beyond immunosuppressive networks for tumour immunity. Immunology. 2006;119:254–64.
9. Wherry EJ, Kurachi M. Molecular and cellular insights into T cell exhaustion. Nat Rev Immunol. 2015;15:486–99.
10. Bi J, Tian Z. NK cell exhaustion. Front Immunol. 2017;8. https://doi.org/10.3389/fimmu.2017.00760.

11. Leach DR, Krummel MF, Allison JP. Enhancement of antitumor immunity by CTLA-4 blockade. Science (80-). 1996;271:1734–6.
12. Ishida Y, Agata Y, Shibahara K, Honjo T. Induced expression of PD-1, a novel member of the immunoglobulin gene superfamily, upon programmed cell death. EMBO J. 1992;11:3887–95.
13. Jenkins RW, Barbie DA, Flaherty KT. Mechanisms of resistance to immune checkpoint inhibitors. Br J Cancer. 2018;118:9–16.
14. Qureshi OS, Zheng Y, Nakamura K, Attridge K, Manzotti C, Schmidt EM, et al. Trans-endocytosis of CD80 and CD86: a molecular basis for the cell-extrinsic function of CTLA-4. Science (80-). Science. 2011;332:600–3. https://doi.org/10.1126/science.1202947.
15. Schnell A, Bod L, Madi A, Kuchroo VK. The yin and yang of co-inhibitory receptors: toward anti-tumor immunity without autoimmunity. Cell Res. 2020:285–99. https://doi.org/10.1038/s41422-020-0277-x Springer Nature.
16. Wing K, Onishi Y, Prieto-Martin P, Yamaguchi T, Miyara M, Fehervari Z, et al. CTLA-4 control over Foxp3+ regulatory T cell function. Science (80-). Science. 2008;322:271–5. https://doi.org/10.1126/science.1160062.
17. Chan DV, Gibson HM, Aufiero BM, Wilson AJ, Hafner MS, Mi QS, et al. Differential CTLA-4 expression in human CD4+ versus CD8 + T cells is associated with increased NFAT1 and inhibition of CD4+ proliferation. Genes Immun. 2014;15:25–32. https://doi.org/10.1038/gene.2013.57 Nature Publishing Group.
18. Khan M, Arooj S, Wang H. NK cell-based immune checkpoint inhibition. Front Immunol. 2020;11:167.
19. Curran MA, Montalvo W, Yagita H, Allison JP. PD-1 and CTLA-4 combination blockade expands infiltrating T cells and reduces regulatory T and myeloid cells within B16 melanoma tumors. Proc Natl Acad Sci U S A. 2010;107:4275–80.
20. Hui E, Cheung J, Zhu J, Su X, Taylor MJ, Wallweber HA, et al. T cell costimulatory receptor CD28 is a primary target for PD-1-mediated inhibition. Science (80-). 2017;355:1428–33. https://doi.org/10.1126/science.aaf1292 American Association for the Advancement of Science.
21. Ahmadzadeh M, Johnson LA, Heemskerk B, Wunderlich JR, Dudley ME, White DE, et al. Tumor antigen-specific CD8 T cells infiltrating the tumor express high levels of PD-1 and are functionally impaired. Blood. 2009;114:1537–44. https://doi.org/10.1182/blood-2008-12-195792.
22. MacFarlane AW, Jillab M, Plimack ER, Hudes GR, Uzzo RG, Litwin S, et al. PD-1 expression on peripheral blood cells increases with stage in renal cell carcinoma patients and is rapidly reduced after surgical tumor resection. Cancer Immunol Res. 2014;2:320–31. https://doi.org/10.1158/2326-6066.CIR-13-0133 American Association for Cancer Research Inc.
23. Pesce S, Greppi M, Tabellini G, Rampinelli F, Parolini S, Olive D, et al. Identification of a subset of human natural killer cells expressing high levels of programmed death 1: A phenotypic and functional characterization. J Allergy Clin Immunol. Mosby Inc. 2017;139:335–346.e3. https://doi.org/10.1016/j.jaci.2016.04.025.
24. Purdy AK, Campbell KS. SHP-2 expression negatively regulates NK cell function. J Immunol. The American Association of Immunologists. 2009;183:7234–43. https://doi.org/10.4049/jimmunol.0900088.
25. Butte MJ, Keir ME, Phamduy TB, Sharpe AH, Freeman GJ. Programmed Death-1 ligand 1 interacts specifically with the B7-1 Costimulatory molecule to inhibit T cell responses. Immunity. 2007;27:111–22. https://doi.org/10.1016/j.immuni.2007.05.016.
26. Ni X, Song Q, Cassady K, Deng R, Jin H, Zhang M, et al. PD-L1 interacts with CD80 to regulate graft-versus-leukemia activity of donor CD8+ T cells. J Clin Invest. 2017;127:1960–77. https://doi.org/10.1172/JCI91138.
27. Cai J, Wang D, Zhang G, Guo X. The role of PD-1/PD-L1 axis in treg development and function: implications for cancer immunotherapy. Onco Targets Ther Dove Medical Press Ltd. 2019:8437–45. https://doi.org/10.2147/OTT.S221340.
28. Garris CS, Arlauckas SP, Kohler RH, Trefny MP, Garren S, Piot C, et al. Successful anti-PD-1 Cancer immunotherapy requires T cell-dendritic cell crosstalk involving the cytokines IFN-γ and IL-12. Immunity. 2018;49:1148–61.
29. Wan C, Keany MP, Dong H, Al-Alem LF, Pandya UM, Lazo S, et al. Enhanced efficacy of simultaneous PD-1 and PD-L1 immune checkpoint blockade in high-grade serous ovarian Cancer. Cancer Res. American Association for Cancer Research Inc. 2021;81:158–73. https://doi.org/10.1158/0008-5472.CAN-20-1674.
30. Stecher C, Battin C, Leitner J, Zettl M, Grabmeier-Pfistershammer K, Höller C, et al. PD-1 blockade promotes emerging checkpoint inhibitors in enhancing T cell responses to allogeneic dendritic cells. Front Immunol. Frontiers Media S.A. 2017;8. https://doi.org/10.3389/fimmu.2017.00572.
31. Anderson AC, Joller N, Kuchroo VK. Lag-3, Tim-3, and TIGIT: co-inhibitory receptors with specialized functions in immune regulation. Immunity. 2016;44:989–1004.
32. Camisaschi C, Casati C, Rini F, Perego M, De Filippo A, Triebel F, et al. LAG-3 expression defines a subset of CD4 + CD25 high Foxp3 + regulatory T cells that are expanded at tumor sites. J Immunol. 2010;184:6545–51.
33. Narayanan S, Ahl PJ, Bijin VA, Kaliaperumal N, Lim G, Wang C, et al. LAG3 is a Central Regulator of NK Cell Cytokine Production. bioRxiv. 2020;01.31.9282.
34. Graydon CG, Mohideen S, Fowke KR. LAG3's enigmatic mechanism of action. Front Immunol Frontiers Media SA. 2021;11:615317. https://doi.org/10.3389/fimmu.2020.615317.
35. Huang RY, Eppolito C, Lele S, Shrikant P, Matsuzaki J, Odunsi K. LAG3 and PD1 co-inhibitory molecules collaborate to limit CD8+ T cell signaling and dampen antitumor immunity in a murine ovarian cancer model. Oncotarget. 2015;6:27359–77.
36. Burova E, Hermann A, Dai J, Ullman E, Halasz G, Potocky T, et al. Preclinical development of the anti-LAG-3 antibody REGN3767: characterization and activity in combination with the anti-PD-1 antibody cemiplimab in human PD-1xLAG-3–knockin mice. Mol Cancer Ther. American Association for Cancer Research Inc. 2019;18:2051–62. https://doi.org/10.1158/1535-7163.MCT-18-1376.
37. Wierz M, Pierson S, Guyonnet L, Viry E, Lequeux A, Oudin A, et al. Dual PD1/LAG3 immune checkpoint blockade limits tumor development in a murine model of chronic lymphocytic leukemia. Blood American Society of Hematology. 2018:1617–21. https://doi.org/10.1182/blood-2017-06-792267.
38. Marcq E, Van Audenaerde JRM, De Waele J, Merlin C, Pauwels P, Van Meerbeeck JP, et al. The search for an interesting partner to combine with PD-L1 blockade in mesothelioma: focus on TIM-3 and LAG-3. Cancers (Basel). MDPI AG. 2021;13:1–14. https://doi.org/10.3390/cancers13020282.
39. Jie HB, Gildener-Leapman N, Li J, Srivastava RM, Gibson SP, Whiteside TL, et al. Intratumoral regulatory T cells upregulate immunosuppressive molecules in head and neck cancer patients. Br J Cancer. 2013;109:2629–35.
40. Ohs I, Ducimetière L, Marinho J, Kulig P, Becher B, Tugues S. Restoration of natural killer cell antimetastatic activity by IL12 and checkpoint blockade. Cancer Res. American Association for Cancer Research Inc. 2017;77:7059–71. https://doi.org/10.1158/0008-5472.CAN-17-1032.
41. Sakuishi K, Ngiow SF, Sullivan JM, Teng MWL, Kuchroo VK, Smyth MJ, et al. TIM3+FOXP3+ regulatory T cells are tissue-specific promoters of T-cell dysfunction in cancer. Oncoimmunology. 2013;2:e23849.
42. Zhu C, Anderson AC, Schubart A, Xiong H, Imitola J, Khoury SJ, et al. The Tim-3 ligand galectin-9 negatively regulates T helper type 1 immunity. Nat Immunol. 2005;6:1245–52. https://doi.org/10.1038/ni1271.
43. Gautron AS, Dominguez-Villar M, de Marcken M, Hafler DA. Enhanced suppressor function of TIM-3+FoxP3+ regulatory T cells. Eur J Immunol. 2014;44:2703–11.
44. van de Weyer PS, Muehlfeit M, Klose C, Bonventre JV, Walz G, Kuehn EW. A highly conserved tyrosine of Tim-3 is phosphorylated upon stimulation by its ligand galectin-9. Biochem Biophys Res Commun. 2006;351:571–6. https://doi.org/10.1016/j.bbrc.2006.10.079.
45. Davidson D, Schraven B, Veillette A. PAG-associated FynT regulates calcium signaling and promotes Anergy in T lymphocytes. Mol Cell Biol. American Society for Microbiology. 2007;27:1960–73. https://doi.org/10.1128/mcb.01983-06.
46. Sehrawat S, Reddy PBJ, Rajasagi N, Suryawanshi A, Hirashima M, Rouse BT. Galectin-9/TIM-3 interaction regulates virus-specific primary and memory CD8 T cell response. PLoS Pathog. 2010;6:1–16. https://doi.org/10.1371/JOURNAL.PPAT.1000882.
47. Yang R, Sun L, Li CF, Wang YH, Yao J, Li H, et al. Galectin-9 interacts with PD-1 and TIM-3 to regulate T cell death and is a target for cancer immunotherapy. Nat Commun Nature Research. 2021;12. https://doi.org/10.1038/s41467-021-21099-2.

48. Liu JF, Ma SR, Mao L, Bu LL, Yu GT, Li YC, et al. T-cell immunoglobulin mucin 3 blockade drives an antitumor immune response in head and neck cancer. Mol Oncol. 2017;11:235–47.
49. Yang M, Du W, Yi L, Wu S, He C, Zhai W, et al. Checkpoint molecules coordinately restrain hyperactivated effector T cells in the tumor microenvironment. Oncoimmunology. 2020;9:1708064.
50. Oweida A, Hararah MK, Phan A, Binder D, Bhatia S, Lennon S, et al. Resistance to radiotherapy and PD-L1 blockade is mediated by TIM-3 upregulation and regulatory T-cell infiltration. Clin Cancer Res. American Association for Cancer Research Inc. 2018;24:5368–80. https://doi.org/10.1158/1078-0432.CCR-18-1038.
51. Kim JE, Patel MA, Mangraviti A, Kim ES, Theodros D, Velarde E, et al. Combination therapy with anti-PD-1, anti-TIM-3, and focal radiation results in regression of murine gliomas. Clin Cancer Res. American Association for Cancer Research Inc. 2017;23:124–36. https://doi.org/10.1158/1078-0432.CCR-15-1535.
52. Xu L, Huang Y, Tan L, Yu W, Chen D, Lu C, et al. Increased Tim-3 expression in peripheral NK cells predicts a poorer prognosis and Tim-3 blockade improves NK cell-mediated cytotoxicity in human lung adenocarcinoma. Int Immunopharmacol. 2015;29:635–41.
53. Seo H, Kim BS, Bae EA, Min BS, Han YD, Shin SJ, et al. IL21 therapy combined with PD-1 and Tim-3 blockade provides enhanced NK cell antitumor activity against MHC class I-deficient tumors. Cancer Immunol Res. American Association for Cancer Research Inc. 2018;6:685–95. https://doi.org/10.1158/2326-6066.CIR-17-0708.
54. Maurya N, Gujar R, Gupta M, Yadav V, Verma S, Sen P. Immunoregulation of dendritic cells by the receptor T cell Ig and Mucin Protein-3 via Bruton's tyrosine kinase and c-Src. J Immunol. 2014;193:3417–25.
55. Wang T, Zhang J, Li N, Li M, Ma S, Tan S, et al. Spatial distribution and functional analysis define the action pathway of Tim-3/Tim-3 ligands in tumor development. Mol Ther. 2021. https://doi.org/10.1016/J.YMTHE.2021.11.015.
56. Sanchez-Correa B, Valhondo I, Hassouneh F, Lopez-Sejas N, Pera A, Bergua JM, et al. DNAM-1 and the TIGIT/PVRIG/TACTILE axis: novel immune checkpoints for natural killer cell-based cancer immunotherapy. Cancers (Basel). 2019;11:877.
57. Alteber Z, Kotturi MF, Whelan S, Ganguly S, Weyl E, Pardoll DM, et al. Therapeutic targeting of checkpoint receptors within the DNAM1 Axis. Cancer Discov. 2021;11:1040–51. https://doi.org/10.1158/2159-8290.CD-20-1248.
58. Li M, Xia P, Du Y, Liu S, Huang G, Chen J, et al. T-cell immunoglobulin and ITIM domain (TIGIT) receptor/poliovirus receptor (PVR) ligand engagement suppresses interferon-γ production of natural killer cells via β-arrestin 2-mediated negative signaling. J Biol Chem. American Society for Biochemistry and Molecular Biology Inc. 2014;289:17647–57. https://doi.org/10.1074/jbc.M114.572420.
59. Joller N, Hafler JP, Brynedal B, Kassam N, Spoerl S, Levin SD, et al. Cutting edge: TIGIT has T cell-intrinsic inhibitory functions. J Immunol. The American Association of Immunologists. 2011;186:1338–42. https://doi.org/10.4049/jimmunol.1003081.
60. Yu X, Harden K, Gonzalez LC, Francesco M, Chiang E, Irving B, et al. The surface protein TIGIT suppresses T cell activation by promoting the generation of mature immunoregulatory dendritic cells. Nat Immunol. 2009;10:48–57. https://doi.org/10.1038/ni.1674.
61. Johnston RJ, Comps-Agrar L, Hackney J, Yu X, Huseni M, Yang Y, et al. The Immunoreceptor TIGIT regulates antitumor and antiviral CD8+ T cell effector function. Cancer Cell. 2014;26:923–37.
62. Hung AL, Maxwell R, Theodros D, Belcaid Z, Mathios D, Luksik AS, et al. TIGIT and PD-1 dual checkpoint blockade enhances antitumor immunity and survival in GBM. Oncoimmunology. Taylor and Francis Inc. 2018;7. https://doi.org/10.1080/2162402X.2018.1466769.
63. Zhang Q, Bi J, Zheng X, Chen Y, Wang H, Wu W, et al. Blockade of the checkpoint receptor TIGIT prevents NK cell exhaustion and elicits potent anti-tumor immunity. Nat Immunol. 2018;19:723–32.
64. Zhu Y, Paniccia A, Schulick AC, Chen W, Koenig MR, Byers JT, et al. Identification of CD112R as a novel checkpoint for human T cells. J Exp Med Rockefeller University Press. 2016;213:167–76. https://doi.org/10.1084/jem.20150785.
65. Li J, Whelan S, Kotturi MF, Meyran D, D'Souza C, Hansen K, et al. PVRIG is a novel natural killer cell immune checkpoint receptor in acute myeloid leukemia. Haematologica. 2021;106. https://doi.org/10.3324/HAEMATOL.2020.258574.
66. Li Y, Zhang Y, Cao G, Zheng X, Sun C, Wei H, et al. Blockade of checkpoint receptor PVRIG unleashes anti-tumor immunity of NK cells in murine and human solid tumors. J Hematol Oncol. 2021;14:100. https://doi.org/10.1186/S13045-021-01112-3.
67. Xu F, Sunderland A, Zhou Y, Schulick RD, Edil BH, Zhu Y. Blockade of CD112R and TIGIT signaling sensitizes human natural killer cell functions. Cancer Immunol Immunother. Springer Science and Business Media Deutschland GmbH. 2017;66:1367–75. https://doi.org/10.1007/s00262-017-2031-x.
68. Murter B, Pan X, Ophir E, Alteber Z, Azulay M, Sen R, et al. Mouse PVRIg has CD8 + T cell-specific coinhibitory functions and dampens antitumor immunity. Cancer Immunol Res. 2019;7:244–56.
69. Whelan S, Ophir E, Kotturi MF, Levy O, Ganguly S, Leung L, et al. PVRIG and PVRL2 are induced in Cancer and inhibit CD8 + T-cell function. Cancer Immunol Res. 2019;7:257–68. https://doi.org/10.1158/2326-6066.CIR-18-0442.
70. Long EO, Barber DF, Burshtyn DN, Faure M, Peterson M, Rajagopalan S, et al. Inhibition of natural killer cell activation signals by killer cell immunoglobulin-like receptors (CD158). Immunol Rev. 2001;181:223–33.
71. Long EO. Negative signaling by inhibitory receptors: the NK cell paradigm. Immunol Rev NIH Public Access. 2008:70–84. https://doi.org/10.1111/j.1600-065X.2008.00660.x.
72. Huard B, Karlsson L. KIR expression on self-reactive CD8+ T cells is controlled by T-cell receptor engagement. Nature. 2000;403:325–8.
73. Ruggeri L, Capanni M, Urbani E, Perruccio K, Shlomchik WD, Tosti A, et al. Effectiveness of donor natural killer cell aloreactivity in mismatched hematopoietic transplants. Science (80-). 2002;295:2097–100.
74. He Y, Bunn PA, Zhou C, Chan D. KIR 2D (L1, L3, L4, S4) and KIR 3DL1 protein expression in non-small cell lung cancer. Oncotarget. 2016;7:82104–11.
75. Sun C, Xu J, Huang Q, Huang M, Wen H, Zhang C, et al. High NKG2A expression contributes to NK cell exhaustion and predicts a poor prognosis of patients with liver cancer. Oncoimmunology. 2016;6:e1264562.
76. Braud VM, Aldemir H, Breart B, Ferlin WG. Expression of CD94-NKG2A inhibitory receptor is restricted to a subset of CD8+ T cells. Trends Immunol. 2003;24:162–4.
77. Le Dréan E, Vély F, Olcese L, Cambiaggi A, Guia S, Krystal G, et al. Inhibition of antigen-induced T cell response and antibody-induced NK cell cytotoxicity by NKG2A: association of NKG2A with SHP-1 and SHP-2 protein-tyrosine phosphatases. Eur J Immunol; 1998;28:264–276. doi: 10.1002/(SICI)1521-4141(199801)28:01<264::AID-IMMU264>3.0.CO;2-O.
78. André P, Denis C, Soulas C, Bourbon-Caillet C, Lopez J, Arnoux T, et al. Anti-NKG2A mAb is a checkpoint inhibitor that promotes anti-tumor immunity by unleashing both T and NK cells. Cell. 2018;175:1731–43.
79. Ruggeri L, Urbani E, André P, Mancusi A, Tosti A, Topini F, et al. Effects of anti-NKG2A antibody administration on leukemia and normal hematopoietic cells. Haematologica Ferrata Storti Foundation. 2016;101:626–33. https://doi.org/10.3324/haematol.2015.135301.
80. Hatherley D, Lea SM, Johnson S, Barclay AN. Structures of CD200/CD200 receptor family and implications for topology, regulation, and evolution. Structure Elsevier. 2013;21:820–32. https://doi.org/10.1016/j.str.2013.03.008.
81. Zhang S, Cherwinski H, Sedgwick JD, Phillips JH. Molecular mechanisms of CD200 inhibition of mast cell activation. J Immunol The American Association of Immunologists. 2004;173:6786–93. https://doi.org/10.4049/jimmunol.173.11.6786.
82. Liu JQ, Hu A, Zhu J, Yu J, Talebian F, Bai XF. CD200-CD200R pathway in the regulation of tumor immune microenvironment and immunotherapy. Adv Exp Med Biol Springer. 2020:155–65. https://doi.org/10.1007/978-3-030-35582-1_8.
83. Coles SJ, Wang ECY, Man S, Hills RK, Burnett AK, Tonks A, et al. CD200 expression suppresses natural killer cell function and directly inhibits patient anti-tumor response in acute myeloid leukemia. Leukemia. 2011;25:792–9.
84. Gorczynski RM, Chen Z, Erin N, Khatri I, Podnos A. Comparison of immunity in mice cured of primary/metastatic growth of EMT6 or 4THM breast cancer by chemotherapy or immunotherapy. PLoS One. 2014;9:e113597.

85. Pallasch CP, Ulbrich S, Brinker R, Hallek M, Uger RA, Wendtner CM. Disruption of T cell suppression in chronic lymphocytic leukemia by CD200 blockade. Leuk Res. 2009;33:460–4.
86. Veillette A, Chen J. SIRPα–CD47 immune checkpoint blockade in anticancer therapy. Trends Immunol Elsevier Ltd. 2018:173–84. https://doi.org/10.1016/j.it.2017.12.005.
87. Kim MJ, Lee JC, Lee JJ, Kim S, Lee SG, Park SW, et al. Association of CD47 with natural killer cell-mediated cytotoxicity of head-and-neck squamous cell carcinoma lines. Tumor Biol. 2008;29:28–34.
88. Liu X, Pu Y, Cron K, Deng L, Kline J, Frazier WA, et al. CD47 blockade triggers T cell-mediated destruction of immunogenic tumors. Nat Med. 2015;21:1209–15.
89. Lian S, Xie R, Ye Y, Xie X, Li S, Lu Y, et al. Simultaneous blocking of CD47 and PD-L1 increases innate and adaptive cancer immune responses and cytokine release. EBioMedicine. 2019;42:281–95.
90. Cheung TC, Oborne LM, Steinberg MW, Macauley MG, Fukuyama S, Sanjo H, et al. T cell intrinsic Heterodimeric complexes between HVEM and BTLA determine receptivity to the surrounding microenvironment. J Immunol. The American Association of Immunologists. 2009;183:7286–96. https://doi.org/10.4049/jimmunol.0902490.
91. Gavrieli M, Watanabe N, Loftin SK, Murphy TL, Murphy KM. Characterization of phosphotyrosine binding motifs in the cytoplasmic domain of B and T lymphocyte attenuator required for association with protein tyrosine phosphatases SHP-1 and SHP-2. Biochem Biophys Res Commun. Academic Press Inc. 2003;312:1236–43. https://doi.org/10.1016/j.bbrc.2003.11.070.
92. Fourcade J, Sun Z, Pagliano O, Guillaume P, Luescher IF, Sander C, et al. CD8 + T cells specific for tumor antigens can be rendered dysfunctional by the tumor microenvironment through upregulation of the inhibitory receptors BTLA and PD-1. Cancer Res. 2012;72:887–96.
93. Jones A, Bourque J, Kuehm L, Opejin A, Teague RM, Gross C, et al. Immunomodulatory functions of BTLA and HVEM govern induction of Extrathymic regulatory T cells and tolerance by dendritic cells. Immunity. 2016;45:1066–77.
94. Chen YL, Lin HW, Chien CL, Lai YL, Sun WZ, Chen CA, et al. BTLA blockade enhances Cancer therapy by inhibiting IL-6/IL-10-induced CD19high B lymphocytes. J Immunother Cancer. 2019;7:313.
95. Celis-Gutierrez J, Blattmann P, Zhai Y, Jarmuzynski N, Ruminski K, Grégoire C, et al. Quantitative Interactomics in primary T cells provides a rationale for concomitant PD-1 and BTLA Coinhibitor blockade in Cancer immunotherapy. Cell Rep. 2019;27:3315–30.
96. Johnston RJ, Su LJ, Pinckney J, Critton D, Boyer E, Krishnakumar A, et al. VISTA is an acidic pH-selective ligand for PSGL-1. Nature. 2019;574:565–70.
97. Lines JL, Pantazi E, Mak J, Sempere LF, Wang L, O'Connell S, et al. VISTA is an immune checkpoint molecule for human T cells. Cancer Res. 2014;74:1924–32.
98. Huang X, Zhang X, Li E, Zhang G, Wang X, Tang T, et al. VISTA: an immune regulatory protein checking tumor and immune cells in cancer immunotherapy. J Hematol Oncol BioMed Central. 2020:83. https://doi.org/10.1186/s13045-020-00917-y.
99. Le Mercier I, Chen W, Lines JL, Day M, Li J, Sergent P, et al. VISTA regulates the development of protective antitumor immunity. Cancer Res. 2014;74:1933–44.
100. Liu J, Yuan Y, Chen W, Putra J, Suriawinata AA, Schenk AD, et al. Immune-checkpoint proteins VISTA and PD-1 nonredundantly regulate murine T-cell responses. Proc Natl Acad Sci U S A. 2015;112:6682–7.
101. Chapoval AI, Ni J, Lau JS, Wilcox RA, Flies DB, Liu D, et al. B7-H3: a costimulatory molecule for T cell activation and IFN-γ production. Nat Immunol. 2001;2:269–74.
102. Prasad DVR, Nguyen T, Li Z, Yang Y, Duong J, Wang Y, et al. Murine B7-H3 is a negative regulator of T cells. J Immunol. 2004;173:2500–6.
103. Lemke D, Pfenning PN, Sahm F, Klein AC, Kempf T, Warnken U, et al. Costimulatory protein 4IgB7H3 drives the malignant phenotype of glioblastoma by mediating immune escape and invasiveness. Clin Cancer Res. 2012;18:105–17.
104. Yamato I, Sho M, Nomi T, Akahori T, Shimada K, Hotta K, et al. Clinical importance of B7-H3 expression in human pancreatic cancer. Br J Cancer. 2009;101:1709–16.
105. Yonesaka K, Haratani K, Takamura S, Sakai H, Kato R, Takegawa N, et al. B7-h3 negatively modulates ctl-mediated cancer immunity. Clin Cancer Res. 2018;24:2653–64.
106. Georgiev H, Ravens I, Papadogianni G, Bernhardt G. Coming of age: CD96 emerges as modulator of immune responses. Front Immunol. Frontiers Media S.A. 2018. https://doi.org/10.3389/fimmu.2018.01072.
107. Chiang EY, Almeida PE, Almeida Nagata DE, Bowles KH, Du X, Chitre AS, et al. CD96 functions as a co-stimulatory receptor to enhance CD8 + T cell activation and effector responses. Eur J Immunol. 2020;50:891–902.
108. Mittal D, Lepletier A, Madore J, Aguilera AR, Stannard K, Blake SJ, et al. CD96 is an immune checkpoint that regulates CD8+ T-cell antitumor function. Cancer Immunol Res. 2019;7:559–71.
109. Sayós J, Martínez-Barriocanal A, Kitzig F, Bellón T, López-Botet M. Recruitment of C-terminal Src kinase by the leukocyte inhibitory receptor CD85j. Biochem Biophys Res Commun. 2004;324:640–7. https://doi.org/10.1016/j.bbrc.2004.09.097.
110. Rouas-Freiss N, Moreau P, Lemaoult J, Carosella ED. The dual role of HLA-G in cancer. J Immunol Res. 2014;2014:359748.
111. Villa-Álvarez M, Sordo-Bahamonde C, Lorenzo-Herrero S, Gonzalez-Rodriguez AP, Payer AR, Gonzalez-Garcia E, et al. Ig-like transcript 2 (ILT2) blockade and Lenalidomide restore NK cell function in chronic lymphocytic leukemia. Front Immunol. 2018;9:2917.
112. Ikehara Y, Ikehara SK, Paulson JC. Negative regulation of T cell receptor signaling by Siglec-7 (p70/AIRM) and Siglec-9. J Biol Chem. 2004;279:43117–25.
113. Varchetta S, Brunetta E, Roberto A, Mikulak J, Hudspeth KL, Mondelli MU, et al. Engagement of Siglec-7 receptor induces a pro-inflammatory response selectively in monocytes. PLoS One. 2012;7:e45821.
114. Higuchi H, Shoji T, Iijima S, Nishijima KI. Constitutively expressed Siglec-9 inhibits LPS-induced CCR7, but enhances IL-4-induced CD200R expression in human macrophages. Biosci Biotechnol Biochem. 2016;80:1141–8.
115. Ohta M, Ishida A, Toda M, Akita K, Inoue M, Yamashita K, et al. Immunomodulation of monocyte-derived dendritic cells through ligation of tumor-produced mucins to Siglec-9. Biochem Biophys Res Commun. 2010;402:663–9.
116. Adams OJ, Stanczak MA, Von Gunten S, Läubli H. Targeting sialic acid-Siglec interactions to reverse immune suppression in cancer. Glycobiology. 2018;28:640–7.
117. Stanczak MA, Siddiqui SS, Trefny MP, Thommen DS, Boligan KF, Von Gunten S, et al. Self-associated molecular patterns mediate cancer immune evasion by engaging Siglecs on T cells. J Clin Invest. 2018;128:4912–23.
118. Jandus C, Boligan KF, Chijioke O, Liu H, Dahlhaus M, Démoulins T, et al. Interactions between Siglec-7/9 receptors and ligands influence NK cell-dependent tumor immunosurveillance. J Clin Invest. 2014;124:1810–20.
119. Robbins SH, Nguyen KB, Takahashi N, Mikayama T, Biron CA, Brossay L. Cutting edge: inhibitory functions of the killer cell Lectin-like receptor G1 molecule during the activation of mouse NK cells. J Immunol. 2002;168:2585–9.
120. Gründemann C, Bauer M, Schweier O, von Oppen N, Lässing U, Saudan P, et al. Cutting edge: identification of E-cadherin as a ligand for the murine killer cell Lectin-like receptor G1. J Immunol. 2006;176:1311–5.
121. Tessmer MS, Fugere C, Stevenaert F, Naidenko OV, Chong HJ, Leclercq G, et al. KLRG1 binds cadherins and preferentially associates with SHIP-1. Int Immunol. 2007;19:391–400. https://doi.org/10.1093/intimm/dxm004.
122. Gründemann C, Schwartzkopff S, Koschella M, Schweier O, Peters C, Voehringer D, et al. The NK receptor KLRG1 is dispensable for virus-induced NK and CD8 + T-cell differentiation and function in vivo. Eur J Immunol. 2010;40:1303–14.
123. Ito M, Maruyama T, Saito N, Koganei S, Yamamoto K, Matsumoto N. Killer cell lectin-like receptor G1 binds three members of the classical cadherin family to inhibit NK cell cytotoxicity. J Exp Med. 2006;203:289–95.
124. Greenberg SA, Kong SW, Thompson E, Gulla SV. Co-inhibitory T cell receptor KLRG1: human cancer expression and efficacy of neutralization in murine cancer models. Oncotarget. 2019;10:1399–406.

125. Latchman Y, McKay PF, Reiser H. Cutting edge: identification of the 2B4 molecule as a counter-receptor for CD48. J Immunol. 1998;161:5809–12.
126. Hosen N, Ichihara H, Mugitani A, Aoyama Y, Fukuda Y, Kishida S, et al. CD48 as a novel molecular target for antibody therapy in multiple myeloma. Br J Haematol. 2012;156:213–24. https://doi.org/10.1111/j.1365-2141.2011.08941.x.
127. Pahima H, Puzzovio PG, Levi-Schaffer F. 2B4 and CD48: a powerful couple of the immune system. Clin Immunol Academic Press Inc. 2019:64–8. https://doi.org/10.1016/j.clim.2018.10.014.
128. Lanuza PM, Pesini C, Arias MA, Calvo C, Ramirez-Labrada A, Pardo J. Recalling the biological significance of immune checkpoints on NK cells: a chance to overcome LAG3, PD1, and CTLA4 inhibitory pathways by adoptive NK cell transfer? Front Immunol. Frontiers Media SA. 2020. https://doi.org/10.3389/fimmu.2019.03010.
129. Wu Y, Kuang DM, Pan WD, Le WY, Lao XM, Wang D, et al. Monocyte/macrophage-elicited natural killer cell dysfunction in hepatocellular carcinoma is mediated by CD48/2B4 interactions. Hepatology. 2013;57:1107–16.
130. Agresta L, Lehn M, Lampe K, Cantrell R, Hennies C, Szabo S, et al. CD244 represents a new therapeutic target in head and neck squamous cell carcinoma. J Immunother Cancer. 2020;8:1–12.
131. Vaidya SV, Stepp SE, McNerney ME, Lee J-K, Bennett M, Lee K-M, et al. Targeted disruption of the 2B4 gene in mice reveals an in vivo role of 2B4 (CD244) in the rejection of B16 melanoma cells. J Immunol. 2005;174:800–7.
132. Duan Q, Zhang H, Zheng J, Zhang L. Turning cold into hot: firing up the tumor microenvironment. Trends Cancer. 2020;6:605–18. https://doi.org/10.1016/J.TRECAN.2020.02.022.
133. Grosser R, Cherkassky L, Chintala N, Adusumilli PS. Combination immunotherapy with CAR T cells and checkpoint blockade for the treatment of solid tumors. Cancer Cell. 2019;36:471–82. https://doi.org/10.1016/J.CCELL.2019.09.006.
134. Cherkassky L, Morello A, Villena-Vargas J, Feng Y, Dimitrov DS, Jones DR, et al. Human CAR T cells with cell-intrinsic PD-1 checkpoint blockade resist tumor-mediated inhibition. J Clin Invest. 2016;126:3130–44. https://doi.org/10.1172/JCI83092.
135. John LB, Devaud C, Duong CPM, Yong CS, Beavis PA, Haynes NM, et al. Anti-PD-1 antibody therapy potently enhances the eradication of established tumors by gene-modified T cells. Clin Cancer Res. 2013;19:5636–46. https://doi.org/10.1158/1078-0432.CCR-13-0458.
136. Hu W, Zi Z, Jin Y, Li G, Shao K, Cai Q, et al. CRISPR/Cas9-mediated PD-1 disruption enhances human mesothelin-targeted CAR T cell effector functions. Cancer Immunol Immunother. 2019;68:365–77. https://doi.org/10.1007/S00262-018-2281-2.
137. Wculek SK, Cueto FJ, Mujal AM, Melero I, Krummel MF, Sancho D. Dendritic cells in cancer immunology and immunotherapy. Nat Rev Immunol Nature Research. 2020:7–24. https://doi.org/10.1038/s41577-019-0210-z.
138. Kodumudi KN, Ramamoorthi G, Snyder C, Basu A, Jia Y, Awshah S, et al. Sequential anti-PD1 therapy following dendritic cell vaccination improves survival in a HER2 mammary carcinoma model and identifies a critical role for CD4 T cells in mediating the response. Front Immunol. 2019;10. https://doi.org/10.3389/FIMMU.2019.01939.
139. Yazdani M, Gholizadeh Z, Nikpoor AR, Mohamadian Roshan N, Jaafari MR, Badiee A. Ex vivo dendritic cell-based (DC) vaccine pulsed with a low dose of liposomal antigen and CpG-ODN improved PD-1 blockade immunotherapy. Sci Rep. 2021;11. https://doi.org/10.1038/S41598-021-94250-0.
140. Sun C, Nagaoka K, Kobayashi Y, Nakagawa H, Kakimi K, Nakajima J. Neoantigen dendritic cell vaccination combined with anti-CD38 and CpG elicits anti-tumor immunity against The immune checkpoint therapy-resistant murine lung Cancer cell line LLC1. Cancers (Basel). 2021;13:5508. https://doi.org/10.3390/CANCERS13215508.
141. Patel SA, Minn AJ. Combination Cancer therapy with immune checkpoint blockade: mechanisms and strategies. Immunity. 2018;48:417–33. https://doi.org/10.1016/J.IMMUNI.2018.03.007.
142. Galluzzi L, Humeau J, Buqué A, Zitvogel L, Kroemer G. Immunostimulation with chemotherapy in the era of immune checkpoint inhibitors. Nat Rev Clin Oncol. 2020;17:725–41. https://doi.org/10.1038/S41571-020-0413-Z.
143. Pauken KE, Dougan M, Rose NR, Lichtman AH, Sharpe AH. Adverse events following Cancer immunotherapy: obstacles and opportunities. Trends Immunol. Elsevier Ltd. 2019:511–23. https://doi.org/10.1016/j.it.2019.04.002.
144. Dougan M, Luoma AM, Dougan SK, Wucherpfennig KW. Understanding and treating the inflammatory adverse events of cancer immunotherapy. Cell. 2021;S0092-8674:00161–6. https://doi.org/10.1016/j.cell.2021.02.011.
145. Hegde PS, Karanikas V, Evers S. The where, the when, and the how of immune monitoring for Cancer immunotherapies in the era of checkpoint inhibition. Clin Cancer Res. 2016;22:1865–74. https://doi.org/10.1158/1078-0432.CCR-15-1507.
146. Sutherland KD, Visvader JE. Cellular mechanisms underlying Intertumoral heterogeneity. Trends Cancer. 2015;1:15–23. https://doi.org/10.1016/J.TRECAN.2015.07.003.
147. Verhagen J, Genolet R, Britton GJ, Stevenson BJ, Sabatos-Peyton CA, Dyson J, et al. CTLA-4 controls the thymic development of both conventional and regulatory T cells through modulation of the TCR repertoire. Proc Natl Acad Sci U S A. 2013:110. https://doi.org/10.1073/pnas.1208573110.
148. Sasikumar PG, Ramachandra M. Small-molecule immune checkpoint inhibitors targeting PD-1/PD-L1 and other emerging checkpoint pathways. BioDrugs Springer International Publishing. 2018:481–97. https://doi.org/10.1007/s40259-018-0303-4.
149. Hommes JW, Verheijden RJ, Suijkerbuijk KPM, Hamann D. Biomarkers of checkpoint inhibitor induced immune-related adverse events—a comprehensive review. Front Oncol Frontiers Media SA. 2021;10:585311. https://doi.org/10.3389/fonc.2020.585311.
150. Jing Y, Liu J, Ye Y, Pan L, Deng H, Wang Y, et al. Multi-omics prediction of immune-related adverse events during checkpoint immunotherapy. Nat Commun. Nature Research. 2020;11. https://doi.org/10.1038/s41467-020-18742-9.

Publisher's Note

UNIVERSITAT DE BARCELONA

IDIBELL